IntechOpen

Sensory Nervous System

Edited by Thomas Heinbockel

SENSORY NERVOUS SYSTEM

Edited by **Thomas Heinbockel**

Sensory Nervous System
http://dx.doi.org/10.5772/68128
Edited by Thomas Heinbockel

Contributors

Lavinia Alberi, Emanuele Brai, Einat Hauzman, Dora Ventura, Daniela Bonci, Stephane Molotchnikoff, Nayan Chanauria, Rudy Lussiez, Afef Ouelhazi, Alyssa A Brewer, Brian Barton, Wolfgang Stein, Margaret DeMaegd, Thomas Heinbockel

Notice

First published in London, United Kingdom, 2018 by IntechOpen
eBook (PDF) Published by IntechOpen, 2019
IntechOpen is the global imprint of INTECHOPEN LIMITED, registered in England and Wales, registration number: 11086078, The Shard, 25th floor, 32 London Bridge Street
London, SE19SG – United Kingdom
Printed in Croatia

British Library Cataloguing-in-Publication Data
A catalogue record for this book is available from the British Library

Additional hard and PDF copies can be obtained from orders@intechopen.com

Sensory Nervous System
Edited by Thomas Heinbockel

p. cm.

Print ISBN 978-1-78923-358-2

Online ISBN 978-1-78923-359-9

eBook (PDF) ISBN 978-1-83881-284-3

Meet the editor

Thomas Heinbockel, Ph.D., is Professor and Director of Graduate Studies in the Department of Anatomy, Howard University College of Medicine, Washington, DC. Dr. Heinbockel's laboratory engages in multidisciplinary research to elucidate organizational principles of neural systems in the brain, specifically the limbic and olfactory system. His research has been directed at understanding brain mechanisms of information processing and their relation to neurological and neuropsychiatric disorders. His lab works also on translational projects, specifically, the development of novel anti-epileptic drugs and pharmacotherapeutic treatment options of drug addiction. His lab analyzes drug actions at the epi- and genetic level using next-generation sequencing technology. Dr. Heinbockel studied biology at the Philipps-University, Marburg, Germany. His studies of the brain started during his M.S. thesis work at the Max-Planck-Institute for Behavioral Physiology, Starnberg/Seewiesen, Germany. Subsequently, he completed a Ph.D. in Neuroscience at the University of Arizona, Tucson, Arizona, USA. After graduating, he was Research Associate at the Institute of Physiology, Otto-von-Guericke-University School of Medicine, Magdeburg, Germany. Prior to his arrival at Howard University, Dr. Heinbockel held joint research faculty appointments in the Department of Anatomy & Neurobiology and the Department of Physiology at the University of Maryland School of Medicine, Baltimore, Maryland, USA. He still maintains an adjunct appointment in these departments.

Contents

Preface

The sensory nervous system is of critical importance in our daily lives and contributes to our personal well-being and safety as well as communication with others. However, it is only when disease or injury impair its function that we fully appreciate the relevance of our sensory modalities. During the past decades, research of our senses has seen an ever-growing interest in this exciting field of study. This book provides the reader with an overview of the current state-of-the-art of research of our senses and focuses on the most important evidence-based developments in this area. This book addresses both the physiology and pathophysiology of our sensory nervous system ranging from molecular, cellular, and systems to cognitive and behavioral topics. Individual chapters focus on recent advances in specific areas of sensory systems in different model organisms and humans. All chapters represent recent contributions to the rapidly developing field of sensory science.

The book contains six chapters and presents reviews in different areas of the sensory nervous system written by experts in their respective fields. The mechanisms of sensory processing in the central nervous system and their relation to neurological diseases are featured prominently as a recurring theme throughout several chapters. This book will be a most valuable resource for neuroscientists and other scientists alike. In addition, it will contribute to the training of current and future neuroscientists who find the sensory nervous system as fascinating as many generations before them.

Chapter One ('Organization and Function of Sensory Nervous Systems'), written by Thomas Heinbockel, introduces to topic of this book by discussing the concept of the sensory nervous system and its relation to other divisions of the nervous system. The chapter briefly discusses the value of model organisms in enhancing our understanding of the evolution of sensory systems. The chapter outlines differences and astounding similarities of sensory nervous systems among members of distant animal taxa with respect to structure and function of the sensory pathways. This key point is illustrated by reviewing the olfactory system of vertebrates and insects.

In Chapter Two ('Long-Distance Modulation of Sensory Encoding via Axonal Neuromodulation'), Margaret L. DeMaegd and Wolfgang Stein discuss how the neuromodulatory system plays a critical role in sensorimotor system function and animal behavior. The authors focus on one neuromodulatory effect on axons, namely ectopic spiking, a process during which action potentials are elicited in the axon trunk and travel antidromically toward the site of sensory transduction. In their chapter, the authors review work on the experimentally advantageous anterior gastric receptor which is a single-cell muscle tendon organ in the crustacean stomatogastric ganglion. This is a well-characterized system for the investigation of cellular and circuit neuromodulation.

Chapter Three ('Are Sensory Neurons In The Cortex Committed To Original Trigger Features?'), written by Nayan Chanauria, Rudy Lussiez, Afef Ouelhazi, and Stephane Molotchnikoff, reviews the plasticity of sensory cortices as a result of injury or exposure to chemicals. The authors

describe how sensory cortices are capable of adapting to intense experiences by going through a re-calibration of corresponding or neighboring sensory area(s) to re-direct the sensory function and exhibit remarkable expansion of neuroplasticity within the brain. The authors also explore how the application of drugs modulates potential plasticity within a sensory system.

Chapter Four ('Olfaction, Among the First Senses to Develop and Decline '), written by Emanuele Brai and Lavinia Alberi, addresses the physiological relevance of our olfactory system because of its fundamental role for survival. The authors review the anatomical structures, cytoarchitecture and neurogenesis in the olfactory pathway. A major focus of the chapter is on how olfaction is the first sense to be impaired before the onset of cognitive symptoms which potentially indicates that olfactory transmission characterizes early neural network imbalances. The authors explore the perspective of using this sense as a diagnostic tool in treating systemic and central nervous system pathologies.

In Chapter Five ('Retinal Topographic Maps: A Glimpse into the Animals' Visual World**'),** Einat Hauzman, Daniela M. O. Bonci and Dora F. Ventura review the visual ecology of a group of diurnal and nocturnal snakes from the Colubridae family which is the largest snake family. The authors compare and contrast species differences in the retinal specializations among the snake species with respect to density and distribution of cells of the retinal ganglion cell layer. The findings are interpreted to reflect evolutionary pressures on the structures of the visual system and could be related to the species' evolutionary history as well as ecological and behavioral features indicating the complexity of the adaptive strategies of the snakes' visual system.

In Chapter Six ('Cloverleaf Clusters: A Common Macrostructural Organization Across Human Visual and Auditory Cortex'), Alyssa A. Brewer and Brian Barton address a key concept of brain function, namely the organization of sensory cortices into modular structures with specific function or computations. The authors describe cortical field maps as an organizational unit and how multiple cortical field maps give rise to a macrostructural pattern called the cloverleaf cluster. The authors discuss this new organizational pattern in the visual and auditory system and its usefulness for determining cortical structure and function and the changes that occur in the sensory cortex following trauma or disease.

I am grateful to InTech – Open Access Publisher for initiating this book project and for asking me to serve as its editor. Many thanks go to Slobodan Momcilovic at InTech for moving the book project ahead in a timely fashion. Thanks are due to all contributors of this book for taking the time to first write a chapter proposal, compose their chapter and, lastly, make my requested revisions to it. Hopefully, all contributors will continue their sensory system research with many intellectual challenges and exciting new directions. I would like to thank my wife Dr. Vonnie D.C. Shields, Associate Dean and Professor, Towson University, Towson, MD and our son Torben Heinbockel for the time that I was able to spend working on this book project during the past year. Finally, I am grateful to my parents Erich and Renate Heinbockel for their continuous support and interest in my work over many years.

Thomas Heinbockel, Ph.D.
Professor and Director of Graduate Studies
Department of Anatomy
Howard University College of Medicine
Washington, DC, USA

Chapter 1

Introductory Chapter: Organization and Function of Sensory Nervous Systems

Thomas Heinbockel

Additional information is available at the end of the chapter

http://dx.doi.org/10.5772/intechopen.78738

1. Introduction

This chapter introduces the concept of the sensory nervous system and briefly discusses the value of model organisms in enhancing our understanding of the evolution of sensory systems. The world around us continuously stimulates our senses. These stimuli come in different varieties (modalities) such as light, sounds, smells, tastants, and somatic sensation (touch, pain, pressure, vibration, heat, cold). Our corresponding senses communicate the outside world to the inside of our body with the help of specific receptors. These are part of the nervous system and connect the periphery with the brain. The nervous system, in turn, can respond to incoming information by generating adaptive signals and behaviors. It is essential for all organisms to be able to perceive stimuli from the environment and to subsequently process and integrate these stimuli with the help of our sensory systems. Animals including humans have a need for information about the processes that go on inside of our body as well as on the outside to maintain homeostasis and to properly respond to the organism's bodily functions and surrounding environment [1].

All of us are familiar with the well-known senses such as seeing, smelling, tasting, and hearing. In addition, animal species have taken advantage of other environmental stimuli for orientation and survival and, thus, provide us with less-known examples of sensory systems, for example, echolocation in bats, heat sensation in snakes, magnetic compass orientation in migratory birds, or polarized light perception in insects. Consequently, the sensory nervous system can show exquisite differences between the many existing animal species. Nevertheless, researchers have found astounding similarities in sensory processing even among members of distant animal taxa with respect to the structure and function of the sensory pathways.

Several fundamental rules govern how the sensory nervous system processes stimuli in different modalities [2]. In each case, specialized receptor cells transduce the environmental signal into an electrical or a neural signal that is sent to the brain by afferent nerve fibers. Both the

receptor cells themselves as well as the synaptic targets of the receptor cells, neurons in the brain, are capable of encoding specific attributes of the stimulus such as its quality and quantity. In some cases, receptor cells and central neurons can transmit information about the temporal dynamics of the stimulus (intermittency) and its location in space. As far as the transmission of sensory information from one relay station in a sensory pathway to the next is concerned, neighboring groups of neurons in a given relay station maintain the spatial relationship of receptor cells in the peripheral sense organs. This has been demonstrated in our spatial senses such as vision and touch. This topological organization helps the organism to convey spatial information about sensory stimuli [3]. Nevertheless, it would be a falsehood to assume that sensory systems convey a perfect and complete picture of the world around us [4]. Even though receptor cells at first glance appear to function as physical devices, they are meant simply to help us make inferences about the world rather than provide us with correct measurements. Neurons along a sensory pathway encode stimulus information and transform this information based on computational rules inherent in the neurons and their synaptic connectivity [4]. Therefore, the information that reaches the brain is not simply a mirror reflection of the environment; rather, the information is exposed to multiple levels of processing.

2. Divisions of the nervous system

How does the sensory nervous system fit into our understanding of the nervous system? A standard way to distinguish different parts of the nervous system is to refer to the central versus peripheral nervous system [5, 6]. The central nervous system includes the brain and spinal cord with about 86 billion neurons and trillions of glial cells in the brain. The peripheral nervous system consists of the nerves and ganglia outside of the brain and spinal cord, and it can be divided into the somatic and the autonomic nervous system. The somatic nervous system comprises peripheral nerve fibers, namely sensory nerve fibers (afferent fibers) that send sensory information to the central nervous system as well as motor nerve fibers (efferent fibers) that project to skeletal muscles. The somatic nervous system affords us voluntary control over our skeletal muscles [2, 6]. In contrast, the autonomic nervous system controls smooth muscles of the viscera (internal organs) and the digestive tract as well as sweat glands, salivary glands, kidney, bladder, pupil, and heart muscle. As the name implies, it works automatically (autonomously), without a person's conscious effort, that is, we do not have a voluntary control over the autonomic nervous system. Accordingly, it is also called the involuntary or the vegetative nervous system. The autonomic nervous system comes in two opposing parts, sympathetic and parasympathetic. The sympathetic division stimulates bodily processes in response to information about the body and the external environment received by the autonomic nervous system, whereas the parasympathetic division has an antagonistic effect by inhibiting bodily functions.

Principally, the sensory nervous system with its different sensory systems is part of the peripheral nervous system or, better, it starts in the periphery and ends in the central nervous system. As a whole, the sensory nervous system detects and encodes stimuli and then sends signals from receptors, that is, sense organs or simple sensory nerve endings, to the central

nervous system, that is, it transduces environmental signals into electrical signals that are propagated along nerve fibers. In contrast, the motor systems respond to information provided by the sensory systems to generate movements and other forms of behavior. The main function of the sensory nervous system is to inform the central nervous system about stimuli impinging on us from the outside or within us. By doing so, it informs us about any changes in the internal and external environment. The central nervous system integrates the sensory information and communicates the information to target organs in our body. Therefore, a given sensory system comprises receptor cells in sense organs, neurons that project from sense organs to the brain, and specific brain areas that process the afferent information coming from the periphery. For each of the five classic senses (vision, touch, hearing, smell, and taste), a corresponding cortical area exists in the brain [5] referred to as sensory cortex, namely visual cortex, somatosensory cortex, auditory cortex, olfactory cortex, and gustatory cortex. Our brain also houses a vestibular cortex to process information from the vestibular organs, the utricle and saccule with the maculae, and the semicircular ducts with the crista ampullaris.

In addition to the sensory cortices, the brain or, more specifically, the cerebral cortex is involved in the control of voluntary movement, for example, in the frontal lobe [6]. Parts of the brain are responsible for encoding sensory information and controlling motor behavior. These are the primary sensory and motor cortices, and they constitute only about one-fifth of the cerebral cortex [2]. Not all brain areas can be assigned easily to either sensory or motor functions. These areas are involved in processing complex stimuli, forming relations between objects and planning adaptive responses including memory formation. The functions are referred to as cognition and are carried out in the association cortices in the parietal, temporal, and frontal lobes such as the prefrontal cortex, posterior parietal cortex, and inferotemporal cortex [2].

3. Relevance of the sensory nervous system

As pointed out so poignantly by Barth et al. [7], "there is no life without sensors and sensing." The authors emphasize that even in bacteria without a nervous system, sensory performance is in place. Sensing and sensory systems are a characteristic property of living animals and have evolved over millions of years by selective pressures to develop many sense organs for specific tasks with magnificent precision [1]. As a result, animals use a stunning diversity of sensory systems to extract information from their environment [8] and have many sensory abilities not know to humans such as ultraviolet, infrared, ultrasound, electromagnetic reception, and skeletal strain detection [7]. On the one hand, the differences between the sensory systems in terms of complexity are obvious. On the other hand, despite all the differences, there are commonalities that have been discovered in sensory systems and the brains [1]. As indicated by these authors, while some animals such as insects and mollusks may vastly differ from humans, they share a surprising number of basic properties of living organisms. The similarities extend to brain functions such as learning and memory and advanced cognitive abilities which traditionally have been associated with primates rather than snails, bees, or birds.

4. The olfactory system

A prominent example of the commonalities of sensory systems is provided by the olfactory system that has been studied in vertebrates and invertebrates for several decades [9–18]. The similarities start in the periphery with olfactory receptor cells located in the olfactory epithelium in the nose of vertebrates or in the paired antennae of insects. The receptor cells are adapted to detect a vast array of odorants by means of receptor proteins that are positioned in the membranes of the receptor cells. The olfactory receptor cells are associated with various types of sensilla in invertebrates (e.g., insects) [19] or the olfactory epithelium lining a portion of the nasal cavity of vertebrates (e.g., mammals) [20]. Individual receptor cells are specialized to respond to one or a few different odorants by expressing one member of a large gene family of olfactory receptor proteins as shown for rodents [20]. Likewise, Clyne et al. [21] and Vosshall et al. [22] identified a novel family of seven transmembrane-domain proteins, which are encoded by 100–200 genes and are likely to function as *Drosophila melanogaster* olfactory receptors. An individual olfactory receptor cell in the antenna of *D. melanogaster* is thought to express one or a few of the candidate olfactory receptor genes, and, therefore, each olfactory receptor cell is functionally distinct [23]. In insects, an antennal receptor cell in male moths might respond to only one component of several chemicals that make up the sex pheromone released by the conspecific females [24–26]. The olfactory receptor cells send their axon to the first central relay station for olfactory information processing in the brain and form synaptic contacts with central neurons. In vertebrates, this takes place in the olfactory bulb; in insects, it occurs in the antennal lobes of the deutocerebrum [27]. In both, the olfactory bulb and the antennal lobes, olfactory information is processed in brain modules, the olfactory glomeruli. Each glomerulus is a discrete anatomical and functional unit and serves as an anatomical address dedicated to collecting and processing specific molecular features about the olfactory environment, conveyed to it by olfactory receptor cell axons expressing specific olfactory receptor proteins [11, 12, 28–30]. Thus, the glomeruli in the antennal lobes of insects and the olfactory bulbs of vertebrates are organized chemotopically [30–35], analogous to visuotopy, in visual systems, and tonotopy, of auditory systems. In both vertebrates and insects, olfactory information is extensively processed at the level of the glomeruli through feedforward and feedback inhibition and modulation provided by centrifugal neurons. Information is subsequently conveyed to a higher-order olfactory center such as the olfactory cortex in vertebrates or the mushroom bodies and lateral horn in insects [36, 37]. These circuit similarities among distant taxa demonstrate the convergence of basic brain mechanisms in sensory systems.

5. Animal model systems

Which animal models are used to study sensory nervous systems? The question relates to finding the best animal model to study a particular sensory system. Most biological and biomedical research focuses on a small number of animal models, the Core Four, mice, zebrafish, fly (*Drosophila*), and worm (*Caenorhabditis*) because of their genetic tractability

[38]. Many other animal species are being used to determine the structure and function of a specific sensory system. This is in part mandated by the fact that not all animal species are equipped with the same senses. And even if they possess a specific sensory system, it might be rudimentary in its anatomy or simply does not perform a function relevant to the species' survival. As the champion for Neuroethology, Hoy [38] points out that there is a need for nongenetic discovery science, like neuroethology, that will mine the biodiversity of neural systems and behavior mechanisms so that the *Core* Four model species will not become the *Final* Four.

As stated by August Krogh many years ago [39] and quoted by others [38, 40], "For a large number of problems there will be some animal of choice or a few such animals on which it can be most conveniently studied." Along the same lines, Bernard [41] stated even earlier (1865) that "In scientific investigation, the smallest processes are of the utmost importance. The happy choice of an animal, an instrument built in a certain way, the use of a reagent instead of another, are often enough to solve the highest general questions (translated from French)." In that sense, the diversity of species finds its way back into neurobiological research and our understanding of the sensory nervous system [42–44].

Acknowledgements

This work was supported in part by grants from the National Science Foundation (NSF IOS-1355034) and the Charles and Mary Latham Trust Fund.

Conflict of interest

The author declares that there is no conflict of interests regarding the publication of this chapter.

Author details

Thomas Heinbockel

Address all correspondence to: theinbockel@howard.edu

Department of Anatomy, Howard University College of Medicine, Washington, DC, USA

References

[1] Barth FG, Giampieri-Deutsch P, Klein HD. Sensory Perception – Mind and Matter. New York: Springer Wien; 2012. ISBN: 978-3-211-99750-5

[2] Purves D, Augustine GJ, Fitzpatrick D, Hall WC, LaMantia AS, White LE. Neuroscience 5th ed. Sunderland: Sinauer; 2012. ISBN 978-0-87893-695-3

[3] Amaral DG, Strick PL. The neural basis of cognition. In: Kandel ER, Schwartz JH, Jessell TM, Siegelbaum SA, Hudspeth AJ, editors. Principles of Neural Science. 5th ed. New York: McGraw-Hill; 2013. pp. 333-335. ISBN 978-0-07-139011-8

[4] Gardner EP, Johnson KO. Sensory coding. In: Kandel ER, Schwartz JH, Jessell TM, Siegelbaum SA, Hudspeth AJ, editors. Principles of Neural Science. 5th ed. New York: McGraw-Hill; 2013. pp 445-447. ISBN 978-0-07-139011-8

[5] Kandel ER, Schwartz JH, Jessell TM, Siegelbaum SA, Hudspeth AJ. Principles of Neural Science. 5th ed. New York: McGraw-Hill; 2013. ISBN 978-0-07-139011-8

[6] Bear M, Connors BW, Paradiso MA. Neuroscience – Exploring the Brain. 4th ed. Philadelphia: Wolters Kluwer; 2016. ISBN 978-0-7817-7817-6

[7] Barth FG, Humphrey JAC, Srinivisan MV. Frontiers in Sensing – From Biology to Engineering. New York: Springer Wien; 2012. ISBN 978-3-211-99748-2

[8] Bleckmann H, Klein A, Meyer G. Nature as a model for technical sensors. In: Barth, FG, Humphrey JAC, Srinivisan MV, editors. Frontiers in Sensing – From Biology to Engineering. New York: Springer Wien; 2012. pp 3-18. ISBN 978-3-211-99748-2

[9] Hildebrand JG. Analysis of chemical signals by nervous systems. Proceedings of the National Academy of Sciences USA. Jan 1995;**92**(1):67-74. ISSN 0027-8424

[10] Hildebrand JG. Olfactory control of behavior in moths: Central processing of odor information and the functional significance of olfactory glomeruli. Journal of Comparative Physiology A. Jan 1996;**178**(1):5-19. ISSN 0340-7594

[11] Christensen TA, Heinbockel T, Hildebrand JG. Olfactory information processing in the brain: Encoding chemical and temporal features of odors. Journal of Neurobiology. May 1996;**30**(1):82-91. ISSN 0022-3034

[12] Hildebrand JG, Shepherd G. Mechanisms of olfactory discrimination: converging evidence for common principles across phyla. Annual Review of Neuroscience. Mar 1997; **20**:595-631. ISSN 0147-006X

[13] Hildebrand JG, Christensen TA, Heinbockel T, Roche King J, Mechaber W, Rössler W, Shields VDC. The olfactory neurobiology of host- and mate-attraction in moths. In: Elsner N, Eysel U, editors. From Molecular Neurobiology to Clinical Neuroscience (Proc 1st Göttingen Conference of the German Neuroscience Society 1999 & 27th Göttingen Neurobiology Conference). Vol. I. New York: Georg Thieme Verlag Stuttgart; 1999. pp. 56-67. ISBN 3-13-118411-6

[14] Lei H, Oland LA, Riffell JA, Beyerlein A, Hildebrand JG. Microcircuits for olfactory information processing in the antennal lobe of *Manduca sexta*. In: Shepherd GM, Grillner S, editors. Handbook of Brain Microcircuits. Oxford University Press; 2010. pp. 417-426. ISBN 978-0-19-538988-3

[15] Shepherd GM, Migliore M, Willhite DC. Olfactory bulb. In: Shepherd GM, Grillner S, editors. Handbook of Brain Microcircuits. New York: Oxford University Press; 2010. pp. 251-262. ISBN 978-0-19-538988-3

[16] Shields VDC, Heinbockel T. Neurophysiological recording techniques applied to insect chemosensory systems. In: Garcia M-D, editor. Zoology. Rijeka, Croatia: Intech Open Access Publisher; chapter 7. 2012. pp. 123-162. ISBN 978-953-51-0360-8

[17] Heinbockel T. Electrophysiological recording and imaging of neuronal signals in brain slices. In: Heinbockel T, editor. Neuroscience. Rijeka, Croatia: Intech Open Access Publisher; chapter 2. 2012. pp. 19-48. ISBN 978-953-51-0617-3

[18] Heinbockel T, Shields VDC, Reisenman CE. Glomerular interactions in olfactory processing channels of the antennal lobes. Journal of Comparative Physiology. A. 2013; **199**:929-946. DOI: 10.1007/s00359-013-0842-6. Epub Jul 28, 2013 (peer-reviewed)

[19] Shields VDC, Hildebrand JG. Recent advances in insect olfaction, specifically regarding the morphology and sensory physiology of antennal sensilla of the female sphinx moth *Manduca sexta*. Microscopy Research and Technique, Vol. 55, No. 5, (Dec 2001), pp. 307–329. ISSN 1059-910X

[20] Buck L, Axel R. A novel multigene family may encode odorant receptors: A molecular basis for odor recognition. Cell. Apr 5, 1991;**65**(1):175-187

[21] Clyne PJ, Warr CG, Freeman MR, Lessing D, Kim J, Carlson JR. A novel family of divergent seven-transmembrane proteins: candidate odorant receptors in *Drosophila*. Neuron. Feb 1999;**22**(2):327-338. ISSN 0896-6273

[22] Vosshall LB, Amrein H, Morozov PS, Rzhetsky A, Axel R. A spatial map of olfactory receptor expression in the *Drosophila* antenna. Cell. Mar 1999;**96**(5):725-736. ISSN 0092-8674

[23] Vosshall LB. The molecular logic of olfaction in *Drosophila*. Chemical Senses. Feb 2001; **26**(2):207-213. ISSN 0379-864X

[24] Kaissling K-E. Peripheral mechanisms of pheromone reception in moths. Chemical Senses. Apr 1996;**21**(2):257-268. ISSN 0379-864X

[25] Kaissling K-E, Thorson J. Insect olfactory sensilla: Structural, chemical and electrical components of the functional organization. In: Sattelle DB, Hall LM, Hildebrand JG, editors. Receptors for Neurotransmitters, Hormones and Pheromones in Insects. North-Holland, Amsterdam: Elsevier; 1980. pp. 261-282. ISSN 0444802312

[26] Kaissling K-E, Hildebrand JG, Tumlinson JH. Pheromone receptor cells in the male moth *Manduca sexta*. Archives of Insect Biochemistry and Physiology. Apr 1989;**10**(4):273-279. ISSN 0739-4462

[27] Homberg U, Christensen TA, Hildebrand TA. Structure and function of the deutocerebrum in insects. Annual Review of Entomology. 1989;**34**:477-501. ISSN 0066-4170

[28] Buck LB. Information coding in the vertebrate olfactory system. Annual Review of Neuroscience. Mar 1996;**19**:517-544. ISSN 0147-006X

[29] Buonviso N, Chaput MA. Response similarity of odors in olfactory bulb output cells presumed to be connected to the same glomerulus: Electrophysiological study using simultaneous single-unit recordings. Journal of Neurophysiology. Mar 1990;**63**(3):447-454. ISSN 0022-3077

[30] Mombaerts P. Targeting olfaction. Current Opinion in Neurobiology. Aug 1996;**6**(4):481-486. ISSN 0959-4388

[31] Sharp FR, Kauer JS, Shepherd GM. Local sites of activity-related glucose metabolism in rat olfactory bulb during olfactory stimulation. Brain Research. Nov 1975;**98**(3):596-600. ISSN 0006-8993

[32] Rodrigues V, Buchner E. [3H]2-deoxyglucose mapping of odor-induced neuronal activity in the antennal lobes of *Drosophila melanogaster*. Brain Research. 1984;**324**:374-378. ISSN 0006-8993

[33] Hansson BS, Christensen TA, Hildebrand JG. Functionally distinct subdivisons of the macroglomerular complex in the antennal lobe of the male sphinx moth *Manduca sexta*. Journal of Comparative Neurology. Oct 1991;**312**(2):264-278. ISSN 1096-9861

[34] Friedrich RW, Korsching SI. Combinatorial and chemotopic odorant coding in the zebrafish olfactory bulb visualized by optical imaging. Neuron. May 1997;**18**(5):737-752. ISSN 0896-6273

[35] Galizia CG, Sachse S, Rappert A, Menzel R. The glomerular code for odor representation is species specific in the honeybee *Apis mellifera*. Nature Neuroscience. May 1999;**2**(5):473-478. ISSN 1097-6256

[36] Homberg U, Montague RA, Hildebrand JG. Anatomy of antenno-cerebral pathways in the brain of the sphinx moth *Manduca sexta*. Cell and Tissue Research. Nov 1988;**254**(2):225-281. ISSN 0302-766X

[37] Strausfeld NJ, Hansen L, Li Y, Gomez RS, Ito K. Evolution, discovery, and interpretations of arthropod mushroom bodies. Learning & Memory. 1998;**5**(1–2):11-37. DOI: 10.1101/lm.5.1.11

[38] Hoy RR. Current Biology. 2014;**24**(21):R1028-R1029

[39] Krogh A. The progress of physiology. American Journal of Physiology. 1929;**90**:243-251

[40] Krebs HA. The August Krogh principle: "For many problems there is an animal on which it can be most conveniently studied". Journal of Experimental Zoology. 1975;**194**:221-226

[41] Bernard C. Introduction à l'étude de la médecine expérimentale. Paris: J. B. Bailliére et fils; Londres: H. Baillière; Madrid: C. Bailly-Baillière; New-York: Baillière-brothers; Leipzig: E. JungTreuttel, 1865. p. 400; 22 cm. Édition originale, 1er tirage

[42] Shepherd GM, Grillner S. Handbook of Brain Microcircuits. New York: Oxford University Press; 2010. ISBN 978-0-19-538988-3

[43] Keifer J, Summers CH. Putting the "biology" back into "neurobiology": the strength of diversity in animal model systems for neuroscience research. Frontiers in Systems Neuroscience. 2016;**10**:69. DOI: 10.3389/fnsys.2016.00069. PMCID: PMC4992696, PMID: 27597819

[44] Yartsev MM. The emperor's new wardrobe: Rebalancing diversity of animal models in neuroscience research. Science. Oct 27, 2017:**358**(6362):466-469. DOI: 10.1126/science.aan8865

Chapter 2

Long-Distance Modulation of Sensory Encoding via Axonal Neuromodulation

Margaret L. DeMaegd and Wolfgang Stein

Additional information is available at the end of the chapter

http://dx.doi.org/10.5772/intechopen.74647

Abstract

The neuromodulatory system plays a critical role in sensorimotor system function and animal behavior. Its influence on axons, however, remains enigmatic although axons possess receptors for a plethora of modulators, and pathologies of the neuromodulatory system impair neuronal communication. The most dramatic neuromodulatory effect on axons is ectopic spiking, a process common to many systems and neurons during which action potentials are elicited in the axon trunk and travel antidromically towards the site of sensory transduction. We argue that ectopic action potentials modify sensory encoding by invading the primary spike initiation zone in the periphery. This is a particularly intriguing concept, since it allows the modulatory system to alter sensory information processing. We demonstrate that aminergic modulation of a proprioceptive axon that elicits spontaneous ectopic action potentials changes spike frequency, which determines the burst behavior of the proprioceptor. Increasing ectopic spike frequency delayed the peripheral burst, caused reductions in spike number and burst duration, and changes in sensory firing frequency. Computational models show these effects depend on slow ionic conductances to modulate membrane excitability. Thus, axonal neuromodulation provides a means to rapidly influence sensory encoding without directly or locally affecting the sites of stimulus reception and spike initiation.

Keywords: proprioception, neuromodulation, sensory encoding, action potential, axon

1. Introduction

Flow of information in neurons of the sensory nervous system, as in the central nervous system, is usually thought of as unidirectional. The function of sensory neurons is to supply the central nervous system with information from the periphery, and this information is transmitted through action potentials (APs) propagating along the sensory axons. While this

concept was introduced early in the history of neuroscience in Cajal's neuron doctrine, it has been challenged many times. Such challenges include examples from retrograde transport from the synaptic terminals to the soma, which affects slow homeostatic processes [1], to APs that backpropagate from the axon initial segment into the dendritic regions where they modulate postsynaptic signaling and contribute to coincidence detection on fast time scales [2, 3]. Even axons, which are traditionally seen as faithful unidirectional conductors, can propagate APs backwards towards the axon origin [4]. Propagation direction depends on where APs are initiated, which is typically a spike initiation zone (SIZ) at the axon initial segment, near the axon hillock. Here, the excitability of the neuronal membrane is at its highest and integrated synaptic or sensory information has easy access.

The last decades have shown that membrane excitability, including that of the axon, is subject to changes depending on a diverse set of intrinsic and extrinsic conditions. The neuromodulatory system, for example, plays a critical role in sensory processing as a major contributor to the plasticity maintaining sensorimotor system function and animal behavior [5]. It typically targets local signal encoding, transmission, and AP initiation by modulating ion channel conductances though metabotropic (typically G-protein coupled) receptors. Modulator influences on long distance communication, however, remain enigmatic even though axons possess receptors for a plethora of modulators [4], and pathologies of the neuromodulatory system impair neuronal communication. Recent evidence suggests that neuromodulator-induced changes in axon membrane excitability facilitate AP propagation dynamics [6–8], and may serve to adapt sensory functions to different behavioral conditions.

The most dramatic change in axonal excitability is ectopic AP generation, a process common to many systems and neurons [4, 9–13]. In this case, axon trunk excitability increases to superthreshold levels, and APs are generated spatially distant from the primary SIZ. Since the axon membrane surrounding the AP initiation site is not refractory, APs propagate in both directions, orthodromically towards the axon terminal and antidromically towards the dendritic sites of signal integration. Excitability changes leading to ectopic spiking can be caused by various influences, including slow changes in local or global neuromodulators, external conditions such as temperature, or in different hormonal or pathological states. On faster time scales, antidromic APs can be elicited by axo-axonic synapses, such as those present in hippocampus [14], cortex [15], and most sensory neurons [16–18]. Furthermore, external axon stimulation is a common technique used by physicians to test reflex function and treat chronic neuropathic pain [19]. Little is known about the origin, control and functional effects of these additional APs. While postsynaptic effects of ectopic APs that propagate orthodromically have been shown, the effects of antidromic APs on information processing are mostly unknown [18].

In pseudounipolar neurons of the sensory system, such as pain fibers, proprioceptors, and somatosensory neurons, ectopic APs traveling towards the periphery may more easily invade the primary SIZ and the sensory dendrites. In these neurons, there is no soma between the axon and sensory dendrites, which is why in this case the latter are often referred to as receptive endings instead. Without a soma between the axon and the receptive endings, these neurons have fewer impedance changes [20] to stop antidromic AP propagation from reaching

the periphery. Despite ectopic APs typically having lower frequencies, AP collisions [21] and failures due to refractory membrane block [22] must be rare whenever the sensory neuron's primary SIZ is silent, giving ectopic APs ample opportunity to invade the receptive endings in the periphery.

We argue, using a 'simple' proprioceptor and computational modeling, that antidromic traveling ectopic APs modify sensory encoding by invading the primary SIZ in the periphery and modulating membrane excitability. This is a particularly intriguing concept, since the frequency of antidromic APs can be determined through external stimulation, or through neuromodulatory or synaptic actions on the axon trunk. These actions may allow humoral and neural influences to alter sensory information as it travels towards the central nervous system. To test our hypothesis, we utilized the experimentally advantageous anterior gastric receptor (AGR, [23, 24]). AGR is a single-cell muscle tendon organ in the crustacean stomatogastric ganglion [25] – a well-characterized system for the investigation of cellular and circuit neuromodulation [26]. AGR generates ectopic APs in its several centimeter-long axon trunk, spatially distant from the primary SIZ in the periphery [27]. To test whether changes in AGR's ectopic AP frequency determine peripheral information encoding, we elicited different ectopic frequencies using extracellular axon stimulations while we chemically elicited peripheral AP bursts.

Our data show that ectopic APs propagated without failures towards the periphery, where they invaded the primary SIZ and caused three distinct frequency-dependent actions on sensory encoding: (1) an increase burst onset latency, (2) a reduction AP number, and (3) a reduction the burst duration. These effects increased when ectopic APs continued throughout the encoding of sensory information and caused significant frequency-dependent decreases in the average and maximum frequency. Using computational models of generic neurons, we show that slow ionic conductances facilitate antidromic AP modification of sensory encoding. Slow ionic conductances, such as those elicited by persistent Sodium, hyperpolarization-activated (HCN), and slow Potassium channels are ubiquitous in neurons and axons [28–30], indicating that sensory modification by antidromic APs may be inherent to many other systems. We conclude that axonal neuromodulation provides a means to rapidly influence sensory encoding via ectopic APs that invade the periphery, without directly or locally affecting the sites of stimulus reception and AP initiation.

2. Materials and methods

2.1. Dissection

The stomatogastric nervous system (STNS) of adult male crabs (*Cancer borealis*) was isolated following standard procedures [31], and superfused with physiological saline (10–12°C, [32]) KCl was increased 10–20 fold for high Potassium (K^+) saline. To maintain osmolarity, NaCl was reduced appropriately. K^+ saline depolarizes the membrane, and its effective concentration was determined for each preparation. Octopamine hydrochloride (OA, Sigma Aldrich)

was diluted in saline to the desired concentration (0.1–100 μM). OA was cooled to 10–12°C and manually applied to the isolated STG in a petroleum jelly well. As a control, saline was applied at the same temperature 3 min before each neuromodulator application. Measurements were taken in steady-state (2–5 min after OA wash in). To prevent cumulative effects due to repeated modulator application, wash-outs were 5 min long with continuous superfusion of cooled saline. Peripheral bursts were elicited with a 0.1–0.5 s puff of K^+ saline to a continuously saline-superfused well around the *pdgn*. To prevent accumulation of modulator effects 60–90 s washout occurred between puffs.

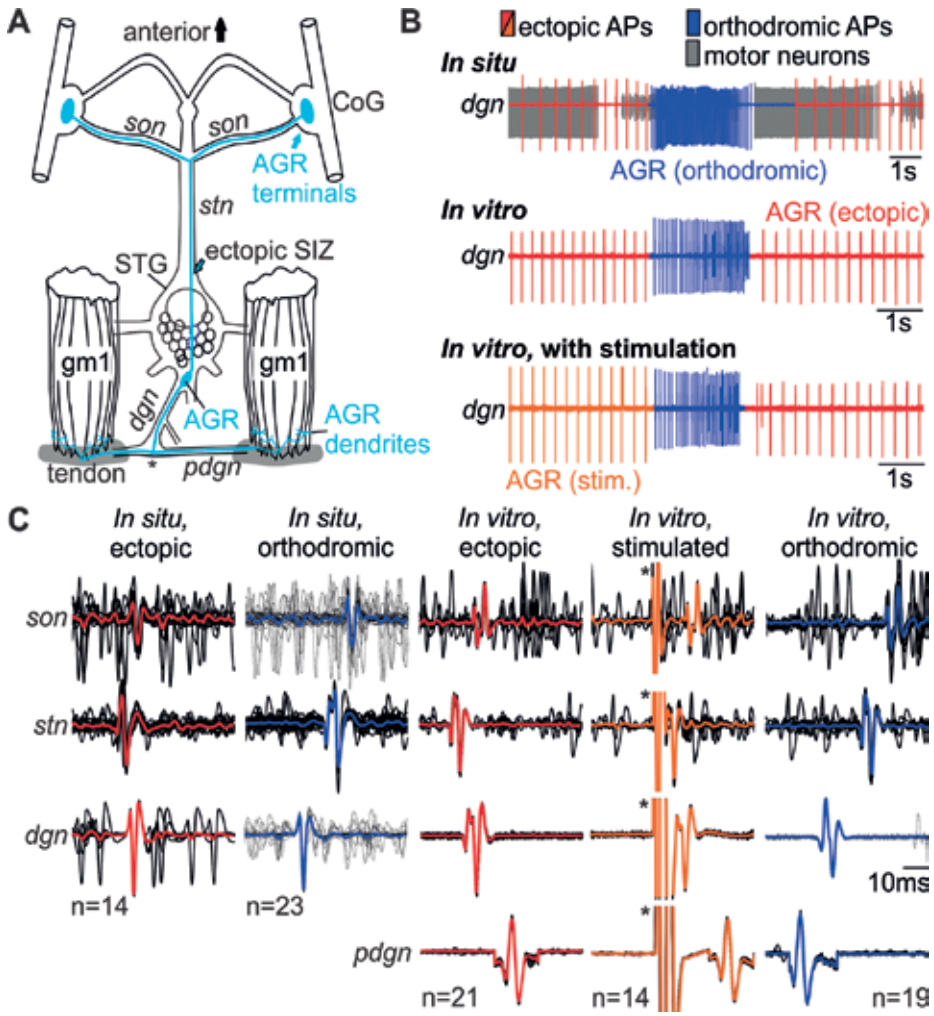

Figure 1. A. Schematic representation of STNS and AGR. AGR projects an axon to the gm1 muscles in the periphery, and to the premotor CoGs. The AGR ectopic SIZ is located in the *stn,* near the anterior end of the STG. The primary SIZ is near the gm1 muscles (*). B. AGR produces spontaneous ectopic APs *in situ* and *in vitro* (original recordings). Ectopic APs can be elicited with stimulation of AGR's central axon. APs have been color coded for clarity. C. Overlay ('multisweep') and average (colored) of nerve recordings containing the AGR axon used to track AP propagation from posterior (*dgn*) to anterior (*son*), in different conditions. Stimulation artifacts are labeled with (*).

2.2. Extracellular recordings, stimulations, and optical imaging

Standard techniques were used for extracellular recordings and data analysis [33]. The activity of AGR was monitored on multiple extracellular recordings simultaneously, namely on the stomatogastric nerve (*stn*), the dorsal gastric nerve (*dgn*), and the supraoesophageal nerve (*son*), see **Figure 1A**. To identify AGR, we used APs recorded on the *dgn* or *stn* and performed a time-correlation analysis (multisweep). Ectopic APs (1–10 Hz) were elicited with extracellular nerve stimulation [34] of the AGR axon trunk. The lipophilic voltage-sensitive dye Di-4-ANNEPDHQ [35] was used according to published protocols [36]. To facilitate access of the dye to the axons, the connective tissue sheath of the *pdgn* was manually removed. We used event-triggered averaging of APs to improve the signal-to-noise ratio of the optically recorded data (similar to [37]).

2.3. Data analysis, statistics and figure preparation

Data were analyzed using scripts for Spike2 (available at www.neurobiologie.de/spike2). To compute the EC_{50} of OA, instantaneous firing frequency. was normalized to control frequencies, then to the minimum and maximum frequency within each animal. Average responses to OA ± SD are plotted. To compare changes in burst parameters, results were normalized to the control bursts measured before stimulation and plotted as a function of the normalized difference. Mean normalized differences ± SD are plotted. Pearson correlation analyses were used to assess changes in AGR peripheral burst activities in response to forcing different AGR ectopic AP frequencies. Tests were computed in SigmaPlot (version 12 for Windows, Systat Software GmbH, Erkrath, Germany). Final figures were prepared with CorelDRAW Graphics Suite (version X7, Corel Corporation, Ottawa, ON, Canada).

2.4. Modeling

Computation models were designed using NEURON [38] using standard Hodgkin-Huxley ionic conductances in a cable model of an unmyelinated axon. The model length was set to 1.213 cm with 10 μm compartments and the axon diameter was 0.6 μm. Axial resistivity (28 Ω*cm) and membrane capacitance (1 $\mu F/cm^2$) were constant through the length of the neuron. The neuron had three sections, the axon (1012 μm), the peripheral SIZ (100 μm), and the dendritic terminal (101 μm). Active channel properties were conserved in the axon and peripheral SIZ, except only the peripheral SIZ had I_h or I_{Ks} (**Table 1**).

Ionic current	$\bar{g}_{max}$ (mS/cm^2)	Gating	Activation function	Tau (ms)	E_x (mV)
I_{Na}	0.4	m^3	1/(1 + exp.(−0.4(36 + v))	0.19exp(−0.05(v + 40)	50
		h	1/(1 + exp.(39.5 + v))	40exp(−0.025(v − 55))	
I_{Kd}	1.09	n^4	1/(1 + exp.(0.125(−33 − v)))	55exp(−0.015(v −28))	−77
I_{Ks}	0.1	n^4	1/(1 + exp.(0.125(−33 − v)))	4000/cosh((v + 73)/12)	−90
I_l	0.0016				−60
I_h	0.103	h	1/(1 + exp.((v + 70)/7)	300 or 3000	−10

Table 1. Parameters of ionic currents used in computational models.

3. Results

3.1. Antidromic ectopic action potentials invade the site of sensory encoding

The effects of antidromic APs on sensory encoding can be challenging to delineate. We use the anterior gastric receptor neuron (AGR) of the crab, *C. borealis* because it is experimentally advantageous. AGR is a bipolar single-cell muscle tendon organ that projects two axons from its cell body - one towards the peripheral gastric mill 1 (gm1) muscles, and one to the commissural ganglia (CoGs, **Figure 1A**), where it innervates premotor control neurons [39]. The CoGs are analogous to the vertebrate brainstem, and contain a set of descending projection neurons that modulate downstream motor circuits in the stomatogastric ganglion (STG) and promote appropriate behavioral responses. The primary function of AGR is to encode information about changes in gm1 muscle tension and to convey this to the CoG networks. Sensory information is encoded as bursts of APs with maximum frequencies between 20 and 30 Hz at the primary SIZ in close proximity to the peripheral gm1 muscles (**Figure 1B**). APs generated at this site are propagated unidirectionally towards the integrating centers in the upstream CoGs. **Figure 1C** shows an *in-situ* recording of AGR, using multiple extracellular recordings at different sites along its axons. AGR burst activity was elicited by isometric gm1 muscle contractions that increased muscle tension (similar to [23]). All APs in this burst were recorded first in the dorsal gastric nerve (*dgn*), through which AGR innervates the gm1 muscles. They then passed through the soma before reaching the stomatogastric (*stn*) and superior esophageal (*son*) nerves, through which the AGR axon innervates the CoGs. The soma lies posterior to the STG, and functionally and physically connects the two AGR axons. Unlike most neuronal somata, AGR's cell body possesses active properties and thus act as a continuation of the axon [40].

In addition to the peripheral SIZ, AGR generates APs at a second SIZ in its axon trunk whenever no sensory bursts are produced (**Figure 1B**, [23]). These APs first occurred in the *stn*, before appearing on the *dgn* and *son* (**Figure 1C**). These spontaneous APs thus traveled bidirectionally from the axon trunk towards the CoGs and the periphery, and were not elicited at the primary SIZ. Previous studies have estimated that these ectopic APs originate approximately 225 microns anterior to the STG neuropil, near the origin of the *stn* [32]. Thus, they were initiated spatially distant from the primary SIZ, at an approximate distance of 1 cm. AGR maintains its firing properties and SIZs even when isolated. In these *in vitro* conditions, the gm1 muscles are dissected away from the peripheral dendrites, removing the source of sensory stimuli, and only STG, CoGs, and the connecting nerves containing AGR's axons were retained (see **Figure 1A**). Sensory-like bursts can be generated when short puffs of K^+ physiological saline are applied locally to the peripheral dendrites. In the experiment shown in **Figure 1B**, a petroleum jelly well was placed around the *pdgn* containing the sensory dendrites of AGR (**Figure 1A**) and a puff of K^+ saline was applied (see Materials and Methods). The elicited APs first appeared on the *pdgn*, demonstrating that they were initiated at the peripheral application site (**Figure 1C**). In contrast, spontaneous APs that occurred in between peripheral bursts, were first recorded on the *stn* and simultaneously on the *dgn*. They continued bidirectionally towards the CoGs, appearing on the *son*, and towards the peripheral AGR dendrites, appearing on the

pdgn. This is consistent with previous results [27, 32] and the intact animal [23], and suggests that these *in vitro* spontaneous tonic APs are generated ectopically in AGR's axon trunk. We used our ability to generate uniform sensory bursts at controlled times and track AP direction to investigate the modulatory effects of antidromic APs on sensory encoding. To control the frequency of ectopic APs in the axon trunk, we elicited APs through extracellular stimulation of the AGR axon in the STG well (**Figure 1B**, [34]). Forced ectopic APs followed the same pattern of propagation as spontaneously generated ectopic APs: bidirectionally from the STG well to the *stn* and *dgn* (**Figure 1C**).

To confirm that ectopic APs traveled without failures throughout the entire length of the AGR axon, we first recorded spontaneous and stimulated APs on the *son*, near the terminal ends of AGR in the CoGs, as well as from the *pdgn*, i.e. the *dgn* branch that responded to K^+ stimulation and contained the primary SIZ. In all recordings (N = 14), ectopic APs reached the *son* and *pdgn* without ever failing.

This provided good evidence that ectopic APs propagated throughout the entire length of AGR. However, extracellular recordings have limited spatial resolution due to the space required to place electrodes. Therefore, it was difficult to determine if ectopic APs truly invaded the axon terminals in the CoG and the sensory encoding region, respectively. While we did not expect AGR's APs to fail when they enter the CoG axon terminals, we decided to intracellularly record from a known postsynaptic target neuron of AGR, the commissural projection neuron 2 (CPN2). **Figure 2A** shows intracellular somatic recordings of CPN2 and AGR. AGR was tonically active and APs were generated at the ectopic AP SIZ. Each AGR AP was followed by a time-locked EPSP in CPN2 (**Figure 2B**), demonstrating that ectopic APs propagated all the way to the axon terminals and elicited postsynaptic responses.

In the periphery, for ectopic APs to modulate sensory encoding, they must affect the primary SIZ. AGR encodes sensory stimuli pertaining to changes in muscle tension, and there are no postsynaptic structures to measure invading antidromic APs. In contrast to the output terminals in the CoGs, the AGR axon splits into several collaterals, with several branches innervating each of the two bilaterally symmetric gm1 muscles (**Figure 1A**). Axonal branching poses a problem for APs if they propagate from a single axon trunk towards a branch point, since the branching increases membrane impedance [20], and may decrease currents promoting AP propagation. This can lead to propagation failures, AP reflections, or both. Sensory APs from the AGR periphery propagate orthodromically from the branches into the main axon trunk, and are thus unlikely to be affected at these branch points. Antidromic APs, however, enter these branches coming from the main axon trunk, and may thus encounter non-permissive conditions. To test whether APs indeed invaded the primary SIZ without failure, we used the voltage sensitive dye, Di-4-ANNEPDHQ to record and identify the AGR axon in the periphery (see Materials and Methods). This dye has two major advantages: it changes fluorescence with membrane potential with high temporal and spatial acuity, which overcomes the limited spatial resolution of the extracellular recordings, and it selectively stains neuronal membranes, making it possible to visually identify and separate individual axons in a nerve bundle [32]. We applied the dye to the *pdgn* well used to isolate and activate the primary SIZ with K^+ saline. This locally stained all axon membranes in the *pdgn*. Besides AGR, the *dgn* contains the axons

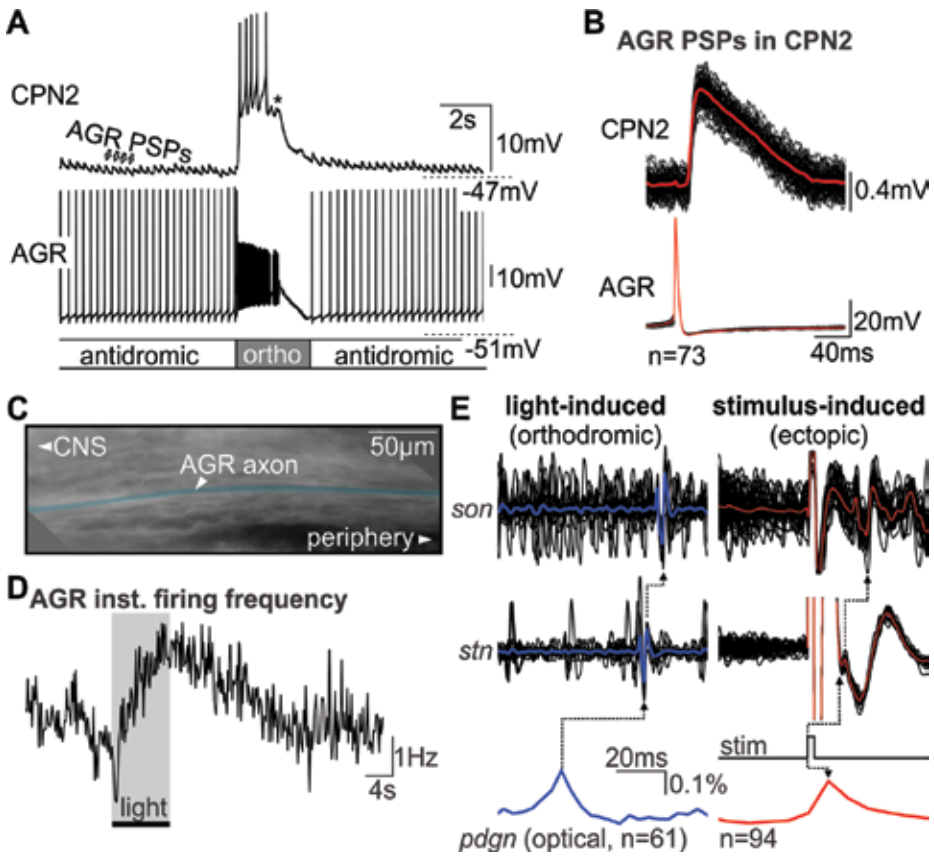

Figure 2. A. Intracellular recordings of AGR and its postsynaptic partner, CoG projection neuron CPN2. EPSPs in CPN2 were time locked to APs in AGR during spontaneous ectopic AP activity, while strong AGR firing elicited a burst of APs (*). B. Multisweep and average of EPSPs in CPN2, triggered by APs in AGR. C. High resolution photo of *pdgn* with AGR's peripheral axon (blue). D. AGR's firing frequency increases when the peripheral (primary) SIZ is illuminated with fluorescent excitation light. E. Optical recordings of primary SIZ. Left: light-induced APs traveled orthodromically towards the CoGs. Right: stimulus evoked ectopic APs traveled antidromically towards the periphery and invaded the primary SIZ.

of several STG motor neurons [41]. We identified the AGR axon by recording the optical signals of all stained axons, and aligning them to APs on the electrical recordings. Only optical signals from the AGR axon were consistently timed to extracellularly recorded AGR activity. We first used spontaneously generated APs to identify the AGR axon in the *dgn*, and then visually tracked the identified axon towards the periphery using the membrane staining. Lipophilic voltage-sensitive dyes such as the one we used here have excitatory side-effects with high-intensity fluorescence illumination [32, 42, 43]. We used this fact to our advantage: the excitation light was focused on a small area the nerve (225 µm, [32]). We found that when illuminated, APs originated in the periphery, i.e. they first appeared on the electrical recording of the *dgn*, and then propagated to the *stn* and *son*. As we moved illumination along the axon, AP frequencies varied substantially. SIZs are defined by an increased propensity to generate APs. Therefore, we determined that the region which generated the highest AP frequency

would be the approximate location of the primary SIZ. **Figure 2C** shows the location on AGR that resulted in the highest firing frequency with illumination in **Figure 2D**. When we optically tracked APs initiated there, we found that they started at the site of illumination, and propagated orthodromically along the AGR axon (**Figure 2E**).

To determine if ectopic APs could penetrate this peripheral area, we first forced ectopic APs by extracellular stimulation of the AGR axon in the STG (see **Figure 1C**) and optically recorded the primary SIZ. Because illumination elicited orthodromic APs, there was a potential for collisions between orthodromic APs and antidromic ectopic APs [21]. To ensure that ectopic APs would not fail to be recorded in the periphery due to collisions, we forced ectopic APs at a higher frequency than the spontaneous firing frequency (1–2 Hz higher than the peripheral frequency). We found that all stimulated APs elicited an optical signal in the periphery time-locked to the stimulus (**Figure 2E**, right). Thus, ectopic APs invaded AGR's stimulus encoding regions. Taken together, we find that AGR has two SIZs, one that spontaneously generates ectopic APs in the axon trunk, and one that generates APs in response to sensory stimuli. While APs encoding sensory stimuli travel unidirectionally in orthodromic direction, ectopic APs travel bidirectionally. Antidromic ectopic APs invade the primary SIZ of AGR.

3.2. Axonal amine modulation increases ectopic action potential frequency

Since AGR's ectopic APs invade the periphery, we hypothesized that these APs modulate sensory encoding occurring there. In the simplest case, ectopic APs will penetrate the sensory SIZ at a constant frequency, leading to a static, continuous effect on sensory encoding. However, AGR's spontaneous ectopic firing frequency is variable. *In vivo*, it varies between 0.7–9.4 Hz (3.66 ± 2.2 Hz, N = 17) between animals, but it can also change quickly within a given animal. Our *in vitro* recordings revealed an average ectopic firing frequency consistent with the *in vivo* data (3.36 ± 0.64 Hz, N = 14). However, the range of frequency changes *in vitro* is smaller in comparison to the *in vivo* range (2.31–4.74 Hz). The STG is subject to heavy neuromodulation from hormones in the blood stream and from peptide and amine modulators released from descending modulatory projection neurons [44–46]. *In vitro*, modulation is reduced, potentially leading to a much reduced variability in activity in comparison to *in vivo* [47]. The reduced modulation may account for the smaller range of AGR frequencies when compared to intact animals.

We have previously shown that the axon of AGR passes through the heavily modulated area in the STG as it projects from the periphery to the CoGs, and possesses receptors for the biogenic amine Octopamine (OA). OA is the invertebrate analog of norepinephrine and present in both the STG and *stn* [48]. We hypothesized that OA would affect the spontaneously generated ectopic APs, and increase their frequency. To test this, we locally applied OA at different concentrations to the recording well containing AGR's ectopic SIZ. We identified the recording well nearest to the ectopic SIZ as shown previously, using a multisweep of several extracellular recording wells. AGR firing frequencies were measured in a steady state for all concentrations of OA. We followed each measurement by washing out OA through superfusion of physiological saline until the ectopic AP firing frequency returned to baseline

frequency. First, we found that the ectopic firing frequency of AGR increased with the application of OA (**Figure 3A**), and it did so in a concentration dependent manner with an EC_{50} of 4.13 µM (**Figure 3B**, sigmoidal fit, R^2 = 0.988, SE of estimate 0.053, $p < 0.001$). The average maximum frequency elicited by OA application ranged from 3.35 ± 1.054 Hz at 0.1 µM OA to 5.09 ± 1.34 Hz at 100 µM OA (N = 6), which corresponded to an average increase of 64.7 ± 47.8% at 100 µM OA. We further found that the latency between OA application and the half-maximum frequency diminished with increasing OA concentration, with an EC_{50} value of 1.00 µM (four parameter logistic curve fit, R^2 0.994, SE of estimate 0.026, $p < 0.001$, **Figure 3B**, N = 6). Finally, the location of the ectopic SIZ remained unchanged and APs did not dislocate at any OA concentration, suggesting that OA exerted it actions directly at the axonal ectopic SIZ (**Figure 3C**). This demonstrates that there is OA concentration dependent ectopic firing frequency modulation in the AGR axon, enabling various frequencies at which ectopic APs will penetrate the periphery.

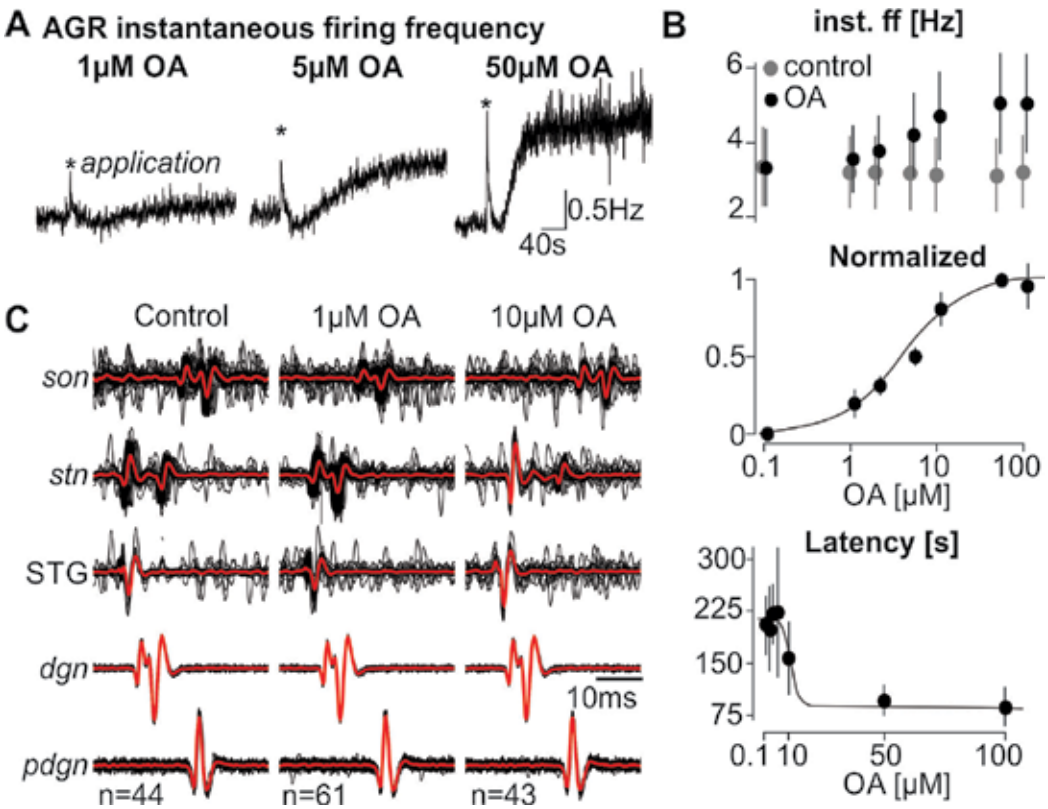

Figure 3. A. AGR firing frequency increases in a concentration dependent manner when OA is applied to the ectopic SIZ. Original recording of an individual animal at three concentrations. B. Dose response curves of AGR instantaneous firing frequency (top: raw; middle: normalized) and response latency (raw) after OA application. C. Multisweeps and averages of nerve recordings that contain the AGR axon to track AP propagation and the location of the ectopic SIZ at different concentrations of OA. OA did not displace the ectopic SIZ.

3.3. Antidromic action potentials have frequency-dependent effects on sensory encoding

Since AGR's ectopic APs invade the periphery at different frequencies, we hypothesized that there is frequency-dependent modulation of sensory encoding occurring there. To test this, we extracellularly forced ectopic APs to a set of fixed firing frequencies (1–10 Hz) and measured the effect on various parameters of stimulus encoding. Ectopic APs were continuously elicited (at least 20 APs at each ectopic frequency) before a local puff K^+ saline was applied to elicit a peripheral burst (**Figure 1B**). Ectopic AP stimulation continued until the first AP in the burst, mimicking the behavior of the spontaneous and modulated ectopic APs in AGR (**Figure 1B**). We then compared changes in the peripheral bursts in control (no ectopic stimulation) to experimental bursts with stimulated ectopic APs preceding the burst. Sensory stimuli can be encoded in the number of APs, the frequency, and the precise timing of APs. We thus measured the change in number of APs per burst, the average and maximum AP frequencies, the durations of peripheral bursts, and their onset latencies (the time between the K^+ saline puff and the first AP of the peripheral burst).

We found that invading ectopic APs had significant influences on several aspects of stimulus encoding. **Figure 4** shows a comparison of a control burst to a burst with forced ectopic frequency of 6 Hz. Burst delay, burst duration and the number of APs in burst were clearly diminished when ectopic APs are present. The smaller number of burst APs was not due to AP collisions, since we (1) were able to account for all ectopic APs in the periphery, and (2) AP collisions could be identified by missing APs on the multisweep recordings. Since ectopic AP stimulation stopped when the first burst spike was detected, we found collisions to be rare (less than 2%). In general, increasing ectopic AP frequencies caused stronger effects on the sensory burst. For example, burst onset latency significantly increased with ectopic AP frequency ($p = 0.01$, Pearson correlation coefficient $R^2 = 0.532$, **Figure 4**Aii), indicating that membrane excitability at the beginning of the burst decreased with higher ectopic AP frequencies. There was also a significant negative correlation between ectopic AP frequency and the number of APs in a burst ($p = 0.001$, Pearson correlation coefficient $R^2 = 0.729$; **Figure 4**Aiii). This resulted in a nearly 30% decrease in the number of APs in a burst at 10 Hz ectopic frequency. Concurrently, burst duration decreased significantly with ectopic AP frequency ($p < 0.001$, Pearson correlation coefficient $R^2 = 0.750$; **Figure 4**Aiv), reaching a nearly 30% decrease at 10 Hz. Neither average nor maximal burst frequency changed significantly with ectopic AP frequency ($R^2 = 0.122$ and 0.0696 respectively, **Figure 4**Av, vi), although both tended to be lower at higher ectopic AP frequencies.

Ectopic APs occur spontaneously and in response to modulator actions at the ectopic SIZ in AGR. However, ectopic APs can also be elicited by synaptic actions at axo-axonic synapses such that the ectopic firing frequency is determined by the occurrence of synaptic potentials in the axon [10, 11, 18]. In this case, ectopic firing would not cease when the sensory burst is elicited. While this is not the case for AGR, the effects of continuous ectopic spiking were tested by continuing the forced ectopic APs throughout the sensory burst. **Figure 4B** shows an example recording for continued ectopic spiking at 6 Hz, in comparison to a control burst without forced ectopic APs. As a consequence of the continued ectopic firing during the sensory burst, AP collisions were more prevalent, although still rare. We estimate less than

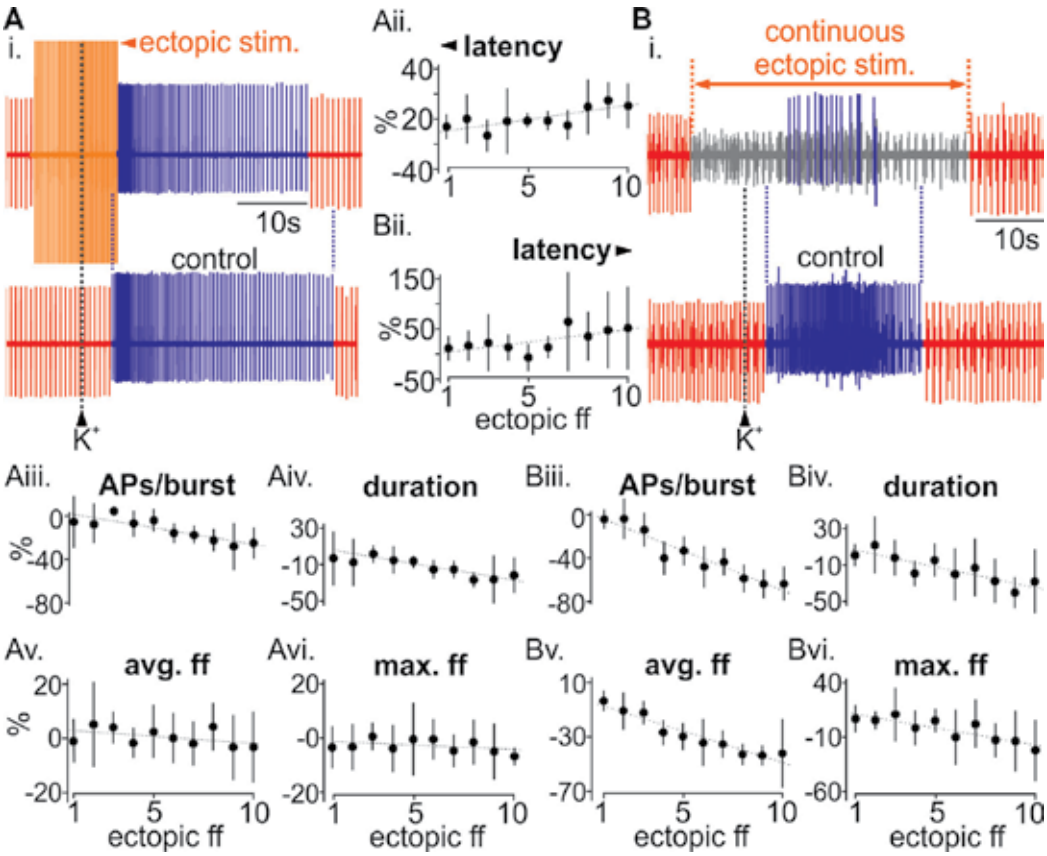

Figure 4. A. Original recordings of AGR ectopic and burst AP activities. i: Control sensory burst (bottom), elicited with high potassium (K^+) in the periphery. Top: With forced ectopic APs that ended at the beginning of the sensory burst. ii: Corresponding changes in latency of elicited sensory bursts at different ectopic AP frequencies (mean ± SD). iii: Number of spikes per burst. iv: Burst duration. v: Average intraburst frequency. vi: Maximum intraburst frequency. B. i: Control sensory burst and burst with ectopic APs that continued throughout. ii–vi: Like in A.

5% of all ectopic APs collided on their way to the periphery. This low number is mostly due to the small distance between ectopic and primary SIZs (about 1 cm), and that propagating APs 'occupy' the axon only for a short amount of time (around 10 ms given the propagation speed of AGR's APs of around 1 m/s). Consequently, even at ectopic frequencies of 10 Hz (interspike intervals of 100 ms), axons were non-refractory for 90% of the time.

Like in the previous experiments, the effects of ectopic spiking on the sensory burst were immediately obvious. In this case, they were more pronounced: burst latency increased significantly with ectopic AP frequency ($p = 0.03$, Pearson correlation coefficient $R^2 = 0.4643$, **Figure 4**Bii), further supporting the notion that membrane excitability at the burst start is lowered when ectopic APs enter the primary SIZ. Burst duration and the number of APs in a burst significantly decreased with ectopic AP frequency (AP number: $p < 0.001$, Pearson correlation coefficient $R^2 = 0.9152$; duration: $p = 0.001$, Pearson correlation coefficient $R^2 = 0.7512$, **Figure 4**Biii, iv), resulting in a greater than 40% reduction for both measurements

at 10 Hz ectopic frequency. In contrast to the previous experiments, average and maximal burst frequency now changed significantly with ectopic AP frequency ($R^2 = 0.9192$ and 0.7525 respectively, $p < 0.001$ and $p = 0.001$, Pearson correlation, **Figure 4**Bv, vi), following the same trend as already seen when ectopic APs did not penetrate the burst.

3.4. Modulation of sensory encoding requires slow ionic conductances in the periphery

Taken together, our data indicate that ectopic APs invade the periphery where they affect sensory bursts in a frequency-dependent manner. This leads to the question; does this axon or its SIZ possesses distinct properties that facilitate the actions of invading ectopic APs, and if so, which properties may these be? To address this question, we created a computational model axon using NEURON [38]. The details of the model are given in the Materials and Methods. Briefly, the model was a linear axon trunk primary SIZ, and a single sensory dendrite. The axon and SIZ possessed active properties and were able to generate APs. The dendritic compartments were passive, i.e. did not possess any voltage-gated ion channels. Ectopic APs were elicited with pulsed current injections (40 nA, 1 ms) at different frequencies into the axon trunk. Ectopic APs propagated from the axon trunk towards the primary SIZ. Sensory bursts were elicited with ramp-and-hold current stimuli into the peripheral dendrites (**Figure 5A**). This assembly allowed us to reproduce ectopic APs that either penetrated the sensory burst (like in the case of strong synaptic inputs via axo-axonal synapses) or stopped upon burst start (like for spontaneous and modulated ectopic APs).

The simplest axonal configuration is probably the one described by Hodgkin and Huxley (HH) in their groundbreaking work on the squid giant axon [49]. HH axons are limited in that they only possess voltage-gated Sodium and Potassium currents in addition to the passive membrane properties. Thus, they may not reflect more complex propagation dynamics and AP modulation reported more recently for a variety of axons [4]. Nevertheless, HH axons explain the properties of AP initiation and propagation observed in many axons. To test which neuronal properties would facilitate the effects ectopic APs have on sensory bursts, we thus first started out with a HH axon that approximated biological firing frequencies. We implemented gate kinetics according to previously published axon models [6], and adjusted them to produce robust firing. We elicited sensory bursts of 3 s duration and approximately 30 Hz frequency. **Figure 5A** shows an example of these bursts following a 6 Hz ectopic stimulation sequence at its arrival at the peripheral SIZ. The corresponding sensory burst and a control burst without ectopic APs are shown as well. The sensory burst was unaffected by the presence of the ectopic APs. To exclude that this was due to the specific ectopic AP frequency used, we varied frequency from 1 to 10 Hz. We found no obvious influences on any burst parameters (**Figure 5C, D, E**, circles), with the exception of a small, but consistent frequency-dependent increase of burst latency with higher ectopic AP frequency (**Figure 5C**, bottom).

Which conductances could enable ectopic APs to affect sensory encoding then? In addition to the standard HH properties, AGR possesses several ionic conductances that may affect sensory encoding [40]. In specific, a slow hyperpolarization-activated cation current (I_h) seems to affect AP frequency in the sensory burst, and a slow Calcium-dependent Potassium current (I_{Ks}) seems to affect burst timing and structure such that firing frequencies during the burst

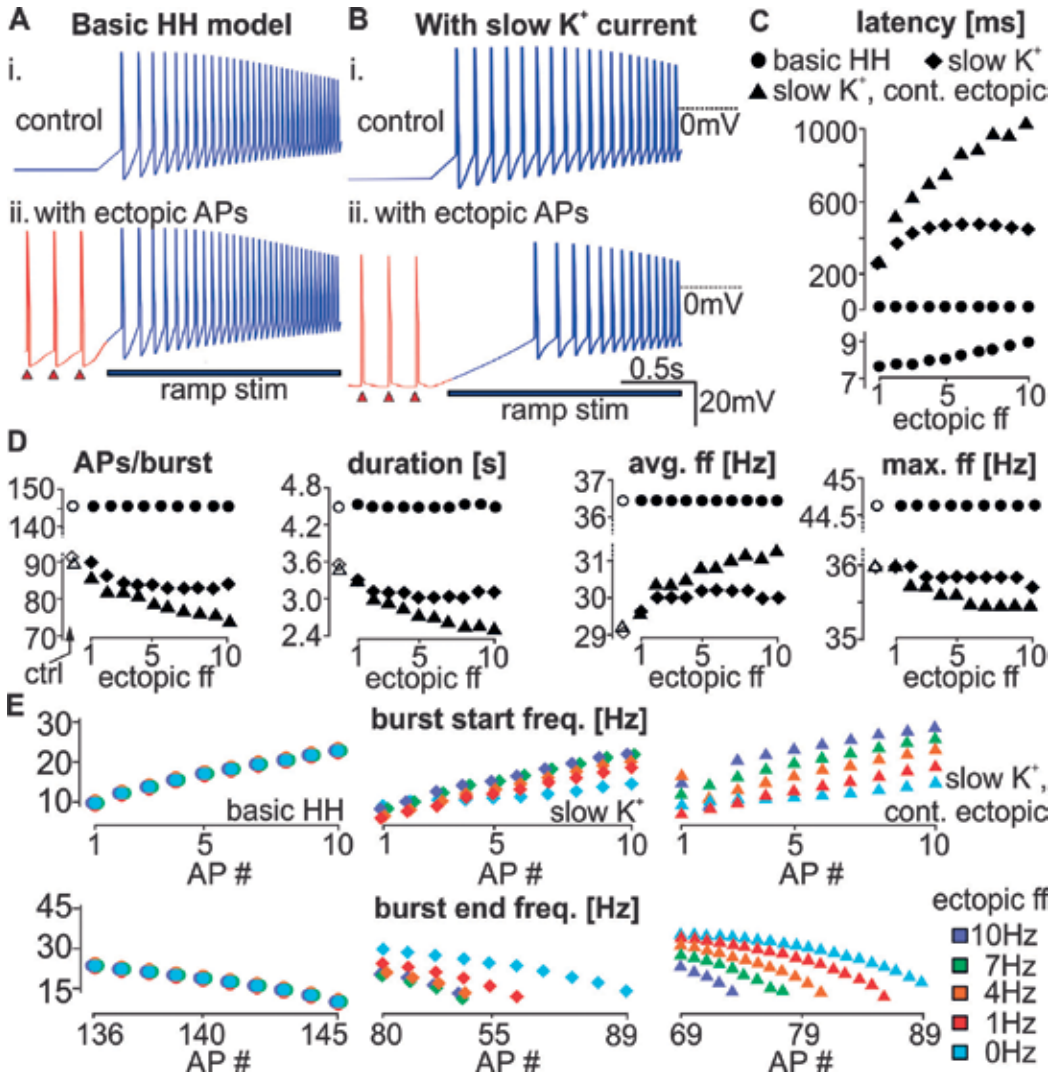

Figure 5. Comparison of membrane potential traces of AGR models without (A) and with (B) I_{Ks} at the primary SIZ. i: Truncated control sensory burst sensory burst, elicited by ramp-and-hold current in the peripheral dendrite. ii: With ectopic APs elicited in the axon trunk. Ectopic APs ended at the beginning of the sensory burst. Red arrowheads indicate ectopic stimulation. C. Corresponding changes in latency at different ectopic AP frequencies. Bottom: magnification of HH model burst latency. D. Changes in burst parameters with ectopic AP frequency. E. Comparison of burst shapes using instantaneous firing frequencies at burst start and end. AP number corresponds to the count of APs in the burst.

accommodate and diminish towards burst end [40]. Slow conductances are common to many sensory neurons, including pain fibers [28, 50], for example. To test whether these slow ionic conductances may enable ectopic APs to exert a frequency-dependent effect on the sensory burst, we added them individually to our axon model. We first implemented I_h, with a time constant of 300 ms, according to previously published data in the stomatogastric ganglion [51].

While the sensory burst was strongly affected by the presence of I_h, this was independent of any ectopic firing, and adding ectopic APs at any frequency had no further influence on the burst (data not shown). This was also the case when we increased the I_h time constant to achieve 10× slower kinetics, as suggested by previous measurements in AGR [40]. Since I_h had no frequency-dependent effects on the sensory burst, we did not consider it further.

In contrast to I_h, Calcium-activated Potassium currents are activated when neurons depolarize, and are slow enough to maintain hyperpolarizing currents. When we implemented I_{Ks} in the primary SIZ, we saw a clear influence when we changed ectopic AP frequencies. **Figure 5B** shows the results from a model with 6 Hz ectopic AP frequency. Changes in ectopic AP frequency had similar effects to the biological system: with increasing ectopic AP frequencies, burst latencies increased, AP numbers in the burst decreased, and burst duration decreased (**Figure 5C, D**, diamonds). There was a small increase in average intraburst firing frequency, and a small decrease in the maximum firing frequency (**Figure 5C, D**). These frequency-dependent effects were most obvious between 1 and 5 Hz ectopic frequencies, and saturated at higher ectopic frequencies.

To also determine the effects of strong synaptic input at the axon trunk, we modeled continuous ectopic firing through the burst. Similar to what we observed experimentally, the effects of changes in ectopic AP frequency were exaggerated in comparison to when ectopic APs stopped with the burst onset. Specifically, there was an increase in burst latency that did not plateau with higher ectopic frequencies (**Figure 5C**). The maximum latency observed at 10 Hz was more than twice that of previous model. The effects on AP number and burst duration were also strengthened, resulting in larger decreases. There were again small effects on the average and maximum intraburst firing frequencies (less than 2 Hz). We noted that these small changes contrasted to the biological experiments. The smaller influence on maximum frequency is likely due to the strength of the ramp-and-hold current used, which was designed to reach biological relevant frequencies (~30 Hz). However, these frequencies are close to maximum frequencies the model can sustain. Consequently, the dynamic range around the maximum frequency might be limited.

To address the difference in average frequency between model and physiology, we assessed burst shape by measuring instantaneous firing frequencies at burst start and burst end (**Figure 5E**). We again compared the basic HH model with the ones containing the I_{Ks}. Firing frequencies in the HH model burst were not different from the control burst at any ectopic AP frequency, both at the beginning or end of the burst. In contrast, both models with I_{KS} showed higher instantaneous firing frequencies at burst start when ectopic AP frequency was increased. Conversely, at the end of the burst, instantaneous firing frequencies were lower. These two effects were stronger in the model where ectopic APs continued through the burst. Together, these effects might explain why there are few changes in average intraburst firing frequency.

In conclusion, our experimental and model data demonstrate that antidromic APs can invade the primary SIZ of sensory neurons, and cause frequency-dependent modulation of sensory

encoding at this site. Our model results suggest that for ectopic APs to exert their effects, ionic conductances with slow kinetics must be present at the primary SIZ.

4. Discussion and conclusions

We demonstrate that modulation of the axon trunk of a proprioceptive neuron influences the encoding of sensory information in the distant periphery. The frequency of ectopic APs initiated in the axon is increased by the biogenic amine Octopamine in a concentration dependent manner, leading to a larger number and higher density of APs that propagate towards and invade the sensory encoding SIZ. We show three frequency-dependent actions on sensory encoding with ectopic APs that stop once an orthodromic burst begins: (1) an increase in the onset latency, (2) a reduction of AP number, and (3) a reduction in the duration of the sensory burst. These effects are strengthened when ectopic APs are elicited throughout the burst, and there is a significant frequency-dependent decrease in the average and maximum burst frequencies. Computational models demonstrate that antidromic APs modify sensory encoding in generic neurons when slow ionic conductances are present. Thus, axonal neuromodulation serves to rapidly influence sensory encoding distantly from the sites of stimulus reception and AP initiation.

4.1. Neuromodulation of sensory systems

Sensory neurons are dynamic and change their responses in a state- and context-dependent manner. Consequently, their AP trains do not solely depend on stimulus properties, but also on internal and external conditions of the neuron. In recent years, increasing evidence about the ability of the neuromodulatory system to influence sensory systems has accumulated. Neuromodulation has been shown to modify the response to identical sensory stimulus and cause significant functional changes in behavior and perception by acting on intrinsic and synaptic properties [5]. Modulators like monoamines, peptides, and opiates, for example, alter reflexes such as startle responses [52]. While initially thought to be related to optimal energy expenditure, it is now clear that altering sensory responses is a widely used phenomenon to allow dynamic adaptations. Thus, neuromodulation allows organisms to modify neuronal and circuit responses to changing external and internal conditions, and allows sensory systems to contribute to not just one, but many behaviors.

More recently, many non-reflex sensory responses have been added to the list of modulated systems, including social communication [53], taste [54], olfaction [55], hearing [56], and pain [57]. For instance, the AP responses of mammalian pain and itch receptors are differentially affected by a variety of immune molecules and neuromodulators that alter nociceptive TRP channel activation during injury, inflammatory, and other pathological conditions [58], including Parkinson disease [59]. Neuromodulators also convey history- and state-dependent sensory responses. The receptor thresholds in newt primary olfactory receptors which determines odor perception sensitivity, for example, are modulated by adrenaline [55]. In the crustacean STNS, the AP response of a muscle stretch receptor is modulated by at least six distinct

modulators, including monoamines, neuropeptides, and GABA [60–62]. These modulators switch how sensory information is encoded (from burst coding to AP coding), and encoding preciseness [63]. Neuromodulation enables the encoding process of both slow and fast processes to be largely plastic.

4.2. Modulation of axons

The actions and functions of neuromodulators on axons, as opposed to synaptic and dendritic regions, remain enigmatic, in part due to the common misconception that axons are only simple and robust carriers of information. Membranes of both myelinated and unmyelinated axon trunks are endowed with ionotropic and metabotropic receptors for transmitters and neuromodulators [4, 64–66], and several different types of ion channels (such as I_h [8, 67–76]; P, N and L type Ca channels [77–84]), providing compelling evidence for axonal neuromodulation. While the origins of axonal modulators are often unknown, it is reasonable to assume that modulation stems from synaptic, paracrine, and endocrine sources [5, 85] and is an intricately balanced process that defines axon excitability. This results in more flexibility of propagation dynamics including conduction velocity and APs number [66, 86–92], thus increasing the computational and processing capabilities of the neuron [93–97]. Conversely, several disorders and pathologies of the neuromodulatory system severely impair neuronal communication and axonal properties [98–100].

4.3. Axonal modulation modifies distant sensory encoding through ectopic action potentials

A lesser-studied phenomenon is how axon modulation affects frequency encoding in neurons. Recent studies have suggested that the size and location of SIZs help regulate neuron excitability and define responses to synaptic inputs and membrane potential changes [101–103]. Moreover, pathologies and modulators can shift SIZ location [11, 32], or generate entirely new SIZs in the axon trunk. For example, hyper-excitability of spinal pain fibers in the dorsal horn is suggested to underlie chronic pain and itch [57]. Similarly, chronic inflammation can hyper-excite proprioceptive sensory axons and lead to ectopic APs that are initiated far from the primary SIZ and travel bi-directionally [11]. While common in many systems and neurons [4], including sensory neurons, the effects ectopic APs that travel antidromically towards the site of sensory reception may have on sensory encoding remain poorly understood.

We argue that antidromic traveling ectopic APs modify sensory encoding by invading the primary SIZ and modulating membrane excitability. This is a particularly intriguing concept, since it allows the modulatory system to alter sensory information before and after it is transduced, and as it travels towards the central nervous system. This is especially true when the ectopic AP frequency changes in different modulatory conditions, as we show for Octopamine modulation of AGR. In the STNS, modulatory descending projection neurons are a major source of neuromodulation [44, 104, 105], and it is reasonable to assume that these neurons modulate the AGR axon [106]. Given that descending modulatory projection neurons are a hallmark of most sensorimotor systems [107], axonal neuromodulation may be common and allow the nervous system to control its own sensory encoding.

The idea that backpropagating APs influence information encoding is not new. Studies in neocortex and hippocampus demonstrate that locally (at the axon initial segment) generated APs backpropagate into the dendritic areas, and modify subsequent signal encoding [2, 108]. To our knowledge, we are the first ones to directly show antidromic ectopic APs can serve a similar function, i.e. that APs generated distantly from the dendritic structures can affect information encoding. A similar phenomenon has been suggested in dorsal root ganglion cells [11, 13, 109]. The implications of antidromic ectopic APs and backpropagating APs from the axon initial segment are distinct though: APs initiated at the axon initial segment will always be elicited by dendritic activity, and therefore backpropagation can only affect future events. It thus can never modify the entirety of the information encoded. In contrast, ectopic APs influenced by axonal neuromodulation are not dependent on incoming sensory or synaptic events, and can thus modulate the entirety of the incoming sensory information. This may be a potential mechanisms by which motor systems control information entering the central nervous system.

4.4. Antidromic action potentials allow more flexibility in sensory encoding

Our data indicate that the effects ectopic APs have on sensory encoding depends on whether ectopic APs continue through the sensory burst or stop when it begins. Specifically, frequency-dependent decreases in average and maximal burst frequency are only present when ectopic APs continue through the burst. Though there are frequency-dependent changes in the burst onset latency, AP number, and burst duration in both paradigms, these effects are stronger when ectopic APs continue through the burst. This may be in particular pertinent to the treatment of neuropathologies using continuous high frequency stimulation [19, 110]. While the high frequency will overrun all sensory information, this may not be necessary to provide the best treatment. Examples for this come from the treatment of chronic neuropathic pain with spinal cord stimulation, where continuous stimulation is used to block all peripheral sensations with a tonic train of stimuli [111]. This prevents the perception of pain, but can result in paresthesia [112]. We show ectopic AP frequencies lower than sensory burst frequencies can change sensory encoding, suggesting high frequency stimulation may not be a prerequisite for treatment. Nevertheless, it seems reasonable to speculate about the relationship of sensory burst frequency and the ectopic APs frequency range, which modulates it. Higher frequencies of either SIZ leads to more 'winner takes all' situations, where the higher frequency SIZ simply overruns the lower frequency SIZ. The potential for modulation is thus limited by the opportunity of the ectopic APs to reach the encoding regions. In other words, the sensory AP frequencies must at some point fall below the ectopic AP frequency to allow them to invade the primary SIZ.

Our computational models indicate that a prerequisite for these actions is the presence of slow ionic conductances. While the detailed biophysical mechanisms that affected particular spike parameters are beyond the scope of this study, slow ionic conductances greatly influence neuronal behavior and responses to synaptic input. For example, transitions between tonic and bursting states are mediated by changes in slow Potassium currents and their functional antagonists, such as I_h, and persistent Sodium or T-type Calcium currents [29, 113]. In axons, slow conductances and membrane potential changes have been implicated in affecting axonal

excitability and AP propagation. For example, slow potassium channels affect AP width and transmitter release in myelinated axons of cortex [30], and slow currents elicited by the Sodium-Potassium pump affect AP propagation in crustacean motor neurons [6]. It would not be surprising to find similar AP-induced, slow accumulating, currents in peripheral sensory axons or dendrites. For AGR, the main effect of the ectopic APs seems to stem from I_{Ks}, or a similar current that imposes a slow inhibitory action that accumulates as ectopic APs invade the primary SIZ. Axon modulation thus appears to give sensory neurons the opportunity to be more flexible, depending on the source and type of modulation, in their ability to encode stimuli. This may be particularly important for time critical processes, and behaviors that rely on time sensitive synaptic processes that require precise AP timing.

Acknowledgements

Many thanks to Carola Städele for helpful discussions of the data. Supported by NSF IOS 1354932.

Author details

Margaret L. DeMaegd and Wolfgang Stein*

*Address all correspondence to: wstein@neurobiologie.de

School of Biological Sciences, Illinois State University, Normal, USA

References

[1] Sanyal S, Kim SM, Ramaswami M. Retrograde regulation in the CNS; neuron-specific interpretations of TGF-beta signaling. Neuron. 2004;**41**(6):845-848

[2] Wu YW, Grebenyuk S, McHugh TJ, Rusakov DA, Semyanov A. Backpropagating action potentials enable detection of extrasynaptic glutamate by NMDA receptors. Cell Reports. 2012;**1**(5):495-505

[3] Stuart GJ, Hausser M. Dendritic coincidence detection of EPSPs and action potentials. Nature Neuroscience. 2001;**4**(1):63-71

[4] Bucher D, Goaillard J-M. Beyond faithful conduction: Short-term dynamics, neuromodulation, and long-term regulation of spike propagation in the axon. Progress in Neurobiology. 2011;**94**(4):307-346

[5] Nadim F, Bucher D. Neuromodulation of neurons and synapses. Current Opinion in Neurobiology. 2014;**29C**:48-56

[6] Zhang Y, Bucher D, Nadim F. Ionic mechanisms underlying history-dependence of conduction delay in an unmyelinated axon. eLife. 2017;**6**:e25382

[7] Ballo AW, Nadim F, Bucher D. Dopamine modulation of I_h improves temporal fidelity of spike propagation in an unmyelinated axon. The Journal of Neuroscience. 2012;**32**(15): 5106-5119

[8] Ballo AW, Keene JC, Troy PJ, Goeritz ML, Nadim F, Bucher D. Dopamine modulates I_h in a motor axon. The Journal of Neuroscience. 2010;**30**(25):8425-8434

[9] Waters J, Schaefer A, Sakmann B. Backpropagating action potentials in neurones: measurement, mechanisms and potential functions. Progress in Biophysics and Molecular Biology. 2005;**87**(1):145-170

[10] Pinault D. Backpropagation of action potentials generated at ectopic axonal loci: Hypothesis that axon terminals integrate local environmental signals. Brain Research Reviews. 1995;**21**(1):42-92

[11] Ma C, LaMotte RH. Multiple sites for generation of ectopic spontaneous activity in neurons of the chronically compressed dorsal root ganglion. The Journal of Neuroscience. 2007;**27**(51):14059-14068

[12] Papatheodoropoulos C. A possible role of ectopic action potentials in the in vitro hippocampal sharp wave-ripple complexes. Neuroscience. 2008;**157**(3):495-501

[13] Dubuc R, Cabelguen JM, Rossignol S. Rhythmic fluctuations of dorsal root potentials and antidromic discharges of primary afferents during fictive locomotion in the cat. Journal of Neurophysiology. 1988;**60**(6):2014-2036

[14] Schmitz D, Schuchmann S, Fisahn A, Draguhn A, Buhl EH, Petrasch-Parwez E, et al. Axo-axonal coupling. A novel mechanism for ultrafast neuronal communication. Neuron. 2001;**31**(5):831-840

[15] Feldmeyer D, Qi G, Emmenegger V, Staiger JF. Inhibitory interneurons and their circuit motifs in the many layers of the barrel cortex. Neuroscience. 2018;**368**:132-151

[16] Fink AJ, Croce KR, Huang ZJ, Abbott LF, Jessell TM, Azim E. Presynaptic inhibition of spinal sensory feedback ensures smooth movement. Nature. 2014;**509**(7498):43-48

[17] Cattaert D, Libersat F, El Manira AA. Presynaptic inhibition and antidromic spikes in primary afferents of the crayfish: a computational and experimental analysis. The Journal of Neuroscience. 2001;**21**(3):1007-1021

[18] Bevengut M, Clarac F, Cattaert D. Antidromic modulation of a proprioceptor sensory discharge in crayfish. Journal of Neurophysiology. 1997;**78**(2):1180-1183

[19] Song Z, Viisanen H, Meyerson BA, Pertovaara A, Linderoth B. Efficacy of kilohertz-frequency and conventional spinal cord stimulation in rat models of different pain conditions. Neuromodulation 2014;**17**(3):226-234; discussion 34-5

[20] Grossman Y, Parnas I, Spira ME. Differential conduction block in branches of a bifurcating axon. The Journal of Physiology. 1979;**295**:283-305

[21] Follmann R, Rosa E, Stein W. Dynamics of signal propagation and collision in axons. Physical Review. E, Statistical, Nonlinear, and Soft Matter Physics. 2015;**92**(3):032707

[22] Zhang X, Roppolo JR, de Groat WC, Tai C. Mechanism of nerve conduction block induced by high-frequency biphasic electrical currents. IEEE Transactions on Biomedical Engineering 2006;**53**(12 Pt 1):2445-2454

[23] Smarandache CR, Daur N, Hedrich UB, Stein W. Regulation of motor pattern frequency by reversals in proprioceptive feedback. The European Journal of Neuroscience. 2008; **28**(3):460-474

[24] Smarandache CR, Stein W. Sensory-induced modification of two motor patterns in the crab, *Cancer pagurus*. The Journal of Experimental Biology. 2007;**210**:2912-2922

[25] Combes D, Simmers J, Moulins M. Structural and functional characterization of a muscle tendon proprioceptor in lobster. The Journal of Comparative Neurology. 1995;**363**(2):221-234

[26] Stein W. Stomatogastric Nervous System. Oxford, United Kingdom: Oxford University Press; 2017. DOI: http://neuroscience.oxfordre.com/view/10.1093/acrefore/9780190264086.001.0001/acrefore–e-153

[27] Daur N, Nadim F, Stein W. Regulation of motor patterns by the central spike-initiation zone of a sensory neuron. The European Journal of Neuroscience. 2009;**30**(5):808-822

[28] Jiang YQ, Sun Q, Tu HY, Wan Y. Characteristics of HCN channels and their participation in neuropathic pain. Neurochemical Research. 2008;**33**(10):1979-1989

[29] He C, Chen F, Li B, Hu Z. Neurophysiology of HCN channels: from cellular functions to multiple regulations. Progress in Neurobiology. 2014;**112**:1-23

[30] Shu Y, Yu Y, Yang J, McCormick DA. Selective control of cortical axonal spikes by a slowly inactivating K^+ current. Proceedings of the National Academy of Sciences of the United States of America. 2007;**104**(27):11453-11458

[31] Gutierrez GJ, Grashow RG. *Cancer borealis* stomatogastric nervous system dissection. Journal of Visualized Experiments. 2009;**25**:e1207

[32] Städele C, Stein W. The site of spontaneous ectopic spike initiation facilitates signal integration in a sensory neuron. The Journal of Neuroscience. 2016;**36**(25):6718-6731

[33] DeMaegd ML, Städele C, Stein W. Axonal conduction velocity measurement. Bio-protocol. 2017;**7**(5):e2152

[34] Städele C, DeMaegd ML, Stein W. Extracellular axon stimulation. Bio-protocol. 2017; **7**(5):e2151

[35] Obaid AL, Loew LM, Wuskell JP, Salzberg BM. Novel naphthylstyryl-pyridium potentiometric dyes offer advantages for neural network analysis. Journal of Neuroscience Methods. 2004;**134**(2):179-190

[36] Follmann R, Goldsmith CJ, Stein W. Spatial distribution of intermingling pools of projection neurons with distinct targets: A 3D analysis of the commissural ganglia in *Cancer borealis*. The Journal of Comparative Neurology. 2017;**525**(8):1827-1843

[37] Städele C, Andras P, Stein W. Simultaneous measurement of membrane potential changes in multiple pattern generating neurons using voltage sensitive dye imaging. Journal of Neuroscience Methods. 2012;**203**(1):78-88

[38] Hines ML, Carnevale NT. NEURON: A tool for neuroscientists. The Neuroscientist. 2001;**7**(2):123-135

[39] Hedrich UB, Smarandache CR, Stein W. Differential activation of projection neurons by two sensory pathways contributes to motor pattern selection. Journal of Neurophysiology. 2009;**102**(5):2866-2879

[40] Daur N, Diehl F, Mader W, Stein W. The stomatogastric nervous system as a model for studying sensorimotor interactions in real-time closed-loop conditions. Frontiers in Computational Neuroscience. 2012;**6**:13

[41] Goldsmith CJ, Städele C, Stein W. Optical imaging of neuronal activity and visualization of fine neural structures in non-desheathed nervous systems. PLoS One. 2014;**9**(7): e103459

[42] Stein W, Andras P. Light-induced effects of a fluorescent voltage-sensitive dye on neuronal activity in the crab stomatogastric ganglion. Journal of Neuroscience Methods. 2010;**188**(2):290-294

[43] Preuss S, Stein W. Comparison of two voltage-sensitive dyes and their suitability for long-term imaging of neuronal activity. PLoS One. 2013;**8**(10):e75678

[44] Stein W. Modulation of stomatogastric rhythms. Journal of Comparative Physiology. A. 2009;**195**(11):989-1009

[45] Daur N, Nadim F, Bucher D. The complexity of small circuits: the stomatogastric nervous system. Current Opinion in Neurobiology. 2016;**41**:1-7

[46] Nusbaum MP, Blitz DM, Marder E. Functional consequences of neuropeptide and small-molecule co-transmission. Nature Reviews. Neuroscience. 2017;**18**(7):389-403

[47] Yarger AM, Stein W. Sources and range of long-term variability of rhythmic motor patterns *in vivo*. The Journal of Experimental Biology. 2015;**218**(Pt 24):3950-3961

[48] Barker DL, Kushner PD, Hooper NK. Synthesis of dopamine and octopamine in the crustacean stomatogastric nervous system. Brain Research. 1979;**161**(1):99-113

[49] Hodgkin AL, Huxley AF. A quantitative description of membrane current and its application to conduction and excitation in nerve. The Journal of Physiology. 1952;**117**:500-544

[50] Momin A, Cadiou H, Mason A, McNaughton PA. Role of the hyperpolarization-activated current I_h in somatosensory neurons. The Journal of Physiology. 2008;**586**(24):5911-5929

[51] Buchholtz F, Golowasch J, Epstein IR, Marder E. Mathematical model of an identified stomatogastric ganglion neuron. Journal of Neurophysiology. 1992;**67**(2):332-340

[52] Davis M. Neurochemical modulation of sensory-motor reactivity: Acoustic and tactile startle reflexes. Neuroscience and Biobehavioral Reviews. 1980;**4**(2):241-263

[53] Hoke KL, Pitts NL. Modulation of sensory-motor integration as a general mechanism for context dependence of behavior. General and Comparative Endocrinology. 2012;**176**(3): 465-471

[54] Lemon CH. Modulation of taste processing by temperature. American Journal of Physiology. Regulatory, Integrative and Comparative Physiology. 2017;**313**(4):R305-RR21

[55] Kawai F, Kurahashi T, Kaneko A. Adrenaline enhances odorant contrast by modulating signal encoding in olfactory receptor cells. Nature Neuroscience. 1999;**2**(2):133-138

[56] Brozoski TJ, Bauer CA. Animal models of tinnitus. Hearing Research. 2016;**338**:88-97

[57] Tsuda M. Modulation of pain and itch by spinal glia. Neuroscience Bulletin. 2017:1-8

[58] Mickle AD, Shepherd AJ, Mohapatra DP. Nociceptive TRP channels: Sensory detectors and transducers in multiple pain pathologies. Pharmaceuticals (Basel). 2016;**9**(4):72

[59] Cury RG, Galhardoni R, Fonoff ET, Perez Lloret S, Dos Santos Ghilardi MG, Barbosa ER, et al. Sensory abnormalities and pain in Parkinson disease and its modulation by treatment of motor symptoms. European Journal of Pain. 2016;**20**(2):151-165

[60] Birmingham JT, Billimoria CP, DeKlotz TR, Stewart RA, Marder E. Differential and history-dependent modulation of a stretch receptor in the stomatogastric system of the crab, *Cancer borealis*. Journal of Neurophysiology. 2003;**90**(6):3608-3616

[61] Birmingham JT. Increasing sensor flexibility through neuromodulation. The Biological Bulletin. 2001;**200**(2):206-210

[62] Birmingham JT, Szuts ZB, Abbott LF, Marder E. Encoding of muscle movement on two time scales by a sensory neuron that switches between spiking and bursting modes. Journal of Neurophysiology. 1999;**82**(5):2786-2797

[63] Billimoria CP, DiCaprio RA, Birmingham JT, Abbott LF, Marder E. Neuromodulation of spike-timing precision in sensory neurons. The Journal of Neuroscience. 2006;**26**(22): 5910-5919

[64] Kamiya H. Kainate receptor-dependent presynaptic modulation and plasticity. Neuroscience Research. 2002;**42**(1):1-6

[65] Sasaki T, Matsuki N, Ikegaya Y. Action-potential modulation during axonal conduction. Science. 2011;**331**(6017):599-601

[66] Swadlow HA, Kocsis JD, Waxman SG. Modulation of impulse conduction along the axonal tree. Annual Review of Biophysics and Bioengineering. 1980;**9**:143-179

[67] Baginskas A, Palani D, Chiu K, Raastad M. The H-current secures action potential transmission at high frequencies in rat cerebellar parallel fibers. The European Journal of Neuroscience. 2009;**29**(1):87-96

[68] Baker M, Bostock H, Grafe P, Martius P. Function and distribution of three types of rectifying channel in rat spinal root myelinated axons. The Journal of Physiology. 1987; **383**:45-67

[69] Ballo AW, Bucher D. Complex intrinsic membrane properties and dopamine shape spiking activity in a motor axon. The Journal of Neuroscience. 2009;**29**(16):5062-5074

[70] Grafe P, Quasthoff S, Grosskreutz J, Alzheimer C. Function of the hyperpolarization-activated inward rectification in nonmyelinated peripheral rat and human axons. Journal of Neurophysiology. 1997;**77**(1):421-426

[71] Kiernan MC, Lin CS, Burke D. Differences in activity-dependent hyperpolarization in human sensory and motor axons. The Journal of Physiology. 2004;**558**(Pt 1):341-349

[72] Soleng AF, Chiu K, Raastad M. Unmyelinated axons in the rat hippocampus hyperpolarize and activate an H current when spike frequency exceeds 1 Hz. The Journal of Physiology. 2003;**552**(Pt 2):459-470

[73] Tomlinson S, Burke D, Hanna M, Koltzenburg M, Bostock H. In vivo assessment of HCN channel current (I(h)) in human motor axons. Muscle & Nerve. 2010;**41**(2):247-256

[74] Eng DL, Gordon TR, Kocsis JD, Waxman SG. Current-clamp analysis of a time-dependent rectification in rat optic nerve. The Journal of Physiology. 1990;**421**:185-202

[75] Poulter MO, Hashiguchi T, Padjen AL. An examination of frog myelinated axons using intracellular microelectrode recording: the role of voltage-dependent and leak conductances on the steady-state electrical properties. Journal of Neurophysiology. 1993;**70**(6): 2301-2312

[76] Takigawa T, Alzheimer C, Quasthoff S, Grafe PA. special blocker reveals the presence and function of the hyperpolarization-activated cation current IH in peripheral mammalian nerve fibres. Neuroscience. 1998;**82**(3):631-634

[77] Callewaert G, Eilers J, Konnerth A. Axonal calcium entry during fast 'sodium' action potentials in rat cerebellar Purkinje neurones. The Journal of Physiology. 1996;**495**(Pt 3): 641-647

[78] Sun BB, Chiu SY. N-type calcium channels and their regulation by GABAB receptors in axons of neonatal rat optic nerve. The Journal of Neuroscience. 1999;**19**(13):5185-5194

[79] Brown AM, Westenbroek RE, Catterall WA, Ransom BR. Axonal L-type Ca^{2+} channels and anoxic injury in rat CNS white matter. Journal of Neurophysiology. 2001;**85**(2):900-911

[80] Fern R, Ransom BR, Waxman SG. Voltage-gated calcium channels in CNS white matter: Role in anoxic injury. Journal of Neurophysiology. 1995;**74**(1):369-377

[81] Ouardouz M, Nikolaeva MA, Coderre E, Zamponi GW, McRory JE, Trapp BD, et al. Depolarization-induced Ca^{2+} release in ischemic spinal cord white matter involves L-type Ca^{2+} channel activation of ryanodine receptors. Neuron. 2003;**40**(1):53-63

[82] Tippens AL, Pare JF, Langwieser N, Moosmang S, Milner TA, Smith Y, et al. Ultrastructural evidence for pre- and postsynaptic localization of Cav1.2 L-type Ca^{2+} channels in the rat hippocampus. The Journal of Comparative Neurology. 2008;**506**(4):569-583

[83] Lohr C, Beck A, Deitmer JW. Activity-dependent accumulation of Ca2+ in axon and dendrites of the leech Leydig neuron. Neuroreport. 2001;**12**(17):3649-3653

[84] Beck A, Lohr C, Deitmer JW. Calcium transients in subcompartments of the leech Retzius neuron as induced by single action potentials. Journal of Neurobiology. 2001; **48**(1):1-18

[85] Bucher D, Marder E. SnapShot neuromodulation. Cell. 2013;**155**(2):482-4e1

[86] Barron DH, Matthews BH. Intermittent conduction in the spinal cord. The Journal of Physiology. 1935;**85**(1):73-103

[87] Krnjevic K, Miledi R. Presynaptic failure of neuromuscular propagation in rats. The Journal of Physiology. 1959;**149**:1-22

[88] Standaert FG. The mechanisms of post-tetanic potentiation in cat soleus and gastrocnemius muscles. The Journal of General Physiology. 1964;**47**:987-1001

[89] Standaert FG. Post-tetanic repetitive activity in the cat soleus nerve. Its origin, course, and mechanism of generation. The Journal of General Physiology. 1963;**47**:53-70

[90] Toennies JF. Reflex discharge from the spinal cord over the dorsal roots. Journal of Neurophysiology. 1938;**1**(4):378-390

[91] Bullock TH. Conduction and transmission of nerve impulses. Annual Review of Physiology. 1951;**13**:261-280

[92] Swadlow HA, Waxman SG. Variations in conduction velocity and excitability following single and multiple impulses of visual callosal axons in the rabbit. Experimental Neurology. 1976;**53**(1):128-150

[93] Debanne D, Campanac E, Bialowas A, Carlier E, Alcaraz G. Axon physiology. Physiological Reviews. 2011;**91**(2):555-602

[94] Debanne D. Information processing in the axon. Nature Reviews. Neuroscience. 2004; **5**(4):304-316

[95] Kress GJ, Mennerick S. Action potential initiation and propagation: Upstream influences on neurotransmission. Neuroscience. 2009;**158**(1):211-222

[96] Segev I, Schneidman E. Axons as computing devices: Basic insights gained from models. Journal of Physiology, Paris. 1999;**93**(4):263-270

[97] Sidiropoulou K, Pissadaki EK, Poirazi P. Inside the brain of a neuron. EMBO Reports. 2006;**7**(9):886-892

[98] Harvey PJ, Li Y, Li X, Bennett DJ. Persistent sodium currents and repetitive firing in motoneurons of the sacrocaudal spinal cord of adult rats. Journal of Neurophysiology. 2006;**96**(3):1141-1157

[99] Melnikov M, Belousova O, Murugin V. Pashenkov capital Em C, Boysmall ka CoCA. The role of dopamine in modulation of Th-17 immune response in multiple sclerosis. Journal of Neuroimmunology. 2016;**292**:97-101

[100] Dobryakova E, Genova HM, DeLuca J, Wylie GR. The dopamine imbalance hypothesis of fatigue in multiple sclerosis and other neurological disorders. Frontiers in Neurology. 2015;**6**:52

[101] Grubb MS, Burrone J. Activity-dependent relocation of the axon initial segment fine-tunes neuronal excitability. Nature. 2010;**465**(7301):1070-1074

[102] Kuba H, Ishii TM, Ohmori H. Axonal site of spike initiation enhances auditory coincidence detection. Nature. 2006;**444**(7122):1069-1072

[103] Kuba H, Oichi Y, Ohmori H. Presynaptic activity regulates Na(+) channel distribution at the axon initial segment. Nature. 2010;**465**(7301):1075-1078

[104] Nusbaum MP, Blitz DM. Neuropeptide modulation of microcircuits. Current Opinion in Neurobiology. 2012;**22**(4):592-601

[105] Nusbaum MP, Beenhakker MP. A small-systems approach to motor pattern generation. Nature. 2002;**417**(6886):343-350

[106] Städele C, Stein W. Control of sensory ectopic spike initiation by descending modulatory projection neurons. BioRxiv. 2015. DOI: https://www.biorxiv.org/about-biorxiv

[107] Nusbaum MP. Modulatory projection neurons. In: Binder MD, Hirokawa N, Windhorst U, editor. Encyclopedia of Neuroscience. Heidelberg, Germany: Springer; 2013. Availble from: http://www.springerreference.com/docs/html/chapterdbid/117087.html

[108] Markram H, Lubke J, Frotscher M, Sakmann B. Regulation of synaptic efficacy by coincidence of postsynaptic APs and EPSPs. Science. 1997;**275**(5297):213-215

[109] Beloozerova IN, Rossignol S. Antidromic discharges in dorsal roots of decerebrate cats. II: Studies during treadmill locomotion. Brain Research. 2004;**996**(2):227-236

[110] Kumar K, Taylor RS, Jacques L, Eldabe S, Meglio M, Molet J, et al. Spinal cord stimulation versus conventional medical management for neuropathic pain: A multicentre randomised controlled trial in patients with failed back surgery syndrome. Pain. 2007; **132**(1–2):179-188

[111] Meyerson BA, Linderoth B. Mechanisms of spinal cord stimulation in neuropathic pain. Neurological Research. 2000;**22**(3):285-292

[112] De Ridder D, Vanneste S, Plazier M, van der Loo E, Menovsky T. Burst spinal cord stimulation: toward paresthesia-free pain suppression. Neurosurgery. 2010;**66**(5):986-990

[113] Harris-Warrick RM. Voltage-sensitive ion channels in rhythmic motor systems. Current Opinion in Neurobiology. 2002;**12**(6):646-651

Chapter 3

Are Sensory Neurons in the Cortex Committed to Original Trigger Features?

Nayan Chanauria, Rudy Lussiez, Afef Ouelhazi and Stephane Molotchnikoff

Additional information is available at the end of the chapter

http://dx.doi.org/10.5772/intechopen.74776

Abstract

Sensory cortices are inherently dynamic and exhibit plasticity in response to a variety of stimuli. Few studies have revealed that depending upon the nature of stimuli, excitation of the corresponding sensory region also evokes a response from other neighboring connected areas. It is even more striking, when somatosensory areas undergo reorganization as a result of an intentional disturbance and further explored as a paradigm to understand neuroplasticity. In addition, it has also been proved that drugs too can be used as a model to explore potential plasticity in sensory systems. To this aim, through electrophysiology in cats, we explored that visual neurons, throughout the cortical column, have a tendency to alter their inherent properties even when presented a non-visual stimulus. Furthermore, it was explored in mice, how the application of drugs (serotonin and ketamine) modulates potential plasticity within the visual system. Indeed, we found a shift in orientation tuning of neurons indicated by Gaussian tuning fits in both scenarios. These results together suggest that sensory cortices are capable of adapting to intense experiences by going through a recalibration of corresponding or neighboring sensory area(s) to redirect the sensory function and exhibit remarkable extent of neuroplasticity within the brain.

Keywords: cortex, neuroplasticity, adaptation, orientation selectivity, tactile learning, cross-modal plasticity, ketamine, serotonin, reorganization, multisensory integration

1. Introduction

Brain's sensory systems translate raw elements of the external world into practical processable data adapted to sensory nervous system analyses. Forthcoming sensory stimuli trigger initial neural representations in the sensory structures that recurrently end in stimulus-specific

modifications. Through different ascending and descending physiological mechanisms, subsequent nerve impulses are enrooted toward appropriate regions of the cortex. The regularity of these processes devises an organized circuitry of neuronal connections elicited by a variety of stimuli [1–3]. Thus, it is the early sensory experience that guides the evolution of neural circuitry in the cortex.

2. Selectivity in critical period and inhibition

During development, the brain undergoes intense episodes of augmented plasticity known as a critical period. The advent of the critical period has been fundamental to understanding brain development. Critical periods are recognized as the epochs during which developing brains mature in a dynamic yet invariable way by anomalous experience. Considering, inhibition makes the postnatal brain undergo a permanent process of change; more often, brain is referred to as "plastic." The critical period is characterized by a heightened increase in excitation and inhibition right after birth, leading to a large restructuring of neuronal networks, and decreasing alternatively with age. It has also been acknowledged that there are multiple critical periods associated with various brain functions wherein early sensory processing have shorter critical periods than for higher complex functions or cognitive/executive functions. This maturation of cortical inhibition just after eye-opening is necessary for the establishment of experience-dependent ocular dominance plasticity in the visual cortex which relies on counteraction between two eyes to drive cortical responses. Moreover, it is presumed that critical period contributes to improving our ability to survive in the dynamic environment in later sensory experiences.

In general, sensory deprivation is associated with powerful cross-modal changes in the cortex which has been used as a paradigm to study neuroplasticity. Lack of sense of vision or hearing during early development may interfere with the calibration process that occurs during the critical period. It has been demonstrated by a number of studies in deaf and blind that cortex reorganizes itself as a result of the loss of sensory modality. This has also been found true in congenital blind and deaf.

2.1. Reorganization of the cortex following sensory deprivation or sensory loss

The most surprising yet striking phenomenon in the cortex takes place during the critical period. It was demonstrated that during the critical period, auditory cortex could develop finely tuned maps for different orientations of visual stimuli when a rerouting of visual input was enforced to an otherwise de-afferent auditory cortex [4]. Another study by Sharma et al. [5] examined and compared intrinsic connections in the rewired primary auditory cortex (A1) to normal A1 and normal primary visual cortex (V1). They found that diverting visual inputs to auditory cortex led to sharp orientation selectivity in rewired A1 and found that A1 maps were like V1 maps, but not as clean as V1. Further, it is also familiar now that during development, there is extensive and undefined emergence of connections that are particularly strong for cortical-cortical networks [6]. Despite having an individual skill associated to every recognized sensory area, nearby associative and auditory cortical areas respond to auditory motion stimuli, including the superior temporal sulcus cortex (STS), which is the sulcus separating

the superior temporal gyrus from the middle temporal gyrus in the temporal lobe of the brain. It could be possible that STS provides auditory input to the MT (middle temporal visual area or V5) during development. The STS in normal adult monkeys consists of pure auditory, pure visual, and multisensory neurons [7]. It seems likely that the auditory input within STS may spread to the nearby middle temporal visual area during development and the undefined contacts may align themselves during the visual deprivation period.

2.1.1. Disappearing of cortical borders in the barrel cortex by tactile learning

In monkeys, another type of tactile learning was used to show whether or not it was possible to change tactile receptive fields in the somatosensory cortex [8]. In this study, authors wanted to simultaneously stimulate two adjacent fingers and see if the somatosensory cortex displayed any kind of adaptation or reorganization (**Figure 1**). To increase their chances to achieve synchronized stimulation of two adjacent fingers, they surgically fused them by connecting the

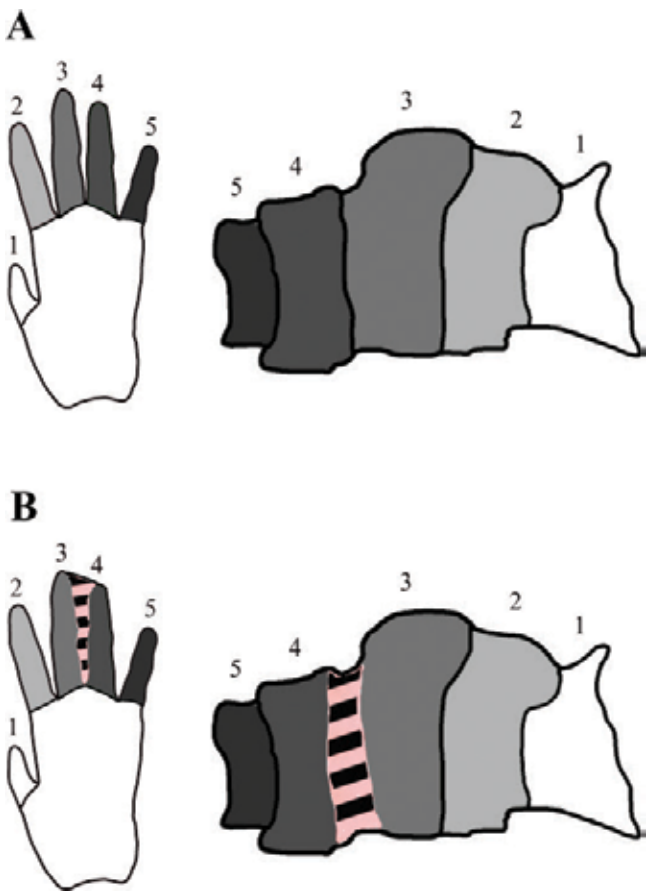

Figure 1. Model of cortical reorganization of area 3b following synchronous-stimulation of two fingers. (A) Normal monkey hand (left) with the associated cortical territory (right) in area 3b of the somatosensory cortex. (B) Fingers 3 and 4 were then surgically merged (left) to achieve synchronized stimulation of both fingers, conducting a reorganization of area 3b (right). Striped area represents overlapping between fingers 3 and 4 (model based on Clark et al. [8]).

skin, creating a syndactyly for digits 3 and 4 of owl adult monkeys. In [8], the strict separation between fingers receptive fields disappeared, allowing them to merge, forming a new single receptive field similar than that of a single unaltered finger. Stimulation of one of the two connected digits resulted not only in the activation of neurons in the previous finger receptive field, but also in the overlapping part of the newly formed cortical territory. Thus, these results suggest that the cortical map of specific body surface is linked to the temporal correlation of afferent stimuli. Tactile learning is then a useful procedure to help organize the somatosensory cortex and maintain tactile memory over long periods of time.

2.1.2. Typical example: reorganization of the barrel cortex following sensory loss by finger amputation

We now know that it is indeed possible to merge fingers' cortical receptive fields in the somatosensory cortex of the adult monkey, using synchronized stimulation of adjacent fingers. However, this experiment was conducted in a situation where no tactile receptors were eliminated. What would happen if the animal encountered some form of sensory loss on the tactile level? This was further explored by Merzenich and his colleagues [9], in an experiment which again involved adult owl monkeys. To test how the cortex would react to sensory loss, monkeys underwent surgical amputations of digit 3, or 2 and 3, and digital nerves were tied to counter their regeneration after the amputation (**Figure 2**). For digit 3 amputated monkeys, cortical mapping was realized before amputation, and 62 days post-surgery. Even though cortical territory for each finger was clearly defined before surgery, the area of the amputated digit was now used to represent adjacent fingers. Finger representations for finger 2 and 4 expended their territory inside the former digit 3 area, activating neurons when fingers were stimulated. As for digits 1 and 5 receptive fields, no changes were observed. As a rule for the brain, plasticity reduces with age, yet these results suggested that somatosensory cortex can reorganize its cortical territories to fully recover from the sensory loss, a beautiful proof of plasticity retained in adult monkeys. Furthermore, they mapped the cortical territories of remaining fingers for dual (digits 2 and 3) amputated monkeys. Just as digit 3 amputated specimens, the remaining fingers receptive fields expanded to the digit less cortical areas. However, in regions previously associated with fingers 2 and 3, it was found that some neurons were not activated by adjacent finger stimulation, rendering these cortical territories silent.

2.2. Congenital blindness

Reorganizing the somatosensory cortex was proved to be possible [8, 9], but only within itself and with sensory loss occurring during adult life. In the study of Kupers et al. [10], experiments were conducted on human late blinds (LB) and early blinds (EB). Human subjects were previously trained with a tongue display unit (TDU), which is a tactile vision sensory substitution system (TVSS) [11, 12], showing that activation of occipital cortex could be achieved and increased using sensory substitution. However, it was not proved that activation of either cortex could be achieved without using sensory substitution. Subjects were then prepared for transcranial magnetic stimulation of the occipital cortex [11], and were asked if they had any reaction. Some subjects affirmed to have experienced tactile sensations on the tongue, following stimulation of occipital cortex. Other regions of the occipital region were then stimulated, each

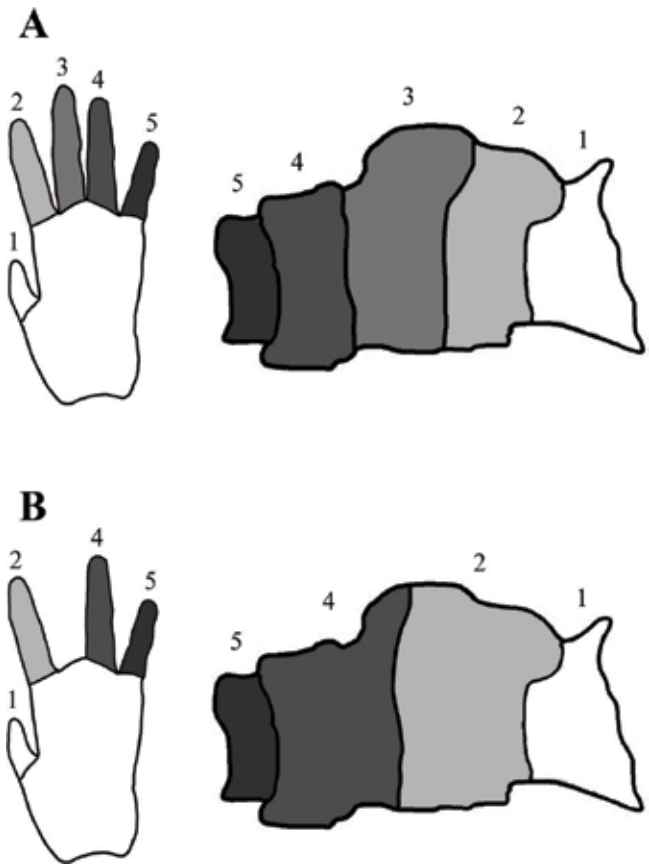

Figure 2. (A) Normal monkey hand (left) with associated cortical territory (right) in area 3b of the somatosensory cortex (B) after finger 3 was surgically amputated (left), area 3b of the somatosensory showed cortical reorganization (right) with fingers 2 and 4 territories expanding into the now deprived finger 3 territory (model based on Merzenich et al. [9]).

of them resulting in an evoked response on different areas of the tongue. Hence, these results proved that early sensory deprived cortices could be involved in cross-modal plasticity, following training with sensory substitution techniques.

2.3. Selectivity modified in adult visual and auditory cortices

For eons, it has been tested and verified that the structure and interneuronal connections of the central nervous system cannot be modified in adulthood. Yet, the past decade investigations carried out on invertebrates [13] and vertebrates [14–20] have revealed that neurons may change their response property or stimulus selectivity exhibited since after birth following an appropriate experimental protocol. To mention a few cases, monocular deprivation produces an amblyopic condition that results in a loss of vision in the affected eye due to unbalanced synaptic drive in the visual cortex. Reversing the deprivation by closing the unaffected eye and stimulating the initially closed eye switches the effect. In this process, the synaptic equilibrium is reversed because the initially deprived eye is strengthened and the companion eye is weakened. Ocular dominance can be shifted even in adult

brains, meaning that neuronal networks maintain potential plasticity from an infant into adulthood. In the auditory system, stimulating neurons with narrow band stimuli excluding the preferred frequency induces responses outside the preferred frequency range [21]. Similarly, cerebral cortex neurons belonging to somatosensory barrels whose whiskers have been cut respond to intact whiskers, suggesting an expansion of the latter's territory [22]. The somatosensory cortex homunculus may be altered with both increased and decreased stimulation [9]. Therefore, neurons in the adult cortex, following manipulation of inputs, display novel response properties that were not present after normal brain's maturation. Most of the investigations studying brain plasticity use a strategy based on the removal or weakening of sensory inputs, such as enucleating eyes, dark rearing, etc., in developing and immature animals. Conclusively, the neuronal plasticity is derived from an absence of excitation. Recording neuronal evoked action potentials in different regions of cortex have profited researchers to deeply explore and understand how separate sensory areas perform individually as well as part of the big sensory systems. It has been unveiled that cells in visual cortex (and elsewhere in cortex) respond to relatively narrow ranges of stimuli features such as the orientation of an elongated edge, direction of stimulus, a direction of whisker displacements, etc. For instance, a typical plot of the response magnitude versus function of orientation reveals a Gaussian type curve, the peak of which indicates the preferred orientation that generates the maximal number of action potentials. Consequently, cortical cells are exquisitely selective to restricted ranges of stimuli properties exhibiting the preferred or optimal stimulus, which usually are acquired during the critical period that follows the birth of the animal. More recently, a collection of published results showed that frequent or forced application of specific non-preferred trigger features, which evoke a feeble response, induces profound modifications of optimal properties exhibited since birth. Studies published in this direction have shown that adaptation diminished responses evoked by the initial optimal orientation, whereas responses evoked by the adapter were considerably augmented. Hence, the original optimal orientation evokes a much weaker response than the response produced by the adapting orientation [16, 23–27].

2.3.1. Cortical neurons exhibit neuroplasticity by acquiring new stimulus features following induction of non-preferred stimulus

Visual adaptation alters perception and tuning selectivity, and these modifications are quite selective suggesting a cortical reorganization of the primary sensory areas. Psychophysical studies revealed that adaptation permits isolating specific sensory channels responsible for eliciting responses induced by a narrow range of properties without affecting responses evoked by stimuli falling outside this range. For instance, adapting an observer to one particular spatial frequency results in a loss of sensitivity to that value of spatial frequency; for this reason, tuning curves present a dip corresponding to the particular band of the adapter [28]. In humans, frequent or prolonged exposure to one particular stimulus generally produces a change in the detectability of the target, because there is a reduced perception to the test stimulus, that is, the threshold becomes elevated due to a selective loss of particular characteristics of the adapter [29]. Prolonged adaptation changes fMRI responses in V1 in an orientation-specific manner [30].

However, in various mammals, adaptation induces more versatile trends. At the single cell level, the effect of adaptation was investigated for several properties in a number of areas and quite a few species. Frenkel et al. [15], showed that repeated presentation of gratings oriented at an orientation to mice induces a specific response potentiating (SRP) to the test orientation. Jin et al. [31], described response suppression resulting in shifts of the peaks of tuning curves away from the adapter, often referred as repulsive shifts. As cortical cells respond well to motion, this property was studied extensively. In primates, V4 adaptation confers a better directionality for cells normally poorly tuned to the direction [32]. In MT of macaque, Kohn and Movshon showed that adaptation causes direction tuning to shift toward the adapted direction; this effect is accompanied by a reduction of direction-tuning bandwidth [33, 34]. On the other hand, Yang and Lisberger [35], reported data demonstrating that adaptation globally reduces the magnitude and the width of direction- and speed-tuned curves. In the same direction, it has also been demonstrated that after monkeys learned to associate directions of motion with static shapes, the neurons of MT area exhibited unexpected selectivity for the static shape, suggesting acquisition of a novel visual property induced by the learning procedure [36]. In parallel, more studies in V1 showed that evoked discharges in response to the originally preferred stimuli are selectively reduced [37–39], but Krekelberg et al. showed that evoked discharges after adaptation are in a direction-dependent manner. Thus, the response enhancement to the adapter stands in contrast to earlier studies where it has been shown that when a neuron is adapted to a particular grating, its sensitivity to that grating is reduced [40–43].

A study [44] carried out on mouse visual cortex and employing the double photon technique disclosed that a single dendritic branch of a cortical cell possesses a collection of synaptic connections for several orientations. In the same cell, these different inputs are located in proximity to the dendritic tree. Repulsive shifts appear to be resulting from a differential weakening of synaptic drives activated by the adapter. The attractive shift required a different explanation. If one assumes that a limited, small area of a dendrite receives contacts from a broad spectrum of properties, one group of inputs will dominate, thus creating a bias that carries the membrane potential across the action potential threshold. The excessive afferent activity ensuing from the lengthened application of a non-preferred stimulus transfers the bias in favor of the adaptor [44]. This produces attractive shifts such as described in the visual and auditory systems. The shifts of tuning curves whether in repulsive or attractive directions are the result of very selective response modulations. The spontaneous activity is unaltered during tests, and responses evoked by stimuli characteristics at distant flanks of the tuning curve are weaker. The response modulations are constrained most closely to the adapter and original optimal property, ruling out a sudden surge of excitability [16, 24, 33, 45]. A second adaptation performed (many minutes sometimes up to 2 h) after the recovery from the first episode of adaptation, yields similar results [46]. Others showed that cortical cells discharge selectively to the null direction (classically, a direction failing to excite the cell), if an appropriate electrical pulse is delivered while the stimulating bar sweeps the cell's receptive field. This emergence of responses to the null direction may last several minutes and well after the conditioning electrical pulse is terminated, suggesting a substantial change of cellular property [47]. Another study in ferrets also explored the critical period for ocular dominance plasticity using intrinsic optical imaging. On comparing ferrets with cats, they found that ferret's critical period

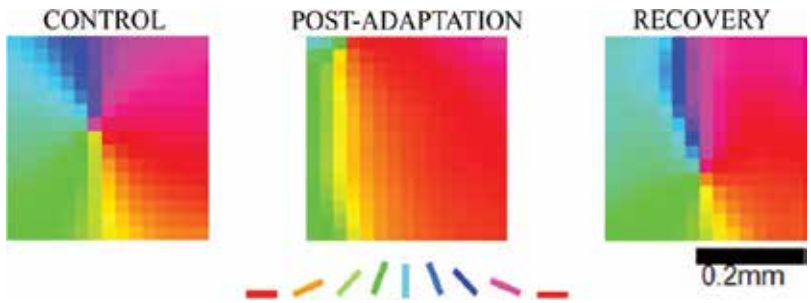

Figure 3. Reorganization of orientation columns in cat primary visual cortex shown by optical imaging.

begins ~75 d which is actually 6–7 days earlier than a cat on conception. Moreover, ferret's LGN becomes laminated and extends axons into visual cortex ~1 week before the cat's LGN does. However, overall, they found the critical period process to be quite similar, yet the development in ferrets appears to be slightly more rapid than cats.

In line with previous reports, few studies from our laboratory through electrophysiology showed that layer 2/3 neurons exhibit attraction and repulsion by changing their orientation selectivity toward or away from adapting orientation or retaining or refracting their orientation tuning in some cases [26, 46]. It was further confirmed by another study using optical imaging that following adaptation for 12 min, the orientation maps are modified in response to the adapter [27] (**Figure 3**). A similar result was obtained in mice by Jeyabalaratnam et al. [48]. Further, a significant study confirmed that a continuous adaptation on the recording site for 12 min yields attractive and repulsive shifts, wherein the shifts carry equivalent averages of a shift in orientation tuning to averages of tuning of neurons recorded from another site away from receptive fields of target neurons. Authors called this as "domino effect" as the reorientation observed after adaptation was found to be guided by the imposed adapter and initiated itself at the site of recording and was followed systematically as a marker by neurons in other columns [49]. Based on this observation and hypothesis, Chanauria et al. [50] demonstrated that the typical behavioral response of visual neurons persists and can be observed in layer 5/6 neurons too when recorded simultaneously with layer 2/3 neurons. Authors further stressed that domino effect does not only exists in layer 2/3 neurons, but also inherently prevails within the neurons throughout the cortical column [50].

At control, each orientation is evenly distributed in the camera-captured zone. However, the post-adaptation situation is no longer the case, as the adapting orientation took over the quasi-totality of the captured zone. After a recovery period, previously preferred orientation regains its control territory (S. Cattan unpublished material).

2.4. Organization of somatosensory cortex and trigger features

All sensory receptors input to the somatosensory cortex, and are then used by the brain to generate a response to the input stimuli by giving information about the environment or position of the body. However, sensory pathways do not only convey information to the somatosensory

cortex but instead, relay the information to specific parts of the cortex [51–53]. It has been shown that using somatotopic maps, a "Sensory Homunculus" can be created, which shows the uneven distribution of cortical areas to different parts of the body. For example, face and hands areas display a bigger area distribution than legs and feet [51]. This was first demonstrated by Penfield and Boldrey [53] using electrical stimulation of the brain during open surgery on consenting patients. Electrical stimulus was applied to a cortical region, and intensity was increased until a response was obtained. Even though this experiment was crucial to the understanding of somatotopic mapping in the brain, it was none the less an invasive and risky experiment. As technology evolved, new tools came into existence and hardware got developed that was now capable of recreating the same experiments, but noninvasively. Techniques like functional magnetic resonance imaging (fMRI) to display brain activity based on blood oxygenation difference became at disposal [51, 52, 54]. The fMRI technique brought a better resolution to the somatotopic maps, showing that each cortical area is dedicated only to a specific part of the body, similarly to receptive fields in the visual cortex [55–57]. The somatosensory cortex is organized in such a way that cortical territories are well-defined and region-specific with respect to body parts. However, some animals harbor some vibrissae, also called "whiskers." Since higher primates possess stimulus-specific cortical territories, it was hypothesized that lower vertebrates also embody the same somatotopic pattern. Indeed, studies conducted on mice proved that their somatosensory cortex is organized similarly to humans. For example cortical areas dedicated to forelimb or hindlimb [58] were found congruent in higher and lower vertebrates, An entire territory dedicated to whiskers inputs was also discovered [59]. These inputs regions with respect to whiskers were called "barrel cortex," because each column in this barrel cortex area of somatosensory cortex was found associated to only one whisker. The barrel cortex occupies an estimated 70% of the primary somatosensory cortex (S1) in mice [59]. Thus, it is no wonder that mice use their whiskers, before their vision, to locate and identify objects not only by their shape [60–64], but also by their texture [65, 66]. The somatosensory cortex is generally shaped to collect and analyze surround information from the environment, with specific structures depending on the species.

2.4.1. Whisking: adaptation and tactile learning

It is convenient to study somatosensory cortex in rodents via the barrel cortices because each whisker is linked to a cortical column, making it "effortless" to identify which neurons will respond to the stimulation of a specific whisker [67, 68]. In [69], the researchers investigated the correlation between spiking and whisking. In their study, neurons were recorded at different levels in the corresponding barrels of stimulated whiskers. It was found that during a whisking episode, neurons from supragranular layers (e.g., L2/3) had lower spiking frequencies than that of infragranular layers (e.g., L5), suggesting that infragranular neurons' spiking frequencies were correlated to whisker position. Once this direction was explored, de Kock and colleagues hypothesized that spiking episodes were correlated to the behavioral state of the rat. To test their hypothesis, they compared the spiking frequencies between three different "behaviors." Their results showed that spiking frequencies in non-whisking awake episodes were similar to whisking episodes under urethane anesthesia. However, when the rats were awake, spiking frequencies were independent between layers, with infragranular (L5) neurons spiking to higher frequencies than supragranular neurons. Moreover, infragranular

neurons (e.g., L6 neurons) did not display significant changes between different behavioral states. Thus, they concluded that behavioral state influenced principally spiking frequencies in L5 neurons. To further confirm their observations, de Kock and de Kock [70] tried to observe cell-type frequencies correlation to a specific behavior state. By analyzing frequencies from supragranular pyramids, slender-tufted and thick-tufted pyramids, L6 pyramids, and granular spiny neurons, it was shown that mainly slender and thick tufted pyramids neurons recorded at 1000–1500 μm, corresponding to L5, displayed significant changes in spiking frequencies for quiet (non-whisking) and whisking states.

2.4.2. Tactile learning

Rodents mainly use their whiskers to acquire information about their surrounding environment. Hence, their natural instinct is to explore new and unfamiliar components of their environment, to get better acquainted with their living space [71]. Wu et al. based their study on this natural instinct [71], used it to investigate the short-term memory of the somatosensory cortex in mice. Their results proved that mice spent more time "exploring" the new panel than that of "exploring" the familiar panel, shown in their arena-based experimental setup. These results suggested that the somatosensory cortex can retain short-term tactile memory by perceptual learning. To further investigate the mechanisms invoked in this tactile memory, they set up the experiments in a way that only tactile stimuli were used by the animal to discriminate the two different textures (suppression of olfactory components, textureless grooved panels for the second trial). In this case, mouse did not express memory in tactile less trial. Moreover, as whisker-less mice did not show the same exploring pattern, their results also demonstrated that this tactile memory was vibrissae-based. With this study, by Wu et al. [71] uncovering the short-term tactile memory of the mice, it was then hypothesized that the effect of perceptual learning can be maintained for a much longer period [72]. With the same kind of experimental setup, trials were separated by 24 h instead of 5 min. After analysis, it was shown that mice spent an average of 65.20% with the novel gratings [72], thus indicating that the perceptual-learning-acquired memory could be maintained for a 24-h period.

2.5. Multisensory integration and cross-modal plasticity

Multisensory stimulation can have a substantial impact on the basic visual perception. Non-visual input, such as auditory stimuli, can affect visual functioning in a myriad of ways. Numerous studies have demonstrated these alluring cross-modal relationships. For example, anatomical and electrophysiological approaches in non-human primates [73, 74] have provided evidence that multisensory interactions can be observed at early primary unimodal stages of sensory processing [1]. This body of evidence suggests that projections from the auditory cortex reach deeper layers of the visual cortex and vice versa. Another study by Muckli and Petro [75] highlights the existence and the importance of non-geniculate input to V1 by associated areas such as auditory cortex. Moreover, a fMRI report by Vetter et al. [76] displayed through task-based approaches in blindfolded healthy adults that, by solely performing an audio task, a response in the visual cortex could be observed. Therefore, primary areas, such as V1 and A1, showcase high multisensory interaction, predominantly a

modulatory influence in response to a complementary stimulus. In a recent study [77], authors have shown that auditory stimulus sharpens the selectivity of visual neurons. In the present investigation, through electrophysiological techniques, we examined the effect of sound on the simultaneously recorded visual cells from supra- and infragranular layers. An auditory stimulus was presented continuously and uninterruptedly for 12 min, and the recordings were performed in area 17 of the visual cortex in anesthetized cats. The effect of the sound stimulus was tested by comparing orientation tunings of neurons before and after the presentation of sound. Indeed, we noticed an intense modulation of response accompanied by a modification of orientation tuning of the neurons. Our data showed that after 12 min presentation of the auditory stimulus, a population of visual cortical neurons experienced modulation of excitation and inhibition and attained new orientation selectivity. In addition, few-layer II–III and V neurons lose their preference and become untuned. These results suggest that visual neurons in either layer change their properties on the application of an auditory stimulus which highlights the cross-modal interactions between visual and auditory systems and a robust reconfiguration of visual cortex induced by sound. An illustration is shown to explain the obtained result. **Figure 4** explains the effect of sound on visual neurons. Sound acts as a non-visual input to the primary visual cortex. Here, instead of a traditional pathway being implicated, a non-geniculate route has been activated. New orientation selectivity is attained by the L2/3 and L5/6 neuron pair recorded from the same site after 12 minutes. The upper curves are L2/3 neuron, whereas bottom curves are L5/6 neuron. Control curves are shown in bold and dotted curves are shown for post-adaptation with sound.

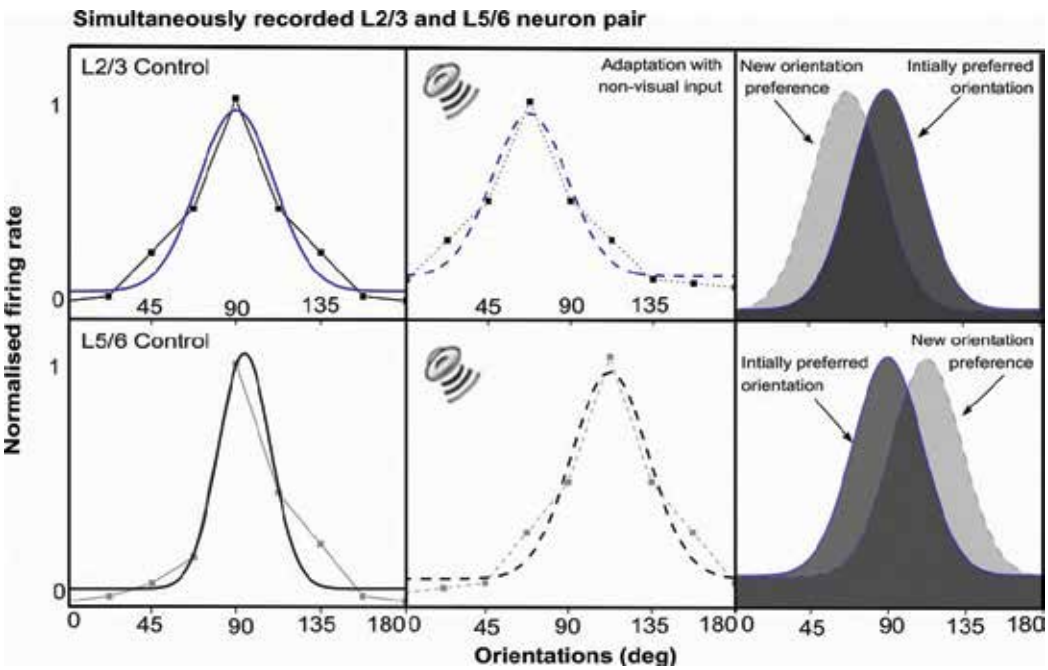

Figure 4. Illustration of effect of a sound stimulus on a pair of simultaneously recorded neurons from L2/3 and L5/6 from a recording site.

The possible explanation to these results could be simply attributed to direct anatomical connections between primary sensory areas within the cortex [73] or an indirect pathway involving arousal of a multisensory area as a mediator to facilitate the modulation of responses [74]. These mediator areas could be pulvinar, superior colliculus or other thalamic nuclei that act as ports of entry of information to primary areas.

The bold curves indicate control tuning curves with respect to raw firing rates, whereas the dotted curves represent raw firing rates. For clarity, raw fits have been fitted with Gauss functions. Curves in upper and lower rows attribute to L2/3 and L5/6 neuron, respectively. On the extreme right (above and below) are non-linear Gaussian fits plotted to infer the exact numerical values of orientation preferences. The superimposition clearly indicates that neuron pair that was similarly tuned initially attained a new selectivity after experience with sound stimulus for 12 min. Modulation of firing rate can be observed and accompanied by the alteration in selectivity. A similar response shift, yet in the opposite direction can be observed in the L5/6 neuron. This indicates that neurons in a column may choose to show a similar response, yet behave independently toward the same stimulus.

2.6. Possible mechanism underlying adaptation and plastic modifications

Recordings of electrical neuronal activity reveal modifications of neuronal properties following adaptation. Since response modifications come about rapidly within a time window of several minutes to a few hours, it seems reasonable to propose that the response alterations following adaptation are carried out by mechanistic processes directly available to neurons. Two-photon microscopy permits visualization of isolated dendritic branches with their spines in vivo. Jia et al. [44], described in V1 that single dendritic branches are divided into several short segments, each selective to one particular orientation. Accordingly, synaptic inputs of different orientation preferences contact a single branch of a dendritic tree. Orientation-tuned neurons, therefore, process their characteristic firing pattern by integrating spatially distributed synaptic inputs responding to multiple orientations. It follows then the most intensely stimulated dendritic segment that drives the neuron above the firing threshold which attributes a novel preferred orientation corresponding to the adapter. Other studies suggest that dendritic structural modifications may happen at a relatively rapid pace. Yang and Lisberger [35] have been able to follow identified dendritic spines over time while mice were submitted to new sensory experiences. The experiments revealed extensive spine remodeling that correlated with behavioral improvement after learning [78, 79]. Also, the remodeling of dendritic branches takes place within a few days following eye suture. Importantly, a small fraction of new spines produced by novel experience, together with most spines formed earlier during development and surviving experience-dependent elimination, are preserved and may provide a structural basis for holding on to memory during the entire life of an animal [35]. A recent [79] study showed that spines and matching axonal boutons of inhibitory neurons undergo rapid changes following retinal lesions. In fact, the same authors suggested that the loss of sensory inputs to inhibitory neurons triggers the plastic dendritic transformation of excitatory cells. The above experiments suggest that daily sensory experience and learning leave small but permanent marks on cortical connections, implying that enduring memories may be associated with the synaptic formation. It may be worth adding that in 1949,

Hebb wrote that "when one cell repeatedly assists in firing another, the axon of the first cell develops synaptic knobs." Nowadays, we may identify it as spine formation on dendrites following prolonged adaptation which produces a sustained, high firing rate in an afferent cell. Cortical orientation maps visualized with intrinsic optical imaging techniques revealed vanishing of pin-wheels without recovery. The prolonged return to preadaptation maps is attributed to structural modifications occurring in dendritic branches [80].

3. Understanding at population level/interareal explorations

In previous sections, we described changes of neuronal selectivity occurring at the single cell level brought about by adaptation. As cells acquire new optimal properties, it is reasonable to postulate that these changes are the consequences of a new equilibrium between excitatory and inhibitory relationships amid reciprocally connected neurons. In other words, adaptation affects a cell's population activity. Intrinsic optical imaging revealed that on the surface of the visual cortex, orientation preference forms parallel slabs [81–83]. These maps exhibit two fundamental features such as linear zones (with orientation remaining the same over these zones) or singularities and fractures (orientation preferences are changing abruptly over a short distance of cortical surface) [84]. Also, investigations have demonstrated that the layout of orientation preference maps is roughly scattered around pinwheel centers, rather than aligned in slabs [80, 85]. Within pinwheels, adjacent neurons at the center of pinwheels display large differences in orientation preference. For example, neurons with orthogonal orientations are in proximity [14, 85]. Such a display makes pinwheel areas particularly susceptible to adaptation since the convergence of a broad range of orientation preferences presents a large potential for reorganization, because there are numerous mutual connections between cells directly or through inhibitory interneurons.

4. Modulation of plasticity by application of drugs

In parallel with physiological processes inducing plasticity, drugs and other substances which operate as a neurotransmitter or selective neurotransmitter reuptake inhibitor and modulate visual plasticity [86]. Indeed, some of them, such as the protein Lynx1, decrease the level of plasticity and provoke stability by locking the cortical network [87].

4.1. Effect of serotonin and fluoxetine on cortical plasticity

Fluoxetine, which is antidepressant and reacts with selective serotonin reuptake inhibitor (SSRI), restores ocular-dominance plasticity in adult rats, when they are treated in a long-term protocol [88, 89]. In line with the previously published data, it has been shown that after the treatment of ischemic stroke patient with fluoxetine, there is facilitation of the motor recovery in comparison to placebo subjects [90]. Similar to the antidepressant fluoxetine, it has been shown that the neurotransmitter serotonin increase the attractive behavior (attractive shift is a shift of a peak of the orientation tuning curve), following adaptation in primary visual cortex V1 in anesthetized adult cats. Few neurons will serve as a reference for the other cells that lose their

stability during adaptation to achieve a new preferred selectivity in the direction of the adapter. Likewise, repulsive neurons shift their orientation tuning peaks away from the direction of forced orientation. In this study, it has been shown that the larger attractive shifts of the peak of the orientation tuning curve (attractive to attractive) are stronger in case of serotonin application if compared to fluoxetine. Hence, this result suggests that for the group of cells that increased the attractive effect during adaptation with drug administration, the effect is due to direct serotoninergic actions; however, the non-significant attractive amplified effect of fluoxetine (SSRI) could be explained by an indirect weaker process such as inhibition of serotonin reuptake. This indirect path is is reported to potentiate after long-term chronic administration in rats [88, 91]. In the same framework, Komlosi et al. [92] showed that the influence of fluoxetine on the polysynaptic transmission is relatively smaller than the serotonin action. In addition, it is shown that both drugs affect amplify the shift magnitude but not the firing magnitude of neurons post-drug administration and adaptation. In other words, serotonin and fluoxetine modulate the plasticity by acting on polysynaptic transmission which affects, for the most part, the selectivity range of a neuron rather than its evoked discharge rate. Thus, these differential effects of both drugs can be explained by the saturation of the firing rates; so, the strength of the evoked discharges remain relatively stable after application of drugs, while the increase in orientation-selectivity can be due to the ability of serotonin and fluoxetine to change the threshold of neurons. Therefore, neurons exhibit a higher firing rate with a new preferred orientation enhanced to the adapter. This explanation suggests that both drugs act at synapse level causing a drift (displacement) toward the adaptor. Based on the fact that spontaneous activity remained unmodified after administration of both drugs, the previous idea seems to be supported. Furthermore, serotonin, as well as fluoxetine, has a partial effect on evoked response magnitude. Indeed, both significantly affect the response amplitude evoked by the adapter and the original preferred orientations but not those that were evoked by flank orientations.

Molecular processes are further developed below:

Overall, fluoxetine (SSRI) and serotonin (neurotransmitter) promote sensitization of refractory cells (which maintain their preference after adaptation) by acting on synaptic components and lead them to learn an non-preferred stimulus, enhance the attractive effect of neurons, and contribute to increasing the plasticity for the repulsive cells. In the primary visual cortex, the ability of neurons to learn a non-preferred stimulus drives synaptic reorganization that serves as a scaffold and contribute to cerebral pharmacological treatments or cognitive mechanisms such as learning or memory.

4.2. Effect of ketamine on cortical plasticity

In a similar direction to previous reports from our laboratory, we sought to examine the effect of ketamine on the modulation of adaptation-induced orientation plasticity in the primary visual cortex of anesthetized mice. Ketamine is widely used in clinical medicine as a short-acting dissociative anesthetic. The preliminary results show that post-adaptation firing rate is lower than that of control. However, even when ketamine was applied on adapted neurons, post-adaptation firing rate did not significantly decrease in comparison with control. As

adaptation is a mechanism used to understand plasticity, we suggest that ketamine acts as a short-term blocker of the orientation plasticity post-adaptation by reducing the response rate following adaptation.

In the same framework, we aimed to investigate the effect of ketamine on the potential plasticity of neurons in V1 of anesthetized mice by comparing several parameters which were measured before and after the application of ketamine. Our data shows that following ketamine, a majority of cells shifted their optimal orientation. The comparison of mean of OSI between control and post-drug application revealed a significant decrease in the OSI post ketamine, which implies that application of ketamine weakened the initial orientation selectivity of neurons in V1. However, the bandwidth of orientation tuning curves did not display any significant modification between the two conditions (before and after ketamine application). The measure of the amplitude of the highest response displayed by the Gaussian-like function shows two populations of cells: one that initially (control condition) had weak amplitudes but increased after ketamine application and the other that initially had strong amplitudes but decreased after ketamine application (**Figure 5**). Thus, ketamine modulates the initial downward or upward amplitudes of Gaussian-like function. However, it was not known to what factor this modulation is correlated. To assess and describe the variability of neuronal response, a Fano factor (FF) was calculated for each neuron by dividing the variance of a neuron by the mean of firing rate of the same neuron. The larger the Fano factor is, the more significant is the variability of the neuronal response and vice versa. The comparison of evoked response variability before and after ketamine application shows that the value of the FF decreases significantly post ketamine, which meant that ketamine declines the cells' potential to respond variably to a large range of orientations. So, ketamine not only narrows the window of the variability of cells' response to stimuli, but also weakens their orientation selectivity. Moreover, it was revealed that following ketamine application, the FF value of spontaneous and evoked response remains similar while they were significantly different in the absence of ketamine. This suggests that ketamine decreases the orientation selectivity of cells and brings their evoked activities in response to stimuli closer to their spontaneous activities (**Figure 5**). The FF values of spontaneous responses calculated before and after ketamine application remained similar that suggests that ketamine does not affect the spontaneous response and its effect is not global but limited to evoked responses. In summary, ketamine causes orientation shifts, modulates the highest amplitude of Gaussian-like function, decreases the orientation selectivity, and narrows the variability range of evoked responses by acting at synaptic transmission while modifying the synaptic functional domain. Globally, ketamine features a sort of inhibitory effect on V1 potential plasticity. Molecular bases underlying cortex plasticity in general and how fluoxetine, serotonin, and ketamine can modulate the cortical plasticity, are discussed in the following section.

4.3. Molecular mechanism of cortical plasticity and pathways related to action of drugs

The studies on mammalian visual cortex have long been a field of discovery of mechanisms leading to plasticity during development and adulthood because of the ease of its handling and measuring results at physiological, anatomical, and molecular levels. Importantly, the experience-dependent plasticity derived from ancestral mechanisms occurs during development [4, 93, 94].

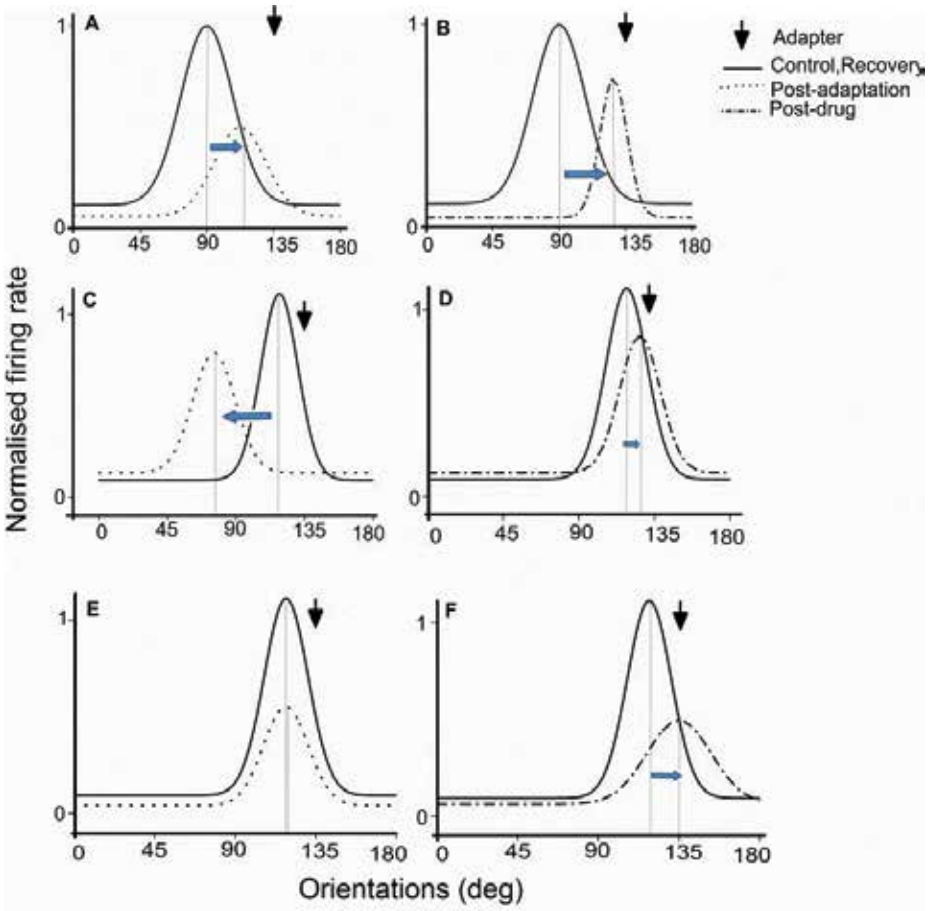

Figure 5. Effect of serotonin on the response of cells. A and B: amplified attractive effect of the drug—(A) model of Gaussian fit of normalized responses of one neuron for control (bold) and post-adaptation (dot). Black arrow represents adapting orientation. Gaussian fits show a shift of the tuning curve (attractive shift). (B) The Gaussian fit of normalized responses of the same neuron after recovery (bold) and after the second adaptation during serotonin application (dashed); the new attractive shift is bigger. C and D: inversion of the repulsive shift by the drug—(C) the Gaussian fit of normalized responses of one neuron for control (bold) and after the first adaptation process (dot). Black arrow represents adapting orientation. Gaussian fits show a shift of the tuning curve (repulsive shift). (D) The Gaussian fit of normalized responses of the same neuron after recovery (bold) and after the second adaptation during serotonin application (dashed). Note the inversion of repulsive shift after drug administration. (E) The Gaussian fit of normalized responses of one neuron for control and post-adaptation conditions (bold and dot curves, respectively). Black arrow represents the adapter. Gaussian fits that are superimposed show a non-significant shift after the first adaptation. (F) The Gaussian fit of normalized responses of the same cell for recovery and second adaptation in the presence of serotonin (bold and dashed curves, respectively). The tuning curve is shifted toward the adapter in the presence of the drug.

4.3.1. Molecular mechanisms of feed-forward plasticity

4.3.1.1. Glutamatergic receptors

Excitatory transmission is mediated by ionotropic glutamatergic channels' receptors AMPA and NMDA, which contribute to regulating membrane depolarization and calcium

permeability, through mGluR (metabotropic glutamate) receptors, which trigger downstream signaling cascades. Evidence exists that each of these receptor types may promote plasticity in visual cortex [95].

Frenkel et al. [15] have shown that a process similar to long-term potentiation (LTP) depending on NMDA receptor activation by repetitive activation leads to increased insertion of synaptic α-amino-3-hydroxy-5-methyl-4-isoxazolepropionic acid (AMPA) receptor allowing strengthening of responses to repeated stimuli. This model of molecular plasticity is present both in juvenile and adult animals. The structure of NMDA receptors varies NR1, and either of NR2A or NR2B subunits, and they regulate the membrane depolarization and intracellular calcium level. Therefore, the excitatory transmission mediated by glutamate-gated NMDA receptor is affected. It is very well known that during post-natal development, the ratio NR2A/NR2B transits from low to high. Decreasing this ratio promotes plasticity by affecting the threshold for LTP. Since it was shown that ketamine blocks the NMDA receptors [96], there is a decrease in plasticity. Indeed, ketamine is an NMDA non-competitive antagonist. When the NMDA receptor is active, ketamine binds to it by sealing the lumen of the channel. Therefore, it creates a physical obstacle to ion currents through the channel pore. When the channel closes, ketamine becomes trapped [97]. Because plasticity requires NMDA receptor activation [98], the deprivation decrease of this activity leads to a reduction in inhibition effect on plasticity. Contrary to the effect of ketamine, it was demonstrated in adult rats that serotonin restores the NMDA-dependent long-term potentiation. Metabotropic glutamate receptors are also involved in cortex plasticity independently of its subtype [95]. It is worth noting that fluoxetine potentiates plasticity by increasing glutamatergic synaptic transmission [99].

In the brain, AMPA receptors are primarily composed of GluR2 and either GluR1 or GluR3 subunits. Synaptic strength, resulting in LTP and, by some effect, plasticity, are significantly determined by AMPA receptor [100]. Other finding shows that ketamine is a non-selective blocker of NMDA channel, and it also acts on AMPA/kainate receptors. Therefore, it seems that ketamine is a blocker of two ionotropic glutamate receptor channel-types in a concentration-dependent manner. This effect was determined by using whole-cell patch clamp technique and mediated by pharmacologically isolated AMPA/kainate receptor channels on membrane proprieties of pyramidal neurons of gerbil neocortex including the auditory cortex. Results show that ketamine lowers the amplitude of fast EPSPs mediated by AMPA/kainate receptor channels. In addition, ketamine increased the resting input resistance (RI). By Ohm's law, a small increase in cellular resistance outweighs the impact on synaptic efficacy, resulting in a corresponding increase in membrane potential that was due in part to a partial blockade of AMPA/kainate receptor channels. The outcome of this is that the reduction of fast synaptic currents attenuates depolarizing changes that contribute to voltage-dependent release of magnesium to achieve the threshold for NMDA receptor channels open states.

4.3.1.2. Calcium: a second messenger

Glutamate-gated AMPA and NMDA receptors regulate intracellular calcium level. As a second messenger, calcium activates many intracellular signaling cascades mainly including three critical kinases (ERK: called ERK, extracellular signal-regulated kinases; PKA: protein kinase

A; and CaMKII alpha: calcium/calmodulin-dependent protein kinase II alpha) [101–104]. These kinases may modulate synaptic strength and induce plasticity by phosphorylating plasticity-regulating molecules or mediating changes in target gene transcription synaptic signaling molecules by activating C-AMP response element-binding protein (CREB) [105]. CREB levels mediated by visual stimulation decrease with age, showing the involvement of other pathways promoting plasticity in the adult cortex [106].

4.3.1.3. GABAergic inhibition and BDNF downstream events

An indirect consequence of adjustments of GABAergic (gamma-aminobutyric acid-mediated) circuitry could be implied in changes in visually evoked responses. It was found that the infusion of brain-derived neurotrophic factor (BDNF) during monocular deprivation probably reduced the GABAergic transmission and reinstalled plasticity [88, 107–109]. The same pathway is induced by chronic treatment of fluoxetine exhibits in rats. Indeed, fluoxetine decreases GABAergic inhibition and thereby increases BDNF expression. Serotonin transmission has a similar effect as it potentiates the BDNF-trkB signaling path. Hence, fluoxetine and serotonin promote plasticity in adult rodents.

4.3.1.4. Structural plasticity

Several investigations demonstrate that sensory experience influences both structure and dynamics of dendritic spines which underlines structural plasticity [110, 111]. In visual cortex, reducing the density of spines leads to a decrease in the deprived-eye drive [112]. Moreover, the spine stabilization is induced by NMDA and AMPA synaptic activation [113]. It appears that ketamine increases spine dynamics by blocking NMDA receptors.

Several studies show that agonists of adrenergic and cholinergic systems facilitate the onset of ocular dominance plasticity [114, 115]. The effect of fluoxetine resulting in a restoration of ocular dominance plasticity to adults, probably due to a correlative reduction in inhibition, underlines an analogous function for the serotoninergic system [99].

Neuromodulators affect plasticity possibly to their ability to modulate thresholds for LTP/LTD induction by modifying the intracellular calcium concentration via second messenger pathways [116, 117]. Moreover, it seems that these neuromodulators systems selectively interact with growth factors to affect plastic changes. For instance, acetylcholine fibers host the majority of the receptors for the neurotrophin nerve growth factor. Therefore, this system may mediate the effects of the growth factor [118, 119] on ocular dominance plasticity.

4.3.1.5. Contribution of neuromodulators to cortical plasticity in relation to feed-forward mechanisms

Adrenergic, cholinergic, and serotoninergic systems are essential for the primary function of visual cortex. Indeed, they control the morphological reorganization of the circuitry. For instance, the application of noradrenaline and serotonin modulates, in an age-dependent manner, the number of synapses. Interestingly, these systems facilitate the ocular dominance

plasticity possibly by modulating thresholds for LTP/LTD induction resulting in modification of intracellular calcium concentration. Maya Vetencourt and co-authors [88] showed that the administration of fluoxetine restores ocular dominance plasticity in adults, possibly due to a correlative reduction in inhibition.

Knowing that preferential orientation of neurons may change following adaptation or could be modified using specific compounds, underlines plasticity within the adult cortex, and adds a ray of hope in various clinical situations. However, the mechanisms responsible for the constant changes in the adult brain are not fully elucidated; that is why, the plasticity is a key property, which we should more investigate.

5. Conclusions

Senses make us alive by detecting a diverse set of external signals with incredible sensitivity and specificity. We are thus capable of detecting changes in our environments and adjusting our behavior appropriately. Sensory cortices are thus referred to as "plastic," wherein changes across brain systems and related behaviors modulate as a function of the time and the nature of experience. There are missing links of knowledge concerning unimodal sensory deprivation on the direct functioning of neighboring primary sensory areas and missing sensory modalities. Moreover, a few cross-modal studies have opened gates toward the understanding of the interaction between multimodal sensory areas. There is a need to determine the multimodal nature of primary sensory areas and the extent to which the structural changes that can be observed ultimately leading to behavioral changes. Future studies implying high-resolution approach would be able to clarify the roles of these areas in compensatory sensory changes and brain reorganization. Still, summarizing from the discussion of the role of sensory areas and sensory regions exhibiting multisensory conduct is it not fair to ask; Is cortex essentially multisensory? Is cortex plastic or elastic? After describing different studies and results from our own and few other protocols, we may suggest that the answer is indeed YES. Cortex is essentially multisensory! Moreover, the argument that brain is plastic or elastic is still yet to be further scrutinized. It may be concluded that external factors govern the dynamics of the brain and the extent and nature of experience at different stages of life could be the most deciding factor or brain plasticity.

Author details

Nayan Chanauria†, Rudy Lussiez†, Afef Ouelhazi† and Stephane Molotchnikoff*

*Address all correspondence to: stephane.molotchnikoff@umontreal.ca

Department of Biological Sciences, University of Montreal, Quebec, Canada

† These authors contributed equally.

References

[1] Adeli M, Rouat J, Molotchnikoff S. Audiovisual correspondence between musical timbre and visual shapes. Frontiers in Human Neuroscience. 2014;**8**:352

[2] Bharmauria V, Bachatene L, Cattan S, Brodeur S, Chanauria N, Rouat J, et al. Network-selectivity and stimulus-discrimination in the primary visual cortex: Cell-assembly dynamics. The European Journal of Neuroscience. 2016;**43**(2):204-219

[3] Bharmauria V, Bachatene L, Cattan S, Chanauria N, Rouat J, Molotchnikoff S. Stimulus-dependent augmented gamma oscillatory activity between the functionally connected cortical neurons in the primary visual cortex. The European Journal of Neuroscience. 2015;**41**(12):1587-1596

[4] Sur M, Rubenstein JL. Patterning and plasticity of the cerebral cortex. Science. 2005;**310**(5749):805-810

[5] Sharma J, Angelucci A, Sur M. Induction of visual orientation modules in auditory cortex. Nature. 2000;**404**(6780):841-847

[6] Innocenti GM, Price DJ. Exuberance in the development of cortical networks. Nature Reviews Neuroscience. 2005;**6**(12):955-965

[7] Beauchamp MS, Lee KE, Argall BD, Martin A. Integration of auditory and visual information about objects in superior temporal sulcus. Neuron. 2004;**41**(5):809-823

[8] Clark SA, Allard T, Jenkins WM, Merzenich MM. Receptive fields in the body-surface map in adult cortex defined by temporally correlated inputs. Nature. 1988;**332**(6163):444-445

[9] Merzenich MM, Nelson RJ, Stryker MP, Cynader MS, Schoppmann A, Zook JM. Somatosensory cortical map changes following digit amputation in adult monkeys. The Journal of Comparative Neurology. 1984;**224**(4):591-605

[10] Kupers R, Fumal A, de Noordhout AM, Gjedde A, Schoenen J, Ptito M. Transcranial magnetic stimulation of the visual cortex induces somatotopically organized qualia in blind subjects. Proceedings of the National Academy of Sciences. 2006;**103**(35):13256-13260

[11] Ptito M, Moesgaard SM, Gjedde A, Kupers R. Cross-modal plasticity revealed by electrotactile stimulation of the tongue in the congenitally blind. Brain. 2005;**128**(3):606-614

[12] Bach-y-Rita P, Kercel W, Sensory S. Substitution and the human–machine interface. Trends in Cognitive Sciences. 2003;**7**(12):541-546

[13] Kandel ER. The biology of memory: A forty-year perspective. The Journal of Neuroscience: The Official Journal of the Society for Neuroscience. 2009;**29**(41):12748-12756

[14] Basole A, White LE, Fitzpatrick D. Mapping multiple features in the population response of visual cortex. Nature. 2003;**423**(6943):986-990

[15] Frenkel MY, Sawtell NB, Diogo AC, Yoon B, Neve RL, Bear MF. Instructive effect of visual experience in mouse visual cortex. Neuron. 2006;**51**(3):339-349

[16] Kohn A. Visual adaptation: Physiology, mechanisms, and functional benefits. Journal of Neurophysiology. 2007;**97**(5):3155-3164

[17] Kokovay E, Temple S. Taking neural crest stem cells to new heights. Cell. 2007;**131**(2): 234-236

[18] McCoy PA, Huang HS, Philpot BD. Advances in understanding visual cortex plasticity. Current Opinion in Neurobiology. 2009;**19**(3):298-304

[19] Sur M, Schummers J, Dragoi V. Cortical plasticity: Time for a change. Current Biology: CB. 2002;**12**(5):R168-R170

[20] Watroba L, Buser P, Milleret C. Impairment of binocular vision in the adult cat induces plastic changes in the callosal cortical map. The European Journal of Neuroscience. 2001;**14**(6):1021-1029

[21] Gourevitch B, Eggermont JJ. Spectro-temporal sound density-dependent long-term adaptation in cat primary auditory cortex. The European Journal of Neuroscience. 2008;**27**(12):3310-3321

[22] Armstrong-James M, Diamond ME, Ebner FF. An innocuous bias in whisker use in adult rats modifies receptive fields of barrel cortex neurons. The Journal of Neuroscience: The Official Journal of the Society for Neuroscience. 1994;**14**(11 Pt 2):6978-6991

[23] Dragoi V, Sharma J, Sur M. Adaptation-induced plasticity of orientation tuning in adult visual cortex. Neuron. 2000;**28**(1):287-298

[24] Ghisovan N, Nemri A, Shumikhina S, Molotchnikoff S. Long adaptation reveals mostly attractive shifts of orientation tuning in cat primary visual cortex. Neuroscience. 2009;**164**(3):1274-1283

[25] Nemri A, Ghisovan N, Shumikhina S, Molotchnikoff S. Adaptive behavior of neighboring neurons during adaptation-induced plasticity of orientation tuning in VI. BMC Neuroscience. 2009;**10**:147

[26] Bachatene L, Bharmauria V, Rouat J, Molotchnikoff S. Adaptation-induced plasticity and spike waveforms in cat visual cortex. Neuroreport. 2012;**23**(2):88-92

[27] Cattan S, Bachatene L, Bharmauria V, Jeyabalaratnam J, Milleret C, Molotchnikoff S. Comparative analysis of orientation maps in areas 17 and 18 of the cat primary visual cortex following adaptation. The European Journal of Neuroscience. 2014;**40**(3):2554-2563

[28] Bouchard M, Gillet PC, Shumikhina S, Molotchnikoff S. Adaptation changes the spatial frequency tuning of adult cat visual cortex neurons. Experimental Brain Research. 2008;**188**(2):289-303

[29] Clifford CW. Perceptual adaptation: Motion parallels orientation. Trends in Cognitive Sciences. 2002;**6**(3):136-143

[30] Tootell RB, Hadjikhani NK, Vanduffel W, Liu AK, Mendola JD, Sereno MI, et al. Functional analysis of primary visual cortex (V1) in humans. Proceedings of the National Academy of Sciences of the United States of America. 1998;**95**(3):811-817

[31] Jin DZ, Dragoi V, Sur M, Seung HS. Tilt aftereffect and adaptation-induced changes in orientation tuning in visual cortex. Journal of Neurophysiology. 2005;**94**(6):4038-4050

[32] Tolias AS, Sultan F, Augath M, Oeltermann A, Tehovnik EJ, Schiller PH, et al. Mapping cortical activity elicited with electrical microstimulation using FMRI in the macaque. Neuron. 2005;**48**(6):901-911

[33] Kohn A, Movshon JA. Neuronal adaptation to visual motion in area MT of the macaque. Neuron. 2003;**39**(4):681-691

[34] Kohn A, Movshon JA. Adaptation changes the direction tuning of macaque MT neurons. Nature Neuroscience. 2004;**7**(7):764-772

[35] Yang J, Lisberger SG. Relationship between adapted neural population responses in MT and motion adaptation in speed and direction of smooth-pursuit eye movements. Journal of Neurophysiology. 2009;**101**(5):2693-2707

[36] Schlack A, Albright TD. Remembering visual motion: Neural correlates of associative plasticity and motion recall in cortical area MT. Neuron. 2007;**53**(6):881-890

[37] Hietanen MA, Crowder NA, Price NS, Ibbotson MR. Influence of adapting speed on speed and contrast coding in the primary visual cortex of the cat. The Journal of Physiology. 2007;**584**(Pt 2):451-462

[38] Priebe NJ, Lampl I, Ferster D. Mechanisms of direction selectivity in cat primary visual cortex as revealed by visual adaptation. Journal of Neurophysiology. 2010;**104**(5):2615-2623

[39] Krekelberg B, van Wezel RJ, Albright TD. Adaptation in macaque MT reduces perceived speed and improves speed discrimination. Journal of Neurophysiology. 2006;**95**(1): 255-270

[40] Movshon JA, Lennie P. Pattern-selective adaptation in visual cortical neurones. Nature. 1979;**278**(5707):850-852

[41] Saul AB, Cynader MS. Adaptation in single units in visual cortex: The tuning of aftereffects in the temporal domain. Visual Neuroscience. 1989;**2**(6):609-620

[42] Levinson E, Sekuler R. Adaptation alters perceived direction of motion. Vision Research. 1976;**16**(7):779-781

[43] Blakemore C, Carpenter RH, Georgeson MA. Lateral inhibition between orientation detectors in the human visual system. Nature. 1970;**228**(5266):37-39

[44] Jia H, Rochefort NL, Chen X, Konnerth A. Dendritic organization of sensory input to cortical neurons in vivo. Nature. 2010;**464**(7293):1307-1312

[45] Marshansky S, Shumikhina S, Molotchnikoff S. Repetitive adaptation induces plasticity of spatial frequency tuning in cat primary visual cortex. Neuroscience. 2011;**172**:355-365

[46] Bachatene L, Bharmauria V, Cattan S, Molotchnikoff S. Fluoxetine and serotonin facilitate attractive-adaptation-induced orientation plasticity in adult cat visual cortex. The European Journal of Neuroscience. 2013;**38**(1):2065-2077

[47] Fregnac Y, Pananceau M, Rene A, Huguet N, Marre O, Levy M, et al. A re-examination of Hebbian-covariance rules and spike timing-dependent plasticity in cat visual cortex in vivo. Frontiers in Synaptic Neuroscience. 2010;**2**:147

[48] Jeyabalaratnam J, Bharmauria V, Bachatene L, Cattan S, Angers A, Molotchnikoff S. Adaptation shifts preferred orientation of tuning curve in the mouse visual cortex. PLoS One. 2013;**8**(5):e64294

[49] Bachatene L, Bharmauria V, Cattan S, Rouat J, Molotchnikoff S. Reprogramming of orientation columns in visual cortex: A domino effect. Scientific Reports. 2015;**5**:9436

[50] Chanauria N, Bharmauria V, Bachatene L, Cattan S, Rouat J, Molotchnikoff S. Comparative effects of adaptation on layers II–III and V–VI neurons in cat V1. The European Journal of Neuroscience. 2016;**44**(12):3094-3104

[51] Kell CA, von Kriegstein K, Rösler A, Kleinschmidt A, Laufs H. The sensory cortical representation of the human penis: Revisiting Somatotopy in the male homunculus. The Journal of Neuroscience. 2005;**25**(25):5984

[52] Cazala F, Vienney N, Stoléru S. The cortical sensory representation of genitalia in women and men: A systematic review. Socioaffective Neuroscience & Psychology. 2015;**5**. DOI: 10.3402/snp.v5.26428

[53] Penfield W, Boldrey E. Somatic motor and sensory representation in the cerebral cortex of man as studied by electrical stimulation. Brain. 1937;**60**(4):389-443

[54] Sanchez-Panchuelo RM, Francis S, Bowtell R, Schluppeck D. Mapping human somatosensory cortex in individual subjects with 7T functional MRI. Journal of Neurophysiology. 2010;**103**(5):2544-2556

[55] Tusa RJ, Palmer LA, Rosenquist AC. The retinotopic organization of area 17 (striate cortex) in the cat. The Journal of Comparative Neurology. 1978;**177**(2):213-235

[56] Tusa RJ, Rosenquist AC, Palmer LA. Retinotopic organization of areas 18 and 19 in the cat. The Journal of Comparative Neurology. 1979;**185**(4):657-678

[57] Hubel DH, Wiesel TN. Receptive fields, binocular interaction and functional architecture in the cat's visual cortex. The Journal of Physiology. 1962;**160**(1):106-154

[58] Maier DL, Mani S, Donovan SL, Soppet D, Tessarollo L, McCasland JS, et al. Disrupted cortical map and absence of cortical barrels in growth-associated protein (GAP)-43 knockout mice. Proceedings of the National Academy of Sciences of the United States of America. 1999;**96**(16):9397-9402

[59] Lee L-J, Erzurumlu RS. Altered Parcellation of neocortical somatosensory maps in N-methyl-ᴅ-aspartate receptor-deficient mice. The Journal of Comparative Neurology. 2005;**485**(1):57-63

[60] Polley DB, Rickert JL, Frostig RD. Whisker-based discrimination of object orientation determined with a rapid training paradigm. Neurobiology of Learning and Memory. 2005;**83**(2):134-142

[61] Anjum F, Turni H, Mulder PGH, van der Burg J, Brecht M. Tactile guidance of prey capture in Etruscan shrews. Proceedings of the National Academy of Sciences. 2006;**103**(44):16544-16549

[62] Connor DH, Clack NG, Huber D, Komiyama T, Myers EW, Svoboda K. Vibrissa-based object localization in head-fixed mice. The Journal of Neuroscience. 2010;**30**(5):1947

[63] Mehta SB, Whitmer D, Figueroa R, Williams BA, Kleinfeld D. Active spatial perception in the Vibrissa scanning sensorimotor system. PLOS Biology. 2007;**5**(2):e15

[64] Krupa DJ, Matell MS, Brisben AJ, Oliveira LM, Nicolelis MAL. Behavioral properties of the trigeminal somatosensory system in rats performing whisker-dependent tactile discriminations. The Journal of Neuroscience. 2001;**21**(15):5752

[65] Boubenec Y, Claverie LN, Shulz DE, Debrégeas G. An amplitude modulation/demodulation scheme for whisker-based texture perception. The Journal of Neuroscience. 2014;**34**(33):10832

[66] Lottem E, Azouz R. Dynamic translation of surface coarseness into whisker vibrations. Journal of Neurophysiology. 2008;**100**(5):2852

[67] Woolsey TA, Van der Loos H. The structural organization of layer IV in the somatosensory region (S I) of mouse cerebral cortex: The description of a cortical field composed of discrete cytoarchitectonic units. Brain Research. 1970;**17**(2):205-242

[68] Welker C, Woolsey TA. Structure of layer IV in the somatosensory neocortex of the rat: Description and comparison with the mouse. The Journal of Comparative Neurology. 1974;**158**(4):437-453

[69] de Kock CPJ, Sakmann B. Spiking in primary somatosensory cortex during natural whisking in awake head-restrained rats is cell-type specific. Proceedings of the National Academy of Sciences. 2009;**106**(38):16446-16450

[70] de Kock CP, Sakmann B. Spiking in primary somatosensory cortex during natural whisking in awake head-restrained rats is cell-type specific. Proceedings of the National Academy of Sciences of the United States of America. 2009;**106**(38):16446-16450.

[71] Wu H-PP, Ioffe JC, Iverson MM, Boon JM, Dyck RH. Novel, whisker-dependent texture discrimination task for mice. Behavioural Brain Research. 2013;**237**(Supplement C):238-242

[72] Pacchiarini N, Fox K, Honey RC. Perceptual learning with tactile stimuli in rodents: Shaping the somatosensory system. Learning & Behavior. 2017;**45**(2):107-114

[73] Ghazanfar AA, Schroeder CE. Is neocortex essentially multisensory? Trends in Cognitive Sciences. 2006;**10**(6):278-285

[74] Driver J, Noesselt T. Multisensory interplay reveals crossmodal influences on 'sensory-specific' brain regions, neural responses, and judgments. Neuron. 2008;**57**(1):11-23

[75] Muckli L, Petro LS. Network interactions: Non-geniculate input to V1. Current Opinion in Neurobiology. 2013;**23**(2):195-201

[76] Vetter P, Smith FW, Muckli L. Decoding sound and imagery content in early visual cortex. Current Biology: CB. 2014;**24**(11):1256-1262

[77] Ibrahim LA, Mesik L, Ji XY, Fang Q, Li HF, Li YT, et al. Cross-modality sharpening of visual cortical processing through layer-1-mediated inhibition and disinhibition. Neuron. 2016;**89**(5):1031-1045

[78] Antonini A, Stryker MP. Rapid remodeling of axonal arbors in the visual cortex. Science. 1993;**260**(5115):1819-1821

[79] Keck T, Scheuss V, Jacobsen RI, Wierenga CJ, Eysel UT, Bonhoeffer T, et al. Loss of sensory input causes rapid structural changes of inhibitory neurons in adult mouse visual cortex. Neuron. 2011;**71**(5):869-882

[80] Godde B, Leonhardt R, Cords SM, Dinse HR. Plasticity of orientation preference maps in the visual cortex of adult cats. Proceedings of the National Academy of Sciences of the United States of America. 2002;**99**(9):6352-6357

[81] Blasdel GG. Differential imaging of ocular dominance and orientation selectivity in monkey striate cortex. The Journal of Neuroscience: The Official Journal of the Society for Neuroscience. 1992;**12**(8):3115-3138

[82] Frostig RD, Lieke EE, Ts'o DY, Grinvald A. Cortical functional architecture and local coupling between neuronal activity and the microcirculation revealed by in vivo high-resolution optical imaging of intrinsic signals. Proceedings of the National Academy of Sciences of the United States of America. 1990;**87**(16):6082-6086

[83] Bonhoeffer T, Grinvald A. Iso-orientation domains in cat visual cortex are arranged in pinwheel-like patterns. Nature. 1991;**353**(6343):429-431

[84] Swindale NV. Cortical organization: Modules, polymaps and mosaics. Current Biology: CB. 1998;**8**(8):R270-R273

[85] Maldonado PE, Godecke I, Gray CM, Bonhoeffer T. Orientation selectivity in pinwheel centers in cat striate cortex. Science. 1997;**276**(5318):1551-1555

[86] Mataga N, Imamura K, Watanabe Y. L-threo-3,4-dihydroxyphenylserine enhanced ocular dominance plasticity in adult cats. Neuroscience Letters. 1992;**142**(2):115-118

[87] Morishita H, Miwa JM, Heintz N, Hensch TK. Lynx1, a cholinergic brake, limits plasticity in adult visual cortex. Science. 2010;**330**(6008):1238-1240

[88] Maya Vetencourt JF, Sale A, Viegi A, Baroncelli L, De Pasquale R, O'Leary OF, et al. The antidepressant fluoxetine restores plasticity in the adult visual cortex. Science. 2008;**320**(5874):385-388

[89] Maya Vetencourt JF, Tiraboschi E, Spolidoro M, Castren E, Maffei L. Serotonin triggers a transient epigenetic mechanism that reinstates adult visual cortex plasticity in rats. The European Journal of Neuroscience. 2011;**33**(1):49-57

[90] Chollet F, Tardy J, Albucher JF, Thalamas C, Berard E, Lamy C, et al. Fluoxetine for motor recovery after acute ischaemic stroke (FLAME): A randomised placebo-controlled trial. The Lancet Neurology. 2011;**10**(2):123-130

[91] Wang C, Liu JL, Sang HF, Lu Y, Dong HL, Xiong LZ. Therapeutic time window of flurbiprofen axetil's neuroprotective effect in a rat model of transient focal cerebral ischemia. Chinese Medical Journal. 2008;**121**(24):2572-2577

[92] Komlosi G, Molnar G, Rozsa M, Olah S, Barzo P, Tamas G. Fluoxetine (prozac) and serotonin act on excitatory synaptic transmission to suppress single layer 2/3 pyramidal neuron-triggered cell assemblies in the human prefrontal cortex. The Journal of Neuroscience: The Official Journal of the Society for Neuroscience. 2012;**32**(46):16369-16378

[93] Crowley JC, Katz LC. Development of ocular dominance columns in the absence of retinal input. Nature Neuroscience. 1999;**2**(12):1125-1130

[94] Sur M, Leamey CA. Development and plasticity of cortical areas and networks. Nature Reviews Neuroscience. 2001;**2**(4):251-262

[95] Tropea D, Van Wart A, Sur M. Molecular mechanisms of experience-dependent plasticity in visual cortex. Philosophical Transactions of the Royal Society of London Series B, Biological Sciences. 2009;**364**(1515):341-355

[96] Chen X, Shu S, Bayliss DA. HCN1 channel subunits are a molecular substrate for hypnotic actions of ketamine. The Journal of Neuroscience: The Official Journal of the Society for Neuroscience. 2009;**29**(3):600-609

[97] Beverly CM, Walters MD, Weber AM, Piedmonte MR, Ballard LA. Prevalence of hydronephrosis in patients undergoing surgery for pelvic organ prolapse. Obstetrics and Gynecology. 1997;**90**(1):37-41

[98] Sawtell NB, Frenkel MY, Philpot BD, Nakazawa K, Tonegawa S, Bear MF. NMDA receptor-dependent ocular dominance plasticity in adult visual cortex. Neuron. 2003;**38**(6):977-985

[99] Gu Q, Singer W. Involvement of serotonin in developmental plasticity of kitten visual cortex. The European Journal of Neuroscience. 1995;**7**(6):1146-1153

[100] Citri A, Malenka RC. Synaptic plasticity: Multiple forms, functions, and mechanisms. Neuropsychopharmacology: Official Publication of the American College of Neuropsychopharmacology. 2008;**33**(1):18-41

[101] Berardi N, Pizzorusso T, Ratto GM, Maffei L. Molecular basis of plasticity in the visual cortex. Trends in Neurosciences. 2003;**26**(7):369-378

[102] Di Cristo G, Berardi N, Cancedda L, Pizzorusso T, Putignano E, Ratto GM, et al. Requirement of ERK activation for visual cortical plasticity. Science. 2001;**292**(5525):2337-2340

[103] Taha S, Hanover JL, Silva AJ, Stryker MP. Autophosphorylation of alphaCaMKII is required for ocular dominance plasticity. Neuron. 2002;**36**(3):483-491

[104] Taha SA, Stryker MP. Ocular dominance plasticity is stably maintained in the absence of alpha calcium calmodulin kinase II (alphaCaMKII) autophosphorylation. Proceedings of the National Academy of Sciences of the United States of America. 2005;**102**(45):16438-16442

[105] Cancedda L, Putignano E, Impey S, Maffei L, Ratto GM, Pizzorusso T. Patterned vision causes CRE-mediated gene expression in the visual cortex through PKA and ERK. The Journal of Neuroscience: The Official Journal of the Society for Neuroscience. 2003;**23**(18):7012-7020

[106] Putignano E, Lonetti G, Cancedda L, Ratto G, Costa M, Maffei L, et al. Developmental downregulation of histone posttranslational modifications regulates visual cortical plasticity. Neuron. 2007;**53**(5):747-759

[107] Di Cristo G, Chattopadhyaya B, Kuhlman SJ, Fu Y, Belanger MC, Wu CZ, et al. Activity-dependent PSA expression regulates inhibitory maturation and onset of critical period plasticity. Nature Neuroscience. 2007;**10**(12):1569-1577

[108] Hensch TK, Fagiolini M, Mataga N, Stryker MP, Baekkeskov S, Kash SF. Local GABA circuit control of experience-dependent plasticity in developing visual cortex. Science. 1998;**282**(5393):1504-1508

[109] Jiang B, Huang ZJ, Morales B, Kirkwood A. Maturation of GABAergic transmission and the timing of plasticity in visual cortex. Brain Research. Brain Research Reviews. 2005;**50**(1):126-133

[110] Lendvai B, Stern EA, Chen B, Svoboda K. Experience-dependent plasticity of dendritic spines in the developing rat barrel cortex in vivo. Nature. 2000;**404**(6780):876-881

[111] Zito K, Svoboda K. Activity-dependent synaptogenesis in the adult mammalian cortex. Neuron. 2002;**35**(6):1015-1017

[112] Mataga N, Mizuguchi Y, Hensch TK. Experience-dependent pruning of dendritic spines in visual cortex by tissue plasminogen activator. Neuron. 2004;**44**(6):1031-1041

[113] Oray S, Majewska A, Sur M. Effects of synaptic activity on dendritic spine motility of developing cortical layer v pyramidal neurons. Cerebral Cortex. 2006;**16**(5):730-741

[114] Bear MF, Singer W. Modulation of visual cortical plasticity by acetylcholine and noradrenaline. Nature. 1986;**320**(6058):172-176

[115] Kasamatsu T, Pettigrew JD. Depletion of brain catecholamines: Failure of ocular dominance shift after monocular occlusion in kittens. Science. 1976;**194**(4261):206-209

[116] Kirkwood A, Rozas C, Kirkwood J, Perez F, Bear MF. Modulation of long-term synaptic depression in visual cortex by acetylcholine and norepinephrine. The Journal of Neuroscience: The Official Journal of the Society for Neuroscience. 1999;**19**(5):1599-1609

[117] Kobayashi M, Imamura K, Kaub PA, Nakadate K, Watanabe Y. Developmental regulation of intracellular calcium by N-methyl-ᴅ-aspartate and noradrenaline in rat visual cortex. Neuroscience. 1999;**92**(4):1309-1322

[118] Maffei L, Berardi N, Domenici L, Parisi V, Pizzorusso T. Nerve growth factor (NGF) prevents the shift in ocular dominance distribution of visual cortical neurons in monocularly deprived rats. The Journal of Neuroscience: The Official Journal of the Society for Neuroscience. 1992;**12**(12):4651-4662

[119] Rossi FM, Sala R, Maffei L. Expression of the nerve growth factor receptors TrkA and p75NTR in the visual cortex of the rat: Development and regulation by the cholinergic input. The Journal of Neuroscience: The Official Journal of the Society for Neuroscience. 2002;**22**(3):912-919

Chapter 4

Olfaction, among the First Senses to Develop and Decline

Emanuele Brai and Lavinia Alberi

Additional information is available at the end of the chapter

http://dx.doi.org/10.5772/intechopen.75061

Abstract

Olfaction is one of the most conserved senses across species. It plays a crucial role in animals' and humans' life by influencing food intake, reproduction and social behavior. The olfactory system is composed of a peripheral neuroepithelium and a central olfactory nerve and is one of the few central nervous system (CNS) structures with direct access to the external environment without passage through the Blood Brain Barrier (BBB). This makes this nerve system of importance for understanding how exogenous stimuli may contribute to neuronal damage as well as for diagnostic and therapeutic purposes. Interestingly, olfactory activity physiologically declines with aging, but its alteration can be further impaired by various neurological conditions. For example, in progressive neurodegenerative disorders, such as Alzheimer's disease (AD), olfaction is the first sense to be impaired before the onset of cognitive symptoms, suggesting that olfactory transmission may characterize early neural network imbalances. In this work, we will explore the main olfactory anatomical structures, the cytoarchitecture, the neurogenesis, several pathological conditions characterized by olfactory deficit and the potential use of this sense to diagnose and treat CNS pathologies.

Keywords: olfaction, olfactory system, olfactory dysfunction, Alzheimer's disease, chronic inflammation, cancer, traumatic brain injury, neurological disorders, olfactory tests, nasal biopsies, diagnosis, therapeutic target

1. Introduction

Olfaction is among the most preserved senses across species based on its fundamental role for survival. In fact, this sense influences vital activities such as feeding, reproductive and social behavior.

The variety of functions modulated by olfaction relies on the direct connectivity of the olfactory tract to the piriform cortex, entorhinal cortex, hippocampus and amygdala regulating innate and acquired olfactory perception, memory, fear and alertness (**Figure 1**). In mammals, the major components of the olfactory system consist of the olfactory neuroepithelium (OE), the primary olfactory area, the olfactory bulb (OB) and its cortical projections, considered as secondary olfactory network areas (**Figure 1**) [1]. The olfactory network is, besides the visual system, the only nerve tract with direct access to the external environment without passage through the BBB and represents a viable and non-invasive source of CNS-derived biomarkers. Furthermore, chemosensory transduction manifests itself through the sense of smell, which is readily testable [2]. The olfactory system starts developing at mid gestation [3–5] and is mainly unchanged in all vertebrates [6, 7]. After birth, olfaction is essential in assisting the development of locomotor activities and spatial orientation as demonstrated in both rodents and humans [8–11]. These evidences underlie how the onset of olfactory deficits may induce a wide range of (reversible or irreversible) impairments with potential life-threatening consequences. The most common alterations consist in either an exaggerated sense of smell "hyperosmia," a reduced sense of smell "hyposmia" or the absence of smell "anosmia". Hyperosmia is often co-symptomatic to schizophrenia and manic disorders [12, 13], whereas hyposmia occurs naturally with aging [14] and is exacerbated in progressive neurodegenerative disorders, such as Alzheimer's disease (AD) and Parkinson's disease (PD) [14–17]. In addition, olfaction can be also completely

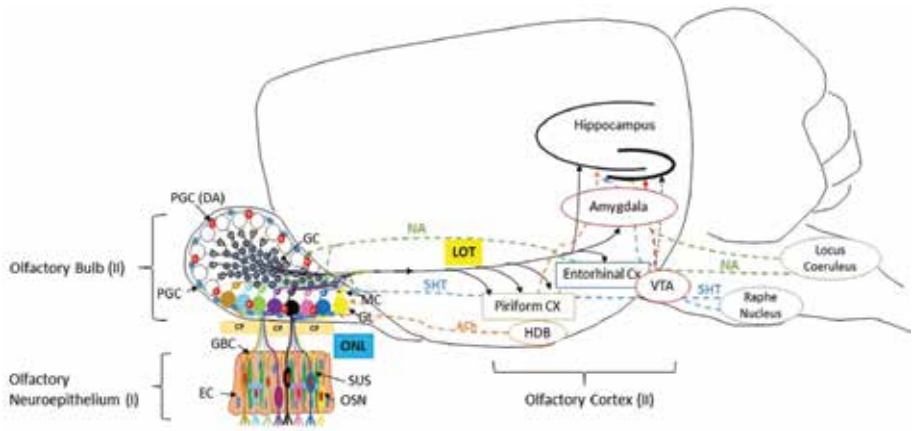

Figure 1. Olfactory system anatomy in the mammalian brain. Drawing of the primary (I) and secondary (II) network areas of the olfactory system and its corticofugal (continuous lines) and centrifugal (dotted lines) connections. The pseudostratified neuroepithelium located in the upper olfactory mucosa is displayed with its major cell types, epithelial cells (EC), globose basal cells (GBC), sustentacular cells (SUS), olfactory sensory neurons (OSNs). The OSNs project their apical dendritic cilia in the nasal cavity and their axons towards the brain to form the olfactory nerve layer (ONL, blue highlight), by passing through small foramina in the cribriform plate (CP). In the olfactory bulb, the ONL terminals synapse with excitatory mitral cells (MC; positive charge) and tufted cells (TC, not represented) in the glomerular layer (GL). Inhibitory periglomerular cells (PGCs; negative charge), dopaminergic PGCs (DA, positive charge) and inhibitory granular cells (GC, negative charge) modulate the activity of MC and TC through dendrodendritic synapses. MC axonal projections assemble to form the lateral olfactory tract (LOT, yellow highlight) projecting to the piriform cortex, entorhinal cortex, amygdala and hippocampus, representing the olfactory cortex (II). Cholinergic terminals (ACh, orange) from the horizontal limb of the diagonal band of Broca (HDB), serotoninergic efferents (5-HT, light blue) from the raphe nuclei, and noradrenergic fibers (NA, green) from the locus coeruleus innervate the olfactory bulb and olfactory cortex. Dopaminergic neurons of the ventral tegmental area (VTA, red) modulate the activity of the olfactory cortex. Cx: cortex.

lost after trauma [16, 18, 19] or certain types of cancer [20–23]. Furthermore, the early olfactory deficit in AD [24] has been shown to be a strong predictor of the progression of dementia [25–28]. Diagnosis of this sense remains underlooked and there is no consensus on the use of olfactory tests to assess/categorize neurological dysfunctions [29]. Interestingly, the studies testing olfaction in Tau and APP mouse models of AD, or α-synuclein models have shown that this sense is significantly altered [30–32]. Moreover, recent studies raise the possibility that endogenous [33–37] (PrP, Aβ, Tau, α-synuclein) and microbial [38, 39] amyloid-like peptides are accumulated in the nasal neuroepithelium and may propagate via retrograde transport to higher brain structures [40]. This might explain why Aβ, Tau, α-synuclein depositions are first observable in the olfactory bulb and olfactory tract, as their accumulation is associated to fibrillary tangle dysgenesis [41] and correlate with Braak staging progression [42].

Despite the strong evidence indicating that olfactory transmission deficit is an early predictor of neurodegenerative processes, the poor understanding of the molecular and cellular mechanisms underlying olfactory activity in the primary as well as secondary olfactory network areas has marred the use of olfaction and olfactory testing as bona fide targets in clinical setting. In this chapter, we elaborate on the anatomical and physiological properties of the olfactory system, its development by sampling the vast literature of olfaction in mammals. We then expand on the role of olfaction in humans and smell deficits as readout of neurological diseases as well as other pathologies. With this work we aim to provide further support for considering the olfactory system as source of physiological and biological biomarker(s) based on its direct connection with the brain and emphasize the use of this easily accessible sensory system as an ideally suited functio-anatomical window for monitoring brain health as well as for therapeutic targeting.

2. Olfactory system anatomy

In vertebrates the olfactory network is activated when an odorant, inhaled through the airways, binds to a specific receptor expressed on specialized neurons, known as olfactory sensory neurons (OSNs) or olfactory receptor neurons (ORNs), embedded in the upper olfactory mucosa. Every OSN expresses a specific odorant receptor (OR), which is activated only when a unique ligand (odor molecule) binds to it [43]. In 1991, Buck and Axel identified 18 genes encoding ORs [44] and for such discovery they were awarded the Nobel Prize in 2004. Few years later, more than 1000 OR genes were discovered in rodents [45] but only 378 OR were found in humans [46]. The OSN are characterized by their unique and exclusive ORs expression. The sorted olfactory signal is then transmitted from the OSNs' axons, bundling as the olfactory nerve layer (ONL) in direction of specific glomeruli located in the OB [47]. Furthermore, innervation of the OB by the OSN axons is spatially segregated along the dorsomedial and lateroventral axis (zone I, II, III, and IV) respecting the spatial positioning of these neurons in the neuroepithelium. This "glomerular convergence" allows OSN projections to be widely dispersed across the bulb, while maintaining specificity for classes of odorant chemicals. For example, the dorsomedial zone I has convergence of OSN axons detecting n-fatty acids or n-aliphatic aldehydes but not alkanes [47–49]. The chemical and anatomical organization of ONL inputs defines the discrete odorant map of the OB, which is further relayed to the connecting mitral (MC) and tufted cells (TC) via axodendritic synapses [48]. Mitral and tufted principal neurons, constituting the output from

the OB to the cortex, are finely tuned through dendrodendritic synapses mostly from periglomerular (PGC) and granular (GC) interneurons. These GABAergic and dopaminergic (DA) neurons are continuously replaced at least in rodents [50–52] and are essential for modulating mitral and tufted cells' firing rates and increasing/decreasing their synchronous firing activity in presence/absence of an odorant [53–55]. Further, cholinergic, serotoninergic and noradrenergic afferents, originating respectively from the horizontal limb of the diagonal band of Broca (HDB) [56], raphe nuclei [57] and locus coeruleus [58], modulate the response of the PGC, MC and GC (**Figure 1**). These centrifugal afferents innervate the bulb in its integrity and appear to be involved in the early deficit observed in AD and PD [59]. From the bulb, axonal projections of the relay MC, form the lateral olfactory tract (LOT) and innervate higher brain areas (**Figure 1**). Neuroimaging studies reveal that the higher olfactory areas encompasse different cerebral structures, which are mainly divided in primary and secondary olfactory regions [60, 61]. The first network area comprises the piriform and entorhinal cortices, the amygdala and hippocampus, whereas the second neuronal hub includes the thalamus, the orbitofrontal cortex, cingulate and insula [60, 62, 63]. In these higher brain areas, the signal is integrated and loses spatial resolution [64]. This decomposition effect has been explained by the combinatorial cortical network ideally suited for decoding of incoming spatially segregated signals [65]. Overall, based on the heterogeneity of brain structures implicated in the modulation and processing of olfactory stimuli, the olfactory deficit phenotype and the degree of severity of olfactory impairment may vary substantially.

3. Adult neurogenesis in the olfactory system

In all mammals, including humans, neurogenesis is maintained in the neuroepithelium through the presence of neural stem cells located close to the basal lamina. In adult rodents two type of cells populate the stem cell niche, globose basal cells (GBC), representing the neural stem cells population and horizontal basal cells (HBC), with ependymal cell characteristics functioning as supporting neurogenic cells. Conversely, in humans there is no distinction between GBC and HBC, with the first appearing as the only population occupying the niche [66]. GBCs comprise transit amplifying *Mash1* positive progenitors and *Ngn-1* expressing Intermediate Neural Progenitors (INPs), ultimately differentiating into OSN [67, 68]. Besides the neurogenic lineage, GBC give also rise to SUS, a glial-like cell type intercalated between OSNs in the epithelium [69, 70] (**Figure 1**). The sustained regenerative capacity of the neuroepithelium can compensate for the vulnerability of the OSNs and SUSs, which are in direct contact with the airways of the nasal cavity exposed to exogenous species, such as microorganisms and possible neurotoxic particles. The interaction between potentially dangerous sources and the cells of the neuroepithelium requires a continuous cell turnover in order to maintain the network functionality. Furthermore, the stem cells of the neuroepithelium represent a source of human neuronal precursors that may be employed for *in-vitro* pharmacology studies, diagnostic and regenerative therapies [71, 72].

In rodents, neurogenesis takes also place in the OB, where both GC and PGC are constantly replaced via the migration of neuronal precursors from the lateral ventricles walls to the rostral migratory stream (RMS), to reach their final destination areas: the periglomerular cell layer

and granule cell layer [73]. It has been long debated whether OB neurogenesis occurs also in humans. Despite the presence of glia cells in the adult human SVZ, potentially representing a quiescent stem cells' population, doublecortin positive migrating neurons are observed in the RMS only until the 6th month of age postnatally [74]. Overall, the events promoting the renewal and replacement of the OB interneurons support the cellular turnover of the OB and its evoked odorant activity. This may have an essential role in the regulation of physiological functions in rodents, such as recognition of pheromones and food intake, or in favoring the distribution of infectious substances, entering into the brain via the nostrils and reaching the OE/OB compartment. On the other hand, the lack of OB neurogenesis in humans might be explained on one side by the reduction of olfactory diversity, since they present less turnover in the CNS networks compared to rodents, and by the compensatory use through other senses (vision, hearing, somatosensation, gustation) requiring less adaptive integration from the renewing interneurons.

4. Signaling transduction in olfaction

Olfactory transduction begins at the level of the cilia of the OSN protruding in the nasal cavity and through cascading amplification mechanisms reducing the threshold for odorant molecules detection. Each olfactory sensory neuron has about 12 ciliary branches, which increase the binding probability of the odorant molecules to the receptors compensating for the sequestration of the molecules in the nasal mucous covering the nasal neuroepithelium. Discrete odorants interact with specific olfactory receptors and activate a sequence of intracellular events leading to ionotropic channel activation and excitatory transmission through the ONL to the brain. In rodents, there are about 1000 genes encoding for different ORs. Each olfactory sensory neuron expresses only one type of OR through a monoallelic stochastic gene selection process occurring during the maturation of the OSN [43]. The ORs are G-protein coupled transmembrane receptors characterized by seven hydrophobic domains, whose diversity determines the heterogeneity and specificity of the response [75]. Upon binding to the odor molecule, a Gα olf protein, associated to the OR, is activated and converts guanosine 5′-diphosphate (GDP) to guanosine 5′-triphosphate (GTP). Further, by detachment of the beta/gamma subunits it activates the adenylate cyclase (AC) transmembrane protein converting ATP into a c-AMP [76]. This secondary messenger, c-AMP, has a high diffusion speed (20 μm/s) [77] and is rapidly sensed by the surrounding ionotropic Ca^{2+}/Na^{+} gated channels (CNG) allowing Ca^{2+}/Na^{+} inflow [78]. The rise in Ca^{2+} activates the Cl(Ca) channels, which extrude Cl-ions, potentiating by about 90% the depolarizing inward current [79, 80]. Intracellular ciliary Ca^{2+} influences the sensitivity of the CGN to c-AMP determining its desensitization or adaptation when exposure to an odor is prolonged or when the interval between exposures is short [81]. This mechanism needs to be taken into account when planning an olfactory testing paradigm in rodent and humans. Finally, unrelated odorants switch off CNG channels in a phenomenon called masking, which preserves the specificity of signal transduction to the OB [82]. These cascading events expand the signal transduction time from 1 millisecond to the order of 100 millisecond [83] producing a molar non-linear amplification of the signal and contributing to the signal persistence. The excitatory signal from the ONL axons is then transferred to the apical dendrites of MC through glutamatergic synapses [84] and modulated through presynaptic and postsynaptic inputs of DAergic and GABAergic afferents of PGC and juxtaglomerular

interneurons spanning one or more glomeruli and regulating the spatiodynamic resolution of the odors evoked responses [85, 86]. Further, firing synchronization and signal amplification is achieved by dendrodendritic inhibitory synapses between GC and MC located in the external plexiform layer [87, 88]. The fine-tuned excitatory signal is relayed through the LOT to the cortical and neocortical structures, where an odor-evoked depression, by presynaptic metabotropic glutamate receptor (mGluR) II/III activation, contributes to signal adaptation and attenuation, typical of the cortical sensory responsiveness [89, 90]. Despite the physiology of olfactory transmission has been well characterized in rodents, much less is known about the physiology of this system in humans.

5. Olfaction in early life, adulthood, aging and mortality

Olfaction is among the most preserved senses throughout species and plays a vital role in daily life, being fundamental for feeding, reproductive and social behavior. Several studies described that in mammals, including humans, the sense of smell is developed during the first weeks of fetal life [9, 22, 91, 92]. Both in rats and humans, it has been shown that the odor of the amniotic fluid and the milk from the mother are perceived and memorized by the fetus, which, after birth, is capable to recognize and distinguish them from those of a surrogate mother [8, 10]. Moreover, experiments of olfactory stimulation in rat pups just after birth (0, 1, 2 hours) show an increase in locomotor activity compared to the unexposed pups [9].

In humans, clinical observations conducted on infants revealed their capability in locating the mother's breast without assistance [93, 94], suggesting that the maternal breast odor is the driving force guiding their orientation and providing a sense of protection [9]. For instance, during hospitalization, the maternal contact and odor have a beneficial effect on relaxing the neonate when crying. These aspects constitute the "non-verbal communication", which plays a fundamental role during the early neonatal phase to build and reinforce the mum-infant bonds [10]. Infants familiarize with odorants during pregnancy through mum's diet, through a chemosensory transmission mother-infant [92]. Thus, in the critical period of early postnatal development, when vision is still poor, olfaction is employed as one of the first senses besides touch to make contact with the external world. Even if with adulthood, olfaction becomes less relevant for survival, particularly in modern humans, it underlies strong odor-cued memories and emotions. These associative processes triggered by odor perception depend on the output of the LOT to the hippocampus and amygdala and have been essential for animals to locate food [95], for the selection of mating candidates [96] and to identify predators [97, 98]. One of the most striking examples of olfactory sensitivity for foraging is the ability of the brown bear to sniff odors from more than 10 miles away, therefore representing a significant threat to campers and hikers carrying food in natural reserves. Studies indicate that the acuity and high sensitivity to odors of larger canid depends on the extended olfactory surface areas of the turbinates rather than the relative size of the olfactory system to the brain [99]. Furthermore, the smell-based mate selection is most prominent in females and appear to be dependent on the HLA variants inherited by the father [100, 101], triggering an emotional and behavioral response aimed at reproductive activity and species' preservation. Finally, the "smell of danger" has been employed in odor-based fear conditioning to test amygdala's function as well

as hippocampal plasticity [102, 103]. Interestingly, fox or cat urine is widely used in testing passive olfactory avoidance in rodents despite these laboratory animals never encountered a predator [104]. This suggests that odor-cued memories are ingrained in the DNA and research demonstrated that are the result of heritable epigenetic modifications [105]. Furthermore, studies in humans showed that most odor-cued memories are formed in the first decade of life [106] and appear stronger than the ones evoked by words or visual cues reflecting accurately one's autobiography throughout life [107, 108]. Finally, olfactory acuity is particularly developed in occupational workers such as sommelier, perfumers and chefs, which can perceive hedonic odors among a mix to deliver unique pleasant and palatable combinations [109, 110]. It remains unclear whether odor protheticity depends on the plasticity of the neuroepithelium or the distribution of the olfactory receptive elements. With aging, humans of both genders progressively lose their olfactory acuity and the ability to identify an odor: more than 50% of individuals aged 65–82 suffer from olfactory deficit [14, 111, 112]. Several factors account for the dysfunction including chronic damage to the neuroepithelium by neurotoxins and misfolded proteins [113], depletion of ciliary ORs, neuroinflammation and reduced vascularization [114]. As a result of the OSN damage with age, bulbar atrophy [115] and glomerular degeneration are associated to neurofibrillary tangle (NFT) depositions and olfactory processing and perception deficits [117]. Olfactory dysfunction (OD) in the elderly represents a source of discomfort and can pose a serious risk to safety [118]. Last, olfactory deficit has been shown to be an early predictor of mortality in old age [119]. This body of data indicates that olfaction is one of the primary form of environmental communication in mammals [120].

6. Olfactory dysfunctions

The olfactory activity is mainly composed of two hierarchical independent processes, where the first, defined as "peripheral", is based on the acuity or capability to perceive an odorant, while the second, named as "central", is involved on the memory or ability to identify an odor [61, 121]. Alteration in peripheral processes is linked to deficits occurring at the olfactory neuroepithelium, specifically at the levels of the OSN. On the other hand, damages to central processes can be attributed to deficits in the OB compartment and in higher cerebral regions, such as cortical and limbic system structures. This observation is supported by studies showing impaired odor identification with unaffected threshold activity in subjects presenting injures in the orbitofrontal cortex or the dorsomedial thalamic nucleus [122]. The integrity of olfactory perception, normosmia, can be impaired by alterations which can be divided in two main categories indicating a (1) quantitative or (2) qualitative impairment of the sense of smell. The first category is composed by anosmia, hyposmia or microsmia and hyperosmia, whereas the second one is represented by dysosmia, subdivided in parosmia and phantosmia or olfactory hallucination. These categories and their definition are summarized in **Table 1**. Apart from normosmia, which represents the physiological condition of the sense of smell, all the other cases can be determined by a wide spectrum of causes. In order to assess olfaction in humans, several tests are nowadays available to monitor the sensitivity of the olfactory system aiming to detect at an early stage the presence of different disorders. A test, which is commonly adopted to evaluate the olfactory responsiveness, is the University of Pennsylvania Smell Identification Test (UPSIT), developed by Doty and colleagues in 1984 [29]. This scratch

Physiological olfactory condition
Normosmia: normal olfactory function
Quantitative olfactory dysfunctions
Anosmia: total loss of smell
Hyposmia: decreased sense of smell
Hyperosmia: increased sense of smell
Qualitative olfactory dysfunctions
Dysosmia: qualitative alteration of the sense of smell. It includes:
(1) Parosmia: odor distortion
(2) Phantosmia: odor perception without the presence of the source

Table 1. Classification of the olfactory conditions.

and smell test enables the evaluation of the general smell function, e.g. odor identification and odor detection, assigning a final score which reflects the individual ability to recognize by exclusion several odors. The original tests includes 40 booklets with 4 odor per booklet, although shorter mini-UPSIT (Brief Smell Identification Test – BSIT) of 12, 15 and 16 odors

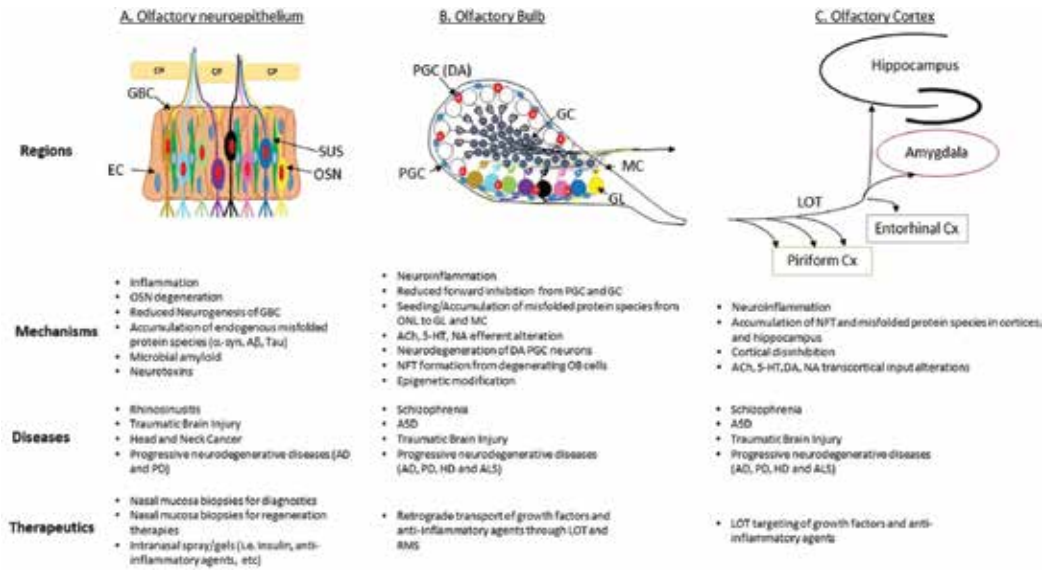

Figure 2. Breakdown of affected regions and potential mechanisms in olfactory deficiencies and window for diagnostic/treatment. Related processes, diseases and possible therapeutic approaches centered on the olfactory neuroepithelium (A), olfactory bulb (B) and olfactory cortex (C). Abbreviations: EC, epithelial cells; GBC, globose basal cells; SUS, sustentacular cells; OSN, olfactory sensory neuron; GC, granule cell; PGC, periglomerular cell; PGC (DA), periglomerular dopaminergic cells; ONL, olfactory nerve layer; CP, cribriform plate; GL, glomerular layer; MC, mitral cell; LOT, lateral olfactory tract; ACh, acetylcholine; DA, dopamine; 5-HT, 5-hydroxytryptamine; NA, noradrenaline; NFT, neurofibrillary tangles; AD, Alzheimer's disease; PD, Parkinson's disease; HD, Huntington's disease; ALS, Amyotropic lateral sclerosis; ASD, autistic spectrum disorders.

have been used before [123–125] and they seem to be a viable solution for testing olfaction on human subjects limiting desensitization mechanisms intrinsic to olfactory transduction. On the other hand, a "forced-choice phenyl ethyl alcohol odor detection threshold test" [26], also called as the Snap and Sniff® Threshold Test, allows for rapid and reliable determinations of olfactory detection thresholds. Subjects are exposed to concentrations of phenyl ethyl alcohol, ranging from 10^{-2} to 10^{-9} log vol/vol in half-log concentration steps, along with blanks for forced-choice testing [126]. This test controls for a subject's response bias or criterion for responding independently of the subject's actual sensory sensitivity. Both tests can be self-administered and are equipped with a score card making olfactory testing accessible and convenient for both clinical and personal use.

Hereafter, we describe some human pathologies which can lead to olfactory dysfunctions (**Figure 2**).

7. Systemic diseases

7.1. Chronic inflammation

Many pathological events are characterized by a persistent inflammatory response, as observed in patients suffering from sinonasal diseases, such as acute or chronic rhinosinusitis, allergic or non-allergic rhinitis [127–129] (**Table 2**). In addition to nasal congestion and altered mucus secretion, these conditions represent a common cause of olfactory impairment [127, 128, 130–132]. For instance, it has been reported that between 14 and 30% of the patients affected by chronic rhinosinusitis (CRS) show olfactory dysfunction [129, 132–134]. The inflammatory event underlying sinonasal pathologies can be divided in two processes: the inflammatory mechanism itself and the conductive (or transport) component [127–129, 135], which compromises the proper diffusion of odorants towards the olfactory neuroepithelium [136–138]. The functionality of the nasal epithelium is affected since the topical inflammation reduces the airflow and subsequently the binding of the odor molecules to the ORs expressed on their cilia. The synthesis of pro-inflammatory factors can induce the loss or impairment of the ORs, which are then unable of signal transmission due to a reduced detection threshold [129, 135]. Several studies suggest that

Pathology	Olfactory impairment	References
Chronic inflammation (Chronic Rhinosinusitis)	Anosmia, hyposmia	127–129, 133, 134
Cancer (Head–neck cancer)	Hyposmia, dysosmia	20, 146, 156, 157
Traumatic brain injury	Reversible anosmia, reversible hyposmia, reversible parosmia	19, 176–179, 184, 185
Neuropsychiatric disorders (Schizophrenia and ASD)	Hyposmia, hyperosmia, dysosmia	60, 61, 189–193, 196–198, 219, 220
Neurodegenerative diseases (Alzheimer's, Parkinson's and Huntington's disease)	Hyposmia	17, 24–26, 226–228, 236–240

Table 2. Summary of the diseases described in this chapter and their observed olfactory alterations.

the relation between CRS and olfactory dysfunction could be multifactorial, since several events can trigger olfactory disbalance in chronic rhinosinusitis cases, such as the different degree of the inflammatory response [131, 132, 137] or the medical or surgical intervention in patients suffering from this pathology [129, 132]. Moreover, it has been described that CRS patients with anosmia present an altered mucus composition, which affects olfactory epithelium neurogenesis [139]. To evaluate and monitor the entity of olfactory loss in CRS subjects various tests can be carried out [140, 141] and also the detection of biomarkers, such as neuron-specific enolase [142] could provide further support in predicting the development of such disorder. All together, these evidence indicate that a constant inflammatory status of the nasal mucosa, in presence of rhinitis, sinusitis and rhinosinusitis can lead to a variable spectrum of olfactory dysfunctions whose severity depends from the inflammatory degree itself. The chronic inflammation in CRS and the absence of the BBB between the primary and secondary olfactory areas poses a serious risk for the propagation of neuroinflammatory species leading to neurodegenerative events. Indeed, a recent report indicates that patients with a history of chronic sinusitis are more prone to develop dementia [143] or stroke [144, 145]. This supports the notion that peripheral sinus inflammation should be promptly treated with pharmacological and surgical approaches, to contain the symptoms of nasal obstruction and prevent the neuroinflammatory spread.

7.2. Cancer

Studies on head and neck cancer (HNC) reported that different symptoms associated to the treatment, such as radiotherapy and chemotherapy, can include smell and taste dysfunction [20] (**Table 2**). The impairment in these senses can appear early in HNC patients and progressively become more severe in the long-term period [146]. Laryngeal cancer patients which are best treated by total laryngectomy, based on removal of the nasal neuroepithelium, suffer from hyposmia and gustatory alteration [21, 147]. In normal conditions the olfactory receptors are not considered as potential contributors in cancerogenesis, but their physiological capability in binding to organic compounds and the subsequent signal transduction essential for survival or migratory events could support their involvement in fostering cancer cells [148–150]. Interestingly, it has been described that some ORs are present in other tissues and organs not related to the "olfactory circuit", such as muscle [151], kidney [152] and lung [22]. Former studies demonstrated that one OR is implicated in the pathobiology of prostate cancer cell migration and proliferation, making this protein a possible parameter to monitor the patient's clinical condition [150, 153, 154]. Recently, Ranzani and colleagues investigated the characteristics of olfactory receptors in cancer cell lineage and tumors. Interestingly, they found that several ORs are expressed in different tumorigenic cell lines and tumors, e.g. the OR2C3 has been observed both in diverse cancer lines and melanomas, suggesting that this receptor might participate to the development of this tumor [23, 155]. Numerous studies showed that more than 70% of cancer cases show taste and smell dysfunctions [156]. Most of these alterations are reported after cancer treatment [157], whereas changes in these senses in pre-treatment phase are not clarified. The reasons could be attributed to multiple events, like (1) mechanical interference, due to tumor obstruction of the chemoreceptor sites; (2) neurological origin, where cancer affects signal transmission; and (3) metabolic, related to a higher urea concentration in the saliva associated to tissue catabolism [23, 158].

Another fundamental aspect which connects cancer and olfaction is the employment of this sense in early detection of this pathology. In particular, canine olfaction and lately electronic

noses (e-noses) represent a promising, non-invasive manner to screen tumors [159–161]. The high sensitivity of dogs in odorants perception render them suitable for this clinical purpose, in fact they are used to distinguish healthy controls and cancer subjects upon exposure of biological samples, whereas the electronic noses present chemo-sensory components able to identify specific biomarkers in exhaled breath [161]. Both canines and e-noses can detect volatile organic compounds (VOCs) in biological specimens. It is well recognized that dogs can perceive specific VOCs in several samples, such as urine, expired breath, blood and stool [162–166]. For instance, diverse VOCs have been identified in the breath of individuals affected by lung, ovarian, prostate, bladder and colorectal tumor [167–170]. The use of electronic noses is increasing as differently from dogs, do not require training and maintenance, are relatively inexpensive and easy to handle. These new devices can analyze volatile molecules present in expired air via gas chromatography and chemosensory apparatus [171–175]. Notably, both canine olfaction and e-noses represent two powerful systems in detecting several kinds of tumors during their asymptomatic stages allowing an earlier and potentially more effective therapy. Overall, it appears that olfactory deficits are involved in the clinical phase of cancer progression, and atypical odor identification can be employed to diagnose mutagenic processes early on.

8. Central nervous system disorders

8.1. Trauma

Traumatic brain injury (TBI) constitutes one of most frequent causes of olfactory dysfunction, affecting both genders [19, 176–178] (**Table 2**). One of the first medical reports about OD, in 1864, described a post-traumatic total loss of smell and a more dated description of anosmia was reported in 1837 after head trauma (HT) from a horse riding accident [179]. Depending on the severity of the trauma, the degree of olfactory impairment can show a quite diverse clinical outcome ranging from microsmia to anosmia [178, 180–182], which can be in both cases partially recovered [181, 182]. Subjects affected by parosmia show a gradual recovery of olfactory ability following a medium-long term period after the accident [178, 181]. The severity of the trauma depends also from the cranial region interested, i.e. frontal injury is associated with a lower olfactory disability compared to the temporal and occipital lobes [181], although there is contradictory evidence on the latter [179]. After head injury, MRI analysis revealed a reduction in olfactory bulb volume as compared to control subjects [178, 181]. The reason why after HT the sense of smell is often permanently lost is due to the failed regeneration of the olfactory neuroepithelium, which directly impacts the signal transmission to the OB. In particular, the axonal re-growth of the OSNs is influenced by the injury degree [183], since it can severely compromise the ONL over its whole length [181]. A crucial aspect, which is widely debated, is the olfactory function recovery after a traumatic brain injury (TBI), which distinguishes the post-TBI hyposmia as mild, medium and severe [178]. Several studies indicate a proportional cause–effect event between trauma severity and olfactory impairment [184, 185], whereas other works suggest that the TBI entity is not directly correlated with the degree of olfactory dysfunction [179, 180]. The trauma can also have indirect consequences on the olfactory system performance, affecting cortical and subcortical areas, which are involved in the physiological olfactory responsiveness. In clinical trials, it has been observed that administration

of therapeutics, such as steroids, might improve the olfactory activity in trauma subjects [186–188]. By favoring the re-absorption of the edema or removal of the hematoma in the affected area, steroids can increase or restore the sense of smell [188]. Overall, these observations indicate that hyposmia is one of the subtlest sensory changes after trauma, which may phenotypically signal regenerative processes in these patients.

8.2. Schizophrenia and autism

A substantial number of studies indicates a correlation between schizophrenia and olfactory impairment (**Table 2**). There are several aspects of olfaction that can be assessed to characterize the schizophrenia-spectrum disorders (SSD). In particular, subjects affected by this neuropsychiatric disease present alterations in performing correctly diverse olfactory tasks, such as odor sensitivity, identification and discrimination, when exposed to different odorants [60, 61, 189–192]. Due to the disbalance in olfactory activity, it has been suggested to consider this deficit as a parameter to identify SSD. Moreover, the negative symptoms which characterize this illness have been related to the dysfunction in olfactory accuracy [193]. Nevertheless, there are controversial reports describing an alteration in the sense of smell in schizophrenia-associated disorders [190, 194] and others showing the absence of olfactory changes between psychotic patients and healthy controls [193, 195, 196]. Starting from this discrepancy, Auster and colleagues addressed whether the presence of olfactory deficits could represent a reliable marker for subjects potentially susceptible to develop schizophrenia. They investigated this aspect comparing the smell functionality in four different groups: (1) schizophrenic individuals, (2) persons with different mental disorders than schizophrenia, (3) subjects affected by schizotypy and (4) healthy controls [193]. To achieve their goal, they modified a common olfaction test, the "Sniffin' Sticks" [193, 197], in order to expand its efficiency for free recall tests in addition to olfaction ability and discrimination. They observed that schizophrenic people appear to have a reduced assortment of pleasant odors compared to healthy subjects and they report smells as less good over the controls [193, 196, 198], being in line with other reports [66, 193, 196, 198, 199]. Functional and structural alterations of the olfactory circuitry have been observed in schizophrenic patients using fMRI analysis [200] and electro olfactogram (EOG) measuring olfactory evoked potentials (EP) [194, 201]. At the biomarker level, cell culture preparations from nasal epithelium showed an alteration in G protein-coupled receptors (GPCRs) cascade, likely affecting the olfactory processing observed in this psychiatric disorder [202]. Another study reported that schizophrenic subjects are characterized by aberrant neuronal differentiation in the nasal neuroepithelium [203] suggesting that neurodevelopmental deficits may underlie the olfactory dysfunction. Indeed, prenatal or perinatal inflammation [204, 205] affect brain development and may cause the excitatory/inhibitory (E/I) disbalance characteristic of schizophrenia. Works in mice have demonstrated that NMDA hypofunction has a characteristic temporal and spatial resolution that explains the onset of schizophrenia: in early postnatal life, NMDA dysfunction occurs first in GABAergic interneurons, leading to excitatory derepression. As a compensatory mechanism, a progressive homeostatic downregulation of glutamatergic of NMDA transmission, results in NMDA hypofunction of cortical excitatory networks in the adult [206]. Based on the composition of the olfactory bulb, with a major inhibitory component and mitral cells representing the only

excitatory neurons, it is conceivable that olfactory transmission defect can arise early on due to the interference of feedforward inhibition of PGC and GC onto mitral cells, necessary for olfactory signal sorting/scaling [207–209]. The connection between neurodevelopmental deficits, E/I imbalance and olfactory deficits in adult life is captured by the numerous studies indicating that the developmental molecule Reelin [210], regulating synaptic plasticity, behavior [211–213] and olfaction [30], is reduced in a subset of interneurons in the prefrontal cortex of schizophrenic patients [214]. Interestingly, Reelin deficiency has also been reported in AD [215–217], suggesting common mechanisms between schizophrenia and progressive neurodegeneration. E/I imbalance also alters dopaminergic transmission. In the setting of local and corticofugal dopaminergic innervation to the bulb, it is expected that olfactory signal transmission may be also affected, as previously demonstrated in rats treated with inhibitors of D2 receptor [218]. This body of studies supports the notion that olfactory impairment may be an early indicator of E/I imbalance.

Only recently the attention has been pointed on the possibility of olfactory deterioration in autism spectrum disorders (ASD), comprising autism (stricto sensu) and Asperger syndrome [219, 220] (**Table 2**). ASD individuals reported an unpleasant strong perception of odors and Galle and colleagues demonstrated that depending on the olfactory tasks performed, a difference in autistic, Asperger and control subjects could be recognized. In particular, the olfactory identification was affected in autistic individuals compared to the other groups [219]. Furthermore, studies using rodent models indicate the olfactory bulb among the brain regions critical for ASD pathogenesis [221–223]. Moreover, the OR2L13G-protein locus, initializing neuronal response to odorants, was shown to be differentially methylated in ASDs suggesting a possible rationale for olfactory dysfunction in these pathologies.

Developmental NMDA hypofunction is also reported in ASD [224, 225]. In both schizophrenia and ASD, E/I imbalances at bulbar and cortical level likely underlie the olfactory transmission alterations.

8.3. Progressive neurodegenerative disorders

Olfactory activity progressively decreases with aging [14] and its decline is even accelerated with chronic neurodegenerative disorders, such as Alzheimer's disease (AD) [25, 26], Parkinson's disease (PD) [17, 24] and Huntington's disease (HD) [226, 227] (**Table 2**). Olfactory dysfunction in PD is very prominent (90% of the cases) [228] and the extent of the impairment is comparable to the one observed in early onset AD and other progressive neurodegenerative disorders. Indeed, in the initial stages of AD the olfactory function is the first to be affected [24], so this sense could represent an early predictor of the disease. Olfactory dysfunction observed in progressive neurodegenerative diseases could underlie impairments in either the olfactory neuroepithelium, OBs, LOT or olfactory cortices [42]. Interestingly, it has been reported that proteinaceous aggregates, like Amyloid-β [33], phosphorylated Tau [34, 35, 229], α-synuclein [230, 231], which are characteristic of AD, PD and HD, are deposited in first instance in the olfactory mucosa where they are thought to exert a bactericidal action [232]. The aberrant accumulation of misfolded proteins can trigger several side effects, causing a transduction deficit and inflammatory responses attempting to reduce/avoid the microbial diffusion into the brain. Based on the absence of the BBB in

the olfactory tract, cells and misfolded proteins can be easily propagated within the brain and subsequently affect other olfactory system components, as olfactory cortices and connected areas (hippocampus and amygdala) [233]. All these cerebral structures and their related functions are damaged in AD, and to a lesser extent in normal aging [42]. Interestingly, OB and olfactory tract axonal atrophy has been already detected in MCI which might progressively evolve in AD [234]. In the initial Braak stages, the OB undergoes axonal atrophy [235] and in the majority of definite AD cases the olfactory impairment correlate with cortical AD pathology [236–240]. These observations implicate an early critical involvement of the olfactory system in neurodegenerative disorders.

Several molecular mechanisms contributing to AD pathobiology have been demonstrated to interfere with olfaction:

1. Amyloid-β, which is overexpressed in AD and contributes to the amyloidogenic pathway, has physiological functions, ranging from metal ion sequestration, synaptic plasticity modulation, and antimicrobial activity [33]. The amyloid peptide shares some aspects with a highly conserved antimicrobial proteins (AMPs) family [232]. Based on their ability to form oligomers and fibrils to surround harmful microbial agents, toxic substances and even aberrant cells, the AMPs produced by the OSNs represent the first and only defensive barrier of the CNS against pathogens. Furthermore, beside its endogenous production, Aβ may also have a microbial origin, aggravating the neurodegenerative process [39, 241]. The gastrointestinal (GI) compartment represents the principal source of the human microbiome and is tightly connected with the CNS through the GI tract-CNS axis, which interconnects these structures via immune system molecules, cytokines, hormones and nervous signals [39, 242–244]. Interestingly, the microorganisms residing in the GI tract can synthesize several peptides including lipopolysaccharides (LPS) and amyloids [241, 242, 245, 246]. These evidence indicate that a mutual benefit host-microbiome is also related to the production of these amyloid exudates within a "homeostatic range", that, when disbalanced, could likely contribute to the etiology of chronic neurodegenerative diseases [247–250]. Therefore, the impairment observed in amyloid turnover and clearance during neurodegenerative pathologies could be attributed to the combination of "human Aβ burden" and the additional microbial Aβ peptides. This growing amyloid load in the OE and GI tract, can cause chronic inflammation which on the long run may affect BBB integrity and functionality [38, 39, 247, 251–253]. Overall, the deposition of insoluble Amyloid-β causes several side effects as (i) olfactory transduction deficit due to interference with OSN surface receptors, (ii) inflammatory responses attempting to reduce/prevent the microbial diffusion and (iii) seeding activity into the brain.
2. ApoE4 carriers have a higher incidence of olfactory deficit and are at risk for developing AD [254]. Moreover, ApoE4 blocks OE cultures neurite outgrowth in contrast to the trophic role of ApoE2 and ApoE3 [255].
3. Reports show SOD upregulation in OE and OB in AD patients compared to healthy controls [256] as well as an increase in oxidative response in AD neuroepithelium [255].
4. Along with network hyperactivity in the early stages of dementia, a reduction of calcium binding proteins has been observed in OSNs [257].

5. Imbalances in Acetylcholine (ACh) [258, 259], Dopamine (DA) [260–262], Serotonin (5-HT) [57, 263], and Norepinephrine (NA) [264] of the centrifugal afferents to the bulb or olfactory cortex affect olfactory transmission but can also influence microglia activation and neuro-inflammatory processes [265, 266].
6. Transient overexpression of hAPP impacts the glomeruli structure and axonal projections towards the corresponding target [267], which is partially rescued by switching off the synthesis of hAPP.
7. Dystrophic axon terminals favor amyloid deposition in AD and other disorders [116].
8. Progressive reduction in neuronal signaling components such as Reelin [268, 269] and Notch [270, 271] in AD may influence olfactory transmission as shown in rodent models [30, 272].

Despite the non-specificity of olfactory dysfunction in neurodegenerative diseases, this deficit is apparent in the pre-symptomatic phase [273, 274]. The underlying mechanisms are still poorly understood and only few studies have analyzed olfactory behavior in animal models of AD (Tg2576 [36], hTau [36]) and PD (*Pink*KO [275], α-Syn [276, 277], Bac Tg [278], VMAT2 [279]). Taken the susceptibility of the olfactory system to early molecular changes occurring in dementia, olfactory functions could be employed to predict/monitor the onset of the cognitive symptoms in AD as well its progression.

9. Olfactory route for diagnostic and therapeutics

The advantage of nasal biopsies in investigating specific olfactory disorders and also related neurodegenerative pathologies is still debated. Several studies suggest that this surgical procedure might not be specific enough to be routinely adopted in identifying primary events which anticipate neurodegenerative diseases [280]. Nevertheless, both the accessibility and heterogeneous cytoarchitecture of the olfactory neuroepithelium, make this specimen valuable for molecular diagnosis of neurological diseases [281]. Furthermore, the increasing precision and accuracy in obtaining nasal biopsies through laser surgery render this procedure safe, fast and with no major consequences, due to the constant neurogenesis occurring in the OE [282]. Nasal biopsies can be employed to detect aberrant misfolded proteins (Aβ, p-Tau, α-Syn, PrP, etc.,), produced by the OSNs, reflecting early neural network imbalances in the asymptomatic phase of different neurological pathologies. Furthermore, the stem cells population residing in the olfactory mucosa is a relevant source of biological material for diagnosing genetic modification related to neurological diseases, performing *in-vitro* pharmacology assays and possibly regenerative therapies after trauma. Thus, nasal mucosa biopsies constitute a useful tool in recognizing susceptible subjects with early subclinical neurodegenerative processes and introduce them well in advance to therapeutics or new medical trials. Sampling of the mucosa has been previously employed in the diagnosis of genetic variants in schizophrenia [71] and as experimental tool to investigate mechanisms underlying a variety of neurological disorders (ranging from schizophrenia, ASD, Rett syndrome, bipolar disorders to

Alzheimer's disease) [71]. Finally, nasal secretions may be also a valuable liquid biopsy to perform longitudinal monitoring of pathological profiles in the progression of AD [283, 284]. Besides the accessibility of the olfactory system for diagnosing brain health, intranasal (IN) drug delivery offers great potential for brain targeting through by-passing the BBB [285]. IN delivery is currently approved for systemic drugs for a wide range of indications, including hormone replacement therapy, osteoporosis, migraine, prostate cancer, and influenza vaccine [286]. Approved CNS applications include IN administration of opioids for chronic cancer pain (fentanyl, buprenorphine and morphine) [287] based on their small molecular weight (200–400 Daltons) and their rapid onset. Repurposing of IN insulin, approved for Diabetes I, is being investigated for the treatment of Insulin hypometabolism in dementia [288]. So far, the clinical studies have demonstrated that IN insulin can revert the cognitive symptoms and reduce the amyloid load in both MCI [289] and early stage AD [290, 291] (https://clinicaltrials.gov/). Nevertheless, the little understanding of the absorbance mechanisms through the nasal route and the biodistribution variability based on nasal secretion and local inflammatory processes are slowing down the development of intranasal CNS drug. Recent preclinical studies in rodents have underlined the potential of IN administration for CNS diseases, as this route shows superior pharmacodynamics [292], allows up to 20 folds higher drug bioavailability [293] and rapid transport through the rostral migratory stream to limbic structures [294]. Nevertheless, more clinical studies are needed to develop IN applications that have prognostic and diagnostic value.

10. Conclusions

Olfaction is one of the most essential senses in mammals throughout life and appears to be a relevant readout for both peripheral and central neural processes. The research in the past 30 years has used mouse models to cast light on important cellular and molecular mechanisms governing odor specification in the olfactory neuroepithelium and olfactory bulb and signal encoding in the cerebral cortex. During the same period, a bulk of clinical studies reported a strong association between many neurological diseases and olfactory deficits, suggesting that olfactory activity can sentinel subtle changes in key brain areas connected to the olfactory system. Nevertheless, the processes underlying this quite ubiquitous phenotypical dysfunction are poorly understood. Indeed, despite the clinical evidence from patients, relevant clinical models of neurological diseases have been rarely tested to unravel the basis of olfactory alteration. We believe that this field needs to close the gap between bench-side and bed-side research to devise better diagnostic and therapeutic strategies, which can exploit the accessibility and non-invasiveness of this cranial nerve.

Acknowledgements

This work is supported by the Swiss National Fund Grant No. 163470.

Conflict of interests

The authors declare no conflict of interests.

Author details

Emanuele Brai[1] and Lavinia Alberi[2,3]*

*Address all correspondence to: lavinia.alberi@unifr.ch

1 Neuro-Bio Ltd, Culham Science Centre, Oxford, UK

2 Swiss Integrative Center for Human Health, Fribourg, Switzerland

3 Department of Medicine, University of Fribourg, Fribourg, Switzerland

References

[1] Wilson DA, Kadohisa M, Fletcher ML. Cortical contributions to olfaction: Plasticity and perception. Seminars in Cell & Developmental Biology. 2006;**17**:462-470

[2] Laing DG, Doty RL, Breipohl W. The Human Sense of Smell. Springer Science & Business Media; 2012

[3] Murray RC, Navi D, Fesenko J, Lander AD, Calof AL. Widespread defects in the primary olfactory pathway caused by loss of Mash1 function. The Journal of Neuroscience. 2003;**23**:1769-1780

[4] Treloar H, Miller A Ray A, Greer C. Development of the olfactory system. In: Menini A, editor. The Neurobiology of Olfaction. Vol. 20092457. CRC Press; 2009. pp. 131-155

[5] de Castro F. Wiring olfaction: The cellular and molecular mechanisms that guide the development of synaptic connections from the nose to the cortex. Frontiers in Neuroscience. 2009;**3**:52

[6] Sarnat HB, Yu W. Maturation and dysgenesis of the human olfactory bulb. Brain Pathology. 2016;**26**:301-318

[7] Walker WF, Liem KF. Functional Anatomy of the Vertebrates: An Evolutionary Perspective. Saunders College Pub.; 1994

[8] Miller SS, Spear NE. Mere odor exposure learning in the rat neonate immediately after birth and 1 day later. Developmental Psychobiology. 2010;**52**:343-351

[9] Miller SS, Spear NE. Olfactory learning in the rat neonate soon after birth. Developmental Psychobiology. 2008;**50**:554-565

[10] Hugill K. The senses of touch and olfaction in early mother–infant interaction. British Journal of Midwifery. 2015;**23**:238-243

[11] Miller SS, Spear NE. Olfactory learning in the rat immediately after birth: Unique salience of first odors. Developmental Psychobiology. 2009;**51**:488-504

[12] Moberg PJ et al. Meta-analysis of olfactory function in schizophrenia, first-degree family members, and youths at-risk for psychosis. Schizophrenia Bulletin. 2014;**40**:50-59

[13] Turetsky BI, Hahn C-G, Borgmann-Winter K, Moberg PJ. Scents and nonsense: Olfactory dysfunction in schizophrenia. Schizophrenia Bulletin. 2009;**35**:1117-1131

[14] Doty RL, Kamath V. The influences of age on olfaction: A review. Frontiers in Psychology. 2014;**5**:20

[15] Devanand DP et al. Olfactory deficits in patients with mild cognitive impairment predict Alzheimer's disease at follow-up. The American Journal of Psychiatry. 2000;**157**:1399-1405

[16] Conti MZ et al. Odor identification deficit predicts clinical conversion from mild cognitive impairment to dementia due to Alzheimer's disease. Archives of Clinical Neuropsychology. 2013;**28**:391-399

[17] Doty RL. Olfaction in Parkinson's disease and related disorders. Neurobiology of Disease. 2012;**46**:527-552

[18] Bakker K, Catroppa C, Anderson V. Anosmia and olfactory outcomes following paediatric traumatic brain injury. Brain Injury. 2016;**30**:191-198

[19] Schofield PW, Moore TM, Gardner A. Traumatic brain injury and olfaction: A systematic review. Frontiers in Neurology. 2014 Jan 22;**5**:5

[20] Álvarez-Camacho M, Gonella S, Campbell S, Scrimger RA, Wismer WV. A systematic review of smell alterations after radiotherapy for head and neck cancer. Cancer Treatment Reviews. 2017;**54**:110-121

[21] Riva G, Sensini M, Corvino A, Pecorari G, Garzaro M. Smell and taste impairment after total laryngectomy. The Annals of Otology, Rhinology, and Laryngology. 2017;**126**:548-554

[22] Gu X et al. Chemosensory functions for pulmonary neuroendocrine cells. American Journal of Respiratory Cell and Molecular Biology. 2014;**50**:637-646

[23] Spotten LE et al. Subjective and objective taste and smell changes in cancer. Annals of Oncology. 2017;**28**:969-984

[24] Rahayel S, Frasnelli J, Joubert S. The effect of Alzheimer's disease and Parkinson's disease on olfaction: A meta-analysis. Behavioural Brain Research. 2012;**231**:60-74

[25] Knupfer L, Spiegel R. Differences in olfactory test performance between normal aged, Alzheimer and vascular type dementia individuals. International Journal of Geriatric Psychiatry. 1986;**1**:3-14

[26] Doty RL, Reyes PF, Gregor T. Presence of both odor identification and detection deficits in Alzheimer's disease. Brain Research Bulletin. 1987;**18**:597-600

[27] Doty RL. The olfactory vector hypothesis of neurodegenerative disease: Is it viable? Annals of Neurology. 2008;**63**:7-15

[28] Mesholam RI, Moberg PJ, Mahr RN, Doty RL. Olfaction in neurodegenerative disease. Archives of Neurology. 1998;**55**:84

[29] Doty RL, Shaman P, Kimmelman CP, Dann MS. University of pennsylvania smell identification test: A rapid quantitative olfactory function test for the clinic. Laryngoscope. 1984;**94**:176-178

[30] Larson J, Hoffman JS, Guidotti A, Costa E. Olfactory discrimination learning deficit in heterozygous reeler mice. Brain Research. 2003;**971**:40-46

[31] Lehmkuhl AM, Dirr ER, Fleming SM. Olfactory assays for mouse models of neurodegenerative disease. Journal of Visualized Experiments. 2014 Aug 25;(90):e51804

[32] Witt RM, Galligan MM, Despinoy JR, Segal R. Olfactory behavioral testing in the adult mouse. Journal of Visualized Experiments. 2009 Jan 28;(23):pii: 949. DOI: 10.3791/949

[33] Kumar DKV et al. Amyloid-peptide protects against microbial infection in mouse and worm models of Alzheimers disease. Science Translational Medicine. 2016;**8**:340ra72-340ra72

[34] Arnold SE et al. Olfactory epithelium amyloid-beta and paired helical filament-tau pathology in Alzheimer disease. Annals of Neurology. 2010;**67**:462-469

[35] Crino PB et al. Beta-amyloid peptide and amyloid precursor proteins in olfactory mucosa of patients with Alzheimer's disease, Parkinson's disease, and Down syndrome. The Annals of Otology, Rhinology, and Laryngology. 1995;**104**:655-661

[36] Wesson DW, Levy E, Nixon RA, Wilson DA. Olfactory dysfunction correlates with amyloid- burden in an Alzheimer's disease mouse model. Journal of Neuroscience. 2010;**30**:505-514

[37] Zanusso G et al. Detection of pathologic prion protein in the olfactory epithelium in sporadic Creutzfeldt–Jakob disease. The New England Journal of Medicine. 2003;**348**:711-719

[38] Blanco LP, Evans ML, Smith DR, Badtke MP, Chapman MR. Diversity, biogenesis and function of microbial amyloids. Trends in Microbiology. 2012;**20**:66-73

[39] Hill JM, Lukiw WJ. Microbial-generated amyloids and Alzheimer's disease (AD). Frontiers in Aging Neuroscience. 2015;**7**:9

[40] Rey NL, Wesson DW, Brundin P. The olfactory bulb as the entry site for prion-like propagation in neurodegenerative diseases. Neurobiology of Disease. 2018 Jan;**109**(Pt B): 226-248. DOI: 10.1016/j.nbd.2016.12.013

[41] Arriagada PV, Louis DN, Hedley-Whyte ET, Hyman BT. Neurofibrillary tangles and olfactory dysgenesis. Lancet. 1991;**337**:559

[42] Attems J, Walker L, Jellinger KA. Olfactory bulb involvement in neurodegenerative diseases. Acta Neuropathologica. 2014;**127**:459-475

[43] Serizawa S, Miyamichi K, Sakano H. One neuron-one receptor rule in the mouse olfactory system. Trends in Genetics. 2004;**20**:648-653

[44] Buck L, Axel R. A novel multigene family may encode odorant receptors: A molecular basis for odor recognition. Cell. 1991;**65**:175-187

[45] Zhang X, Zhang X, Firestein S. Comparative genomics of odorant and pheromone receptor genes in rodents. Genomics. 2007;**89**:441-450

[46] Fleischer J, Breer H, Strotmann J. Mammalian olfactory receptors. Frontiers in Cellular Neuroscience. 2009;**3**:9

[47] Mori K, Nagao H, Yoshihara Y. The olfactory bulb: Coding and processing of odor molecule information. Science. 1999;**286**:711-715

[48] Mori K, Yoshihara Y. Molecular recognition and olfactory processing in the mammalian olfactory system. Progress in Neurobiology. 1995;**45**:585-619

[49] Mori K. Maps of odorant molecular features in the mammalian olfactory bulb. Physiological Reviews. 2006;**86**:409-433

[50] Lledo P-M, Saghatelyan A, Lemasson M. Inhibitory interneurons in the olfactory bulb: From development to function. The Neuroscientist. 2004;**10**:292-303

[51] Yoshihara S-I, Takahashi H, Tsuboi A. Molecular mechanisms regulating the dendritic development of Newborn olfactory bulb interneurons in a sensory experience-dependent manner. Frontiers in Neuroscience. 2016 Jan 12;**9**:514

[52] Lledo P-M, Merkle FT, Alvarez-Buylla A. Origin and function of olfactory bulb interneuron diversity. Trends in Neurosciences. 2008;**31**:392-400

[53] Angelo K, Margrie TW. Population diversity and function of hyperpolarization-activated current in olfactory bulb mitral cells. Scientific Reports. 2011;**1**:50

[54] Burton SD. Inhibitory circuits of the mammalian main olfactory bulb. Journal of Neurophysiology. 2017;**118**:2034-2051

[55] Rapid feedforward inhibition and asynchronous excitation regulate granule cell activity in the mammalian main olfactory bulb. The Journal of Neuroscience. 2015 Oct 21;**35**(42):14103-14122. DOI: 10.1523/JNEUROSCI.0746-15.2015

[56] Záborszky L, Carlsen J, Brashear HR, Heimer L. Cholinergic and GABAergic afferents to the olfactory bulb in the rat with special emphasis on the projection neurons in the nucleus of the horizontal limb of the diagonal band. The Journal of Comparative Neurology. 1986;**243**:488-509

[57] Petzold GC, Hagiwara A, Murthy VN. Serotonergic modulation of odor input to the mammalian olfactory bulb. Nature Neuroscience. 2009;**12**:784-791

[58] Shipley MT, Halloran FJ, de la Torre J. Surprisingly rich projection from locus coeruleus to the olfactory bulb in the rat. Brain Research. 1985;**329**:294-299

[59] Kratskin I, Belluzzi O. Anatomy and neurochemistry of the olfactory bulb. In: Handbook of Olfaction and Gustation. New York, NY: Marcel Dekker. 2003. pp. 139-164

[60] Good KP, Sullivan RL. Olfactory function in psychotic disorders: Insights from neuroimaging studies. World Journal of Psychiatry. 2015;**5**:210-221

[61] Atanasova B et al. Olfaction: A potential cognitive marker of psychiatric disorders. Neuroscience and Biobehavioral Reviews. 2008;**32**:1315-1325

[62] Zatorre RJ, Jones-Gotman M, Evans AC, Meyer E. Functional localization and lateralization of human olfactory cortex. Nature. 1992;**360**:339-340

[63] Savic I, Gulyas B, Larsson M, Roland P. Olfactory functions are mediated by parallel and hierarchical processing. Neuron. 2000;**26**:735-745

[64] Buonviso N, Revial MF, Jourdan F. The projections of mitral cells from small local regions of the olfactory bulb: An anterograde tracing study using PHA-L (*Phaseolus vulgaris* Leucoagglutinin). The European Journal of Neuroscience. 1991;**3**:493-500

[65] Haberly LB. Parallel-distributed processing in olfactory cortex: New insights from morphological and physiological analysis of neuronal circuitry. Chemical Senses. 2001; **26**:551-576

[66] Hahn C-G et al. In vivo and in vitro neurogenesis in human olfactory epithelium. The Journal of Comparative Neurology. 2005;**483**:154-163

[67] DeHamer MK, Guevara JL, Hannon K, Olwin BB, Calof AL. Genesis of olfactory receptor neurons in vitro: Regulation of progenitor cell divisions by fibroblast growth factors. Neuron. 1994;**13**:1083-1097

[68] Doetsch F. The glial identity of neural stem cells. Nature Neuroscience. 2003;**6**:1127-1134

[69] Beites CL, Kawauchi S, Crocker CE, Calof AL. Identification and molecular regulation of neural stem cells in the olfactory epithelium. Experimental Cell Research. 2005; **306**:309-316

[70] Goldstein BJ, Schwob JE. Analysis of the globose basal cell compartment in rat olfactory epithelium using GBC-1, a new monoclonal antibody against globose basal cells. The Journal of Neuroscience. 1996;**16**:4005-4016

[71] Lavoie J, Sawa A, Ishizuka K. Application of olfactory tissue and its neural progenitors to schizophrenia and psychiatric research. Current Opinion in Psychiatry. 2017;**30**:176-183

[72] Costanzo RM, Yagi S. Olfactory epithelial transplantation: Possible mechanism for restoration of smell. Current Opinion in Otolaryngology & Head and Neck Surgery. 2011;**19**:54-57

[73] Lim DA, Alvarez-Buylla A. The adult ventricular-subventricular zone (V-SVZ) and olfactory bulb (OB) neurogenesis. Cold Spring Harbor Perspectives in Biology. 2016;**8**:a018820

[74] Sanai N et al. Unique astrocyte ribbon in adult human brain contains neural stem cells but lacks chain migration. Nature. 2004;**427**:740-744

[75] Jones DT, Reed RR. Golf: An olfactory neuron specific-G protein involved in odorant signal transduction. Science. 1989;**244**:790-795

[76] Bakalyar HA, Reed RR. Identification of a specialized adenylyl cyclase that may mediate odorant detection. Science. 1990;**250**:1403-1406

[77] Chen C, Nakamura T, Koutalos Y. Cyclic AMP diffusion coefficient in frog olfactory cilia. Biophysical Journal. 1999;**76**:2861-2867

[78] Dhallan RS, Yau KW, Schrader KA, Reed RR. Primary structure and functional expression of a cyclic nucleotide-activated channel from olfactory neurons. Nature. 1990;**347**:184-187

[79] Gonzalez-Silva C et al. Ca^{2-} activated Cl− channels of the ClCa family express in the cilia of a subset of rat olfactory sensory neurons. PLoS One. 2013;**8**:e69295

[80] Mura CV, Delgado R, Delgado MG, Restrepo D, Bacigalupo J. A CLCA regulatory protein present in the chemosensory cilia of olfactory sensory neurons induces a Ca^{2-} activated Cl^{-} current when transfected into HEK293. BMC Neuroscience. 2017 Aug 11;**18**(1):61

[81] Kurahashi T, Menini A. Mechanism of odorant adaptation in the olfactory receptor cell. Nature. 1997;**385**:725-729

[82] Chen T-Y, Takeuchi H, Kurahashi T. Odorant inhibition of the olfactory cyclic nucleotide-gated channel with a native molecular assembly. The Journal of General Physiology. 2006;**128**:365-371

[83] Takeuchi H, Kurahashi T. Identification of second messenger mediating signal transduction in the olfactory receptor cell. The Journal of General Physiology. 2003;**122**:557-567

[84] Dudley CA, Moss RL. Electrophysiological evidence for glutamate as a vomeronasal receptor cell neurotransmitter. Brain Research. 1995;**675**:208-214

[85] Aroniadou-Anderjaska V, Zhou FM, Priest CA, Ennis M, Shipley MT. Tonic and synaptically evoked presynaptic inhibition of sensory input to the rat olfactory bulb via GABA(B) heteroreceptors. Journal of Neurophysiology. 2000;**84**:1194-1203

[86] Pírez N, Wachowiak M. In vivo modulation of sensory input to the olfactory bulb by tonic and activity-dependent presynaptic inhibition of receptor neurons. The Journal of Neuroscience. 2008;**28**:6360-6371

[87] Huang L, Garcia I, Jen H-I, Arenkiel BR. Reciprocal connectivity between mitral cells and external plexiform layer interneurons in the mouse olfactory bulb. Frontiers in Neural Circuits. 2013;**7**:32

[88] Isaacson JS, Strowbridge BW. Olfactory reciprocal synapses: Dendritic signaling in the CNS. Neuron. 1998;**20**:749-761

[89] Best AR, Wilson DA. Coordinate synaptic mechanisms contributing to olfactory cortical adaptation. The Journal of Neuroscience. 2004;**24**:652-660

[90] Chung S, Li X, Nelson SB. Short-term depression at thalamocortical synapses contributes to rapid adaptation of cortical sensory responses in vivo. Neuron. 2002;**34**:437-446

[91] Schaal B. Olfaction in infants and children: Developmental and functional perspectives. Chemical Senses. 1988;**13**:145-190

[92] Schaal B, Marlier L, Soussignan R. Human foetuses learn odours from their pregnant mother's diet. Chemical Senses. 2000;**25**:729-737

[93] Varendi H, Porter RH. Breast odour as the only maternal stimulus elicits crawling towards the odour source. Acta Paediatrica. 2001;**90**:372-375

[94] Varendi H, Porter RH, Winberg J. Does the newborn baby find the nipple by smell? Lancet. 1994;**344**:989-990

[95] Stoddart DM, Michael Stoddart D. Detection of food. In The Ecology of Vertebrate Olfaction. Springer Verlag. 1980. pp. 63-84

[96] Brennan PA, Keverne EB. Neural mechanisms of mammalian olfactory learning. Progress in Neurobiology. 1997;**51**:457-481

[97] Takahashi LK, Nakashima BR, Hong H, Watanabe K. The smell of danger: A behavioral and neural analysis of predator odor-induced fear. Neuroscience and Biobehavioral Reviews. 2005;**29**:1157-1167

[98] Dielenberg RA, McGregor IS. Defensive behavior in rats towards predatory odors: A review. Neuroscience and Biobehavioral Reviews. 2001;**25**:597-609

[99] Green PA et al. Respiratory and olfactory turbinal size in canid and arctoid carnivorans. Journal of Anatomy. 2012;**221**:609-621

[100] Jacob S, McClintock MK, Zelano B, Ober C. Paternally inherited HLA alleles are associated with women's choice of male odor. Nature Genetics. 2002;**30**:175-179

[101] Penn DJ, Potts WK. The evolution of mating preferences and major histocompatibility complex genes. The American Naturalist. 1999;**153**:145-164

[102] Otto T, Cousens G, Herzog C. Behavioral and neuropsychological foundations of olfactory fear conditioning. Behavioural Brain Research. 2000;**110**:119-128

[103] Paschall GY, Davis M. Olfactory-mediated fear-potentiated startle. Behavioral Neuroscience. 2002;**116**:4-12

[104] Blozovski D, Cudennec A. Passive avoidance learning in the young rat. Developmental Psychobiology. 1980;**13**:513-518

[105] Parsons RG, Ressler KJ. Implications of memory modulation for post-traumatic stress and fear disorders. Nature Neuroscience. 2013;**16**:146-153

[106] Van Toller S, Kendal-Reed M. A possible protocognitive role for odor in human infant development. Brain and Cognition. 1995;**29**:275-293

[107] Chu S, Downes JJ. Odour-evoked autobiographical memories: Psychological investigations of proustian phenomena. Chemical Senses. 2000;**25**:111-116

[108] Willander J, Larsson M. Smell your way back to childhood: Autobiographical odor memory. Psychonomic Bulletin & Review. 2006;**13**:240-244

[109] Doty RL. On the protheticity of olfactory pleasantness and intensity. Perceptual and Motor Skills. 1997;**85**:1439-1449

[110] Nakano S, Ayabe-Kanamura S. The influence of olfactory contexts on the sequential rating of odor pleasantness. Perception. 2016;**46**:393-405

[111] Attems J, Walker L, Jellinger KA. Olfaction and aging: A mini-review. Gerontology. 2015; **61**:485-490

[112] Choudhury ES, Moberg P, Doty RL. Influences of age and sex on a microencapsulated odor memory test. Chemical Senses. 2003;**28**:799-805

[113] Loo AT, Youngentob SL, Kent PF, Schwob JE. The aging olfactory epithelium: Neurogenesis, response to damage, and odorant-induced activity. International Journal of Developmental Neuroscience. 1996;**14**:881-900

[114] Naessen R. An enquiry on the morphological characteristics and possible changes with age in the olfactory region of man. Acta Oto-Laryngologica. 1971;**71**:49-62

[115] Hummel T et al. Correlation between olfactory bulb volume and olfactory function in children and adolescents. Experimental Brain Research. 2011;**214**:285-291

[116] Cai Y et al. An age-related axon terminal pathology around the first olfactory relay that involves amyloidogenic protein overexpression without plaque formation. Neuroscience. 2012;**215**:160-173

[117] Wilson RS, Arnold SE, Schneider JA, Tang Y, Bennett DA. The relationship between cerebral Alzheimer's disease pathology and odour identification in old age. Journal of Neurology, Neurosurgery, and Psychiatry. 2007;**78**:30-35

[118] Gopinath B, Sue CM, Kifley A, Mitchell P. The association between olfactory impairment and total mortality in older adults. The Journals of Gerontology. Series A, Biological Sciences and Medical Sciences. 2012;**67**:204-209

[119] Wilson RS, Yu L, Bennett DA. Odor identification and mortality in old age. Chemical Senses. 2011;**36**:63-67

[120] Muller-Schwarze, D. Chemical Ecology of Vertebrates. Cambridge University Press; 2006

[121] Martzke JS, Kopala LC, Good KP. Olfactory dysfunction in neuropsychiatric disorders: Review and methodological considerations. Biological Psychiatry. 1997;**42**:721-732

[122] Jones-Gotman M, Zatorre RJ. Olfactory identification deficits in patients with focal cerebral excision. Neuropsychologia. 1988;**26**:387-400

[123] Lawton M et al. Equating scores of the University of Pennsylvania Smell Identification Test and Sniffin' sticks test in patients with Parkinson's disease. Parkinsonism & Related Disorders. 2016;**33**:96-101

[124] Weierstall R, Pause BM. Development of a 15-item odour discrimination test (Düsseldorf odour discrimination test). Perception. 2012;**41**:193-203

[125] Wilson RS, Arnold SE, Tang Y, Bennett DA. Odor identification and decline in different cognitive domains in old age. Neuroepidemiology. 2006;**26**:61-67

[126] Doty RL. Olfactory dysfunction and its measurement in the clinic. World Journal of Otorhinolaryngology-Head and Neck Surgery. 2015;**1**:28-33

[127] Ciofalo A et al. Olfactory dysfunction in acute rhinosinusitis: Intranasal sodium hyaluronate as adjuvant treatment. European Archives of Oto-Rhino-Laryngology. 2017; **274**:803-808

[128] Klimek L, Eggers G. Olfactory dysfunction in allergic rhinitis is related to nasal eosinophilic inflammation. The Journal of Allergy and Clinical Immunology. 1997;**100**:158-164

[129] Raviv JR, Kern RC. Chronic rhinosinusitis and olfactory dysfunction. In: Hummel T, Welge-Lüssen A, editors. Taste and Smell. Vol. 63. Karger; 2006. pp. 108-124

[130] Kohli P et al. The prevalence of olfactory dysfunction in chronic rhinosinusitis. Laryngoscope. 2017;**127**:309-320

[131] Rombaux P, Huart C, Levie P, Cingi C, Hummel T. Olfaction in chronic rhinosinusitis. Current Allergy and Asthma Reports. 2016;**16**

[132] Sánchez-Vallecillo MV, Fraire ME, Baena-Cagnani C, Zernotti ME. Olfactory dysfunction in patients with chronic rhinosinusitis. International Journal of Otolaryngology. 2012;**2012**:1-5

[133] Holbrook EH, Leopold DA. An updated review of clinical olfaction. Current Opinion in Otolaryngology & Head and Neck Surgery. 2006;**14**:23-28

[134] Seiden AM, Duncan HJ. The diagnosis of a conductive olfactory loss. Laryngoscope. 2001;**111**:9-14

[135] Mott AE, Leopold DA. Disorders in taste and smell. The Medical Clinics of North America. 1991;**75**:1321-1353

[136] Jafek BW, Moran DT, Eller PM, Rowley 3rd JC, Jafek TB. Steroid-dependent anosmia. Archives of Otolaryngology – Head & Neck Surgery. 1987;**113**:547-549

[137] Kern RC. Chronic sinusitis and anosmia: Pathologic changes in the olfactory mucosa. Laryngoscope. 2000;**110**:1071-1077

[138] Stevens MH. Steroid-dependent anosmia. Laryngoscope. 2001;**111**:200-203

[139] Robinson AM, Conley DB, Shinners MJ, Kern RC. Apoptosis in the aging olfactory epithelium. Laryngoscope. 2002;**112**:1431-1435

[140] El Rassi E et al. Sensitivity analysis and diagnostic accuracy of the brief smell identification test in patients with chronic rhinosinusitis. International Forum of Allergy Rhinology. 2016;**6**:287-292

[141] Soler ZM, Kohli P, Storck KA, Schlosser RJ. Olfactory impairment in chronic Rhinosinusitis using threshold, discrimination, and identification scores. Chemical Senses. 2016 Jul 28. pii: bjw080. DOI: 10.1093/chemse/bjw080

[142] Tsybikov NN, Egorova EV, Kuznik BI, Fefelova EV, Magen E. Neuron-specific enolase in nasal secretions as a novel biomarker of olfactory dysfunction in chronic rhinosinusitis. American Journal of Rhinology & Allergy. 2016;**30**:65-69

[143] Yasue M et al. Prevalence of sinusitis detected by magnetic resonance imaging in subjects with dementia or Alzheimer's disease. Current Alzheimer Research. 2015;**12**:1006-1011

[144] Kang J-H, Wu C-S, Keller JJ, Lin H-C. Chronic rhinosinusitis increased the risk of stroke: A 5-year follow-up study. Laryngoscope. 2013;**123**:835-840

[145] Wu C-W, Chao P-Z, Hao W-R, Liou T-H, Lin H-W. Risk of stroke among patients with rhinosinusitis: A population-based study in Taiwan. American Journal of Rhinology & Allergy. 2012;**26**:278-282

[146] Bansal M et al. Radiation related morbidities and their impact on quality of life in head and neck cancer patients receiving radical radiotherapy. Quality of Life Research. 2004;**13**:481-488

[147] Caldas ASC et al. Gustatory and olfactory dysfunction in laryngectomized patients. Brazilian Journal of Otorhinolaryngology. 2013;**79**:546-554

[148] Kalbe B et al. Helional-induced activation of human olfactory receptor 2J3 promotes apoptosis and inhibits proliferation in a non-small-cell lung cancer cell line. European Journal of Cell Biology. 2017;**96**:34-46

[149] Maßberg D et al. The activation of OR51E1 causes growth suppression of human prostate cancer cells. Oncotarget. 2016;**7**:48231-48249

[150] Sanz G et al. Promotion of cancer cell invasiveness and metastasis emergence caused by olfactory receptor stimulation. PLoS One. 2014;**9**:e85110

[151] Griffin CA, Kafadar KA, Pavlath GK. MOR23 promotes muscle regeneration and regulates cell adhesion and migration. Developmental Cell. 2009;**17**:649-661

[152] Pluznick JL et al. Olfactory receptor responding to gut microbiota-derived signals plays a role in renin secretion and blood pressure regulation. Proceedings of the National Academy of Sciences of the United States of America. 2013;**110**:4410-4415

[153] Neuhaus EM et al. Activation of an olfactory receptor inhibits proliferation of prostate cancer cells. The Journal of Biological Chemistry. 2009;**284**:16218-16225

[154] Rodriguez M et al. PSGR promotes prostatic intraepithelial neoplasia and prostate cancer xenograft growth through NF-κB. Oncogene. 2014;**3**:e114

[155] Ranzani M et al. Revisiting olfactory receptors as putative drivers of cancer. Wellcome Open Research. 2017;**2**:9

[156] Bernhardson B-M, Tishelman C, Rutqvist LE. Self-reported taste and smell changes during cancer chemotherapy. Supportive Care in Cancer. 2008;**16**:275-283

[157] Hong JH et al. Taste and odor abnormalities in cancer patients. The Journal of Supportive Oncology. 2009;**7**:58-65

[158] Kamath S, Booth P, Lad TE, Kohrs MB, McGuire WP. Taste thresholds of patients with cancer of the esophagus. Cancer. 1983;**52**:386-389

[159] Bijland LR, Bomers MK, Smulders YM. Smelling the diagnosis: A review on the use of scent in diagnosing disease. The Netherlands Journal of Medicine. 2013;**71**:300-307

[160] Jezierski T, Walczak M, Ligor T, Rudnicka J, Buszewski B. Study of the art: Canine olfaction used for cancer detection on the basis of breath odour. Perspectives and limitations. Journal of Breath Research. 2015;**9**:027001

[161] Brooks SW, Moore DR, Marzouk EB, Glenn FR, Hallock RM. Canine olfaction and electronic nose detection of volatile organic compounds in the detection of cancer: A review. Cancer Investigation. 2015;**33**:411-419

[162] Amundsen T, Sundstrøm S, Buvik T, Gederaas OA, Haaverstad R. Can dogs smell lung cancer? First study using exhaled breath and urine screening in unselected patients with suspected lung cancer. Acta Oncologica. 2014;**53**:307-315

[163] Horvath G, Andersson H, Nemes S. Cancer odor in the blood of ovarian cancer patients: A retrospective study of detection by dogs during treatment, 3 and 6 months afterward. BMC Cancer. 2013;**13**:396

[164] McCulloch M et al. Diagnostic accuracy of canine scent detection in early- and late-stage lung and breast cancers. Integrative Cancer Therapies. 2006;**5**:30-39

[165] Sonoda H et al. Colorectal cancer screening with odour material by canine scent detection. Gut. 2011;**60**:814-819

[166] Taverna G et al. Olfactory system of highly trained dogs detects prostate cancer in urine samples. The Journal of Urology. 2015;**193**:1382-1387

[167] Banks R, Selby P. Clinical proteomics—Insights into pathologies and benefits for patients. Lancet. 2003;**362**:415-416

[168] Carpagnano GE, Foschino-Barbaro MP, Resta O, Gramiccioni E, Carpagnano F. Endothelin-1 is increased in the breath condensate of patients with non-small-cell lung cancer. Oncology. 2004;**66**:180-184

[169] Okano T et al. Plasma proteomics of lung cancer by a linkage of multi-dimensional liquid chromatography and two-dimensional difference gel electrophoresis. Proteomics. 2006;**6**:3938-3948

[170] Phillips M et al. Volatile organic compounds in breath as markers of lung cancer: A cross-sectional study. Lancet. 1999;**353**:1930-1933

[171] Asimakopoulos AD et al. Prostate cancer diagnosis through electronic nose in the urine headspace setting: A pilot study. Prostate Cancer and Prostatic Diseases. 2014;**17**:206-211

[172] Di Natale C et al. Lung cancer identification by the analysis of breath by means of an array of non-selective gas sensors. Biosensors & Bioelectronics. 2003;**18**:1209-1218

[173] Krilaviciute A et al. Detection of cancer through exhaled breath: A systematic review. Oncotarget. 2015;**6**:38643-38657

[174] Peled N et al. Use of a nanoparticle-based artificial olfactory system, NaNose, to distinguish malignant from benign pulmonary nodules. Journal of Clinical Orthodontics. 2010;**28**:10521-10521

[175] Peng G et al. Detection of lung, breast, colorectal, and prostate cancers from exhaled breath using a single array of nanosensors. British Journal of Cancer. 2010;**103**:542-551

[176] Doty RL. Studies of human olfaction from the University of Pennsylvania Smell and Taste Center. Chemical Senses. 1997;**22**:565-586

[177] Hummel T, Landis BN and Hüttenbrink K-B. Smell and taste disorders. GMS Current Topics in Otorhinolaryngology, Head and Neck Surgery. 2011;**10**:Doc04

[178] Proskynitopoulos PJ, Stippler M, Kasper EM. Post-traumatic anosmia in patients with mild traumatic brain injury (mTBI): A systematic and illustrated review. Surgical Neurology International. 2016;**7**:S263-S275

[179] Sumner D. Post-traumatic anosmia. Brain. 1964;**87**:107-120

[180] Haxel BR, Grant L, Mackay-Sim A. Olfactory dysfunction after head injury. The Journal of Head Trauma Rehabilitation. 2008;**23**:407-413

[181] Doty RL et al. Olfactory dysfunction in patients with head trauma. Archives of Neurology. 1997;**54**:1131-1140

[182] Reden J et al. Recovery of olfactory function following closed head injury or infections of the upper respiratory tract. Archives of Otolaryngology – Head & Neck Surgery. 2006; **132**:265-269

[183] Costanzo RM. Regeneration and rewiring the olfactory bulb. Chemical Senses. 2005; **30**(Suppl 1):i133-i134

[184] Levin HS, High WM, Eisenberg HM. Impairment of olfactory recognition after closed head injury. Brain. 1985;**108**(Pt 3):579-591

[185] van Damme PA, Freihofer HP. Disturbances of smell and taste after high central midface fractures. Journal of Cranio-Maxillo-Facial Surgery. 1992;**20**:248-250

[186] Fujii M, Fukazawa K, Takayasu S, Sakagami M. Olfactory dysfunction in patients with head trauma. Auris Nasus Larynx. 2002;**29**:35-40

[187] Jiang R-S et al. Steroid treatment of posttraumatic anosmia. European Archives of Oto-Rhino-Laryngology. 2010;**267**:1563-1567

[188] Ikeda K, Sakurada T, Takasaka T, Okitsu T, Yoshida S. Anosmia following head trauma: Preliminary study of steroid treatment. The Tohoku Journal of Experimental Medicine. 1995;**177**:343-351

[189] Pełka-Wysiecka J et al. Odors identification differences in deficit and nondeficit schizophrenia. Pharmacological Reports. 2016;**68**:390-395

[190] Turetsky BI, Moberg PJ. An odor-specific threshold deficit implicates abnormal intracellular cyclic AMP signaling in schizophrenia. The American Journal of Psychiatry. 2009;**166**:226-233

[191] Brewer WJ, Pantelis C. Olfactory sensitivity: Functioning in schizophrenia and implications for understanding the nature and progression of psychosis. Vitamins and Hormones. 2010;**83**:305-329

[192] Robabeh S, Mohammad JM, Reza A, Mahan B. The evaluation of olfactory function in patients with schizophrenia. Global Journal of Health Science. 2015;**7**:319-330

[193] Auster TL, Cohen AS, Callaway DA, Brown LA. Objective and subjective olfaction across the schizophrenia spectrum. Psychiatry. 2014;**77**:57-66

[194] Turetsky BI et al. Physiologic impairment of olfactory stimulus processing in schizophrenia. Biological Psychiatry. 2003;**53**:403-411

[195] Compton MT, Chien VH. No association between psychometrically-determined schizotypy and olfactory identification ability in first-degree relatives of patients with schizophrenia and non-psychiatric controls. Schizophrenia Research. 2008;**100**:216-223

[196] Kamath V, Bedwell JS. Olfactory identification performance in individuals with psychometrically-defined schizotypy. Schizophrenia Research. 2008;**100**:212-215

[197] Hummel T, Sekinger B, Wolf SR, Pauli E, Kobal G. 'Sniffin' sticks': Olfactory performance assessed by the combined testing of odor identification, odor discrimination and olfactory threshold. Chemical Senses. 1997;**22**:39-52

[198] Moberg PJ et al. Impairment of odor hedonics in men with schizophrenia. The American Journal of Psychiatry. 2003;**160**:1784-1789

[199] Doop ML, Park S. On knowing and judging smells: Identification and hedonic judgment of odors in schizophrenia. Schizophrenia Research. 2006;**81**:317-319

[200] Kiparizoska S, Ikuta T. Disrupted olfactory integration in schizophrenia: Functional connectivity study. The International Journal of Neuropsychopharmacology. 2017; **20**:740-746

[201] Turetsky BI, Hahn C-G, Arnold SE, Moberg PJ. Olfactory receptor neuron dysfunction in schizophrenia. Neuropsychopharmacology. 2009;**34**:767-774

[202] Borgmann-Winter KE et al. Altered G protein coupling in olfactory neuroepithelial cells from patients with schizophrenia. Schizophrenia Bulletin. 2016;**42**:377-385

[203] Arnold SE et al. Dysregulation of olfactory receptor neuron lineage in schizophrenia. Archives of General Psychiatry. 2001;**58**:829-835

[204] Watkins CC, Andrews SR. Clinical studies of neuroinflammatory mechanisms in schizophrenia. Schizophrenia Research. 2016;**176**:14-22

[205] Brown AS, Derkits EJ. Prenatal infection and schizophrenia: A review of epidemiologic and translational studies. The American Journal of Psychiatry. 2010;**167**:261-280

[206] Nakazawa K, Jeevakumar V, Nakao K. Spatial and temporal boundaries of NMDA receptor hypofunction leading to schizophrenia. NPJ Schizophrenia. 2017;**3**:7

[207] Lagier S et al. GABAergic inhibition at dendrodendritic synapses tunes gamma oscillations in the olfactory bulb. Proceedings of the National Academy of Sciences of the United States of America. 2007;**104**:7259-7264

[208] Egger V, Urban NN. Dynamic connectivity in the mitral cell-granule cell microcircuit. Seminars in Cell & Developmental Biology. 2006;**17**:424-432

[209] Gire DH, Schoppa NE. Control of on/off glomerular signaling by a local GABAergic microcircuit in the olfactory bulb. Journal of Neuroscience. 2009;**29**:13454-13464

[210] Hong SE et al. Autosomal recessive lissencephaly with cerebellar hypoplasia is associated with human RELN mutations. Nature Genetics. 2000;**26**:93-96

[211] Brosda J, Dietz F, Koch M. Impairment of cognitive performance after reelin knockdown in the medial prefrontal cortex of pubertal or adult rats. Neurobiology of Disease. 2011;**44**:239-247

[212] Sui L, Wang Y, Ju L-H, Chen M. Epigenetic regulation of reelin and brain-derived neurotrophic factor genes in long-term potentiation in rat medial prefrontal cortex. Neurobiology of Learning and Memory. 2012;**97**:425-440

[213] Imai H et al. Dorsal forebrain-specific deficiency of Reelin-Dab1 signal causes Behavioral abnormalities related to psychiatric disorders. Cerebral Cortex. 2017;**27**:3485-3501

[214] Guidotti A et al. Decrease in reelin and glutamic acid decarboxylase67 (GAD67) expression in schizophrenia and bipolar disorder: A postmortem brain study. Archives of General Psychiatry. 2000;**57**:1061-1069

[215] Botella-López A et al. Reelin expression and glycosylation patterns are altered in Alzheimer's disease. Proceedings of the National Academy of Sciences of the United States of America. 2006;**103**:5573-5578

[216] Fehér Á, Juhász A, Pákáski M, Kálmán J, Janka Z. Genetic analysis of the RELN gene: Gender specific association with Alzheimer's disease. Psychiatry Research. 2015; **230**:716-718

[217] Seripa D et al. The RELN locus in Alzheimer's disease. Journal of Alzheimer's Disease. 2008;**14**:335-344

[218] Escanilla O, Yuhas C, Marzan D, Linster C. Dopaminergic modulation of olfactory bulb processing affects odor discrimination learning in rats. Behavioral Neuroscience. 2009;**123**:828-833

[219] Galle SA, Courchesne V, Mottron L, Frasnelli J. Olfaction in the autism spectrum. Perception. 2013;**42**:341-355

[220] Tonacci A et al. Olfaction in autism spectrum disorders: A systematic review. Child Neuropsychology. 2015;**23**:1-25

[221] Katayama Y et al. CHD8 haploinsufficiency results in autistic-like phenotypes in mice. Nature. 2016;**537**:675-679

[222] Cho H et al. Changes in brain metabolic connectivity underlie autistic-like social deficits in a rat model of autism spectrum disorder. Scientific Reports. 2017;**7**

[223] Huang T-N, Hsueh Y-P. Brain-specific transcriptional regulator T-brain-1 controls brain wiring and neuronal activity in autism spectrum disorders. Frontiers in Neuroscience. 2015;**9**:406

[224] Canitano R, Pallagrosi M. Autism spectrum disorders and schizophrenia spectrum disorders: Excitation/inhibition imbalance and developmental trajectories. Frontiers in Psychiatry. 2017;**8**:69

[225] Gao R, Penzes P. Common mechanisms of excitatory and inhibitory imbalance in schizophrenia and autism spectrum disorders. Current Molecular Medicine. 2015;**15**:146-167

[226] Moberg PJ, Doty RL. Olfactory function in Huntington's disease patients and at-risk offspring. The International Journal of Neuroscience. 1997;**89**:133-139

[227] Lemiere J. Huntington's Disease: Early Detection and Progression of Cognitive Changes in Patients and Asymptomatic Mutation Carriers. Leuven: University Press; 2004

[228] Hawkes CH, Doty RL. The Neurology of Olfaction. Cambridge University Press. 2009

[229] Kovács T, Cairns NJ, Lantos PL. Beta-amyloid deposition and neurofibrillary tangle formation in the olfactory bulb in ageing and Alzheimer's disease. Neuropathology and Applied Neurobiology. 1999;**25**:481-491

[230] Ubeda-Bañon I et al. Alpha-synucleinopathy in the human olfactory system in Parkinson's disease: Involvement of calcium-binding protein- and substance P-positive cells. Acta Neuropathologica. 2010;**119**:723-735

[231] Rey NL, Petit GH, Bousset L, Melki R, Brundin P. Transfer of human α-synuclein from the olfactory bulb to interconnected brain regions in mice. Acta Neuropathologica. 2013;**126**:555-573

[232] Kagan BL et al. Antimicrobial properties of amyloid peptides. Molecular Pharmaceutics. 2011;**9**:708-717

[233] Kovács T. The olfactory system in Alzheimer's disease: Pathology, pathophysiology and pathway for therapy. Translational Neuroscience. 2012 Sep;**237**(1):1-7

[234] Davies DC, Brooks JW, Lewis DA. Axonal loss from the olfactory tracts in Alzheimer's disease. Neurobiology of Aging. 1993;**14**:353-357

[235] Kovács T, Cairns NJ, Lantos PL. Olfactory centres in Alzheimer's disease: Olfactory bulb is involved in early Braak's stages. Neuroreport. 2001;**12**:285-288

[236] Ohm TG, Braak H. Olfactory bulb changes in Alzheimer's disease. Acta Neuropathologica. 1987;**73**:365-369

[237] Struble RG, Clark HB. Olfactory bulb lesions in Alzheimer's disease. Neurobiology of Aging. 1992;**13**:469-473

[238] Attems J, Lintner F, Jellinger KA. Olfactory involvement in aging and Alzheimer's disease: An autopsy study. Journal of Alzheimer's Disease. 2005;**7**:149-157 (discussion 173-80)

[239] Attems J, Jellinger KA. Olfactory tau pathology in Alzheimer disease and mild cognitive impairment. Clinical Neuropathology. 2006;**25**:265-271

[240] Talamo BR et al. Pathological changes in olfactory neurons in patients with Alzheimer's disease. Nature. 1989;**337**:736-739

[241] Dua P, Y Z. Microbial sources of amyloid and relevance to Amyloidogenesis and Alzheimer's disease (AD). Journal of Alzheimer's, Parkinsonism and Dementia. 2015 Mar;**5**(1):177

[242] Bhattacharjee S, Lukiw WJ. Alzheimer's disease and the microbiome. Frontiers in Cellular Neuroscience. 2013;**7**:153

[243] Catanzaro R et al. The gut microbiota and its correlations with the central nervous system disorders. Panminerva Medica. 2015;**57**:127-143

[244] Friedland RP. Mechanisms of molecular mimicry involving the microbiota in neurodegeneration. Journal of Alzheimer's Disease. 2015;**45**:349-362

[245] Syed AK, Boles BR. Fold modulating function: Bacterial toxins to functional amyloids. Frontiers in Microbiology. 2014;**5**:401

[246] Rhee SH. Lipopolysaccharide: Basic biochemistry, intracellular signaling, and physiological impacts in the gut. Intestinal Research. 2014;**12**:90-95

[247] Marques F, Sousa JC, Sousa N, Palha JA. Blood-brain-barriers in aging and in Alzheimer's disease. Molecular Neurodegeneration. 2013;**8**:38

[248] Shoemark DK, Allen SJ. The microbiome and disease: Reviewing the links between the oral microbiome, aging, and Alzheimer's disease. Journal of Alzheimer's Disease. 2015;**43**:725-738

[249] Tran L, Greenwood-Van Meerveld B. Age-associated remodeling of the intestinal epithelial barrier. The Journals of Gerontology. Series A, Biological Sciences and Medical Sciences. 2013;**68**:1045-1056

[250] Oakley R, Tharakan B. Vascular hyperpermeability and aging. Aging and Disease. 2014; **5**:114-125

[251] Hammer ND, Wang X, McGuffie BA, Chapman MR. Amyloids: Friend or foe? Journal of Alzheimer's Disease. 2008;**13**:407-419

[252] Higaki S, Gebhardt BM, Lukiw WJ, Thompson HW, Hill JM. Effect of immunosuppression on gene expression in the HSV-1 latently infected mouse trigeminal ganglion. Investigative Ophthalmology & Visual Science. 2002;**43**:1862-1869

[253] Stilling RM, Dinan TG, Cryan JF. Microbial genes, brain & behaviour – epigenetic regulation of the gut-brain axis. Genes, Brain, and Behavior. 2013;**13**:69-86

[254] Sliger M, Lander T, Murphy C. Effects of the ApoE epsilon4 allele on olfactory function in Down syndrome. Journal of Alzheimer's Disease. 2004;**6**:397-402 (discussion 443-9)

[255] Hussain A, Luong M, Pooley A, Nathan BP. Isoform-specific effects of apoE on neurite outgrowth in olfactory epithelium culture. Journal of Biomedical Science. 2013;**20**:49

[256] Kulkarni-Narla A, Getchell TV, Schmitt FA, Getchell ML. Manganese and copper-zinc superoxide dismutases in the human olfactory mucosa: Increased immunoreactivity in Alzheimer's disease. Experimental Neurology. 1996;**140**:115-125

[257] Yamagishi M, Takami S, Getchell TV. Ontogenetic expression of spot 35 protein (Calbindin-D28K) in human olfactory receptor neurons and its decrease in Alzheimer's disease patients. Annals of Otology, Rhinology & Laryngology. 1996;**105**:132-139

[258] Pignatelli A, Belluzzi O. Cholinergic modulation of dopaminergic neurons in the mouse olfactory bulb. Chemical Senses. 2008;**33**:331-338

[259] Arendt T, Bigl V, Arendt A, Tennstedt A. Loss of neurons in the nucleus basalis of Meynert in Alzheimer's disease, paralysis agitans and Korsakoff's disease. Acta Neuropathologica. 1983;**61**:101-108

[260] Huisman E, Uylings HBM, Hoogland PV. A 100% increase of dopaminergic cells in the olfactory bulb may explain hyposmia in Parkinson's disease. Movement Disorders. 2004;**19**:687-692

[261] Mundiñano I-C et al. Increased dopaminergic cells and protein aggregates in the olfactory bulb of patients with neurodegenerative disorders. Acta Neuropathologica. 2011;**122**:61-74

[262] Loopuijt LD, Sebens JB. Loss of dopamine receptors in the olfactory bulb of patients with Alzheimer's disease. Brain Research. 1990;**529**:239-244

[263] Kovacs GG et al. Nucleus-specific alteration of raphe neurons in human neurodegenerative disorders. Neuroreport. 2003;**14**:73-76

[264] Zarow C, Lyness SA, Mortimer JA, Chui HC. Neuronal loss is greater in the locus coeruleus than nucleus basalis and substantia nigra in Alzheimer and Parkinson diseases. Archives of Neurology. 2003;**60**:337-341

[265] Feinstein DL et al. Noradrenergic regulation of inflammatory gene expression in brain. Neurochemistry International. 2002;**41**:357-365

[266] De Simone R, Ajmone-Cat MA, Carnevale D, Minghetti L. Activation of alpha7 nicotinic acetylcholine receptor by nicotine selectively up-regulates cyclooxygenase-2 and prostaglandin E2 in rat microglial cultures. Journal of Neuroinflammation. 2005;**2**:4

[267] Cheng N, Bai L, Steuer E, Belluscio L. Olfactory functions scale with circuit restoration in a rapidly reversible Alzheimer's disease model. Journal of Neuroscience. 2013; **33**:12208-12217

[268] Knuesel I et al. Age-related accumulation of Reelin in amyloid-like deposits. Neurobiology of Aging. 2009;**30**:697-716

[269] Cuchillo-Ibañez I, Balmaceda V, Mata-Balaguer T, Lopez-Font I, Sáez-Valero J. Reelin in Alzheimer's disease, increased levels but impaired signaling: When more is less. Journal of Alzheimer's Disease. 2016;**52**:403-416

[270] Brai E, Alina Raio N, Alberi L. Notch1 hallmarks fibrillary depositions in sporadic Alzheimer's disease. Acta Neuropathologica Communications. 2016;**4**:64

[271] Marathe S, Jaquet M, Annoni J-M, Alberi L. Jagged1 is altered in Alzheimer's disease and regulates spatial memory processing. Frontiers in Cellular Neuroscience. 2017;**11**:220

[272] Brai E et al. Notch1 activity in the olfactory bulb is odour-dependent and contributes to olfactory behaviour. The European Journal of Neuroscience. 2014;**40**:3436-3449

[273] Albers MW, Tabert MH, Devanand DP. Olfactory dysfunction as a predictor of neurodegenerative disease. Current Neurology and Neuroscience Reports. 2006;**6**:379-386

[274] Markopoulou K et al. Assessment of olfactory function in MAPT-associated neurodegenerative disease reveals odor-identification irreproducibility as a non-disease-specific, general characteristic of olfactory dysfunction. PLoS One. 2016;**11**:e0165112

[275] Glasl L et al. Pink1-deficiency in mice impairs gait, olfaction and serotonergic innervation of the olfactory bulb. Experimental Neurology. 2012;**235**:214-227

[276] Kim YH, Lussier S, Rane A, Choi SW, Andersen JK. Inducible dopaminergic glutathione depletion in an alpha-synuclein transgenic mouse model results in age-related olfactory dysfunction. Neuroscience. 2011;**172**:379-386

[277] Fleming SM et al. Olfactory deficits in mice overexpressing human wildtype alpha-synuclein. The European Journal of Neuroscience. 2008;**28**:247-256

[278] Nuber S et al. A progressive dopaminergic phenotype associated with neurotoxic conversion of α-synuclein in BAC-transgenic rats. Brain. 2013;**136**:412-432

[279] Taylor TN, Caudle WM, Miller GW. VMAT2-deficient mice display Nigral and Extranigral pathology and motor and nonmotor symptoms of Parkinson's disease. Parkinsons Disease. 2011;**2011**:124165

[280] Jellinger KA. Olfactory bulb alpha-synucleinopathy has high specificity and sensitivity for Lewy body disorders. Acta Neuropathologica. 2009;**117**:215-216 (author reply 217-8)

[281] Lavoie J et al. The olfactory neural epithelium as a tool in neuroscience. Trends in Molecular Medicine. 2017;**23**:100-103

[282] Narayan S et al. Olfactory neurons obtained through nasal biopsy combined with laser-capture microdissection: A potential approach to study treatment response in mental disorders. Journal of Visualized Experiments. 2014 Dec 4;(94). DOI: 10.3791/51853

[283] Henkin RI, Velicu I. cAMP and cGMP in nasal mucus: Relationships to taste and smell dysfunction, gender and age. Clinical & Investigative Medicine. 2008;**31**:71

[284] Henkin RI, Velicu I. 30 Insulin receptors as well as insulin are present in saliva and nasal mucus. Journal of Investigative Medicine. 2006;**54**:S378

[285] Illum L. Is nose-to-brain transport of drugs in man a reality? The Journal of Pharmacy and Pharmacology. 2004;**56**:3-17

[286] Pires A, Fortuna A, Alves G, Falcão A. Intranasal drug delivery: How, why and what for? Journal of Pharmacy & Pharmaceutical Sciences. 2009;**12**:288-311

[287] Grassin-Delyle S et al. Intranasal drug delivery: An efficient and non-invasive route for systemic administration: Focus on opioids. Pharmacology & Therapeutics. 2012; **134**:366-379

[288] Willette AA, Modanlo N, Kapogiannis D, Alzheimer's Disease Neuroimaging Initiative. Insulin resistance predicts medial temporal hypermetabolism in mild cognitive impairment conversion to Alzheimer disease. Diabetes. 2015;**64**:1933-1940

[289] Craft S et al. Intranasal insulin therapy for Alzheimer disease and amnestic mild cognitive impairment: A pilot clinical trial. Archives of Neurology. 2012;**69**:29-38

[290] Claxton A et al. Long-acting intranasal insulin detemir improves cognition for adults with mild cognitive impairment or early-stage Alzheimer's disease dementia. Journal of Alzheimer's Disease. 2015;**44**:897-906

[291] Reger MA et al. Intranasal insulin improves cognition and modulates beta-amyloid in early AD. Neurology. 2008;**70**:440-448

[292] Wong YC, Zuo Z. Brain disposition and catalepsy after intranasal delivery of loxapine: Role of metabolism in PK/PD of intranasal CNS drugs. Pharmaceutical Research. 2013;**30**:2368-2384

[293] Hanson LR et al. Intranasal deferoxamine provides increased brain exposure and significant protection in rat ischemic stroke. The Journal of Pharmacology and Experimental Therapeutics. 2009;**330**:679-686

[294] Scranton RA, Fletcher L, Sprague S, Jimenez DF, Digicaylioglu M. The rostral migratory stream plays a key role in intranasal delivery of drugs into the CNS. PLoS One. 2011;**6**:e18711

Chapter 5

Retinal Topographic Maps: A Glimpse into the Animals' Visual World

Einat Hauzman, Daniela M.O. Bonci and
Dora F. Ventura

Additional information is available at the end of the chapter

http://dx.doi.org/10.5772/intechopen.74645

Abstract

The vertebrates' retina has a highly conserved laminar organization of 10 alternating nuclear and plexiform layers. Species differences in the retinal specializations, i.e., areas of higher cell density, among the species, represent specific regions of the visual field of higher importance for a better spatial resolution and indicate distinct evolutionary pressures on the structures of the visual system, which can be related to many aspects of the species evolutionary history. In this chapter, we analyzed the density and distribution of cells of the retinal ganglion cell layer (GCL) and estimated the upper limits of the spatial resolving power of 12 species of snakes from the Colubridae family, 6 diurnal and 6 nocturnal, which inhabit different habitats. Our results revealed lower visual acuity in nocturnal species, compared to diurnal, and we observed different types of retinal specialization, horizontal streak, *area centralis*, or scattered distribution, with higher cell density in different retinal regions, depending on the species. These variations may be related to ecological and behavioral features, such as daily activity pattern, habitat, and substrate preferentially occupied, hunting strategies and diet. This comparative study indicates the complexity of the adaptive strategies of the snakes' visual system.

Keywords: retina, visual ecology, visual acuity, ganglion cells, snakes

1. Introduction

1.1. The visual system

The sensory systems allow the animals to interact properly with their environment and with other organisms. The perception of the surrounding environment is essential for the animals'

survival, and in most vertebrates, the visual system plays a crucial role in basic activities such as foraging behavior, sheltering, flight from predators, and breeding. Functional and anatomical differences of the visual structures often reflect distinct selective pressures implied by the ecological niches.

In all vertebrates, three layers of tissue concentrically arranged form the eyes. The sclera is the outermost layer composed by highly interconnected collagen fibers that support the eye. In the anterior part of the eye, the fibers of the sclera assume an orderly conformation that confers transparency to the sclera, forming the cornea, a lens through which the light can pass. The cornea, together with the crystalline lens, located between the anterior chamber and the vitreous humor, a gelatinous substance that fills the eyeball, enable the focusing of the image in the retina. The second layer is the uvea, formed by the iris, ciliary body, and choroid, and provides nutrients and oxygen to third and innermost layer, the retina, a tissue formed by a network of nerve and glial cells [1, 2].

1.1.1. The retina

In all vertebrates, the retina has an organizational pattern of 10 layers of body cells, nerve plexuses, limiting membranes, pigment epithelium, and nerve fibers (**Figure 1**). This laminar tissue, responsible for capturing and initiating the processing of luminous information for image formation, has a complex organization, with five main types of neurons: photoreceptors, bipolar cells, horizontal cells, amacrine cells, and ganglion cells. The neuroanatomist Santiago Ramón y Cajal was the first to describe, in 1893 [1], this thin neural tissue, with a 10-layered division.

The retinal pigment epithelium is the outermost layer, formed by epithelial cells with pigment granules, and has a number of metabolic functions essential for retinal homeostasis and activity, such as nutrients and oxygen supply, and cycling of the photosensitive chromophore (retinal) [3–6]. The photoreceptor layer (PL) is formed by the outer and inner segments of these

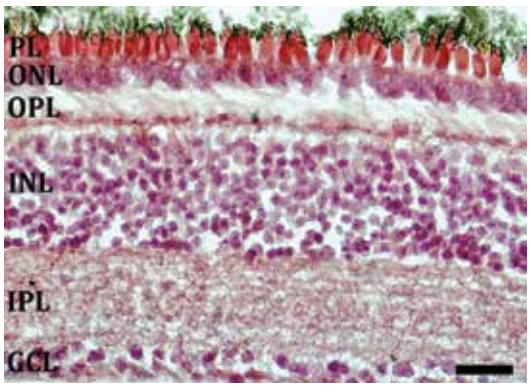

Figure 1. Photomicrograph of a cross section of the diurnal snake, *Tomodon dorsatus*, labeled with hematoxylin and eosin. PL, photoreceptor layer; ONL, outer nuclear layer; OPL, outer plexiform layer; INL, inner nuclear layer; IPL, inner plexiform layer; GCL, ganglion cell layer. Scale bar = 20 μm.

neurons (cones and rods), specialized in capturing and converting the light energy into electrochemical energy and transmitting this information to the cells of the following layer. The outer limiting membrane (OLM), located below the PL, is formed by the extensions of Müller cells (glial cells) and is followed by the outer nuclear layer (ONL), with the photoreceptors nuclei. These first-order neurons make synaptic contact with second order neurons, bipolar and horizontal cells, in the outer plexiform layer (OPL). Bipolar, horizontal, and amacrine cell bodies are located in the inner nuclear layer (INL), and these cells make synaptic contact with the ganglion cells (third order neurons), in the inner plexiform layer (IPL). The cell bodies of ganglion cells and displaced amacrine cells form the ganglion cell layer (GCC). The ganglion cell axons form the nerve fiber layer (NFL) and come together to form the optic nerve, which conducts information from the retina to the higher visual centers in the brain. The inner limiting membrane (ILM) is also composed of laterally contacting extensions of Müller cells [1].

The photoreceptors contain visual photopigments, which are responsible for capturing luminous information and initiating visual processing. Two main types of photoreceptors are usually present in vertebrate retinas, cones, and rods. The outer segments of these cells consist of stacked membranous disks containing the visual photopigments. The latter are formed by a membrane protein, opsin or rhodopsin, coupled to a chromophore, responsible for the absorption of photons and the beginning of the visual processing [7, 8]. The higher number of photopigments in rods provides greater absorption capacity of photons, which makes these cells more sensitive to light compared to cones. Rods are responsible for the scotopic (nocturnal) vision system, which is highly sensitive, with a large capacity of light capturing and signal amplification generated by a single photoizomerization event and the great synaptic convergence, with many rods attached to one ganglion cell, through the bipolar cells, but with a low visual acuity, due to the high degree of convergence. The photopic (diurnal) visual system mediated by cones has less sensitivity but greater visual acuity [7–9]. Under high luminous intensity, rods are saturated, while cones are activated. During the night, rods are activated with the illumination below the activation threshold of cones [10]. Nocturnal animals usually have retinas with predominance of rods, whereas diurnal animals possess greater amount of cones. Different types of photopigments capture maximally photons with different wavelengths. The presence of distinct photoreceptors in the retina, with different opsin types, together with a postreceptor mechanism capable of comparing the signal transmitted by these neurons, is the first step to enable the color vision [11].

More recently, a third photoreceptor class was described in the inner retina of many vertebrates [12–14]. The melanopsin-containing ganglion cells, known as intrinsically photosensitive retinal ganglion cells (ipRGCs), are activated directly by light. These cells give rise to circuits that process important physiological functions, such as the circadian rhythm synchronization and pupillary light reflex [15–17]. They constitute the nonimage forming visual system. The ipRGCs represent about 1–3% of the retinal ganglion cells in mammals [14, 18]. In other vertebrates, as fish [19, 20] and birds [21, 22], melanopsin-containing neurons were described not only in the GCL but also in the other retinal layers.

The ganglion cells are on average larger than the other retinal neurons and have myelinated axons, with large diameters, capable of transmitting the electrical messages of the visual signal

generated by the photoreceptors and processed in the inner retina [7], to the receptive areas of the brain, many millimeters or centimeters away from the retina. Their density and topographic distribution in the retina are important factors in determining the upper limits for the spatial resolution power of the eye [23–26].

In short, the highly complex and standardized laminar pattern of the retina is observed in all vertebrates. However, remarkable differences related to the specific cell types, and their density and distribution in the retina, the so-called retinal specializations, are observed among the different species and are related to specific habitats, behaviors, and the species' visual ecology.

1.1.2. Retinal specializations

A higher concentration of retinal neurons is observed in regions of greater demand for a good image quality [24, 25, 27–34]. Some studies have shown that cell distribution correlates better with species behavior and habitat than with phylogeny, and that phylogenetically related species may have different patterns of distribution and organization of the neural elements and vice versa [28–30, 35, 36]. The retinal specializations are areas of higher cell density compared to neighboring areas and include visual streaks, *area centralis*, and fovea [2, 32, 37, 38]. Visual streaks are elongated regions of higher cell density and can be horizontal or vertical. The horizontal streak is common in vertebrates that occupy habitats whose visual field is dominated by the horizon, such as the air-land interface of terrestrial species or water-land interface of aquatic species [32] (**Figure 2**). The horizontal streak provides a panoramic view of the environment without the need for a high degree of eye movement [28, 32]. Examples of horizontal streaks are observed, for instance, in retinas of the turtle *Trachemys scripta elegans* [39, 40], alpacas *Vicugna pacos* [41], and the agouti *Dasyprocta aguti* [30, 42]. The vertical streak

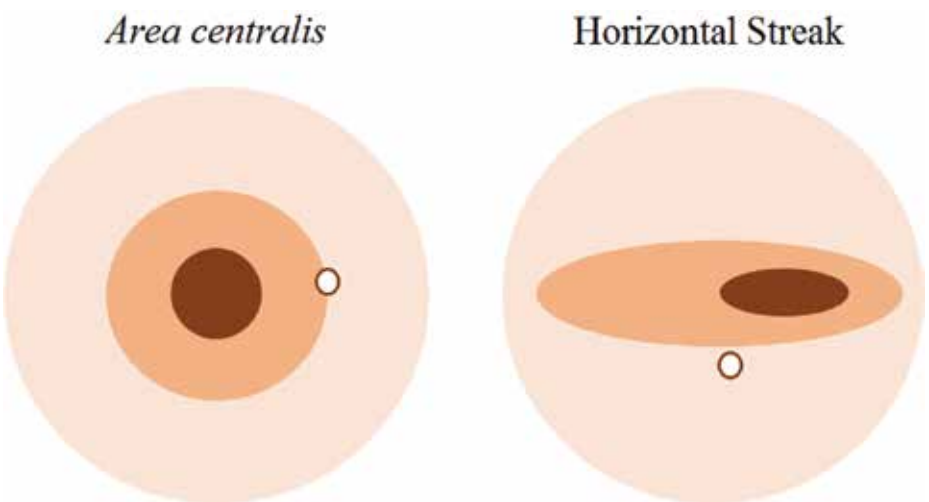

Figure 2. Representation of an *area centralis* located in the central retina, and a horizontal streak extended along the retinal meridian axis. The variation in cell density is represented by the color gradient, where the darker color indicates the region of higher density. The white spots represent the optic nerve head.

is also defined as an elongated increase in cell density but extends along the dorso-ventral axis of the retina and is usually located in the temporal region. This specialization is more unusual and can be observed in retinas of species whose visual field is dominated by a vertically oriented feature, such as the tree branches seen by the sloth *Choloepus didactylus* [43], the trunk of the African elephant *Loxodonta africana* [44], or the water column, seen by vertically migrating species, as the teleost fish *Howella sherborni* [45].

Many species have a circular area of higher cell density called *area centralis* (**Figure 2**). This type of specialization does not have the advantage of perceiving the panoramic visual field like that provided by the horizontal streak and requires a greater degree of eye movement to locate prey and the presence of potential predators [28, 32]. The *area centralis* is usually located in the temporal region of the retina, thus included in the frontal binocular visual field, which is also determined by the position of the eyes on the head. In some species, there is a concentric arrangement of the isodensity contours within the *area centralis*, while in others, the cellular arrangement is described as anisotropic, because the isodensity contours are not concentric and the density distribution is irregular [32, 38].

According to Hughes' "terrain theory" [28], terrestrial animals inhabiting open fields generally have a horizontal streak with high density of photoreceptors and ganglion cells. Since the streak provides a panoramic view of the environment, there is no need for eye movements for detection of objects along the horizon line, an appropriate feature for the field extension vision and perception of the approach of predators. Arboreal species or those from dense forests generally have an *area centralis*, with a higher density of cones and ganglion cells, which confers better acuity to this circular region. The specific function of the *area centralis* may vary depending on the predominant type of retinal ganglion cell [38, 46]. About 20 different types of ganglion cells have been described in the retina of mammals [47, 48] and can be distinguished based on their morphology, stratification pattern, and specific functions.

Some primates, reptiles, and birds have a fovea, a specialization of the *area centralis*, characterized by the lateral displacement of cells from the inner layers of the retina and an increase in the density of ganglion cells in the perifoveal region [2, 32, 49]. In the fovea, there is an increase in the density of photoreceptors with more elongated outer segments and smaller diameter, and the presence of only cones favors greater acuity in this region [2, 37, 39, 50]. There are two main types of foveae—the convexiclivate fovea, with a steep slope on both sides of the depression, as observed in some fish and birds, or the concaviclivate fovea with a shallow depression, as in monkeys and humans [32]. In some species, as the sacred kingfisher bird, *Halcyon sancta*, the presence of two foveae has been described; a temporal that acts in the binocular vision and a nasal involved in monocular vision [51].

1.1.3. Spatial resolving power

Variations in the visual acuity may reflect ecological differences among species and are limited by the diffraction and optical aberration characteristics of the eye, the density of photoreceptors and ganglion cells, and by variables such as refraction error, ambient illumination, and contrast [52]. Lisney and Collin [26] analyzed the retinas of several species of elasmobranchs (sharks and rays) and observed that species with lower resolution power tend to be relatively

less active and feed on benthic invertebrates and small fish, while more active, predatory species that usually feed on larger prey have a greater eye resolving power.

The visual acuity of an animal can be measured using different approaches, such as behavioral tests, response to a stimulus, ocular movements (preferential look), electrophysiological recording, or it can be estimated from anatomical data [41]. Because the ganglion cells constitute the final output of visual information from the retina to the higher visual centers, their density represents a limiting factor of the spatial resolution power of the eye and the ability of the animal to distinguish fine details of the objects [24]. Thus, the peak density of ganglion cells in combination with the eye focal length may be used to infer the maximum spatial resolution power of an animal [24, 25, 33, 34, 53]. These estimated values are usually very close to the acuity values obtained from more direct methods for many species in which both measurements were compared [54–58].

The retinal specializations and the spatial resolution power of the eye are closely associated with the animals' visual ecology. Studies on these aspects of the visual system, which include the analysis of the density and distribution of retinal neurons and the specific area of higher degree of visual acuity, bring valuable information on the species biology and are often more related to ecological and behavioral features than to phylogeny. In order to better understand the evolution and functioning of this complex sensory system, it is of great value to compare closely related species with ecological differences. An excellent model for this type of comparative study is the group of snakes, given their great diversity and the variety of ecological niches occupied by phylogenetically close species.

1.2. Snakes: characteristics of the group and adaptations of the visual system

The infraorder Serpentes is characterized by body stretching, absence of limbs, eyelids and external ears, and the presence of forked tongue [59] and is subdivided into two main groups. The Scolecophidia group (blind snakes) is composed by small fossorial snakes with reduced eyes that feed on small prey as termites and ants. The Alethinophidia group is composed by a greater diversity of species, with two major groups, the paraphyletic Henophidia group, with about 180 species, including pythons and boas, and the Caenophidia group, with about 2500 species [60, 61]. Snakes from the Caenophidia group are found in virtually every portion of the biosphere, except for the poles, some islands, and the ocean deep [62]. The great diversity of this group, with species adapted to a great variety of habitats, can be explained by the occurrence of a number of adaptations that favored their dispersion [63–65] and the specialization of their sensory systems that evolved to allow their survival and adaptive radiation. The Caenophidia group is therefore characterized by a great diversity of species, with differences in the circadian activity patterns and in the habitats occupied, including terrestrial, arboreal, cryptozoic or fossorial, as well as aquatic environments, which include marine or fresh water habitats [66].

Despite the great diversity of snake' species and ecological and behavioral features, very few studies have investigated their retinal specializations. To date, only three studies described the distribution of neurons in snakes' retinas. Wong [67] described a visual streak for cones and

GCL cells in retinas of the terrestrial *Thamnophis sirtalis*. The arboreal *Philodryas olfersii* has a horizontal streak and two discrete anisotropic *area centralis* in the central and temporal regions of the retina, while the closely related species, the terrestrial *P. patagoniensis*, has an anisotropic *area centralis* in the ventro-nasal retina [36]. In retinas of marine snakes from the Hydrophiidae family, Hart et al. [34] observed a horizontal streak in *Lapemis curtus*, *Aipysurus laevis*, and *Disteira major*, with discrete *area* in the temporal and nasal quadrants. The species *L. curtus* and *D. major* also have a ventral *area*.

The upper limits of spatial resolving power, estimated based on the ganglion cell peak density and the eye focal length, varied between 2.3 and 2.8 cpg in diurnal and terrestrial snakes [36, 67] and were lower in marine species, ranging between 1.1 and 2.3 cpd [34]. The lower values of marine snakes were attributed to reduced eye size and differences in the photic properties of water compared to air. A higher visual acuity, 4.9 cpd, was measured by recording evoked responses from telencephalon in the aquatic snake *Nerodia sipedon pleuralis* [68]. Compared to other reptiles, snakes had lower values of visual acuity: 6.1 cpd in the red-eared slider turtle (*Trachemys scripta elegans*) [69], 6.8 cpd in the sleepy lizard (*Tiliqua rugosa*) [70], and 13.6 cpd in the anoline lizard (*Anolis carolinensis*) [71]. Compared to mammals, snakes had higher values than the opossum *Didelphis aurita* (1.3 cpd) [72], rats (1 cpd) [73, 74], and mice (0.6 cpd) [75] but lower than cats (10 cpd) [54], and humans (60 cpd) [76].

In short, the diversity of species and the variability of habitats used by snakes point to important adaptations of their visual system. Studies on the characteristics and adaptations of the visual system of snakes are extremely scarce in view of the large number of species. Based on their ecological diversity, caenophidian snakes represent a good model for testing hypotheses of correlations between retinal specializations and behavioral ecology. Thus, we analyzed and compared the density and distribution of the GCL cells and estimated the eye spatial resolving power of 12 species from the Colubridae family, with variety regarding their daily activity pattern, and the preferential substrate: arboreal, terrestrial, fossorial, or aquatic. The analysis revealed the presence of different specialization types, visual streak or *area centralis* located in different regions of the retina, depending on the species. The population of GCL cells and the estimated upper limit of the spatial resolving power varied among diurnal and nocturnal species. The diversity of retinal specializations observed in this study seems to be related to a variety of ecological and behavioral features, pointing to the complexity of the evolution and adaptations of the retinal structure.

2. Assessing cell density and topographic distribution across the retinas and estimating the spatial resolving power

In this study, retinas of 12 Colubridae snakes, 6 considered as primarily nocturnal and 6 as primarily diurnal (**Table 1**), were collected and dissected for wholemount and Nissl-staining technique. The adult specimens were obtained at the Butantan Institute, São Paulo, Brazil, and were euthanized with a lethal injection of sodium thiopental (thiobarbiturate ethyl sodium, 30 mg/kg). Following euthanasia, the eyes were enucleated, and the axial length was

Family	Subfamily	Tribe	Species	Biome	Habitat	Substrate	Activity pattern
Colubridae	Colubrinae		*Chironius bicarinatus*	AF	F	Ar/Te	D
			Spillotes pullatus	AF	F	Ar/Te	D
	Dipsadinae		*Atractus pantostictus*	CE/AF	F	Su	N
			Atractus reticulatus	CE/AF	F	Su	N
			Dipsas albifrons	AF	F	Ar/Te	N
			Sibynomorphus mikanii	CE/AF	F, O	Te	N
			Sibynomorphus neuwiedi	AF	F	Ar/Te	N
			Erythrolamprus aesculapii	CE/AF	F, O	Te	D
		Xenodontini	*Erythrolamprus miliaris*	AF	F	Aq/Te	D
			Erythrolamprus poecilogyrus	CE	F, O	Te	D
		Pseudoboini	*Oxyrhopus guibei*	CE	F, O	Te	N
		Tachymenini	*Tomodon dorsatus*	AF	F	Te	D

CE, Cerrado; AF, Atlantic Rain Forest; O, open area; F, forested area; Ar, arboreal; Te, terrestrial; Su, subterranean; Aq, aquatic; D, primarily diurnal; N, primarily nocturnal. Biome, habitat and substrate were determined based on [78]. Activity pattern was stablished based on [77, 79].

Table 1. Species, habitat and daily activity pattern.

measured. The cornea, ciliary body, and lens were removed, and the lens diameters were measured. A small radial incision was made in the dorsal region of each eyecup, for retinal orientation. The retinas were dissected from the eyecup, the pigment epithelium was separated, and the vitreous humor was removed. The retinas were fixed in 10% formalin. After these procedures, the specimens were fixed in 10% formaldehyde and preserved in the herpetological collection of the Butantan Institute. The animal procedures were done in accordance with the ethical principles of animal management and experimentation established by the Brazilian Animal Experiment College (COBEA). Species daily activity pattern and ecological features were established based on [77–79] (**Table 1**).

The retinas were flattened on gelatinized slides, with the GCL side facing up. Small radial incisions were made to allow the retinas to flatten and adhere to the slide. To label the retinal ganglion cells, we used Nissl-Staining procedures as described previously [36]. Glial cells were identified by their dark staining, small size, and rounded profile [34, 67, 83] and were not included in the counts. However, ganglion cells and displaced amacrine cells could not be reliably differentiated from each other, and both were included in the GCL cell counting [36, 80–85]. To analyze the density and distribution of GCL cells in wholemount retinas, we used a systematic random sampling and the fractionator principle [53, 82, 86–88]. The coordinates of the retinal edges were plotted on an Excel spreadsheet, and cells were counted at regular intervals defined by a sampling grid, ranging from 220 × 220 μm up to 680 × 680 μm, depending on the size of each retina (**Table 2**). The coordinates of the sampled fields were plotted on the same Excel spreadsheet, as well as the number of cells counted per field. The counting was performed directly under a Leica DMRXE microscope with a 100× oil objective

Species	Counting Frame (μm × μm)	Grid (μm × μm)	Area sampling fraction	Number of sites counted
Diurnal				
C.bicarinatus	74 × 74	620 × 620	0.014	154
E. aesculapi	74 × 74	520 × 520	0.020	125
E. miliaris	74 × 74	320 × 320	0.054	217
E. poecilogyrus	74 × 74	320 × 320	0.054	155
S. pullatus	74 × 74	680 × 680	0.010	190
T. dorsatus	74 × 74	320 × 320	0.050	184
Nocturnal				
A. pantostictus	74 × 74	230 × 230	0.100	55
A. reticulatus	74 × 74	220 × 220	0.110	56
D. petersi	74 × 74	340 × 340	0.048	160
O. guibei	74 × 74	310 × 310	0.057	117
S. mikanii	74 × 74	320 × 320	0.053	133
S. neuwiedii	74 × 74	220 × 220	0.115	272

Table 2. Stereological parameters used to estimate the number and distribution of retinal ganglion cell layer (GCL) cells in retinas of colubrid snakes, using the optical fractionator method.

(numerical aperture, NA = 1.25), equipped with a Nikon Digital Sight DS-U3 DSRi1 camera and the software NIS-Elements AR Microscope Imaging (Nikon Instruments, Melville, NY, USA). A counting frame at 74 × 74 μm was imposed on each sampled frame (**Table 2**). Cells were counted when inserted fully inside the counting frame or if touched the acceptance lines, without touching the rejection lines [86]. The number of cells quantified at each sampled field was entered in the Excel spreadsheet and converted into density value of cells per mm^2, by dividing the number of cells by the frame sampling area. The total number of GCL cells was estimated by multiplying the total number of cells counted by the inverse of the area sampling fraction (asf). The asf is calculated dividing the area of the counting frame by the area of the sampling grid, according to the algorithm: N total = ΣQ × 1/asf, where ΣQ is the number of counted cells [53, 89, 90] (**Table 2**). The average cell density of each retina was estimated from the average density values of each sampled field. The coefficients of error (CE) were calculated using the method proposed by Scheaffer et al. [91] and were <0.02 for all retinas, indicating that the total cell number estimates had a high degree of accuracy [53, 87, 92].

The coordinates of each sampled frame and the cell density values were used to elaborate the topographic maps, with the software OriginPro 8.1 (Northampton, MA, USA). The position of the retina was determined based on the radial incision made in the dorsal region during the dissection procedures and based on the optic nerve located in the ventral and temporal retinal quadrant in snakes. The reconstructed images were processed using the software Adobe Photoshop CS3 (Adobe Systems, Inc.).

We estimated the theoretical upper limits of the spatial resolving power based on the peak density of presumed ganglion cells and the estimated focal length of the eye. The focal length of the eye is represented by the posterior nodal distance (PND), which corresponds to the distance from the lens center to the choroid-retina border [93, 94]. In a broad analysis of different vertebrate species, Pettigrew and colleagues [24] proposed that the PND of diurnal vertebrates has a mean of 0.67 of the eye's axial length and that of nocturnal vertebrates has a mean of 0.52 of the eye's axial length. However, Hauzman and colleagues [36] estimated a focal length of 0.52 for diurnal colubrids. In this study, we accessed the eye's focal length of two colubrids, the diurnal *Tomodon dorsatus* and the nocturnal *Sibynomorphus neuwiedi* (**Figure 3**). For the other species analyzed, the PND was inferred from the measured axial length of the eye and the PND values obtained from the nocturnal and the diurnal species. To assess the focal length, we used the method described by Lisney and Collin [26], and for both species, the estimated focal length was 0.52 of the eye's focal length (**Figure 3**).

To estimate the theoretical peak of spatial resolving power, we applied the method proposed by Hart [85], wherein the distance **d** subtended by one degree on the retina is determined from the PND and calculated according to the formula: $\mathbf{d} = (2\pi PND)/360$. Assuming that the spacing between the ganglion cells is the limiting factor of the spatial resolving power, we applied two different approaches, one in which we assume that the retinal ganglion cell fields are arranged in approximately a hexagonal array and the other in which we assume that the ganglion cell fields are arranged in an approximately square lattice. For both approaches, we estimated the average spacing between the cells using the value of peak density of GCL cells. Assuming a hexagonal array, the average spacing between the cells (S) was estimated

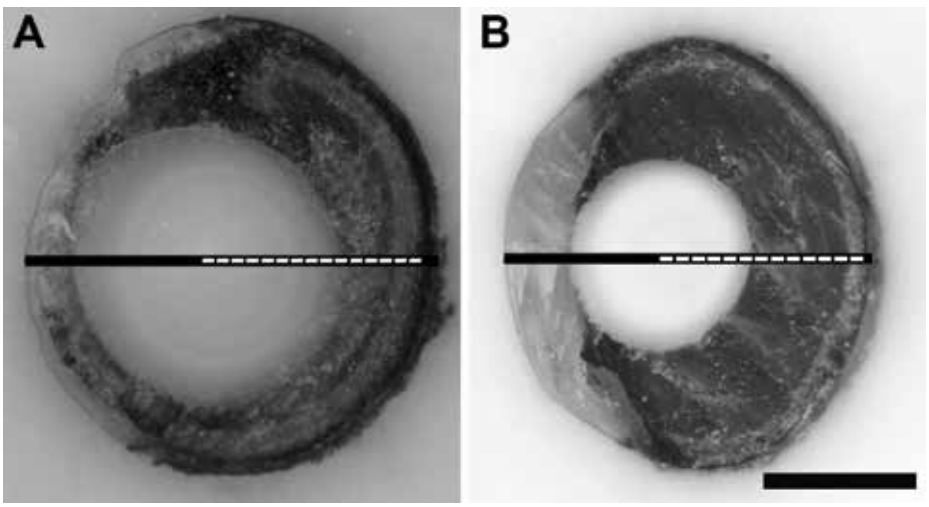

Figure 3. Transversal section of the eye of the nocturnal snake *S. neuwiedi* (A) and the diurnal *T. dorsatus* (B). The posterior nodal distance (PND) from the lens center to the edge of the retina-choroid is represented by the white dashed line, and correspond to about 52% of the axial length of the eye. Scale bar 1 mm.

according to the formula: S2 = 2/(D√3), where D is the peak density of GCL cells in mm^2. In the second approach, the linear density (cells/mm) was estimated by calculating the square root of D (cells mm^{-2}), and then was divided by 2, because at least two cells are required to detect 1 cycle of a given spatial frequency [90]. The maximum spatial (Nyquist) frequency (v) of a sinusoidal grating resolvable by these cell arrangements [95] was calculated using the formula $v = 1/(S\sqrt{3})$. This value was multiplied by the distance **d** to obtain the value of spatial resolution in cycles per degree [24, 90].

Statistical analyses were performed using the program SPSS v.20.0 Statistic (IBM Corporation, Armonk, NY, USA), to compare the population of GCL cells and the estimated upper limit of the spatial resolving power in diurnal and nocturnal colubrids, using the parametric t test and the nonparametric Mann-Whitney test. All data were log 10 transformed prior to analysis. The distribution of values for each variable in each group was evaluated by the Kolmogorov-Smirnov test, and the homoscedasticity between the groups was assessed by the Levene test. The t test for independent samples was performed to verify possible differences between the mean of the groups, for each variable analyzed. There was no disagreement in terms of statistical significance between the Mann-Whitney tests performed, which reinforces the results of the t tests. The level of significance for all comparisons was 5%.

In the retinal wholemounts, we were able to differentiate the neuron population (ganglion cells and displaced amacrine cells) from the nonneuron cell population (glial cells) (**Figure 4**). Diurnal and nocturnal colubrid snakes differed statistically in the total population of GCL cells and the estimated spatial resolution but not in the mean density of GCL cells. The average cell

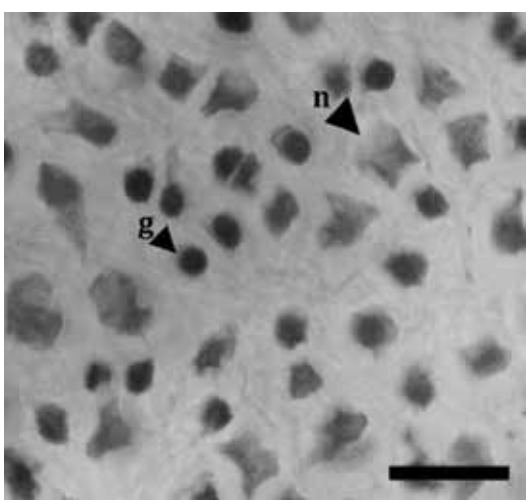

Figure 4. Photomicrograph of the Nissl-stained retinal GCL of the diurnal snake *T. dorsatus*. n, neurons; g, glia cells. The digital image was processed using adobe Photoshop CS3 for scaling, resolution, and adjustment of the levels of brightness and contrast. Scale bar = 10 μm.

Species	Retinal area (mm^2)	Total number of cells	CE	Mean cell density (cells/mm^2)	Eye axial length (mm)	Peak density of GCL cells (cells/mm^2)	Visual acuity (cpd)*	Visual acuity (cpd)**
Diurnal								
C. bicarinatus	59	394,096	0.01	6721 ± 1634	5.5	11,623	2.9	2.7
E. aesculapii	33	247,386	0.01	7474 ± 2308	4.5	12,176	2.4	2.3
E. miliaris	22	172,525	0.01	7842 ± 2034	4.0	12,281	2.2	2.0
E. poecilogyrus	16	110,153	0.01	7016 ± 2258	3.0	13,381	1.7	1.6
S. pullatus	88	614,553	0.01	7025 ± 1355	7.0	10,815	3.5	3.3
T. dorsatus	19	195,131	0.01	10,297 ± 1934	4.0	14,759	2.4	2.2
Mean ± SD	39 ± 28	288,974 ± 186,079		7729 ± 1318	4.7 ± 1.4	12,506 ± 1389	2.5 ± 0.6	2.3 ± 0.6
Nocturnal								
A pantostictus	3	31,404	0.02	11,019 ± 2410	1.3	16,788	0.8	0.8
A reticulatus	3	23,007	0.02	8490 ± 2177	1.8	11,992	1.0	0.8
D. albifrons	18	97,524	0.02	5341 ± 1189	3.5	7933	1.5	1.4
O. guibei	11	59,285	0.02	5327 ± 1140	2.9	8798	1.3	1.2
S. mikanii	14	58,621	0.02	4270 ± 1175	3.9	7195	1.6	1.5
S. neuwiedii	13	77,298	0.01	5987 ± 1200	3.7	9531	1.8	1.6
Mean ± SD	10 ± 6	57,856 ± 27,815		6739 ± 2530	2.9 ± 1.1	10,373 ± 3550	1.3 ± 0.4	1.2 ± 0.4

CE, Schaeffer coefficient of error; PND, posterior nodal distance; cpd, cycles per degree; SD, standard deviation of the mean.
*Estimated visual acuity assuming a hexagonal array.
**Estimated visual acuity assuming a square array.

Table 3. Stereological analysis of the population of cells in the retinal ganglion cell layer (GCL) of colubrid snakes, and the anatomical parameters used to estimate the upper limit of spatial resolution.

population in the GCL was 57.856 ± 27.815 cells in the retinas of nocturnal snakes and 288.974 ± 186.079 cells in retinas of diurnal snakes ($t(10) = 4.7$, $p = 0.001$) (**Table 3** and **Figure 5**). The mean cell density was 6.739 ± 2.530 cells/mm^2 in nocturnal species and 7.729 ± 1.318 cells/mm^2 in diurnal species ($t(10) = 1.2$, $p = 0.28$) (**Table 3** and **Figure 5**). The mean spatial resolution assuming a hexagonal arrangement was 1.3 ± 0.4 cpd in nocturnal snakes and 2.5 ± 0.6 cpd in diurnal snakes ($t(10) = 3.9$, $p = 0.003$) (**Table 3** and **Figure 5**). Similar values were obtained for the assumption of a square lattice: 1.2 ± 0.4 cpd and 2.3 ± 0.6 cpd, in nocturnal and diurnal species, respectively (**Table 3**).

The ganglion cell isodensity contour maps showed different types of retinal specializations, which may be related to species daily activity pattern and differences in habitat preferentially used (**Figure 6**). Poorly defined horizontal streaks with higher cell densities in the temporal

http://dx.doi.org/10.5772/intechopen.74645

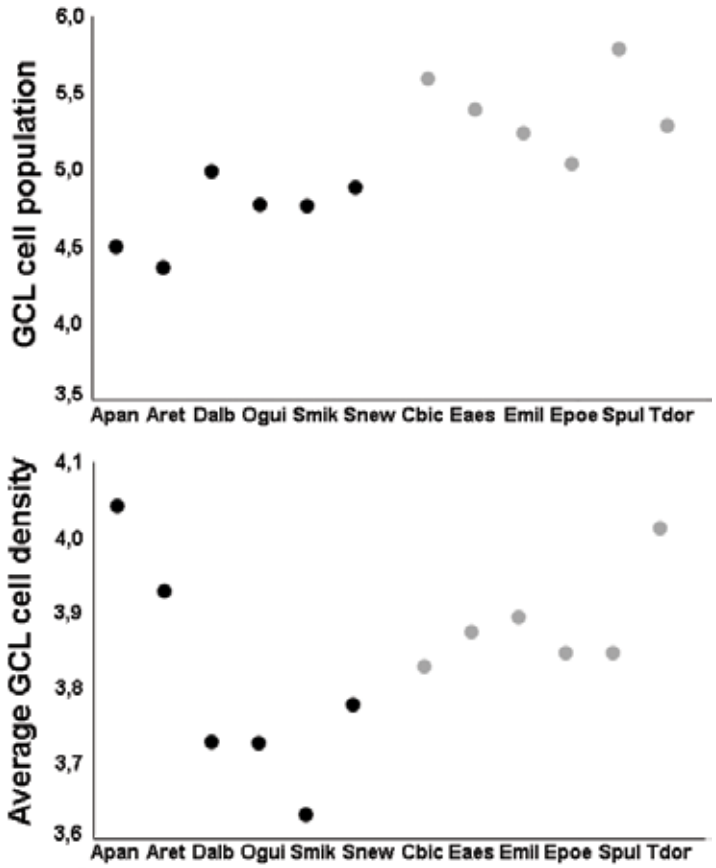

Figure 5. Total number (upper plot) and mean density (lower plot) of GCL cells in nocturnal (black) and diurnal (gray) colubrid snakes. All of the data were $\log_{10}$ transformed. Apan, *A. pantostictus*; Aret, *A. reticulatus*; Dalb, *D. albifrons*; Ogui, *O. guibei*; Smik, *S. mikanii*; Snew, *S. neuwiedii*; Cbic, *C. bicarinatus*; Eaes, *E. aesculapii*; Emil, *E. miliaris*; Epoe, *E. poecilogyrus*; Spul, *S. pullatus*; Tdor, *T. dorsatus*.

region were observed in diurnal species that inhabit distinct habitats: the arboreal species *C. bicarinatus* and *S. pullatus*, the terrestrial species *E. aesculapii* and *E. poecilogyrus*, and the semiaquatic species *E. miliaris*. In the terrestrial snake *T. dorsatus*, we observed a scattered distribution with anisotropic *area centralis* in the ventro-temporal retina. Among the nocturnal species, we observed anisotropic *area centralis* located in the dorso-temporal retina of the fossorial species *A. pantostictus* and *A. reticulatus*. An anisotropic *area centralis* in the temporal retina was observed in the terrestrial and nocturnal snake *O. guibei*, and a scattered GCL cell distribution was observed in the other three nocturnal species: the semiarboreal snakes *D. albifrons* and *S. neuwiedi*, with higher density in the ventral retina, and the terrestrial snake *S. mikanii*, with higher density in the central retina. Examples of horizontal streaks, anisotropic *area*, and scattered and nondefined distributions are shown in **Figure 6**.

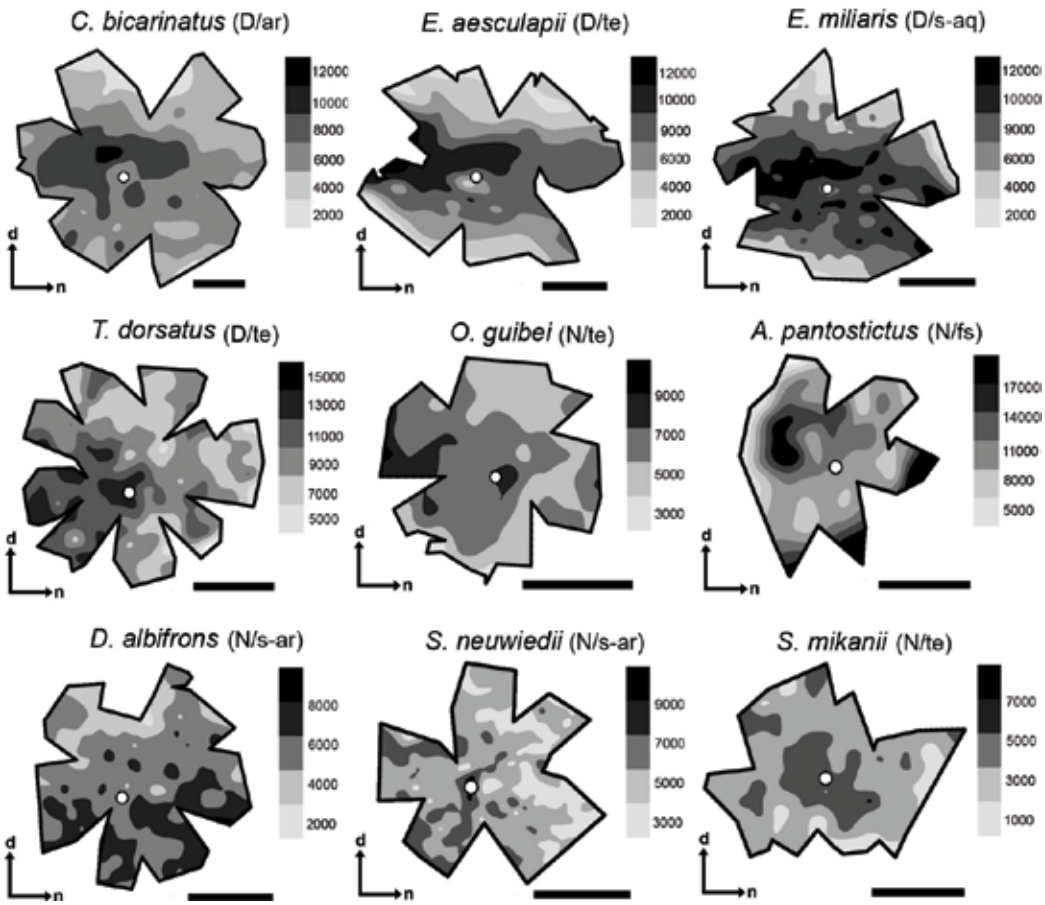

Figure 6. Topographic maps showing the distribution of cells in the GCL in retina of diurnal and nocturnal Colubrid snakes. The upper three maps show poorly defined horizontal streaks in diurnal species. The middle maps show anisotropic *area centralis* in diurnal and nocturnal species and the lower three maps show scattered and nondefined distributions in retinas of nocturnal snakes. The daily activity pattern and species habitat are indicated next to the name of each species, in the order (activity pattern/habitat): D, primarily diurnal; N, primarily nocturnal; ar, arboreal; fs, fossorial; s-ar, semiarboreal; s-aq, semiaquatic; te, terrestrial. The gray gradient bars represent the number of cells per mm^2. The position of the optic nerve head is depicted as a white circle. d = dorsal; n = nasal. Scale bars = 2 mm, except for C. bicarinatus and E. aesculapii, where scale bar = 1 mm.

3. Discussion

3.1. Density of GCL cells and the estimated spatial resolving power

To our knowledge, this is the first study to evaluate and describe the density and distribution of neurons in retinas of nocturnal Colubridae snakes. The average of the total population of GCL cells was significantly lower in nocturnal species (57,856 ± 27,815 cells) compared to diurnal species (288,974 ± 186,079 cells). No significant difference of the mean density of GCL

cells was observed between diurnal and nocturnal species, although this may reflect the low species sampling, with a high sampling variability (**Figure 5**). Among the nocturnal snakes, the fossorial *A. reticulatus* had the lowest value of GCL cell population (23,007 cells), while the highest was seen in the semiarboreal *D. albifrons* (97,524 cells). Among diurnal snakes, the semiaquatic *E. miliaris* had the lowest value (172,525 cells) and the arboreal *S. pullatus* (614,553 cells) the highest.

Data from the literature show similar density values for diurnal and terrestrial snakes. The population of GCL cells in the semiarboreal *P. olfersii* was 307,605 ± 80,422 cells, in the terrestrial *P. patagoniensis* 350,294 ± 64,756 cells and in the terrestrial *T. sirtalis* 209,800 ± 1150 cells [36, 67]. The estimated densities in diurnal marine snakes were lower than those observed for diurnal terrestrial species (104,011 cells in *A. laevis*, 31,977 cells in *D. major*, and 72,597 cells in *L. curtus*) [34] and were similar to the values estimated for the nocturnal colubrids.

The upper limits of the spatial resolving power were also significantly higher in diurnal snakes (2.5 ± 0.6 cpd), which points to the importance of a better image quality in snakes with diurnal habits that actively forage during photoperiods of higher illumination. Similar values were reported for other terrestrial and diurnal species: 2.6 cpd in *P. olfersii*, 2.7 cpd in *P. patagoniensis*, and 2.3 cpd in *T. sirtalis* [34, 36, 67]. The average spatial resolving power in nocturnal colubrids was 1.3 ± 0.4 cpd, which was similar to the values estimated for the marine snakes *D. major* and *L. curtus*: 1.1 cpd and 1.6 cpd, respectively [34]. The marine *A. laevis* had a higher estimated visual acuity (2.3 cpd), which was associated to its crevice-foraging hunting strategies [34]. The lower values estimated for marine and for primarily nocturnal terrestrial species may be associated to the smaller eye's axial diameter and shorter focal length. In nocturnal snakes, visual acuity may be compensated by light sensitivity.

Morphological studies revealed that diurnal snakes from the Caenophidia group, which include the Colubridae and Hydrophiidae families, have pure cone retinas, with no typical rod-like photoreceptor [2, 34, 36, 67, 96–98], and a lower photoreceptor density, compared to nocturnal species [36, 98]. The presence of only cones in retinas of diurnal snakes should contribute to higher spatial resolution [99], given the lower convergence from cones to ganglion cells.

These important differences in the retinal morphology and the upper limits of the spatial resolving power between diurnal and nocturnal snakes and between aquatic and terrestrial snakes indicate how the variety of environments and circadian activity patterns plays a role in the adaptation of the visual system and influence essential aspects of vision.

3.2. Distribution of neurons in the retina and visual ecology of snakes

This comparative study on the distribution of GCL neurons in retinas of Colubridae snakes revealed the variety of retinal specializations, which indicates the complexity of the adaptive strategies of the snakes' visual system. In the literature, only three studies described the density and topography of neurons in snake retinas [34, 36, 67], and this is the first study to describe the distribution of neurons in retinas of nocturnal snakes. In general, the diurnal species had a poorly defined visual streak extending along the meridional axis of the retina

with peak density of cells in the temporal region, while nocturnal species had an anisotropic *area centralis* in different regions of the retina, or a scattered and nondefined distribution, depending on the species (**Table 4**).

According to the terrain theory proposed by Hughes [28], species that inhabits open areas where the visual field is dominated by the horizon should preferably have a horizontal streak, which favors the panoramic view of the environment, without the constant need for eye or head movements. On the other hand, animals that live in forested areas, where the visual field is obstructed by foliage and should have an *area centralis*, which favors the spatial resolution of this circular area. However, the distribution pattern observed in snakes' retinas does not support this theory. For instance, visual streaks were observed in arboreal snakes that inhabit preferentially forested areas, such as *P. olfersii* [36], *C. bicarinatus* and *S. pullatus*, and on the other hand, *area centralis* were observed in species that inhabit preferentially open areas, such as *P. patagoniensis* [36] and *O. guibei*.

In the literature, we find some studies that showed the presence of a horizontal streak in species of mammals where the horizon is not a relevant feature of their habitat or the absence of this type of distribution in species that inhabit open fields [30, 100, 101]. Stone [102] suggested that the topography of the retina must be a phylogenetically inherited trait and does not necessarily represent an adaptive condition of a lifestyle of a given species. However, if this

Subfamily	Species	Biome	Habitat	Substrate	Activity pattern	Diet	Retinal specialization
Colubrinae	*C. bicarinatus*	AF	F	Ar/Te	D	an	HS
	S. pullatus	AF	F	Ar/Te	D	ma, av	HS
Dipsadinae	*A. pantostictus*	CE, AF	F	Su	N	ol	AC—dorsal
	A. reticulatus	CE, AF	F	Su	N	ol	AC—dorsal
	D. albifrons	AF	F	Ar/Te	N	mo	Diffuse—ventral
	S. mikanii	CE, AF	F, O	Te	N	mo	Diffuse—central
	S. neuwiedii	AF	F	Ar/Te	N	mo	Diffuse—ventral
	E. aesculapii	CE, AF	F, O	Te	D	sn	HS
	E. miliaris	AF	F	Aq/Te	D	an, fi	HS
	E. poecilogyrus	CE	F, O	Te	D	an	HS
	O. guibei	CE	F, O	Te	N	ma, li	AC—temporal
	T. dorsatus	AF	F	Te	D	mo	AC—ventral
	P. olfersii	CE, AF	F	Ar/Te	D	an, ma	HS*
	P. patagoniensis	CE, AF	O	Te	D	an, ma	AC—ventral*

AF, Atlantic Rain Forest; CE, Cerrado; F, forested area; O, open area; Ar, arboreal; Te, terrestrial; Su, subterranean; Aq, aquatic; D, primarily diurnal; N, primarily nocturnal; an, anurans; ma, mammals; av., birds; ol, annelids; mo, mollusks; sn, snakes; fi, fish; li, lizards; HS, horizontal streak; AC, *area centralis*. Ecological features (biome, habitat, substrate, activity patter and diet) were stablished based on [77–79].
*Data from Hauzman et al. [36].

Table 4. Snake species, ecological features and retinal specializations.

proposition was applied to snakes, one would expect to observe the same pattern of cell distribution in the retinas of the phylogenetically close-related species *P. olfersii* and *P. patagoniensis* [36], for example, or in the nocturnal Dipsadinae and close-related species *S. mikanii*, *S. neuwiedi* and *D. albifrons*, which was not the case.

Based on the results obtained for *Philodryas* retinas, Hauzman et al. [36] suggested that the microhabitat may have a more important role in the visual ecology of snakes than the habitat. The terrestrial species *P. patagoniensis*, for example, although it occupies open areas, has its visual field obstructed by foliage. Thus, an *area centralis* in the ventral region of the retina (**Table 4**) favors the spatial resolution of the superior visual field, which allows the view of aerial predators, an important defense mechanism for crawling animals [36]. The same was suggested for sea snakes with an *area centralis* in the ventral retina, *L. curtus* and *D. major* [34]. In our analysis, we also observed a ventral *area* in the retina of the primarily diurnal and terrestrial *T. dorsatus* and a scattered distribution of cells but with higher densities in the ventral retina of the primarily nocturnal and semiarboreal snakes *D. albifrons* and *S. neuwiedi* (**Table 4**). On the other hand, the two fossorial snakes, *A. pantostictus* and *A. reticulatus*, had an *area centralis* located in the dorsal region of the retina (**Table 4**). Snakes with fossorial habits usually have adaptations related to the necessity to reduce friction and allow digging tunnels in compact soil [66]. These species tend to have smaller and compact heads, almost indistinct from the rest of the body, a reduced number of scales on the head, small eyes, and shorter tails [103–105]. The retinal specializations with an *area centralis* in the dorso-temporal region may improve the spatial resolving power of the inferior and frontal visual field, thereby helping the digging habit and the search for annelids as prey [77]. Furthermore, we also observed an *area centralis* in the central retina of the primarily diurnal snake *E. poecilogyrus*, which may improve the lateral monocular vision, and a temporal *area centralis* in the retina of the primarily nocturnal snake *O. guibei*, which may improve frontal vision (**Table 4**).

A horizontal streak was observed in different diurnal snakes that inhabit a variety of habitats and occupy different substrates: terrestrial, arboreal, or aquatic (**Table 4**). This type of retinal specialization results in the formation of a sharper image that favors the visual acuity along the naso-temporal axis, and is related to the ability of a panoramic view of the visual field, without the need for head movements [32], which would reveal the location of the snake for a possible prey or for visually oriented predators. Thus, a visual streak would be an important adaptation for locomotion and foraging in different substrates. In the literature, a visual streak was observed in the semiarboreal *P. olfersii* [36], in the terrestrial *T. sirtalis* [67], and in the sea snakes *L. curtus*, *D. major* and *A. laevis* [34]. In this study, we observed this type of retinal specialization in primarily diurnal species that occupy predominantly forested areas: the terrestrial snake *E. aesculapii*, the semiaquatic snake *E. miliaris*, and the semiarboreal species *C. bicarinatus* and *S. pullatus*. We thus suggest that this type of specialization is widely spread among snakes and may be important for foraging behavior in different substrates.

In summary, the variation of the types of retinal specialization in snakes may be related to ecological and behavioral features such as the daily activity pattern, the habitat and substrate preferentially occupied, hunting strategies, and diet. Snakes that actively forage during the day and prey on fast and visually oriented preys may benefit from a horizontal streak that

enables the screening of the environment without the constant need for eye and head movements. On the other hand, snakes are active during the night spend most of the day camouflaged resting [106] and may not have the necessity of a panoramic view of the environmental provided by a visual streak. The presence of an *area centralis* or a diffuse distribution of GCL cells may also be related to food items, in that these types of distribution are observed in snakes that feed on slow moving preys, as snails and slugs: the nocturnal species *D. albifrons*, *S. mikanii*, *S. neuwiedi*, and the diurnal snake *T. dorsatus*. Mollusks are also relatively smaller and easier to handle and ingest compared to other types of prey and that may decrease the time of exposure to potential predators during feeding [107], which may also exert distinct selective pressure on the retinal specializations.

4. Conclusion and future directions

In conclusion, this broad study reveals that the retinal topography in Colubridae snakes may have suffered influences not only from the preferential habitat, microhabitat, and substrate used by the species but also to a range of features and behaviors such as daily activity pattern, foraging strategies, and diet. We suggest that horizontal streak with higher cell density in the temporal retina is a more common feature of primarily diurnal snakes from forested areas, which feed on fast moving preys. An *area centralis* is more common in nocturnal species or those that feed on slow moving preys. We also speculate that retinal specializations may have resulted from adaptations to environments and habitats that have undergone drastic and recent changes, and many features and specific adaptations of the species visual system may not be associated with the current environment but may indicate traits of the evolutionary history of the species.

It is also important to emphasize that these anatomical and morphological analyses of the visual system should be expanded not only to a broader species sampling but should also be combined with other studies, which include electrophysiological and behavioral approaches. Electrophysiological recordings, for instance, can be performed to compare the visual acuity measured with a more direct technique, with the upper limits of the eye spatial resolving power estimated from anatomical data. In addition, behavioral tests can be designed to verify how a specific morphological feature of the retina is ultimately associated to certain behaviors and to the species' visual ecology.

Acknowledgements

The authors are grateful to Francisco Luís Franco for access to the snakes. This project was funded by the Foundation of Research Support in the State of Sao Paulo (FAPESP) with Fellowships to EH (PhD 2010/51670-8 and post doc 2014/25743-9) and DMOB (post doc 2011/17423-6) and research grants to DFV (2008/58731-2, 2014/26818-2 and 2009/06026-6). DFV is a CNPq 1 A Productivity Fellow.

Author details

Einat Hauzman*, Daniela M.O. Bonci and Dora F. Ventura

*Address all correspondence to: hauzman.einat@gmail.com

Department of Experimental Psychology, Psychology Institute, University of São Paulo, São Paulo, Brazil

References

[1] Ramón y Cajal S. La rétine des vertebrés. La Cellule. 1893;**9**:17-257

[2] Walls GL. The Vertebrate Eye and its Adaptative Radiation. Bloomfield Hills: Cranbook Inst of Science; 1942

[3] Steinberg RH. Interactions between the retinal pigment epithelium and the neural retina. Documenta Ophthalmologica. 1985;**60**:327-346

[4] Bok D. The retinal pigment epithelium: A versatile partner in vision. Journal of Cell Science. 1993;(Suppl. 17):189-195

[5] Strauss O. The retinal pigment epithelium in visual function. Physiological Reviews. 2005;**85**:845-881

[6] Amram B, Cohen-Tayar Y, David A, Ashery-Padan R. The retinal pigmented epithelium-from basic developmental biology research to translational approaches. The International Journal of Developmental Biology. 2017;**61**(3-4-5):225

[7] Ali MA, Klyne MA. Vision in Vertebrates. New York and London: Plenum Press; 1985. 272 p

[8] Bowmaker JK. The evolution of vertebrate visual pigments and photoreceptors. In: Cronly-Dillon J, Gregory RL, editors. Vision and Visual Dysfunction. Evolution of the Eye and Visual System. Vol. 2. London: Macmilla Press; 1991

[9] Dowling JE. The Retina: An Approachable Part the Brain. Cambridge, Mass: Belknap Press of Harvard University Press; 1987

[10] Turner PL, Mainster MA. Circadian photoreception: Ageing and the eye's important role in systemic health. British Journal of Ophthalmology. 2008;**92**:1439-1444

[11] Jacobs GH, Rowe MP. Evolution of vertebrate colour vision. Clinical & Experimental Optometry. 2004;**87**:206-216

[12] Provencio I, Jiang G, De Grip WJ, Hayes WP, Rollag MD. Melanopsin: An opsin in melanophores, brain, and eye. Proceedings of the National Academy of Sciences of the United States of America. 1998;**95**:340-345

[13] Panda S, Sato TK, Castrucci AM, Rollag MD, DeGrip WJ, Hogenesch JB, Povencio I, Kay SA. Melanopsin (Opn4) requirement for normal light-induced circadian phase shifting. Science. 2002;**298**:2213-2216

[14] Panda S, Provencio I, Tu DC, Pires SS, Rollag MD, Castrucci AM. Melanopsin is required for non-image-forming photic responses in blind mice. Science. 2003;**301**:525-527

[15] Berson DM, Dunn FA, Takao M. Phototransduction by retinal ganglion cells that set the circadian clock. Science. 2002;**295**(5557):1070-1073

[16] Hattar S, Liao HW, Takao M, Berson DM, Yau KW. Melanopsin-containing retinal ganglion cells: Architecture, projections, and intrinsic photosensitivity. Science. 2002; **295**:1065-1070

[17] Foster RG, Hankins MW. Non-rod, non-cone photoreception in the vertebrates. Progress in Retinal and Eye Research. 2002;**21**:507-527

[18] Dacey DM, Liao H, Peterson B, Robinson F, Smith VC, Pokorny J, Yau KW, Gamlin PD. Melanopsin-expressing ganglion cells in primate retina signal color and irradiance and project to the LGN. Nature. 2005;**433**:749-754

[19] Davies WI, Zheng L, Hughes S, Tamai TK, Turton M, Halford S, Foster RG, Whitmore D, Hankins MW. Functional diversity of melanopsins and their global expression in the teleost retina. Cellular and Molecular Life Sciences. 2011;**68**(24):4115-4132

[20] Bellingham J, Whitmore D, Philp AR, Wells DJ, Foster RG. Zebrafish melanopsin: Isolation, tissue localisation and phylogenetic position. Brain Research. Molecular Brain Research. 2002;**107**:128-136

[21] Bailey MJ, Cassone VM. Melanopsin expression in the chick retina and pineal gland. Brain Research. Molecular Brain Research. 2005;**134**:345-348

[22] Verra DM, Contín MA, Hicks D, Guido ME. Early onset and differential temporospatial expression of melanopsin isoforms in the developing chicken retina. Investigative Ophthalmology & Visual Science. 2011;**52**(8):5111-5120

[23] Thibos LN, Cheney FE, Walsh DJ. Retinal limits to the detection and resolution of gratings. Journal of the Optical Society of America. A. 1987;**4**:1524-1529

[24] Pettigrew JD, Dreher B, Hopkins CS, McCall MJ, Brown M. Peak density and distribution of ganglion cells in the retinae of microchiropteran bats: Implications for visual acuity. Brain, Behavior and Evolution. 1988;**32**:39-56

[25] Collin SP, Pettigrew JD. Quantitative comparison of the limits on visual spatial resolution set by the ganglion cell layer in twelve species of reef teleosts. Brain, Behavior and Evolution. 1989;**34**:184-192

[26] Lisney TJ, Collin SP. Retinal ganglion cell distribution and spatial resolving power in elasmobranchs. Brain, Behavior and Evolution. 2008;**72**:59-77

[27] Hughes EC. The Sociological Eye: Selected Papers. New Jersey: Transaction Publishers; 1971

[28] Hughes A. The topography of vision in mammals of contrasting life styles: Comparative optics and retinal organization. In: Crescitelli F, editor. The Visual System in Vertebrates: Handbook of Sensory Physiology. Vol. VII/5. Berlin, Heidelberg: Springer; 1977. pp. 613-756

[29] Silveira LCL. Organização do Sistema Visual de Roedores da Amazônia: Óptica Ocular e Distribuição das Células Ganglionares Retinianas. Instituto de Ciências Biológicas; 1985. p. 427

[30] Silveira LCL, Picanço-Diniz CW, Oswaldo-Cruz E. Distribution and size of ganglion cells in the retina of large Amazon rodents. Visual Neuroscience. 1989;**2**:221-235

[31] Collin SP. Behavioural ecology and retinal cell topography. In: Archer SN, Djamgoz MBA, Loew ER, Partridge JC, Vallerga S, editors. Adaptive Mechanisms in the Ecology of Vision. Dordrecht: Kluwer Academic Publishers; 1999. pp. 509-535

[32] Collin SP. A web-based archive for topographic maps of retinal cell distribution in vertebrates. Clinical & Experimental Optometry. 2008;**91**:85-95

[33] Pettigrew JD, Manger PR. Retinal ganglion cell density of the black rhinoceros (*Dicero bicornis*): Calculating visual resolution. Visual Neuroscience. 2008;**25**:215-220

[34] Hart NS, Coimbra JP, Collin SP, Westhoff G. Photoreceptor types, visual pigments, and topographic specializations in the retinas of Hydrophiid sea snakes. The Journal of Comparative Neurology. 2012;**520**:1246-1261

[35] Thompson I. Considering the evolution of vertebrate neural reina. In: Cronly-Dillon J, Gregory RL, editors. Vision and Visual Dysfunction. Evolution of the Eye and Visual System. Vol. 2. London: Macmillan Press; 1991

[36] Hauzman E, Bonci DMO, Grotzner SR, Mela M, Liber AMP, Martins SL, Ventura DF. Comparative study of photoreceptor and retinal ganglion cell topography and spatial resolving power in Dipsadidae snakes. Brain, Behavior and Evolution. 2014; **84**:197-213

[37] Brown KT. A linear area centralis extending across the turtle retina and stabilized to the horizontal by non visual cues. Vision Research. 1969;**9**(9):1053-1054

[38] Moore BA, Tyrell LP, Kamilar JM, Collin S, Dominy NJ, Hall MI, et al. Structure and function of regional specializations in the vertebrate retina. In: Kaas JH, editor. Evolution of Nervous Systems. Vol. 1. 2nd ed. Cambridge: Academic Press; 2017. pp. 351-372

[39] Granda AM, Haden KW. Retinal oil globule counts and distribution in two species of turtles: *Pseudemys scripta elegans* and *Chelonia mydas mydas*. Vision Research. 1970;**1**:79-84

[40] Grötzner SR. Densidade e topografia dos fotorrecptores da retina da tartaruga *Trachemys scripta elegans* com imunocitoquímica de opsinas. Instituto de Psicologia: Tese (Doutorado) Universidade de São Paulo; 2005. 158 p

[41] Wang HH, Gallagher SK, Byers SR, Madl JE, Gionfriddo JR. Retinal ganglion cell distribution and visual acuity in alpacas (*Vicugna pacos*). Veterinary Ophthalmology. 2015;**18**: 35-42

[42] Rocha FAF, Ahnelt PK, Peichl L, Saito CA, Silveira LCL, Lima SMA. The topography of cone photoreceptors in the retina of a diurnal rodent, the agouti (*Dasyprocta aguti*). Visual Neuroscience. 2009;**26**:167-175

[43] BLS A-D-C, Pessoa VF, Bousfield JD, Clarke RJ. Ganglion cell size and distribution in the retina of the two-toed sloth (*Choloepus didactylus*). Brazilian Journal of Medical and Biological Research. 1989;**22**:233-236

[44] Stone J, Halasz P. Topography of the retina in the elephant *Loxodonta africana*. Brain, Behavior and Evolution. 1989;**34**:84-95

[45] Collin SP, Partridge JC. Retinal specialisations in the eyes of deep-sea teleosts. Journal of Fish Biology. 1996;**49**(Suppl. A):157-174

[46] Rahman ML, Aoyama M, Sugita S. Number, distribution and size of retinal ganglion cells in the jungle crow (*Corvus macrorhynchos*). Anatomical Science International. 2006; **86**:252-259

[47] Kolb H, Nelson R, Mariani A. Amacrine cells, bipolar cells and ganglion cells of the cat retina: A Golgi study. Vision Research. 1981;**21**:1081-1114

[48] Moraes AMM, Oliveira MM, Hokoc JN. Retinal ganglion cells in the south American opossum (*Didelphis aurita*). The Journal of Comparative Neurology. 2000;**418**(2):193-216

[49] Walls GL. Significance of the foveal depression. Archives of Ophthalmology. 1937;**18**: 912-919

[50] Polyak SL. The Retina. Chicago: University of Chicago Press; 1941

[51] Moroney MK, Pettigrew JD. Some observations on the visual optics of kingfishers (Aves, Caraciformes, Alcedinidae). Journal of Comparative Physiology. A. 1987;**160**:137-149

[52] Smith G, Atchison DA. The Eye and Visual Optical Instrument. New York: Cambridge University Press; 1997

[53] Coimbra JP, Trevia N, Marceliano ML, da Silveira Andrade-Da-Costa BL, Picanço-Diniz CW, Yamada ES. Number and distribution of neurons in the retinal ganglion cell layer in relation to foraging behaviors of tyrant flycatchers. The Journal of Comparative Neurology. 2009;**514**:66-73

[54] Cleland BG, Crewther DP, Crewther SG, Mitchell DE. Normality of spatial resolution of retinal ganglion cells in cats with strabismic amblyopia. The Journal of Physiology. 1982; **326**:235-249

[55] Hall SE, Mitchell DE. Grating acuity of cats measured with detection and discrimination tasks. Behavioural Brain Research. 1991;**44**:1-9

[56] Timney B, Keil K. Visual acuity in the horse. Vision Research. 1992;**32**:2289-2293

[57] Evans KE, McGreevy PD. The distribution of ganglion cells in the equine retina and its relationship to skull morphology. Anatomia, Histologia, Embryologia. 2007;**36**:151-156

[58] Reymond L. Spatial visual acuity of the eagle *Aquila audax*: A behavioural, optical and anatomical investigation. Vision Research. 1985;**25**:1477-1491

[59] Coates M, Ruta M. Nice snake, shame about the legs. Trends in Ecology & Evolution. 2000;**15**:503-507

[60] Vidal N, Hedges SB. Molecular evidence for a terrestrial origin of snakes. Proceedings of the Royal Society B: Biological Sciences (Supplement). 2004;**271**:S226-S229

[61] Uetz P, editor. The Reptile Database. 2006. http://www.reptile-database.org [Accessed October 27, 2017]

[62] Lillywhite HB, Henderson RW. Behavioral and functional ecology of arboreal snakes. In: Seigel RA, Collins JT, editors. Snakes: Ecology and Behaviour. San Francisco: McGraw-Hill; 1993. pp. 1-48

[63] Cadle JE. Geographic distribution: Problems in phylogeny and zoogeography. In: Seigel RA, Collins JT, Novak SS, editors. Snakes: Ecology and Evolutionary Biology. New York: McGraw-Hill Publishing Company; 1987. pp. 77-105

[64] McDowell SB. Systematics. In: Seigel RA et al, editors. Snakes: Ecology and Evolutionary Biology. New York: MacMillan; 1987. pp. 3-50

[65] Ford NB, Burghardt GM. Perceptual mechanisms and the behavioral ecology of snakes. In: Seigel RA, Collins JT, editors. Snakes: Ecology and Behavior. San Francisco: McGraw-Hill; 1993. pp. 117-164

[66] Greene HW. Snakes. The Evolution of Mystery in Nature. Berkeley: University of California Press; 1997. 351 p

[67] Wong R. Morphology and distribution of neurons in the retina of the American garter snake (*Thamnophis sirtalis*). The Journal of Comparative Neurology. 1989;**283**:597-601

[68] Baker RA, Gawne TJ, Loop MS, Pullman S. Visual acuity of the midland banded water snake estimated from evoked telencephalic potentials. Journal of Comparative Physiology. A, Neuroethology, Sensory, Neural, and Behavioral Physiology. 2007;**193**:865-870

[69] Northmore DP, Granda AM. Ocular dimensions and schematic eyes of freshwater and sea turtles. Visual Neuroscience. 1991;**7**:627-635

[70] New ST, Bull CM. Retinal ganglion cell topography and visual acuity of the sleepy lizard (*Tiliqua rugosa*). Journal of Comparative Physiology. A. 2011;**197**(6):703-709

[71] Fleishman LJ. The influence of the sensory system and the environment on mption patterns in the visual displays of anoline lizards and other vertebrates. The American Naturalist. 1992;**139**:S36-S61

[72] Silveira LCL, Picanço-Diniz CW, Oswaldo-Cruz E. Contrast sensitivity function and visual acuity of the opossum. Vision Research. 1982;**22**(11):1371-1377

[73] Dean P. Visual pathways and acuity in hooded rats. Behavioural Brain Research. 1981;**3**: 239-271

[74] Prusky GT, West PWR, Douglas RM. Behavioral assessment of visual acuity in mice ans rats. Vision Research. 2000;**40**:2201-2209

[75] Gianfranceschi L, Fiorentini A, Maffei L. Behavioural visual acuity of wild type and bcl2 transgenic mouse. Vision Research. 1999;**39**:569-574

[76] Campbell FW, Gubisch RW. The effect of chromatic aberration on visual acuity. The Journal of Physiology. 1967;**192**:345-358

[77] Marques OAV, Eterovic A, Sazima I. Serpentes da Mata Atlântica: Guia Ilustrado para Serra do Mar. Holos: Ribeirão Preto; 2001

[78] Marques OAV, Pereira DN, Barbo FE, Germano VJ, Sawaya RJ. Os répteis do Município de São Paulo: Diversidade e ecologia da fauna pretérita e atual. Biota Neotropica. 2009; **9**(2):139-150

[79] Torello-Viera NF, Marques OAV. Daily activity of neotropical dipsadids snakes. South American Journal of Herpetology. 2017;**12**(2):128-135

[80] Wassle H, Peichl L, Boycott BB. Morphology and topography of on- and off-alpha cells in the cat retina. Proceedings of the Royal Society of London—Series B: Biological Sciences. 1981;**212**:157-175

[81] Peichl L. Topography of ganglion cells in the dog and wolf retina. The Journal of Comparative Neurology. 1992;**324**:603-620

[82] Coimbra JP, Nolan PM, Collin SP, Hart N. Retinal ganglion cell topography and spatial resolving power in penguins. Brain, Behavior and Evolution. 2012;**80**:254-268

[83] Ehrlich D. Regional specialization of the chick retina as revealed by the size and density of neurons in the ganglion cell layer. The Journal of Comparative Neurology. 1981;**195**: 643-657

[84] Hayes BP. Cell populations of the ganglion cell layer: Displaced amacrine and matching amacrine cells in the pigeon retina. Experimental Brain Research. 1984;**56**:565-573

[85] Hart NS. Vision in the peafowl (Aves: *Pavo cristatus*). The Journal of Experimental Biology. 2002;**205**:3925-3935

[86] Gundersen HJG. Notes on the estimation of the numerical density of arbitrary profiles: The edge effect. Journal of Microscopy. 1977;**111**:219-223

[87] Ullmann JFP, Moore BA, Temple SH, Fernandez-Juricic E, Collin SP. The retinal wholemount technique: A window to understanding the brain and behaviour. Brain, Behavior and Evolution. 2012;**79**:26-44

[88] Lisney TJ, Stecyk K, Kolominsky J, Schmidt BK, Corfield JR, Iwaniuk AN, Wylie DR. Ecomorphology of eye shape and retinal topography in waterfowl (Aves: Anseriformes: Anatidae) with different foraging modes. Journal of Comparative Physiology. A, Neuroethology, Sensory, Neural, and Behavioral Physiology. 2013;**199**:385-402

[89] West MJ, Slomianka L, Gundersen HJ. Unbiased stereological estimation of the total number of neurons in the subdivisions of the rat hippocampus using the optical fractionator. The Anatomical Record. 1991;**231**:482-497

[90] Coimbra JP, Hart N, Collin SP, Manger PR. Scene from above: Retinal ganglion cell topography and spatial resolving power in the giraffe (*Giraffa camelopardalis*). The Journal of Comparative Neurology. 2013;**521**:2042-2057

[91] Scheaffer RL, Mendenhall W, Ott L. Elementary Survey Sampling. 5th ed. Boston: PWS-Kent; 1996

[92] Boire D, Dufour JS, Theoret H, Ptito M. Quantitative analysis of the retinal ganglion cell layer in the ostrich, *Struthio camelus*. Brain, Behavior and Evolution. 2001;**58**:343-355

[93] Sivak JG. The accommodative significance of the 'ramp' retina of the eye of the stingray. Vision Research. 1976;**16**:531-534

[94] Sivak JG. Optical characteristics of the eye of the spiny dogfish (*Squalus acanthias*). Revue Canadienne de Biologie. 1978;**37**:209-217

[95] Snyder AW, Miller WH. Photoreceptor diameter and spacing for highest resolving power. Journal of the Optical Society of America. 1977;**67**:696-698

[96] Underwood G. A Contribution to the Classification of Snakes. London: Trustees of the British Museum (Natural History); 1967

[97] Underwood G. The eye. In: Gans C, Parson TS, editors. Biology of the Reptilia, Morphology B. Vol. 2. New York: Academic Press; 1970. pp. 1-97

[98] Caprette CL. Conquering the cold shudder: The origin and evolution of snakes eyes [Ph. D. Thesis]. The Ohio State University; 2005. 107 p

[99] Jacobs GH, Fenwick JA, Crognale MA, Deegan JF II. The al cone retina of the garter snake: Spectral mechanisms and photopigment. Journal of Comparative Physiology. A. 1992;**170**:701-707

[100] Freeman B, Tancred E. Number and distribution of ganglion cells in the retina of the brush-tailed possum, *Trichosurus vulpecula*. The Journal of Comparative Neurology. 1978;**177**:557-567

[101] Schiviz AN, Ruf T, Kuebber-Heiss A, Schubert C, Ahnelt PK. Retinal cone topography of artiodactyl mammals: Influence of body height and habitat. The Journal of Comparative Neurology. 2008;**507**:1336-1350

[102] Stone J. Parallel Processing in the Visual System. London: Plenum; 1983

[103] Marx H, Rabb GB. Phyletic analysis of fifty characters of advanced snakes. Fieldiana: Zoology, Chicago. 1972;**63**:1-320

[104] Savitzky AH. Coadapted character complexes among snakes: Fossoriality, piscivory, and durophagy. American Zoologist. 1983;**23**:397-409

[105] Scartozzoni RR. Morfologia de serpentes aquáticas neotropicais: Um estudo comparativo [Dissertação de Mestrado]. São Paulo: Universidade de São Paulo; 2005. p. 102

[106] Martins M. História natural de uma taxocenose de serpentes de mata na região de Manaus, Amazônia Central, Brasil. Tese [Doutorado em Ciências]. Campinas: Instituto de Biologia, Universidade Estadual de Campinas; 1994. pp. 98

[107] Sazima I, Martins M. Presas grandes e serpentes jovens. Memorias Do Instituto Butantan. 1990;**52**(3):73-79

Chapter 6

Cloverleaf Clusters: A Common Macrostructural Organization across Human Visual and Auditory Cortex

Alyssa A. Brewer and Brian Barton

Additional information is available at the end of the chapter

http://dx.doi.org/10.5772/intechopen.77964

Abstract

One of the fundamental properties of mammalian brains is that sensory regions of cortex are organized into multiple, functionally specialized cortical field maps (CFMs). An individual CFM is composed of two orthogonal topographical representations, reflecting two essential aspects of a sensory feature space. Each CFM is thought to subserve a specific computation or set of computations that underlie particular perceptual behaviors by enabling the comparison and combination of the information carried by the various specialized neuronal populations within this cortical region. Multiple adjacent CFMs, in turn, have now been shown by multiple laboratories to be organized in visual and auditory cortex into a macrostructural pattern called the cloverleaf cluster. CFMs within cloverleaf clusters tend to share properties such as receptive field distribution, cortical magnification, and processing specialization. This chapter will review the evidence for CFM and cloverleaf cluster organization across human visual and auditory cortex and will discuss the utility of these measurements for determining cortical structure and function and for investigating what changes occur in sensory cortex following various types of trauma or disease.

Keywords: visual field map, visual cortex, auditory field map, auditory cortex, cloverleaf cluster, cortical field map, cortical mapping, phase-encoded fMRI, population receptive field mapping

1. Introduction

Measurements in visual, auditory, and somatosensory cortices across numerous species of mammals have demonstrated that cortical field maps (CFMs) are a fundamental way for the brain

to represent sensory information [1–5]. CFMs arise from organized inputs from sensory organs (e.g., retina, cochlea, skin) that maintain the topographic organization of the sensory receptors in the cortex. Thus neurons whose sensory receptive fields are positioned next to one another in sensory feature space are located next to one another in cortex within a CFM. Knowledge of the properties of these CFMs is vital for understanding how specific sensory computations are processed across the brain. Basic stimulus features are processed in lower-level cortical regions, which then send information onto the next stage in the cortical hierarchy to undergo progressively more complex computations [6]. A common aspect of these sensory pathways is that the topography of the sensory receptors embodies the most fundamental stimulus information, which is conserved throughout most of the cortical hierarchy [7, 8].

A growing number of measurements in the visual and auditory systems have shown sensory CFMs to be organized into a macrostructural pattern called cloverleaf clusters, indicating that CFMs and cloverleaf clusters may both be fundamental organizing principles in cortical sensory processing [2, 4, 7–11]. Such organization may provide a basic framework for the complex processing and analysis of input from sensory receptors [12]. CFMs within clusters tend to share properties such as receptive field distribution, processing specialization, and cortical magnification (e.g., [10, 11, 13]). It is likely that this cluster organization, like the topographic organization of CFMs, allows for efficient connectivity among neurons that represent neighboring aspects in sensory feature space [14–17]. Since the axons contained within one cubic millimeter of cortex can extend 3–4 km in length, efficient connectivity is vital for sustainable energetics in cortex [18]. The cloverleaf cluster organization may thus be important for minimizing the length of axons connecting sensory maps within and between clusters, allowing for a more efficient ratio of brain matter to skull capacity.

The definition and characterization of CFMs and cloverleaf clusters have been indispensable in the investigation of the structure and function of human cortex, as these *in vivo* measurements allow for the systematic exploration of computations across a particular sensory cortex (for reviews, see [8, 12]). In addition, they can serve as excellent and dependable independent localizers for investigations of particular functions across individuals (e.g., [3, 4, 10, 13, 19, 20]). Thus, measuring the organization of individual CFMs helps elucidate the stages of distinct sensory processing pathways and can be used to track how the cortex changes under various disorders [21–28]. This chapter will review our current knowledge of the CFM and cloverleaf cluster organization across human visual and auditory cortex.

2. Techniques for measuring cortical field maps and cloverleaf clusters

2.1. Phase-encoded fMRI paradigms are used for measuring visual and auditory field maps

Obtaining a high quality measurement of topographic responses is the first step in accurately defining CFMs and requires choosing a set of stimuli that is appropriate for the sensory domain of interest. A highly accurate and powerful paradigm for measuring human CFMs *in vivo* relies on phase-encoded fMRI measurements (also known as "traveling wave"

measurements; **1**) [3, 4, 7, 29–32]. This technique uses two sets of periodic stimuli that each contain a set of stimulus values presented in an orderly sequence across a range of interest at a given frequency per scan (typically 6–8 cycles per scan; **Figure 1Aiii**, **1Biii**), which allows the use of a Fourier analysis to determine the cortical responses [31]. The phase-encoded paradigm only considers activity that is at this signal frequency, excluding low-frequency physiological noise, among other things. The statistical threshold for phase-encoded cortical activity is commonly determined by coherence, which is equal to the amplitude of the blood-oxygenation-dependent (BOLD) signal modulation at the frequency of stimulus presentation (e.g., 6 stimulus cycles per scan), divided by the square root of the power over all other frequencies except the first and second harmonic (e.g., 12 and 18 cycles per scan) [7, 12, 31].

For measuring CFMs of visual space (known as retinotopic or visual field maps), one stimulus set is designed to elicit each voxel's preferred eccentricity typically by presenting

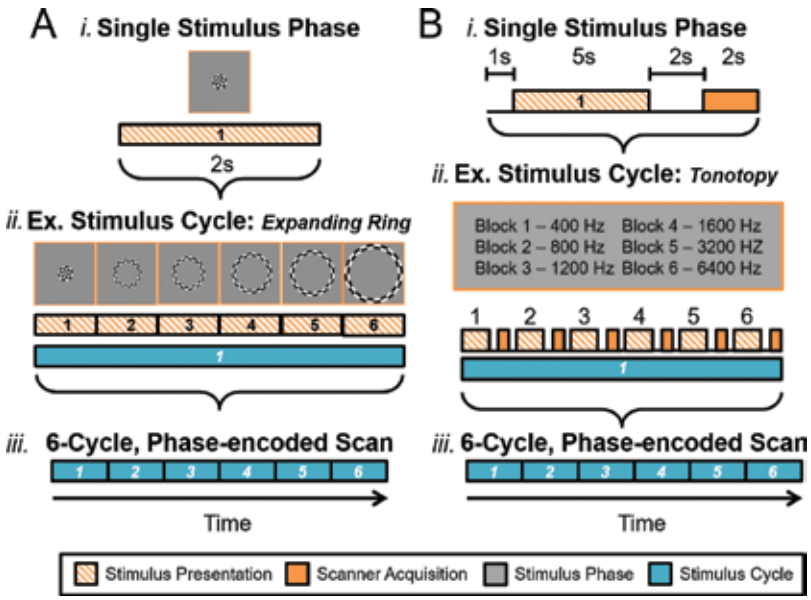

Figure 1. Diagrams of phase-encoded fMRI paradigms for cortical field mapping experiments. **(A)** An example phase-encoded fMRI paradigm for visual field mapping. *(i) Top diagram* shows the components of a single block of one stimulus presentation (striped orange) for one position (i.e., stimulus phase) of an expanding ring stimulus composed of a black and white moving checkerboard pattern. Note that scanner acquisition occurs simultaneously with the stimulus presentation in this case [7, 12]. *(ii) Middle diagram* shows 6 blocks (striped orange) that together compose one stimulus cycle (teal). Each phase of the expanding ring stimulus is displayed above the blocks; one block thus represents one stimulus position in the "phase-encoded" sequence. The term "traveling wave" is also used to describe this type of stimulus presentation, as the stimuli produce a sequential activation of representations across a topographically organized cortical region. *(iii) Lower diagram* displays how 6 cycles (teal)—each repeating the same blocks—compose a full, single scan. **(B)** an example phase-encoded fMRI paradigm for auditory field mapping. *(i) Top diagram* shows the components of a single block of one stimulus presentation (striped orange) followed by an fMRI data acquisition period (solid orange). The sparse-sampling paradigm separates the auditory stimulus presentation from the noise of the scanner acquisition [35]. The timing of the acquisition is set to collect the peak cortical response to the auditory stimulus, in accordance with the approximate hemodynamic delay. *(ii) Middle diagram* similarly shows 6 blocks (striped orange + solid orange) grouped together into one stimulus cycle (teal). Each block, or stimulus phase, in each cycle now represents a specific frequency. An example of this sequence for tonotopic measurements is displayed in Hz. *(iii) Lower diagram* again shows a full, single scan comprising 6 cycles. Note legend in inset.

a high-contrast, flickering checkerboard stimulus shaped like a ring, which expands or contracts in discrete even steps between the central fovea and the periphery to sequentially activate distinct eccentricity representations of visual space (**Figure 1Aii**). The second, orthogonal visual stimulus then activates the preferred polar angle of each fMRI voxel by displaying the same checkerboard pattern now shaped as a wedge spanning a small range of polar angles over all eccentricities. The wedge pattern sequentially activates all polar angles around the central fixation point by rotating clockwise or counterclockwise in discrete steps.

The phase-encoded methods are adapted for auditory field map measurements by combining a phase-encoded stimulus with the sparse-sampling paradigm often used in auditory measurements (**Figure 1B**) [4, 33–36]. Sparse-sampling allows the auditory stimulus presentation to avoid contamination from the noise of the MR scanner during data acquisition by separating the two in time (**Figure 1Bi**) [37–39].

The value of the stimulus (e.g., 5° of visual angle for eccentricity; 400 Hz frequency for tonotopy) that most effectively drives each cortical location is then estimated from the pattern of responses (**Figure 2**). The cortical response at a specific location is said to be "in phase" throughout the scan with the stimulus that most effectively activates it, hence the term "phase-encoded" mapping. The alternative term "traveling wave" arises from the sequential activation of one neighboring cortical location after the other to create a wave-like pattern of activity across the CFM during the stimulus presentation. It is important to note that the phase-encoded methods will not produce a significant BOLD signal in cortex if the stimulus representation in the region is not organized topographically, as there would be no differential activation across the cortical representation [2, 7, 20].

The analysis of phase-encoded cortical field mapping data must be done within individual subjects. Each CFM in sensory cortex can vary dramatically in size and anatomical location across individuals, leading to shifts in cytoarchitectural and topographic boundaries [40–45]. Primary visual cortex, for example, can vary in size by at least a factor of three, independent of brain size [41]. Consequently, when these data are group-averaged across subjects, especially by aligning the data to an average brain through such atlases as Talairach space [46] or Montreal Neurological Institute (MNI) coordinates [47], the measurements are blurred to such an extent that the gradients composing the CFMs are either inaccurate or missing. Relying on whole-brain anatomical co-alignment for cortical averaging will cause different CFMs to be averaged together incorrectly into one measurement, blurring together data from adjacent areas within each subject and making it impossible to differentiate computations in adjacent areas.

2.2. Population receptive field modeling has been developed for measuring visual field maps

A model-based method has been developed for visual field mapping that allows for additional information to be collected about visual field maps (VFMs) by modeling the population receptive field (pRF) of each voxel within a VFM (**Figure 2A**; for complete details, see [48]). Because VFMs are retinotopically organized, the population of RFs in each voxel within a VFM is expected to have similar representations of visual space, allowing for their combined pRF to be estimated as a single, two-dimensional Gaussian. The pRF modeling approach

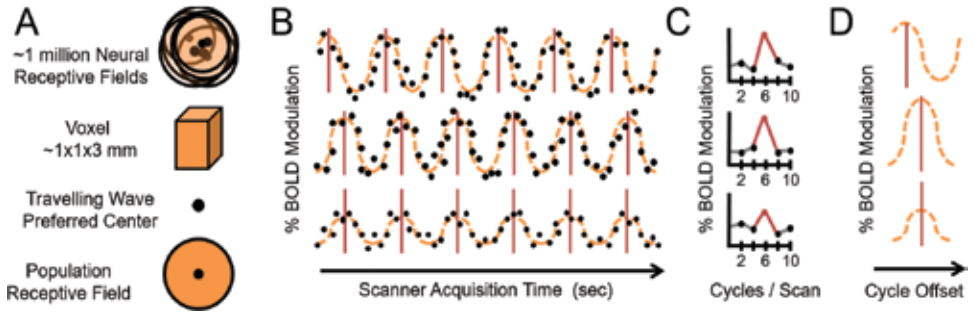

Figure 2. Schematic of measurements of individual voxels in phase-encoded cortical field mapping. **(A)** *Top:* there are on the order of ~1 million neurons within a typical voxel measured with a standardly used 3 T MRI scanner, depending on the size of the voxel [8, 49]. For a voxel within a CFM, the neurons each have similarly tuned receptive fields (orange circles with black outlines) with preferred centers of maximal response (black dots). Note how the overlapping receptive fields concentrate coverage in one region of sensory space (darker orange) corresponding to the average receptive field of the group. *Middle/top:* each typical voxel is on the order of 1 × 1 × 3 mm for cortical field mapping experiments, though voxels are often slightly larger (e.g., 3 × 3 × 3 mm) for other types of experiments [7]. *Middle/bottom:* phase-encoded (i.e., traveling wave) measurements take advantage of the fact that nearby neurons in sensory cortex have similar preferred centers (black dot) in order to estimate an average preferred center for the population of neurons in a given voxel. *Bottom:* Population receptive field (pRF) modeling in visual field mapping takes advantage of the fact that nearby neurons in retinotopic cortex have similar receptive fields in order to estimate not only a preferred center, but also a pRF for the population of neurons in a given voxel [48]. **(B)** Schematic of three example phase-encoded time series with different stimulus responses. Each row represents the activity and analysis of a time series of a single 6-cycle scan of one type of experimental stimuli (e.g., expanding rings) for a single voxel. Black dots indicate simulated raw data points of percent blood-oxygen-level-dependent (BOLD) modulation (i.e., response amplitude). The orange dotted lines represent sinusoidal fits of the simulated data points; each orange line characterizes the average BOLD activation in a different example voxel. The red lines indicate the peak activations per cycle for this imaginary set of voxels. *Top* and *middle rows* represent time series of voxels with the same % BOLD modulation, but different timing of peak responses. This difference in peaks indicates differences in stimulus selectivity (i.e., responses to different "phases" of a stimulus). Note the offset of the red lines between the two rows. For example, the *top row* might represent a voxel with a preferred eccentricity tuning of 3° eccentric to fixation, whereas the *middle row* might have a preferred tuning of 6° eccentric to fixation. *Middle* and *bottom rows* represent time series of voxels with the same timing of peak responses, indicating matching stimulus selectivity; for example, both might have a preferred eccentricity tuning of 6° eccentric to fixation. However, the *bottom row* has much lower % BOLD modulation than the *middle row*. Such a difference in response amplitude can be due to several factors, such as differences in receptive field tuning or local vasculature [8, 11]. **(C)** Schematic of three example Fourier power spectra corresponding to the schematic time series in **(B)**. In the phase-encoded paradigm, only BOLD responses that match the stimulus frequency of 6 cycles per scan (red peak) are considered as data. The responses must also be above a predetermined statistical threshold, typically measured in coherence or percent variance explained [7, 48]. Gray lines denote noise frequencies. **(D)** Schematic of three example averaged stimulus cycles corresponding to the schematic Fourier spectra in **(C)** and to averages of the time series in **(B)**. Each orange dotted line represents the sinusoidal fit for the average, while the peak activation is again marked by the red line. The timing of the peak of each averaged cycle is used to calculate the phase of the preferred stimulus independently for each voxel. Typical pseudocolor overlays on 3-D or flattened brain renderings as shown in **Figures 7** and **10** use color to denote cortical responses to this peak activation (e.g., [4, 12, 33, 34]). Note how the *top* measurement has an earlier peak (red line) that corresponds to an earlier phase of the stimulus (i.e., an earlier presentation time in the cycle) while the *middle* and *bottom* measurements' peaks are shifted to later in time (e.g., [7]). The *bottom* example has a lower % BOLD modulation than the other two schematics, but the same peak activation as the middle example. Adapted from [7].

provides an accurate estimate of not only the preferred center for each voxel's pRF (as with phase-encoded mapping alone), but also its size. In addition, this analysis can be done for any visual stimulus that periodically moves through visual space (e.g., moving bar), rather than just expanding rings and rotating wedges. Research is currently underway to develop a similar pRF model for auditory field maps (AFMs).

3. Fundamental organizing principles of sensory cortex

3.1. What criteria are used to identify a cortical field map?

The term "map" has often been imprecisely applied to topographical gradients or other similar patterns of cortical organization, but the study of cortical sensory processing requires the explicit definition a "cortical field map" according to very precise criteria (**Figures 3** and **4**). First, by definition, each CFM must be composed of at least two orthogonal, non-repeating topographical representations of fundamental sensory dimensions (**Figure 3**) [4, 12, 13, 29, 32]. In the visual system, the retinotopic sensory dimensions arise from the orthogonal aspects of visual space: eccentricity (e.g., center to periphery) and polar angle (e.g., "around the clock") [12, 31]. In the auditory system, the sensory feature space is composed of two aspects of

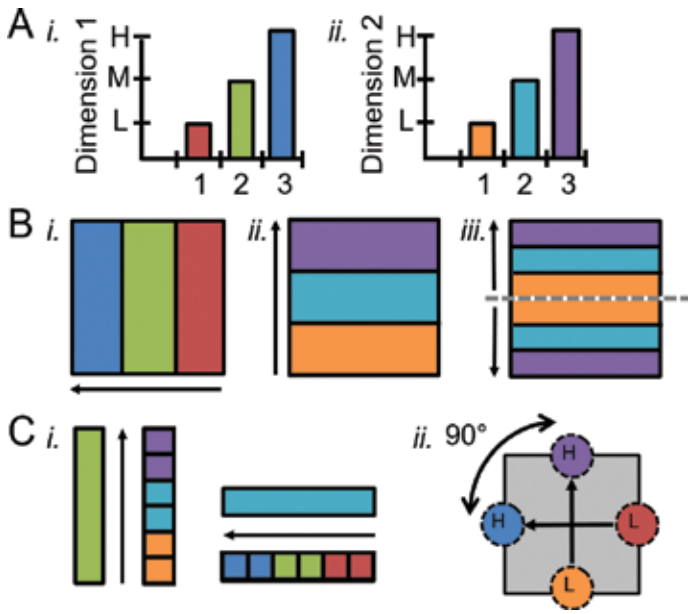

Figure 3. A cortical field map is defined by two orthogonal gradients representing two orthogonal dimensions of sensory space. **(A)** (*i*) Three stimulus values for one sensory dimension (e.g., eccentricity or tonotopy) are depicted in the graph: 1 - low (L, red); 2 - medium (M, green); 3 - high (H, blue). (*ii*) Three stimulus values for a second sensory dimension (e.g., polar angle or periodotopy) are depicted in the second graph: 1 - low (L, orange); 2 - medium (M, aqua); 3 - high (H, purple). **(B)** (*i*) Schematic of a single gradient of dimension 1. Black arrow denotes low-to-high gradient for dimension 1. With only measurements of dimension 1, one cannot determine whether the region within dimension 1 contains one or more CFMs without measuring a second, orthogonal gradient. (*ii*) Schematic of a single gradient of dimension 2 overlapping the dimension 1 gradient in (*i*) to form a single CFM like V1 or hA1. Black arrow denotes low-to-high gradient for dimension 2. Note the orthogonal orientation of the two gradients (*i* vs. *ii*) composing this CFM. (*iii*) Schematic of an alternative gradient organization for dimension 2 overlapping the same dimension 1 gradient in (*i*). Black arrows denote two low-to-high gradients of dimension 2. The dotted gray line denotes the boundary dividing this region into two CFMs. **(C)** (*i*) In a properly defined CFM, measurements along the cortical representation of a single value of dimension 1 (e.g., green) span all values of dimension 2 (e.g., orange to cyan to purple), and vice versa. *(ii)* Schematic of vectors drawn along a single CFM from centers of low-stimulus-value regions of interest (ROIs) to high-stimulus-value ROIs for dimensions 1 (e.g., red to blue) and 2 (e.g., orange to purple). The offset measured between the low-to-high vectors for each dimension should be approximately 90° to be considered orthogonal and thus allow for each voxel/portion of the map to represent a unique combination of dimension 1 and dimension 2 values [4, 7, 10, 12].

http://dx.doi.org/10.5772/intechopen.77964

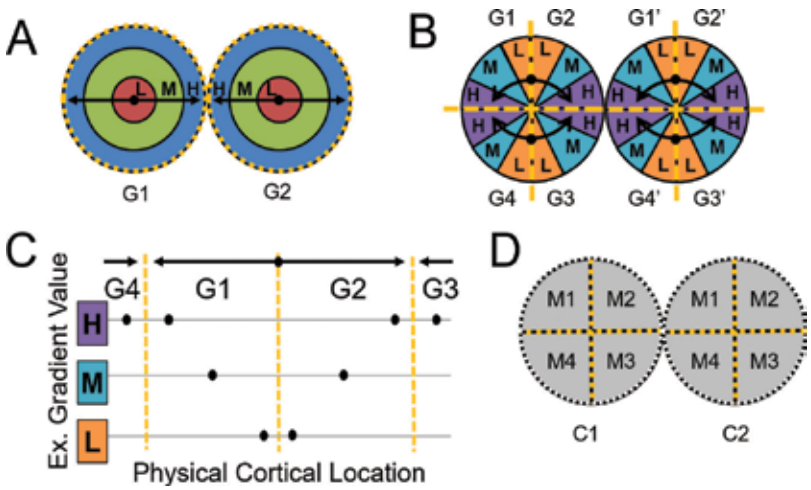

Figure 4. Cortical field map and cloverleaf cluster boundaries are defined along gradient reversals. **(A)** The schematic depicts representations of dimension 1 (e.g., eccentricity or tonotopy) along a flattened cortical surface. Note the repeating patterns of gradient values that denote multiple, repeating representations of low-to-high gradients for the same dimension (e.g., red to green to blue; G1: gradient one; G2: gradient two). Black arrows highlight gradient directions (low, L, to medium, M, to high, H). The gradients for this dimension fall in concentric circles that merge at the outer high (H, blue) representations. Dashed yellow lines mark gradient "reversals" at the edges of the concentric gradients. Note that it is not possible to determine how many CFMs exist within these two gradient sets without additional information from a second representation of an orthogonal dimension. **(B)** The schematic depicts representations of dimension 2 (e.g., polar angle or periodotopy) along the same flattened cortical surface. Again note the multiple, repeating representations of gradient values from low (orange) to medium (cyan) to high (purple) that now run "around the clock" (G3: gradient three; G4: gradient four). Dashed yellow lines mark again mark gradient "reversals," which now are organized like spokes on a wheel. **(C)** The diagram demonstrates how gradient boundaries for one dimension of a CFM are determined. Black dots denote hypothetical measurement points along the cortical surface shown in **(B)**. Arrows and yellow lines are as in **(B)**. Two gradients that span the full range of dimension 2 measurements can be divided into G1 and G2, with the representations of stimulus values increasing from low to high across the cortical surface in one gradient to the boundary where the representations in the next map then reverse back from high to low along the cortical surface in the next gradient. **(D)** Schematic shows the four CFMs defined by these sets of gradients representing the two orthogonal dimensions and arranged in a cloverleaf cluster [4, 7, 9, 10]. Black and yellow dotted lines demark boundaries defined by gradient reversals of dimension 1 and 2 representations, respectively (M1: map one; M2: map two; M3: map three; M4: map four; C1: cluster one; C2: cluster two).

sound: spectral (i.e., tone) and temporal (i.e., period or temporal envelope) information [4, 50]. **Figure 3B** demonstrates the importance of measurements of two orthogonal sensory dimensions for defining CFMs. A region of cortex with a single large gradient for one dimension could denote a single CFM (**Figure 3Bi,ii**) or many CFMs (**Figure 3Bi,iii**). As the number of neighboring gradients increases, the determination of the CFM organization grows increasingly complex. Thus, the number of CFMs in any region cannot be determined without checking for gradient reversals in the representation of the second, orthogonal dimension.

Similarly, two overlapping gradients that are parallel rather than orthogonal will not represent all the points in sensory space uniquely. For example, a region of visual cortex with parallel eccentricity and polar angle gradients would represent a narrow spiral of visual space rather than the entire visual field [7, 20, 51, 52]. Orthogonality can be examined by first estimating the direction of each gradient using a vector drawn from low-to-high stimulus values and then measuring the angle between the vectors for each gradient (**Figure 3Cii**) [4]. In addition, orthogonality can be confirmed by checking that measurements along the cortical

representation of a single value of the first dimension will span all values of the second dimension, and vice versa (**Figure 3Ci**). The orthogonality of each CFM can be determined for individual subjects and can then be compared across the individual subjects.

Second, each of these topographical representations must be organized as an orderly gradient that is generally contiguous (**Figures 3**, **4AB**) [20, 52]. For such a gradient to arise, a large number of voxels must be organized such that they span an entire range of sensory space, in order from one boundary to the other (e.g., from upper to lower vertical meridian for visual polar angle). A topographical gradient is therefore one of the most highly organized features of the cortical surface that we can measure using fMRI; the likelihood of two, orthogonal, overlapping, orderly gradients arising as a spurious pattern from noise is extraordinarily low (for a calculation of the probability of spurious gradients arising from noise, see [11]).

Third, each CFM should represent a substantial portion of sensory space. There may be some differences among CFMs based on the cortical magnification of specific subsets of sensory space, such as the relatively increased foveal representation along the ventral visual cortex, but a large portion of sensory space is still expected to be represented (e.g., [19, 20]). Obtaining a high quality measurement of topographic responses across sensory space is dependent upon choosing a set of phase-encoded stimuli that is appropriate for the sensory domain of interest. The range of values in the stimulus set and the sampling density of those values across feature space both influence the accuracy and precision of the measurement. In addition, the specificity of the representations may undergo some degree of blurring due to such factors as the inherent spatial spread of the fMRI signal, overlapping broad receptive fields, and measurement noise [30, 53–55]. In auditory cortex, in particular, the intensity (or loudness) of the tonotopic stimulus alone can alter the width of the receptive fields of neuron in primary auditory cortex (PAC) and consequently increase the lateral spread of the BOLD signal measured in neuroimaging [56]. Careful consideration should thus be given to the stimulus parameters and how they may affect the cortical responses.

Fourth, the general features of the gradient representations composing the CFMs should be consistent across individuals. It is important to note, however, that even well-accepted CFMs in visual cortex (e.g., V1) can vary dramatically in size and anatomical location [12, 20, 41, 57], as can cytoarchitectural and topographic boundaries in PAC [40, 42–45, 58]. Despite these variations, the general topographical pattern of adjacency among specific CFMs and cloverleaf clusters will be preserved across individuals. The measurement of CFMs provides one of the few *in vivo* ways to localize the distinct borders of a particular cortical region across individuals reliably.

The boundaries of a CFM are determined by carefully delineating the edges of each of the orthogonal gradients measured in a particular cortical region of interest (ROI) within a single hemisphere of an individual subject (**Figures 3** and **4**). Representations of one dimension may be repeated across a region of cortex or may exist in isolation. In isolation, the boundary can be drawn where the gradient responses end, although there will likely be some blurring or spreading of the representation along this edge [12, 20, 31, 48]. Two repeating and adjacent gradients that each span the full range of one dimension (e.g., visual field polar angle) can be divided into two sections at the point at which the gradients reverse (**Figures 3B**, **4**). At the gradient reversal, the representations of stimulus values increase

from low to high (or vice versa) across the cortical surface in one section to the boundary where the representations in the next CFM then reverse back from high to low (or vice versa) along the cortical surface in the next section (**Figure 4C**).

3.2. How are cortical field maps distinguished from sensory gradients or cortical areas?

A pervasive mistake in cortical field mapping has been the attempt to define a CFM using only a single cortical gradient (for reviews, see [2, 7, 8]). As described above, it is vital to understand that the representation of one dimension of sensory space – one topographical gradient along cortex – is not sufficient to define a CFM (**Figures 3**, **4**). A lone gradient simply reveals that this particular feature of sensory space is represented in that region of cortex.

In addition, we describe measurements of "cortical field maps" rather than use the phrase "cortical areas," as the definition of CFMs is specifically coupled to the topographical measurement, while cortical area definitions are based on a different and potentially conflicting set of criteria. Cortical areas have most extensively been identified in visual and auditory cortex using various combinations of the following measurements: 1) cytoarchitecture, 2) patterns of connectivity, 3) topography of sensory representations, and 4) functional responses [6, 7, 12, 20]. Because these separate types of measurements can at times produce conflicting results, the definition of cortical areas has led to many controversies in the naming of sensory areas. Observations of one or two cortical area criteria have often been used to propose the presence of a distinct cortical area; such definitions may then view the topography – the defining feature of CFMs – as secondary. Multiple CFMs may be present within what has been otherwise defined as a single cortical area. For example, cytoarchitecture was used to define Brodmann areas 18 and 19, which compose much of occipital visual cortex beyond primary visual cortex (V1). However, this same region of visual cortex is tiled with numerous VFMs (for additional discussion, see [7, 12]). Because of the significant complexity and confusion that such conflicting definitions can produce, our understanding of how to divide up cortex into distinct regions is still evolving and our naming schemes may vary based on the level of processing we are considering (e.g., first-order vision motion computations vs. the entire visual motion processing pathway). For current investigations of human visual and auditory cortex, sensory system researchers primarily rely on the topographical measurement of CFMs, which is the most well-established the measurement of cortical areas in the *in vivo* human brain at this time [7, 12].

3.3. Cloverleaf clusters: macrostructural organization of cortical field maps

Groups of adjacent CFMs have now been shown by multiple laboratories to be organized within visual and auditory cortex into a macrostructural pattern called the cloverleaf cluster. These clusters of CFMs have been described as a cloverleaf due to the organization of the individual CFMs within the cluster appearing like the leaves of a clover plant (**Figure 4D**). Brewer and associates first described cloverleaf clusters in human visual cortex [2, 7, 12, 20]; subsequent measurements demonstrated the presence of these clusters in other parts of human visual cortex [10, 11], in macaque visual cortex [9], and in human auditory cortex [4].

Figure 4 demonstrates how CFMs are arranged in a spatial pattern of clusters at a scale of several centimeters. Cloverleaf clusters are composed of groups of adjacent CFMs; one dimension of sensory topography is represented in concentric, circular bands from center to periphery of the cluster (e.g., vision: eccentricity; audition: tonotopy; **Figure 4A**), and the second, orthogonal dimension divides this confluent representation into multiple CFMs with radial bands spanning the cluster center to periphery (e.g., vision: polar angle; audition: periodotopy; **Figure 4B**). This type of macrostructural organization is now referred to as being radially orthogonal [7]. While the namesake clover plant is most commonly seen with a four-leaf organization, cloverleaf clusters may contain any number of CFMs. However, only an even number of CFMs will produce a smooth progression of representations around the cluster from the border of one CFM to the next. Measurements to date have shown that these clusters have consistent locations relative to one another, but that the maps within each cluster may be oriented somewhat differently, as if, in each individual's brain, the clusters themselves each may be positioned at a slightly different rotation about the cluster's central representation. Such inter-subject variability in cloverleaf cluster positions is consistent with our understanding of the variability in molecular gradient expression underlying the development of topographical gradients in cortex [26, 59–62]. Careful analysis across individual subjects can identify common CFMs by analyzing the pattern of CFMs and cloverleaf clusters across sensory cortex. This variability in cluster rotation and as well anatomical location again highlights the need for individual-subject data analysis.

The cloverleaf cluster organization of the CFMs may be important not only for the definition of CFMs, but may also play a role in coordinating neural computations. Neurons within each cluster are thought to share common computational resources. For example, CFMs within a cluster might have common mechanisms to coordinate neural timing or short-term information storage [2]. Similarly, it is likely that functional specializations for perception are organized by cloverleaf clusters rather than by single CFMs [20, 63]. VFMs within a cluster, for example, have very similar total surface areas, and each cluster's total surface area is reliable across subjects [11]. Each cloverleaf cluster can be functionally differentiated by its pattern of coherence measurements (i.e., BOLD response), cortical magnification, and pRF sizes. These distinctions indicate that VFMs within individual cloverleaf clusters are not only anatomically but also functionally related [7, 9, 17]. The cluster organization is not necessarily thought to be driving the common functions, but rather reflects how multiple stages in a sensory processing pathway might arise during development across individuals and during evolution across species.

4. The visual system

4.1. Overview

The visual field spatial arrangement is a fundamental physical property of a visual image [2]. While an image may still be identifiable despite alterations of such properties as its color, motion, contrast, or rotation, scrambling its spatial arrangement typically destroys our ability to identify or reconstruct the original image. This visual field spatial arrangement is encoded by the circuitry of the retina and then preserved and repeated through visual cortex

to produce a unifying matrix of visuospatial organization throughout the visual processing hierarchy, despite the diverse computations being performed across regions (e.g., [7, 12, 64]). As cortex interprets different aspects of the visual image—such as its motion or orientation—the cortical circuitry is organized using receptive fields organized within VFMs to preserve the critical spatial image information.

Neurons in lower-level VFMs perform computations on low-level visual features within a specific retinal location; these computations grow increasingly complex as the stimulus features are processed along the cortical hierarchy. Even though they may contain neurons primarily with large receptive fields, higher-order visual regions may still preserve the visuospatial organization of the image on the retina by retaining sufficient dispersion of receptive field centers through slight differences in the preferred tuning of neuronal responses to visual space [65]. Thus the occurrence of retinotopic organization in higher-order areas can still provide the position and stimulus size invariances typically attributed to high-order object- and face-responsive visual regions [7, 11, 48, 66, 67]. Current research is demonstrating that the majority of higher-order visual areas are organized according to visual space, maintaining retinotopically organized, dispersed receptive field centers despite increasingly large receptive field sizes [7, 11, 19, 65, 68–73].

Whether the spatial organization in visual cortex remains truly retinotopic or changes to a broader spatiotopic organization – one based on external space rather than retinal space – is still under investigation and cannot be determined with typical visual field mapping methods [69, 70, 74, 75]. In any case, this extensive preservation of visuospatial organization produces a common frame of reference for passing information up or down the visual hierarchy. Such visual-location-based "channels" could explain how higher-order areas subserving visual-attention can simultaneously influence many lower-level visual areas in spatially specific patterns [74, 76–80]. Another option may be that retinotopic organization is preserved across the cortical hierarchy even without a critical role for visual location information in the computations of a higher-order cortical region merely because changing the neuronal arrangement after it is established at the level of the retina and early visual cortex may be too costly or disruptive during development.

4.2. Low-level VFMs are arranged within a cloverleaf cluster on the medial occipital surface

Human visual cortex includes the entire occipital lobe and extends significantly into the parietal and temporal lobes (**Figure 5**), composing about 20% of cortex [12]. The medial wall of occipital cortex in each hemifield contains four hemifield representations of visual space known as V1, V2, V3, and hV4 (**Figures 6**, **7**; for detailed reviews, see [7, 12]). V1 consistently occupies the calcarine sulcus, bounded on either side by the split-hemifield representations of V2 and V3 on the lingual gyrus and cuneus. Human V4 (designated hV4 because of the unclear homology to macaque V4) is positioned as a complete hemifield on the ventral occipital surface adjacent to ventral V3 along the posterior fusiform gyrus [20, 82]. These four VFMs compose the medial aspect of the occipital pole cluster (m-OP cluster), which supports low-level visual computations [2, 7, 20].

Because it receives direct inputs from the retinogeniculate pathway, V1 is considered to be primary visual cortex, and it is the first place in retina-to-cortex pathway where information

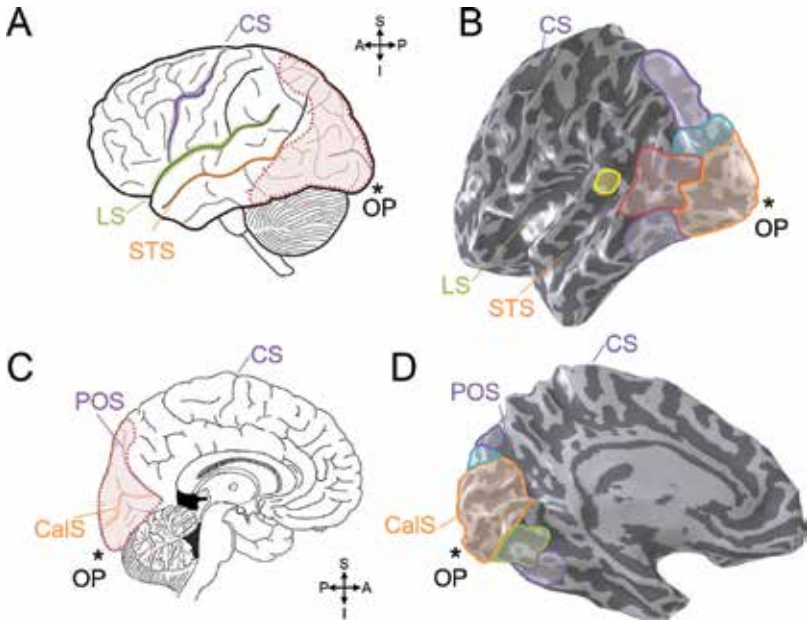

Figure 5. Visual cortex in the human brain. **(A)** Diagram of the lateral view of the human left cerebral hemisphere. Black lines denote major sulci. The general location of visual cortex is marked in red within the red dotted line [7, 12]. CS: Central sulcus (purple); LS: lateral sulcus, also known as the lateral or Sylvian fissure (green); STS: superior temporal sulcus (orange); OP*: occipital pole. Inset legend shows approximate anatomical directions for the views in **(A, B)**. S: superior; I: inferior; A: anterior; P: posterior. **(B)** 3-D rendering of the lateral view of an individual left hemisphere cortical surface. Light gray indicates gyri; dark gray indicates sulci. The locations of several VFM cloverleaf clusters as well as regions currently under investigation are shown by the colored ROIs: orange, OP cluster (occipital pole cluster, lateral subdivision including LO-1, LO-2, LOC) [2, 7, 81]; cyan, V3A/B cluster [2, 13]; red, hMT+ cluster (human medial temporal complex, V5) [2, 4, 9, 10, 12]; yellow, pSTS cluster (posterior superior temporal sulcus) [11]; purple, regions along the dorsal cortex (intraparietal sulcus) and ventral cortex (fusiform and parahippocampal gyri) currently under investigation (for reviews, see [4, 12]). **(C)** Diagram of the medial view of the human left cerebral hemisphere. Inset legend shows approximate anatomical directions for the views in **(C, D)**. POS: Parietal-occipital sulcus (purple); CalS: calcarine sulcus (orange). Other details are as in **(a)**. **(D)** 3-D rendering of the medial view of the left hemisphere cortical surface from the same individual. The locations of several VFM cloverleaf clusters as well as regions currently under investigation are again shown by the colored ROIs (n.b., clusters that span medial and lateral cortex match in color): orange, OP cluster (medial subdivision including V1, V2, V3, hV4) [2, 7]; cyan, V3A/B cluster; green, VO cluster (ventral occipital) [2, 20]; purple, dorsal and ventral regions currently under investigation. Other details are as in **(B)**.

from the two eyes is combined to form binocular cells. In addition, V1 is an important site of basic calculations such as orientation, color, and motion. Each computation is performed across the entire visual field, yet V1 appears at the level of fMRI measurements consist of a single, contiguous representation of visual space. In essence, V1 is composed of several VFMs overlaid on one another, each of which performs a single computation (i.e., separated maps for color, orientation, and motion). In this arrangement, a very intricate mosaic of neurons subserving these computations allows for each computation to be performed over each portion of the visual field. These mosaics, including pinwheel orientation columns, blobs/interblobs, and ocular dominance columns, are still being extensively investigated (e.g., [83–85]). These computations divide up into more specialized processing of the visual image after V1, with V2 and hV4 supporting low-level color and form processing, respectively, and V3 playing a role in low-level motion computations [12, 20, 51].

http://dx.doi.org/10.5772/intechopen.77964

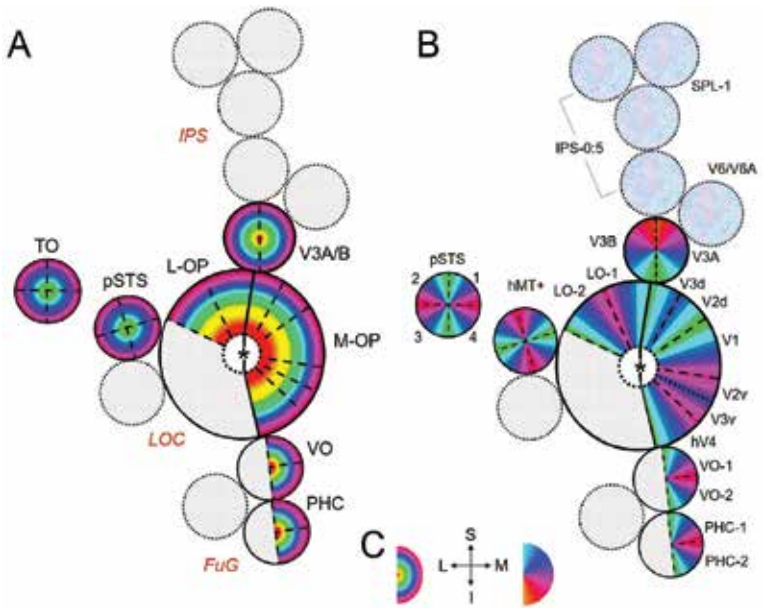

Figure 6. Schematic of human visual field map clusters. Schematics of eccentricity and polar angle representations within VFM clusters as would be viewed on a flattened left hemisphere. Color overlays represent the position in visual space that produces the strongest response at that cortical location. "*" marks occipital pole. Gray regions denote areas in which cloverleaf clusters are currently being investigated. **(A)** Diagram of eccentricity representations. Black labels denote published clusters: M-OP, medial aspect of occipital pole cluster; L-OP, lateral aspect of occipital pole cluster (partially defined); V3A/B, visual areas 3A and 3B cluster; TO, temporal occipital cluster; pSTS, posterior superior temporal sulcus cluster; VO cluster, ventral occipital cluster (partially defined); PHC cluster, parahippocampal cluster (partially defined). Red italicized labels denote anatomical regions currently under investigation: IPS, intraparietal sulcus; LOC, lateral occipital cortex; FuG, fusiform gyrus. **(B)** Diagram of polar angle representations. Black labels denote VFM names. Blue-magenta textured circles along IPS denote regions where polar angle representations have been measured, but not consistent eccentricity gradients. **(C)** *Right:* Color legend for eccentricity representations. *Middle:* Legend inset denotes approximate anatomical locations for the schematic. S: Superior; I: inferior; L: lateral; M: medial. *Left*: Color legend for polar angle representations.

V1, V2, V3, and hV4 each contain a foveal representation positioned at the occipital pole, with progressively more peripheral representations extending into more anteromedial cortex, forming complete eccentricity gradients (**Figure 7Ai,Bi,Ci**; e.g., [12, 29, 30, 32]). The region where the individual foveal representations meet at the occipital pole is commonly termed the "foveal confluence" [86]. Although fMRI measurements of eccentricity gradients depict these foveal representations as merging into one combined foveal region, careful fMRI measurements of polar angle gradients have demonstrated that distinct boundaries exist between even the most central foveal representations of V1, V2, V3, and hV4 [20, 86, 87].

The boundaries between each map are delineated by reversals in the polar angle gradients along the medial surface (**Figure 7 Aii**, **Bii**, **Cii**; e.g., [12, 29, 30, 32]). V1 has a contiguous polar angle gradient representing a full hemifield, while V2 and V3 have split-hemifield representations (i.e., quarterfields), which are named by their positions ventral or dorsal to V1: V2d, V2v, V3d, V3v. Because of their relatively consistent anatomical locations and unique concentric polar angle gradients, these three VFMs are typically the first landmarks identified in visual field mapping analyses [31, 32]. However, as noted above, the surface areas of these

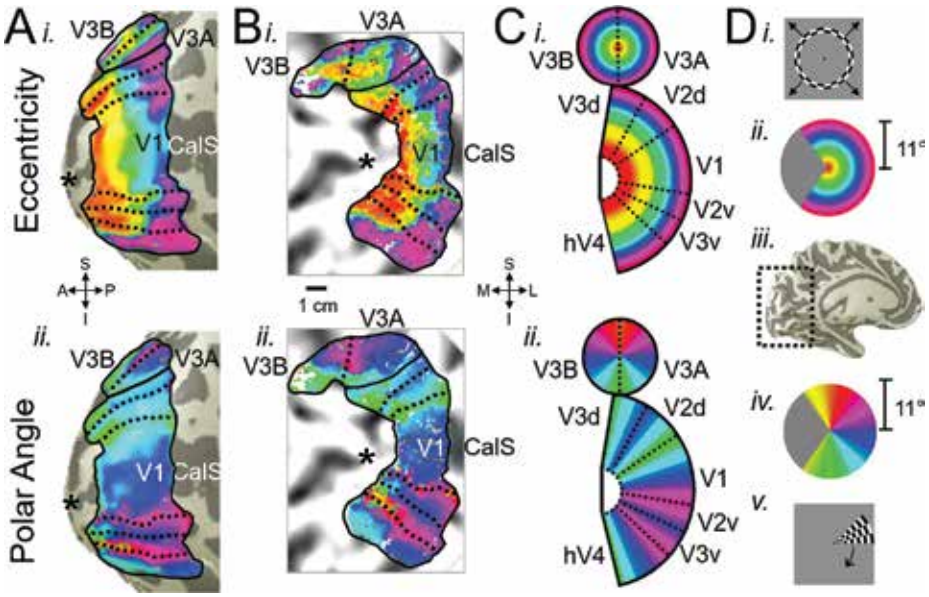

Figure 7. Example visual field map cloverleaf cluster data in human cortex. The pseudocolor data overlays on inflated 3-D **(A)** and flattened **(B)** representations of a single left hemisphere of one subject and the colors in the schematic **(C)** represent the location in visual space that creates the strongest response at that cortical position (see color legends in **(D)**). Solid black lines mark VFM boundaries at peripheral eccentricity reversals, which separate cloverleaf clusters from each other. Dotted black lines denote VFM boundaries along polar angle reversals, which separate individual VFMs within cloverleaf clusters. Light gray on the inflated/flattened cortex images indicates gyri; dark gray indicates sulci. **(A)** (*i*) Eccentricity gradient data are shown for the medial OP cluster and the V3A/B cluster. (*ii*) Polar angle gradients within the same VFM clusters are displayed. Inset legend denotes the anatomical orientation for the inflated brain images; A: anterior; P: posterior; S: superior; I: inferior. **(B)** (*i*) A view of the same eccentricity gradients is now shown on a flattened view of the cortical sheet. (*ii*) A view of the polar angle gradients within the same VFM clusters is displayed. Inset legend denotes the anatomical orientation for the flattened brain images. M: Medial; L: lateral; S: superior; I: inferior. Scale bar signifies 1 cm along the flattened cortical surface. **(C)** (*i*) Schematic of the eccentricity gradients of these VFM clusters; (*ii*) schematic of the polar angle aspect of these VFM clusters. VFMs within these clusters are labeled here and correspond to the VFMs displayed in **(A, B)**. **(D)** (*i*) One phase of the expanding ring stimulus used to measure eccentricity. (*ii*) color legend for eccentricity representations; (*iii*) inflated 3-D brain rendering, with dotted lines and arrow indicating the cropped view shown in **(C)**; (*iv*) color legend for polar angle representations; and (*v*) one phase of the rotating wedge stimulus used to measure polar angle. All data for **(A–D)** are from the left hemisphere of one subject collected using phase-encoded fMRI paradigm with moving-bar visual stimuli spanning 11° of visual angle. Coherence ≥0.25. Adapted from [11].

three VFMs fluctuate significantly among individuals independent of overall brain size [41]. While V1 is always located along the fundus of the calcarine sulcus in normal individuals, an increase in V1 size will consequently shift the specific positions of V2 and V3 along the neighboring gyri and sulci. VFMs beyond V3, such as the contiguous hV4 hemifield, continue to shift variably along the cortical surface in accordance with variable individual VFM sizes.

4.3. VFMs compose several cloverleaf clusters along the ventral stream

Several more VFMs representing extensive, contiguous hemifields of visual space are positioned along the fusiform gyrus anterior to hV4 (**Figures 5 BD**, **6**, **7**). These VFMs are named by their anatomical location and number within a cluster: VO-1 and VO-2, for ventral-occipital cortex, and PHC-1 and PHC-2, for parahippocampal cortex. VO-1

and VO-2 partially compose the VO cluster, share a distinct foveal representation, and subserve mid-level color and form processing [20]. Similarly, PHC-1 and PHC-2 partially compose the PHC cluster, share another discrete foveal representation, and display varying degrees of scene selectivity [19]. The eccentricity gradients reverse between clusters along the ventral surface, while the polar angle gradient reversals again divide up the clusters into individual hemifield VFMs.

In contrast to the measurements in posterior medial and VFMs, it has been much more difficult to measure retinotopic organization within the lateral occipital cortex, a region encompassing the object-responsive lateral occipital complex (LOC; **Figures 5B**, **6**). The LOC was originally thought to lack retinotopic organization or have only an "eccentricity bias" [88–90]. Recent studies along the dorsal aspect of the LOC, however, have described two VFMs, called LO-1 and LO-2 for "lateral occipital" (**Figure 6**). LO-1 is positioned just anterior to the lateral aspect of V3d, reversing from the upper vertical meridian representation at the boundary into its representation of a full hemifield of visual space with the hemifield of LO-2 at its inferior edge [81, 91]. The foveal representations of these two VFMs join with the confluent foveal representations of V1, V2, V3, and hV4 on the occipital pole to form part of the lateral aspect of the occipital pole cluster (l-OP cluster). In addition, regions just inferior to LO-2 have been shown to be responsive to lateralized visual stimuli, but have not yet been divided into specific VFMs [92–95]. Emerging data suggest that lateral occipital cortex inferior to LO-2 will also consist of multiple VFMs, which would complete the l-OP cluster subserving mid-to-high level object recognition. As noted above, the responses to object stimuli in this region could remain both invariant to stimulus size and position over a wide field of view while retaining visuospatial information [67].

4.4. VFMs also compose several cloverleaf clusters along the dorsal stream

4.4.1. Lateral occipital-temporal cortex

Just anterior to LOC along the bank of the inferior temporal sulcus, motion-selective cortex comprises a distinct cloverleaf cluster, alternatively known as the TO (temporal-occipital) or MT (medial-temporal) cluster (**Figures 5B**, **6**) [2, 10, 96, 97]. This cloverleaf cluster consists of the four VFMs of the hMT+ (human MT complex) thought to be involved in successive stages of visual motion processing [9, 10, 96, 98, 99]. The dorsal two hemifield VFMs are positioned just anterior to the LO maps, merging with that cluster at an eccentricity gradient reversal. These VFMs have been alternatively termed TO-1 and TO-2 or MT and MST, respectively, based on the likely homology to the VFMs of the MT cluster in macaque monkey [9, 10, 97]. These two VFMs share a distinct foveal representation with two VFM along more ventral lateral occipital cortex that are likely homologous to macaque FST and V4 t.

Anterior, but not adjacent, to the TO cluster, is a recently discovered additional cloverleaf cluster on the posterior superior temporal sulcus (pSTS): the pSTS cluster (**Figures 5B**, **6**) [11]. The pSTS clusters consists of four VFMs labeled pSTS-1, pSTS-2, pSTS-3, pSTS-4 and is located in a region implicated in high-order visual processing dealing with complex aspects of face and motion processing [100, 101]. In addition, this cortex has been associated with high-order multisensory processing, including the integration of auditory and visual information about objects [102, 103]. Thus, these CFMs may have multimodal tuning.

4.4.2. VFMs, cloverleaf clusters, and polar angle gradients in dorsal parietal and frontal cortex

Beyond the medial half of the dorsal boundary of V3d, a series of hemifield VFMs run from the transverse occipital sulcus (TOS) up along the intraparietal sulcus (IPS) (**Figures 5B**, **6**; e.g., [12, 76]). The first VFMs here bordering V3d are V3A and V3B, which share a discrete foveal representation within the TOS (**Figure 7**) [11, 13, 104, 105]. Measurements of V3A suggest that it has some similarities to macaque V3A and V3d, and it is thought to play a role in motion processing; the computations subserved by V3B are not yet resolved, but the basic parameters of its computations match that of V3A [11, 13, 104, 106, 107].

Moving anteriorly along the IPS from V3A and V3B, measurements find that visuospatial responses here are activated by attentionally demanding, phase-encoded stimuli, consistent with the description of this parietal region as subserving spatial attention [70, 74, 77–79, 106, 107]. The first VFM along the IPS is IPS-0 (formerly called V7), which has a foveal representation distinct from the one shared by V3A and V3B and represents a full hemifield of contralateral visual space [77, 107]. A series of polar angle representations then runs from IPS-0 along the medial wall of the IPS (**Figure 6B**). These representations have primarily been described as reversing smoothly through a strip of several hemifield representations from IPS-0 to IPS-5, with another polar angle representation termed SPL-1 (superior parietal lobule) just medial to these maps [70–72, 74, 76, 77, 79, 108]. Also along the medial wall of the parietal cortex and just anterior to V3d in the parieto-occipital sulcus are two additional polar angle gradients involved in particular types of motion processing, such as self-motion and visuomotor integration: V6 and V6A [109, 110]. V6 and V6A both contain relatively coarse polar angle representations of the contralateral hemifield and potentially eccentricity representations of the far periphery. It is important to note that, except for V6, these parietal representations are all descriptions of polar angle gradients rather than complete VFMs (**Figure 3**). Thus the full extent of VFMs and cloverleaf clusters along the IPS remains to be determined [7].

Several polar angle representations of the contralateral hemifield have also been measured in frontal cortex by a few studies using a variety of stimuli including phase-encoded paradigms, memory-guided saccade tasks, and visual spatial attention tasks (**Figure 6B**) [69, 70, 73, 76, 78, 79]. These topographic representations are positioned in precentral cortex (pre-CC), dorsolateral prefrontal cortex (DLPFC), the frontal eye fields (FEF), and the supplementary eye fields (SEF), cortical regions involved in the complex visual processing of spatial attention and eye movement control. Like the polar angle measurements along the IPS, these frontal regions also lack measurements of orthogonal eccentricity representations. As research progresses, we expect overlapping eccentricity gradients will be found, forming VFMs likely organized into cloverleaf clusters.

5. The auditory system

5.1. Overview

The auditory system encodes the complex sound waves we encounter in our daily environments as the intensity of their individual component frequencies, analogous to a Fourier analysis (**Figure 8A**). Higher frequency variations are transduced near the opening of the

cochlea of the inner ear, with decreasing frequencies transduced further down the membrane. This topographic gradient of frequencies, or tones, from low to high is referred to as tonotopy (or, less commonly, cochleotopy – a map of the cochlea). Spectral sound representation in the form of tonotopic gradients is thus one aspect of the fundamental auditory reference frame. This basic auditory information and tonotopic organization is preserved through multiple subcortical areas and at least through low-level auditory cortex (for reviews, see [8, 111–113]).

The second, orthogonal aspect of the fundamental auditory reference frame is temporal sound information, termed periodicity (**Figure 8B**) [4, 114, 115]. Periodicity information is thought to be coded in the auditory nerve through neural activity time-locked to the periodicity of the amplitude modulation (i.e., the length of time from peak-to-peak of the temporal envelope) [114, 116]. The temporally varying aspects of sound are expected to be encoded by neurons tuned to sounds of certain durations as well as neurons selective for the onset and offset of sounds Periodotopy thus refers to the topographic organization of neurons that respond differentially to sounds of different temporal envelope modulation rates.

Auditory processing in human and non-human primate cortex resides bilaterally within the temporal hemispheres near the lateral sulcus (**Figure 9A**) [8, 42, 117–121]. In the model system of macaque monkey, the first stage of cortical processing lies along the superior temporal gyrus (STG) and consists of three primary auditory areas: A1, R, and RT [122]. In contrast to visual cortex in which V1 is a single area defined as primary visual cortex, primary auditory cortex is

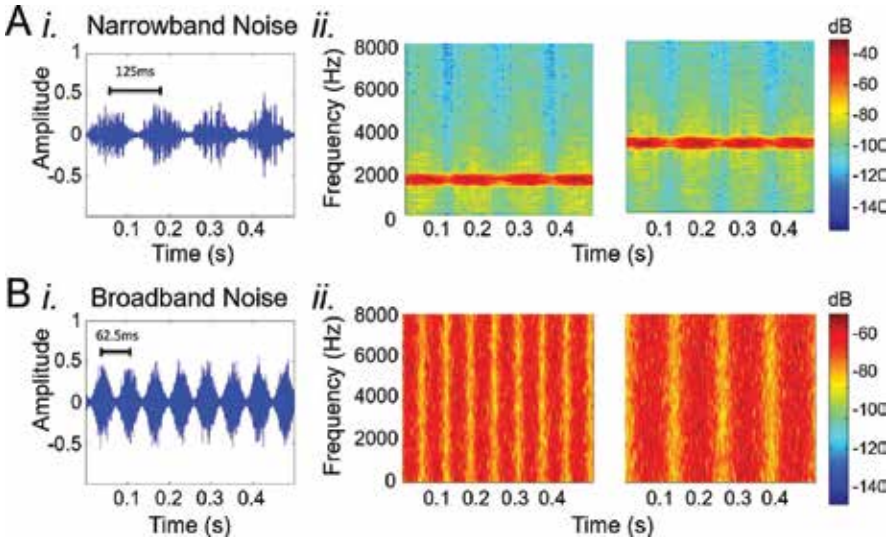

Figure 8. Example auditory field mapping stimuli. **(A)** Examples of a narrowband noise stimulus set (*i*) sound amplitude (arbitrary units) for this stimulus set as a function of time in seconds. (*ii*) Sound spectrograms for two narrowband noise stimuli with center frequencies (CF) of 1600 Hz (*left*) and 3200 Hz (*right*). Higher amplitudes in decibels (dB) are represented as "warmer" colors across frequencies (vertical axis, dB legend on right) and time in seconds (horizontal axis). **(B)** Examples of a broadband noise stimulus set (*i*) sound amplitude (arbitrary units) for this stimulus set as a function of time in seconds. (*ii*) sound spectrograms for two broadband noise stimuli with amplitude modulation (AM) rates of 8 Hz (*left*) and 16 Hz (*right*). Higher amplitudes are again represented as "warmer" colors across frequencies (vertical axis, dB legend on right) and time in seconds (horizontal axis). Narrowband noise stimuli hold periodicity constant and vary frequency, while broadband noise stimuli maintain constant frequency information and vary periodicity.

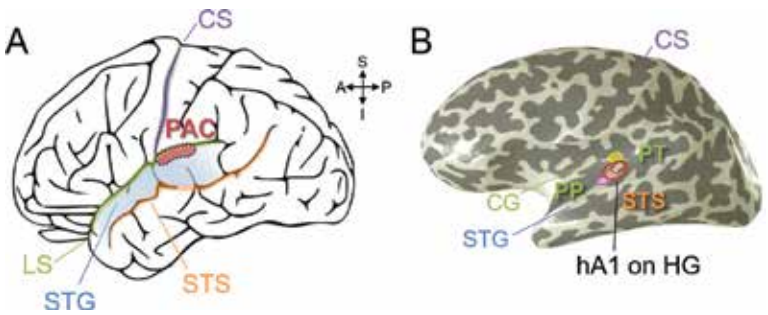

Figure 9. Early auditory cortex in the human brain. **(A)** Diagram of the lateral view of the human left cerebral hemisphere. Black lines mark major sulci. The approximate location of primary auditory cortex (PAC) is denoted by the red overlay within the black dotted line. The white dotted line within the red area shows the spread of PAC into the lateral sulcus (LS) along Heschl's gyrus (HG) that is not visible in this view. Inset legend shows anatomical directions for both brain images. S: Superior; I: inferior; A: anterior; P: posterior. PAC: primary auditory cortex (red); CS: Central sulcus (purple); LS: lateral sulcus, also known as the lateral or Sylvian fissure (green); STG: superior temporal gyrus (blue); STS: superior temporal sulcus (orange). **(B)** Inflated 3-D rendering of an individual left hemisphere cortical surface. Light gray indicates gyri; dark gray indicates sulci. The specific location of the hA1 auditory field map for this subject is marked with the black dotted lines. hA1 lies at the tip of HG. Note that HG is a single gyrus in this subject. CG: Circular gyrus (green); PP: planum polare (green); PT: planum temporale (green). Green labels are sections within LS. The three colored ROIs on HG denote the locations of the cloverleaf clusters comprising the core and belt AFMs: Yellow, hCM/hCL cluster; red, HG cluster including hA1, hR, hRM, hMM, hML, hAL; magenta, hRTM/hRT/hRTL cluster [4, 8]. Additional cloverleaf clusters are under investigation in the surrounding regions of auditory cortex along LS.

considered to be a core of these three AFMs, as all three contain the dense thalamic inputs from the thalamus, the expanded layer IV, and the high expression of cytochrome oxidase, acetylcholinesterase, and parvalbumin characteristic of primary sensory cortices [117, 118, 121, 123–128]. Secondary levels of cortical processing are then mediated by a set of eight belt regions, situated with four areas along both the lateral (CL, ML, AL, RTL) and medial (CM, RM, MM, RTM) sides of the core [129–131]. On the lateral side of the belt, an additional two regions compose the parabelt, which serves as a tertiary level of auditory processing that distributes information to neighboring auditory regions as well as multimodal areas across cortex [123, 132].

Due in part to methodological limitations, many studies of human audition over the past few decades have focused on psychoacoustics research of audition at the behavioral level or on neuroimaging investigations of speech production and comprehension in high-order cortex. In contrast, research about the structure and function of lower-level auditory processing in human cortex has been comparatively limited. An understanding of how lower-level auditory cortex is organized is crucial, however, for expanding our understanding of both the cortical pathways supporting basic auditory behavior and the auditory inputs available to speech processing networks.

Recent research has revealed that the cortical organization underlying lower-level human auditory processing resembles that of macaque core, belt, and parabelt structure, but with a rotation of these regions from the STG to Heschl's gyrus (HG), an anatomical structure within the lateral sulcus unique to humans (**Figure 9**) [4, 43, 58, 121]. The human auditory system also has similarities to the human visual system at several levels, from the fundamental organization of processing lower-level auditory information within AFMs and cloverleaf clusters

[4, 8] to the dual-stream model for higher-level speech processing in which ventral pathways support comprehension and dorsal pathways subserve sensorimotor integration [133]. AFMs, like VFMs, comprise two orthogonal representations of dimensions of sensory feature space: tonotopy (maps of tones, the spectral content of sounds) and periodotopy (maps of periods, the temporal content of sounds). Furthermore, these AFMs are organized into several cloverleaf clusters; the discovery of this cross-modal presence of cloverleaf clusters demonstrates that such cluster organization is a fundamental aspect of sensory cortex (**Figures 9**-**11**) [4, 134].

5.2. AFMs compose three cloverleaf clusters overlapping Heschl's gyrus

The history of auditory field mapping was complicated by the long delay between our ability to measure tonotopic gradients in human cortex and the discovery of human and non-human primate orthogonal periodotopic representations. Basing their investigations on only tonotopic responses, neuroimaging researchers futilely attempted to reach a consensus about the organization of human auditory cortex. As expected from schematics in **Figure 3**, the measurement of only one topographical representation led to a number of variable, conflicting, and ultimately unusable interpretations of the organization of human PAC and surrounding regions (for detailed discussions, see [8, 134]).

The relatively recent discoveries of periodotopic gradients in the macaque monkey midbrain brain and human auditory cortex have now allowed for an accurate definition of the first auditory field maps [4, 115]. This finding is supported by evidence from human psychoacoustic studies, which show that separable filter banks exist not only for frequency spectra, but also temporal information, signifying the presence of neurons with receptive fields tuned to ranges of frequencies and periods [50, 135–137]. Additionally, gradients representing temporal acoustic information have been measured in other animal models, including domestic cat PAC and chinchilla inferior colliculus [82, 138].

Eleven AFMs have been defined in human auditory cortex to date and show clear homologies to the eleven core and belt subfields of auditory cortex identified in human cytoarchitectural studies and in non-human primate cytoarchitectural, connectivity, and tonotopic measurements (**Figures 10**, **11**) [4, 8, 42, 118, 119, 122, 123, 126, 139–141]. The naming of the human AFMs follows that of the suspected homology to macaque, but appends an "h" to indicate human [4].

Three separate sets of concentrically organized tonotopic gradients overlap HG, running from STG to the circular sulcus (CiS; **Figure 10A**, **11C**). The first complete auditory cloverleaf cluster measured in humans – the HG Cluster – is centered on the primary, circular tonotopic gradient on Heschl's Gyrus (HG; **Figures 9**-**11**) [8]. The low-tone representation in this cluster is positioned centrally and expands in iso-tone bands out to high-tone representations. A reversal in the anteromedial high-tone region of the HG cluster divides the HG cluster from the CM/CL cluster. Abutting the HG cluster where HG meets STG, there exist another tonotopic reversal into the RT cluster. More research is required to determine the full extent of the CM/CL and RT clusters.

Periodotopic gradient reversals along HG divide the tonotopic representation of the central HG cluster into two AFMs each of core, medial belt, and lateral belt: hA1, hR, hMM, hRM, hML, and hAL (**Figures 10B**, **11D**). HA1 lies within this cluster at the tip of HG and is the largest of the core and belt AFMs. It is thought to subserve the most basic of cortical auditory computations, and this is reflected in its detailed tonotopic and periodotopic gradients [123]. The anterior/medial aspect of hA1 is tuned to high tones, and the posterior/lateral aspect is tuned to low tones. Just past the tip of HG and the high-tone reversal in the circular sulcus (CiS), a high-periodicity gradient reversal divides the tonotopic representation of the CM/CL cluster into hCM, and hCL, two regions that have been implicated in early language and speech processing as well as audiovisual integration [142]. Similarly, at the base of HG, a set of periodotopic gradients divides the partial third cloverleaf cluster into hRT, hRTM, and hRTL. These AFMs along STG in macaque have been shown to be involved in lower-level processing of stimuli like temporally modulated environmental sounds [129, 130]. Now that these AFMs and cloverleaf clusters can be reliably identified in individual subjects, researchers can

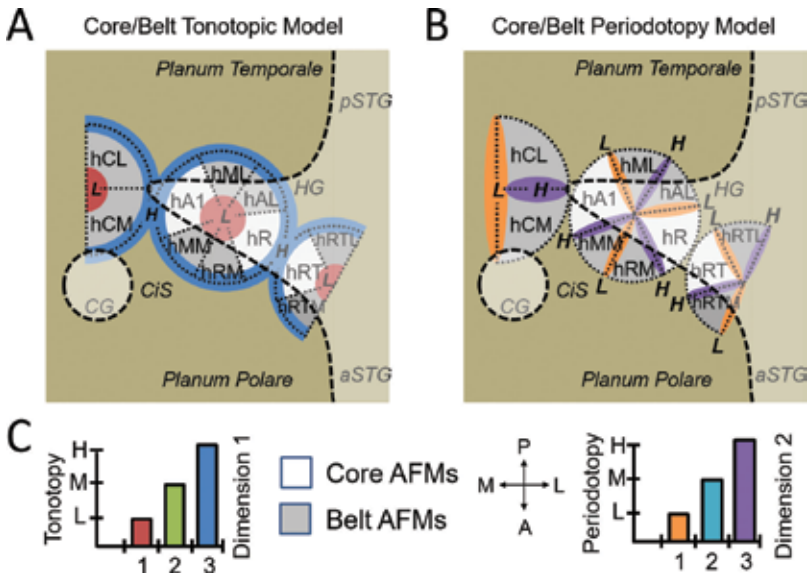

Figure 10. Diagrams of auditory field map cloverleaf clusters overlapping Heschl's gyrus. (A, B) Approximate locations of core AFMs (hA1, hR, hRT) are shown in white, and belt AFMs (hML, hAL, hRTL, hRTM, hRM, hMM, hCM, hCL) are shown in gray, as defined by [4]. Schematics were created from individual-subject data drawn from multiple phase-encoded fMRI experiments. Diagrams are oriented along the same global anatomical axes. Darker beige background indicates the plane of the lateral sulcus, while lighter beige overlay indicates gyri. The edges of gyri are also noted with dashed black lines. HG: Heschl's gyrus. a/p STG: anterior/posterior superior temporal gyrus; CiS: circular sulcus; CG: circular gyrus. **(A)** Diagram depicts the locations of tonotopic representations overlaid along the core (white) and belt (gray) AFMs. The approximate locations of low (L) and high (H) tonotopic representations are shown in red and blue, respectively. Dotted black lines mark the boundaries between AFMs within these three cloverleaf clusters: hCM/hCL cluster (partial cluster defined to date); HG cluster with hA1; hRTM/hRT/hRTL cluster (partial cluster defined to date). **(B)** Diagram now shows periodotopic representations overlaid along the same example region of cortex. L and H now refer to the approximate locations of low (orange) or high (purple) periodotopic representations, respectively. **(C)** Color legends for tonotopy schematic (*left*), core/belt AFMs (*middle left*), and periodotopy schematic (*right*). Inset legend (*middle right*) shows anatomical directions for both diagrams. M: Medial; L: lateral; A: anterior; P: posterior. For a detailed review, see [8].

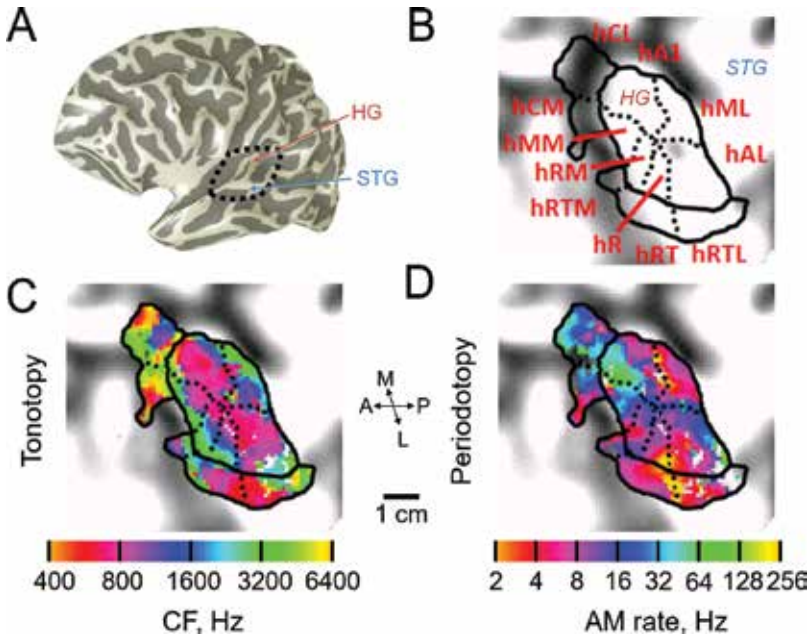

Figure 11. Example auditory field map cloverleaf cluster data in human cortex. **(A)** Inflated 3-D rendering of an individual left hemisphere cortical surface. Light gray indicates gyri; dark gray indicates sulci. HG: Heschl's gyrus, blue; STG: superior temporal gyrus, red. Black dotted line indicates HG and surrounding regions presented in **(B-D)**. **(B)** Flattened cortical surface of HG and surrounding regions. Solid black lines indicate AFM boundaries between maps along tonotopic reversals, which separate cloverleaf clusters from one another. Dotted black lines indicate AFM boundaries along periodotopic reversals between maps within a cloverleaf cluster. Red text indicates AFM names. **(C)** Tonotopic gradients measured using narrowband noise stimuli with a phase-encoded fMRI paradigm. Color overlay indicates the preferred frequency range for each voxel. CF: Center frequency in Hz. For clarity, only voxels within the core and belt AFMs are shown. Coherence ≥0.20. **(D)** Periodotopic representations measured using broadband noise stimuli with a phase-encoded fMRI paradigm. Color overlay is shown on the same flattened cortical surface as in **(C)** and now indicates the preferred period range for each voxel. AM rate: amplitude modulation rate in Hz. Other details are as in **(C)**. Inset scale bar denotes 1 cm along the flattened cortical surfaces. Inset legend shows anatomical directions for both datasets. M: Medial; L: lateral; A: anterior; P: posterior. Adapted from [4].

begin to investigate the specific functions subserved by each AFM. Based on emerging data, we also expect that neighboring cortex like planum temporale (PT) and STG will also contain AFMs organized into cloverleaf clusters.

6. Considerations for defining additional CFMs and cloverleaf clusters

To date, cloverleaf clusters have been shown to both be common to multiple sensory systems across human cortex and conserved across some primate species [2, 7, 9, 10, 20, 134, 143]. As we continue to delineate additional CFM clusters and study their functional responses, it is important to consider what homologies may exist across sensory domains and species as well as potential ways CFMs may be altering under evolutionary pressures. Evolution is an

ongoing process; CFMs and clusters are not necessarily, and in fact are unlikely to be, at an optimal evolutionary endpoint. Thus it is important to keep in mind that the cortical sensory representations that we are measuring may not be perfectly organized. In addition, with 25 million years of divergent evolution between humans and macaque monkeys, some CFMs and clusters may be unique to one species or the other [144].

Figure 12 depicts several ways in which CFMs may have changed or be in the process of changing across species or sensory domains (for extended discussion, see [5]). The size of a CFM itself (**Figure 12B**) or the total number of CFMs devoted to a particular sensory processing pathway (**Figure 12D**) may increase or decrease, reflecting an expansion or reduction of the

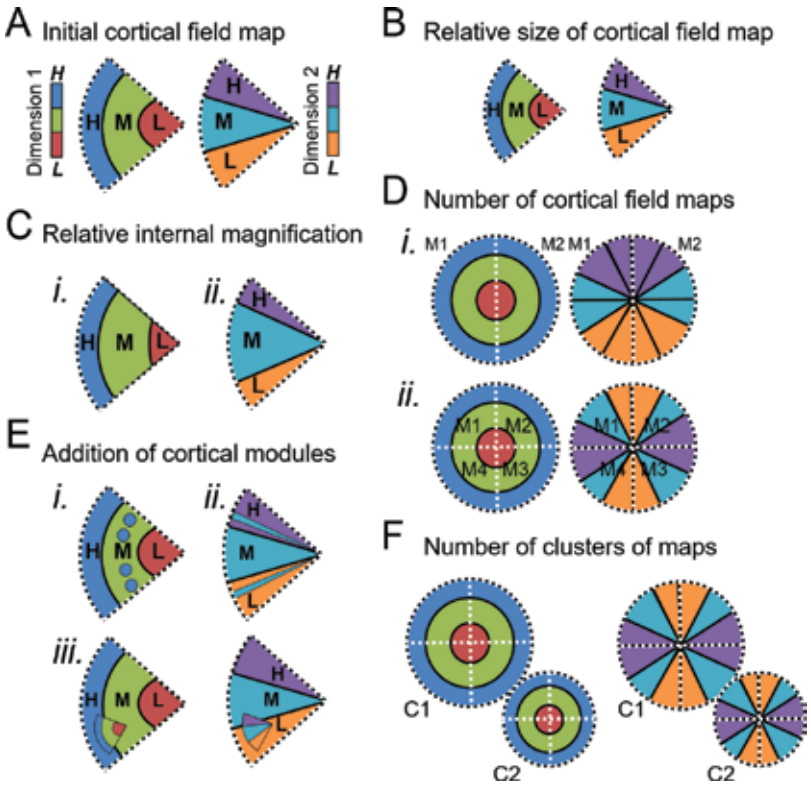

Figure 12. Potential cortical field map changes over evolution. Schematic diagrams depict numerous ways CFMs might change over the course of evolution. Consideration of such changes is important for evaluating potential homology of CFMs across sensory cortices and among species (for extended discussion, see [5]). **(A)** Each schematic shows two pictures of the same CFM, one for each orthogonal dimension (e.g., dimension 1: tonotopy or eccentricity; dimension 2: periodotopy or polar angle). The subsequent schematics depict changes to this CFM. **(B)** Overall size of CFM may be reduced. **(C)** The magnification of a particular part of the internal representations may increase for dimension 1 (*i*) and/or dimension 2 (*ii*). **(D)** The number of CFMs for a particular computation may increase or decrease (e.g., (*i*) two CFMS; (*ii*) four CFMs). **(E)** Additional representations may be in the process of emerging or combining within a complete CFM. (*i*) Additional segments of H (high; blue) representations of dimension 1 are present within the M (medium; green) representations. (*ii*) Additional segments of M (medium; teal) representations of dimension 2 are present within the H (high; purple) and L (low; orange) representations. (*iii*) A smaller complete CFM exists within the larger CFM. **(F)** New clusters of maps may emerge in neighboring regions.

importance of the particular behavior this cortex subserves. The internal structure of a CFM may be altered in the magnification of specific sections of the representations (**Figure 12C**) or may contain additional, emerging representation subsections (**Figure 12E**). Similarly, the number of cloverleaf clusters may be modified. Thus the homology of CFMs across species is very important for understanding functional similarities in different model systems, but care must also be taken to recognize what differences may exist.

In addition to the likely role of cloverleaf clusters in efficiently grouping together neurons performing associated computations, the emergence of new cloverleaf clusters during evolution as an organizational unit across cortex could facilitate the development of expanded or even novel cortical computations for an emerging species [8, 145]. In other words, once a particular organizational unit such as the cloverleaf cluster has arisen in one sensory modality, the same organizational unit might be duplicated and repeated across the brain as it evolves, following consistent genetic mechanisms during development [145]. Now that CFMs and cloverleaf clusters have been established as fundamental organizational principles in visual and auditory cortex, we can use this knowledge to guide measurements of similar topographic groupings in other sensory domains (e.g., somatosenstaion, pain matrix, olfaction; [3, 4, 146]).

7. Conclusion

Human visual and auditory cortex thus interestingly share a common organizational scheme, with each sensory system compartmentalized into CFMs that are themselves arranged on a larger scale into cloverleaf clusters. This fundamental organization provides a basic framework for the complex processing and analysis of input from sensory receptors. Such similarity may be common across many sensory domains, which may aid in the future identification of CFMs in the representation of other senses and in homologous regions in related species. The detailed examination of these CFMs and clusters in individual subjects can also be applied to the careful analysis of the computational stages of sensory processing and to the detailed tracking of cortical changes in a variety of diseases.

Acknowledgements

This material is based upon work supported by the National Science Foundation under Grant Number 1329255 and by startup funds from the Department of Cognitive Sciences at the University of California, Irvine.

Conflict of interest

The authors declare that this research was conducted in the absence of any commercial or financial relationships that could be interpreted to be a potential conflict of interest.

Author details

Alyssa A. Brewer[1,2]* and Brian Barton[1]

*Address all correspondence to: aabrewer@uci.edu

1 Department of Cognitive Sciences, University of California, Irvine, CA, USA

2 Department of Language Science, University of California, Irvine, CA, USA

References

[1] Kaas JH. Topographic maps are fundamental to sensory processing. Brain Research Bulletin. 1997;**44**(2):107-112

[2] Wandell BA, Brewer AA, Dougherty RF. Visual field map clusters in human cortex. Philosophical Transactions of the Royal Society of London. Series B, Biological Sciences. 2005;**360**(1456):693-707. DOI: 10.1098/rstb.2005.1628

[3] Sanchez-Panchuelo RM, Francis S, Bowtell R, Schluppeck D. Mapping human somatosensory cortex in individual subjects with 7T functional MRI. Journal of Neurophysiology. 2010;**103**(5):2544-2556. DOI: 10.1152/jn.01017.2009

[4] Barton B, Venezia JH, Saberi K, Hickok G, Brewer AA. Orthogonal acoustic dimensions define auditory field maps in human cortex. Proceedings of National Academy of Science U S A. 2012;**109**(50):20738-20743. DOI: 10.1073/pnas.1213381109

[5] Krubitzer LA, Seelke AM. Cortical evolution in mammals: The bane and beauty of phenotypic variability. Proceedings of the National Academy of Sciences. 2012;**109** (Supplement 1):10647-10654

[6] Van Essen DC. Organization of Visual Areas in macaque and human cerebral cortex. In: Chalupa LM, Werner JS, editors. The Visual Neurosciences. Boston: Bradford Books; 2003. pp. 507-521

[7] Brewer AA, Barton B. Visual field map organization in human visual cortex. In: Molotchnikoff S, Rouat J, editors. Visual Cortex - Current Status and Perspectives. Rijeka, Croatia: InTech; 2012. pp. 29-60. DOI: 10.5772/51914

[8] Brewer AA, Barton B. Maps of the auditory cortex. Annual Review of Neuroscience. 2016;**39**:385-407. DOI: 10.1146/annurev-neuro-070815-014045

[9] Kolster H, Mandeville JB, Arsenault JT, Ekstrom LB, Wald LL, Vanduffel W. Visual field map clusters in macaque extrastriate visual cortex. The Journal of Neuroscience. 2009;**29**(21):7031-7039. DOI: 10.1523/JNEUROSCI.0518-09.2009

[10] Kolster H, Peeters R, Orban GA. The retinotopic organization of the human middle temporal area MT/V5 and its cortical neighbors. The Journal of Neuroscience. 2010;**30**(29):9801-9820. DOI: 10.1523/JNEUROSCI.2069-10.2010

[11] Barton B, Brewer AA. Visual field map clusters in high-order visual processing: Organization of V3A/V3B and a new cloverleaf cluster in the posterior superior temporal sulcus. Frontiers in Integrative Neuroscience. 2017;**11**:4. DOI: 10.3389/fnint.2017.00004

[12] Wandell BA, Dumoulin SO, Brewer AA. Visual field maps in human cortex. Neuron. 2007;**56**(2):366-383. DOI: 10.1016/j.neuron.2007.10.012

[13] Press WA, Brewer AA, Dougherty RF, Wade AR, Wandell BA. Visual areas and spatial summation in human visual cortex. Vision Research. 2001;**41**(10-11):1321-1332

[14] Mitchison G. Neuronal branching patterns and the economy of cortical wiring. Proceedings: Biological Sciences. 1991;**245**(1313):151-158. DOI: 10.1098/rspb.1991.0102

[15] Chklovskii DB, Koulakov AA. Maps in the brain: What can we learn from them? Annual Review of Neuroscience. 2004;**27**:369-392. DOI: 10.1146/annurev.neuro.27.070203.144226

[16] Shapley R, Hawken M, Xing D. The dynamics of visual responses in the primary visual cortex. Progress in Brain Research. 2007;**165**:21-32. DOI: 10.1016/S0079-6123(06)65003-6

[17] Moradi F, Heeger DJ. Inter-ocular contrast normalization in human visual cortex. Journal of Vision. 2009;**9**(3):13 1-13 1322. DOI: 10.1167/9.3.13

[18] Braitenberg V, Schüz A. Cortex: Statistics and Geometry of Neuronal Connectivity. 2nd ed. 1998

[19] Arcaro MJ, McMains SA, Singer BD, Kastner S. Retinotopic organization of human ventral visual cortex. The Journal of Neuroscience. 2009;**29**(34):10638-10652. DOI: 10.1523/JNEUROSCI.2807-09.2009

[20] Brewer AA, Liu J, Wade AR, Wandell BA. Visual field maps and stimulus selectivity in human ventral occipital cortex. Nature Neuroscience. 2005;**8**(8):1102-1109. DOI: 10.1038/nn1507

[21] Baseler HA, Brewer AA, Sharpe LT, Morland AB, Jagle H, Wandell BA. Reorganization of human cortical maps caused by inherited photoreceptor abnormalities. Nature Neuroscience. 2002;**5**(4):364-370. DOI: 10.1038/nn817

[22] Hoffmann MB, Tolhurst DJ, Moore AT, Morland AB. Organization of the visual cortex in human albinism. The Journal of Neuroscience. 2003;**23**(26):8921-8930

[23] Hoffmann MB, Kaule FR, Levin N, Masuda Y, Kumar A, Gottlob I, et al. Plasticity and stability of the visual system in human achiasma. Neuron. 2012;**75**(3):393-401. DOI: 10.1016/j.neuron.2012.05.026

[24] Baseler HA, Gouws A, Haak KV, Racey C, Crossland MD, Tufail A, et al. Large-scale remapping of visual cortex is absent in adult humans with macular degeneration. Nature Neuroscience. 2011;**14**(5):649-655. DOI: 10.1038/nn.2793

[25] Fine I, Wade AR, Brewer AA, May MG, Goodman DF, Boynton GM, et al. Long-term deprivation affects visual perception and cortex. Nature Neuroscience. 2003;**6**(9):915-916. DOI: 10.1038/nn1102

[26] Muckli L, Naumer MJ, Singer W. Bilateral visual field maps in a patient with only one hemisphere. Proceedings of National Academy of Sciences U S A. 2009;**106**(31):13034-13039. DOI: 10.1073/pnas.0809688106

[27] Brewer AA, Barton B. Visual cortex in aging and Alzheimer's disease: Changes in visual field maps and population receptive fields. Frontiers in Psychology. 2014;**5**:74. DOI: 10.3389/fpsyg.2014.00074

[28] Brewer AA, Barton B. Changes in visual cortex in healthy aging and dementia. In: Moretti DV, editor. Update on Dementia. Rijeka, Croatia: InTech; 2016. pp. 273-310. DOI: 10.5772/61983

[29] DeYoe EA, Carman GJ, Bandettini P, Glickman S, Wieser J, Cox R, et al. Mapping striate and extrastriate visual areas in human cerebral cortex. Proceedings of National Academy of Sciences (USA). 1996;**93**:2382-2386

[30] Engel SA, Glover GH, Wandell BA. Retinotopic organization in human visual cortex and the spatial precision of functional MRI. Cerebral Cortex. 1997;**7**(2):181-192

[31] Engel SA, Rumelhart DE, Wandell BA, Lee AT, Glover GH, Chichilnisky EJ, et al. fMRI of human visual cortex. Nature. 1994;**369**(6481):525. DOI: 10.1038/369525a0

[32] Sereno MI, Dale AM, Reppas JB, Kwong KK, Belliveau JW, Brady TJ, et al. Borders of multiple visual areas in humans revealed by functional magnetic resonance imaging. Science. 1995;**268**(5212):889-893

[33] Humphries C, Liebenthal E, Binder JR. Tonotopic organization of human auditory cortex. NeuroImage. 2010;**50**(3):1202-1211. DOI: 10.1016/j.neuroimage.2010.01.046

[34] Talavage TM, Sereno MI, Melcher JR, Ledden PJ, Rosen BR, Dale AM. Tonotopic organization in human auditory cortex revealed by progressions of frequency sensitivity. Journal of Neurophysiology. 2004;**91**(3):1282-1296. DOI: 10.1152/jn.01125.2002

[35] Petkov CI, Kayser C, Augath M, Logothetis NK. Optimizing the imaging of the monkey auditory cortex: Sparse vs. continuous fMRI. Magnetic Resonance Imaging. 2009;**27**(8):1065-1073. DOI: 10.1016/j.mri.2009.01.018

[36] Joly O, Baumann S, Balezeau F, Thiele A, Griffiths TD. Merging functional and structural properties of the monkey auditory cortex. Frontiers in Neuroscience. 2014;**8**:198. DOI: 10.3389/fnins.2014.00198

[37] Bandettini PA, Jesmanowicz A, Van Kylen J, Birn RM, Hyde JS. Functional MRI of brain activation induced by scanner acoustic noise. Magnetic Resonance in Medicine. 1998;**39**(3):410-416

[38] Gaab N, Gabrieli JD, Glover GH. Assessing the influence of scanner background noise on auditory processing. II. An fMRI study comparing auditory processing in the absence and presence of recorded scanner noise using a sparse design. Human Brain Mapping. 2007;**28**(8):721-732. DOI: 10.1002/hbm.20299

[39] Scarff CJ, Dort JC, Eggermont JJ, Goodyear BG. The effect of MR scanner noise on auditory cortex activity using fMRI. Human Brain Mapping. 2004;**22**(4):341-349. DOI: 10.1002/hbm.20043

[40] Clarke S, Morosan P. Architecture, connectivity, and transmitter receptors of human auditory cortex. In: Poeppel D, Overath T, Popper A, Richard R, editors. The Human Auditory Cortex. New York: Springer; 2012. pp. 11-38

[41] Dougherty RF, Koch VM, Brewer AA, Fischer B, Modersitzki J, Wandell BA. Visual field representations and locations of visual areas V1/2/3 in human visual cortex. Journal of Vision. 2003;**3**(10):586-598. DOI: 10:1167/3.10.1

[42] Galaburda A, Sanides F. Cytoarchitectonic organization of the human auditory cortex. The Journal of Comparative Neurology. 1980;**190**(3):597-610. DOI: 10.1002/cne.901900312

[43] Morosan P, Rademacher J, Schleicher A, Amunts K, Schormann T, Zilles K. Human primary auditory cortex: Cytoarchitectonic subdivisions and mapping into a spatial reference system. NeuroImage. 2001;**13**(4):684-701. DOI: 10.1006/nimg.2000.0715

[44] Rademacher J, Caviness VS Jr, Steinmetz H, Galaburda AM. Topographical variation of the human primary cortices: Implications for neuroimaging, brain mapping, and neurobiology. Cerebral Cortex. 1993;**3**(4):313-329

[45] Rademacher J, Morosan P, Schormann T, Schleicher A, Werner C, Freund HJ, et al. Probabilistic mapping and volume measurement of human primary auditory cortex. NeuroImage. 2001;**13**(4):669-683. DOI: 10.1006/nimg.2000.0714

[46] Talairach J, Tournoux P. Col-Planar Stereotax Atlas of the Human Brain. New York: Thieme Medical Publishers; 1988

[47] Collins DL, Neelin P, Peters TM, Evans AC. Automatic 3D intersubject registration of MR volumetric data in standardized Talairach space. Journal of Computer Assisted Tomography. 1994;**18**(2):192-205

[48] Dumoulin SO, Wandell BA. Population receptive field estimates in human visual cortex. NeuroImage. 2008;**39**(2):647-660. DOI: 10.1016/j.neuroimage.2007.09.034

[49] Hoffmann MB, Seufert PS, Schmidtborn LC. Perceptual relevance of abnormal visual field representations: Static visual field perimetry in human albinism. The British Journal of Ophthalmology. 2007;**91**(4):509-513. DOI: 10.1136/bjo.2006.094854

[50] Santoro R, Moerel M, De Martino F, Valente G, Ugurbil K, Yacoub E, et al. Reconstructing the spectrotemporal modulations of real-life sounds from fMRI response patterns. Proceedings of National Academy of Sciences USA. 2017;**114**(18):4799-4804. DOI: 10.1073/pnas.1617622114

[51] Wade AR, Brewer AA, Rieger JW, Wandell BA. Functional measurements of human ventral occipital cortex: Retinotopy and colour. Philosophical Transactions of the Royal Society of London. Series B, Biological Sciences. 2002;**357**(1424):963-973. DOI: 10.1098/rstb.2002.1108

[52] Tyler CW, Wade AR. Extended concepts of occipital retinotopy. Current Medical Imaging Review. 2005;**1**:3190329

[53] Hart HC, Hall DA, Palmer AR. The sound-level-dependent growth in the extent of fMRI activation in Heschl's gyrus is different for low- and high-frequency tones. Hearing Research. 2003;**179**(1-2):104-112

[54] Logothetis NK, Wandell BA. Interpreting the BOLD signal. Annual Review of Physiology. 2004;**66**:735-769. DOI: 10.1146/annurev.physiol.66.082602.092845

[55] Menon RS, Kim SG. Spatial and temporal limits in cognitive neuroimaging with fMRI. Trends in Cognitive Sciences. 1999;**3**(6):207-216

[56] Tanji K, Leopold DA, Ye FQ, Zhu C, Malloy M, Saunders RC, et al. Effect of sound intensity on tonotopic fMRI maps in the unanesthetized monkey. NeuroImage. 2010;**49**(1):150-157. DOI: 10.1016/j.neuroimage.2009.07.029

[57] Amunts K, Schleicher A, Burgel U, Mohlberg H, Uylings HB, Zilles K. Broca's region revisited: Cytoarchitecture and intersubject variability. The Journal of Comparative Neurology. 1999;**412**(2):319-341

[58] Leonard CM, Puranik C, Kuldau JM, Lombardino LJ. Normal variation in the frequency and location of human auditory cortex landmarks. Heschl's gyrus: Where is it? Cerebral Cortex. 1998;**8**(5):397-406

[59] Brewer AA, Barton B. Developmental plasticity: FMRI investigations into human visual cortex. In: Papageorgiou TD, Christopoulos G, Smirnakis S, editors. Advanced Brain Neuroimaging Topics in Health and Disease - Methods and Applications. Rijeka, Croatia: InTech; 2014. pp. 305-334. DOI: 10.5772/58256

[60] Brewer AA. Visual maps: To merge or not to merge. Current Biology. 2009;**19**(20): R945-R947. DOI: 10.1016/j.cub.2009.09.016

[61] Katz LC, Shatz CJ. Synaptic activity and the construction of cortical circuits. Science. 1996;**274**(5290):1133-1138

[62] Polleux F, Ince-Dunn G, Ghosh A. Transcriptional regulation of vertebrate axon guidance and synapse formation. Nature Reviews. Neuroscience. 2007;**8**(5):331-340. DOI: 10.1038/nrn2118

[63] Bartels A, Zeki S. The architecture of the colour Centre in the human visual brain: New results and a review. The European Journal of Neuroscience. 2000;**12**(1):172-193

[64] Van Essen DC. In: Chalupa L, Werner J, editors. Organization of Visual Areas in Macaque and Human Cerebral Cortex. Boston: Bradford; 2003

[65] Lehky SR, Sereno AB. Population coding of visual space: Modeling. Frontiers in Computational Neuroscience. 2011;**4**:155. DOI: 10.3389/fncom.2010.00155

[66] Haak KV, Winawer J, Harvey BM, Renken R, Dumoulin SO, Wandell BA, et al. Connective field modeling. NeuroImage. 2012;**66C**:376-384. DOI: 10.1016/j.neuroimage.2012.10.037

[67] DiCarlo JJ, Maunsell JH. Anterior inferotemporal neurons of monkeys engaged in object recognition can be highly sensitive to object retinal position. Journal of Neurophysiology. 2003;**89**(6):3264-3278. DOI: 10.1152/jn.00358.2002

[68] Lehky SR, Sereno ME, Sereno AB. Characteristics of eye-position gain field populations determine geometry of visual space. Frontiers in Integrative Neuroscience. 2015;**9**:72. DOI: 10.3389/fnint.2015.00072

[69] Hagler DJ Jr, Riecke L, Sereno MI. Parietal and superior frontal visuospatial maps activated by pointing and saccades. NeuroImage. 2007;**35**(4):1562-1577. DOI: 10.1016/j.neuroimage.2007.01.033

[70] Kastner S, DeSimone K, Konen CS, Szczepanski SM, Weiner KS, Schneider KA. Topographic maps in human frontal cortex revealed in memory-guided saccade and spatial working-memory tasks. Journal of Neurophysiology. 2007;**97**(5):3494-3507. DOI: 10.1152/jn.00010.2007

[71] Konen CS, Kastner S. Representation of eye movements and stimulus motion in topographically organized areas of human posterior parietal cortex. The Journal of Neuroscience. 2008;**28**(33):8361-8375. DOI: 10.1523/JNEUROSCI.1930-08.2008

[72] Swisher JD, Halko MA, Merabet LB, McMains SA, Somers DC. Visual topography of human intraparietal sulcus. The Journal of Neuroscience. 2007;**27**(20):5326-5337. DOI: 10.1523/JNEUROSCI.0991-07.2007

[73] Hagler DJ Jr, Sereno MI. Spatial maps in frontal and prefrontal cortex. NeuroImage 2006;**29**(2):567-577. DOI: 10.1016/j.neuroimage.2005.08.058

[74] Sereno MI, Pitzalis S, Martinez A. Mapping of contralateral space in retinotopic coordinates by a parietal cortical area in humans. Science. 2001;**294**(5545):1350-1354. DOI: 10.1126/science.1063695

[75] Sereno MI, Huang RS. A human parietal face area contains aligned head-centered visual and tactile maps. Nature Neuroscience. 2006;**9**(10):1337-1343. DOI: 10.1038/nn1777

[76] Silver MA, Kastner S. Topographic maps in human frontal and parietal cortex. Trends in Cognitive Sciences. 2009;**13**(11):488-495. DOI: 10.1016/j.tics.2009.08.005

[77] Silver MA, Ress D, Heeger DJ. Topographic maps of visual spatial attention in human parietal cortex. Journal of Neurophysiology. 2005;**94**(2):1358-1371. DOI: 10.1152/jn.01316.2004

[78] Saygin AP, Sereno MI. Retinotopy and attention in human occipital, temporal, parietal, and frontal cortex. Cerebral Cortex. 2008;**18**(9):2158-2168. DOI: 10.1093/cercor/bhm242

[79] Szczepanski SM, Konen CS, Kastner S. Mechanisms of spatial attention control in frontal and parietal cortex. The Journal of Neuroscience. 2010;**30**(1):148-160. DOI: 10.1523/JNEUROSCI.3862-09.2010

[80] Lauritzen TZ, D'Esposito M, Heeger DJ, Silver MA. Top-down flow of visual spatial attention signals from parietal to occipital cortex. Journal of Vision. 2009;**9**(13):181-184. DOI: 10.1167/9.13.18

[81] Larsson J, Heeger DJ. Two retinotopic visual areas in human lateral occipital cortex. The Journal of Neuroscience. 2006;**26**(51):13128-13142. DOI:10.1523/JNEUROSCI.1657-06.2006

[82] Langner G, Albert M, Briede T. Temporal and spatial coding of periodicity information in the inferior colliculus of awake chinchilla (Chinchilla laniger). Hearing Research. 2002;**168**(1-2):110-130

[83] Adams DL, Sincich LC, Horton JC. Complete pattern of ocular dominance columns in human primary visual cortex. The Journal of Neuroscience. 2007;**27**(39):10391-10403. DOI: 10.1523/JNEUROSCI.2923-07.2007

[84] Bartfeld E, Grinvald A. Relationships between orientation-preference pinwheels, cytochrome oxidase blobs, and ocular-dominance columns in primate striate cortex. Proceedings of National Academy of Sciences U S A. 1992;**89**(24):11905-11909

[85] Livingstone MS, Hubel DH. Anatomy and physiology of a color system in the primate visual cortex. The Journal of Neuroscience. 1984;**4**(1):309-356

[86] Schira MM, Tyler CW, Breakspear M, Spehar B. The foveal confluence in human visual cortex. The Journal of Neuroscience. 2009;**29**(28):9050-9058. DOI: 10.1523/JNEUROSCI.1760-09.2009

[87] Schira MM, Tyler CW, Spehar B, Breakspear M. Modeling magnification and anisotropy in the primate foveal confluence. PLoS Computational Biology. 2010;**6**(1). DOI: 10.1371/journal.pcbi.1000651

[88] Hasson U, Hendler T, Ben Bashat D, Malach R. Vase or face? A neural correlate of shape-selective grouping processes in the human brain. Journal of Cognitive Neuroscience. 2001;**13**(6):744-753. DOI: 10.1162/08989290152541412

[89] Malach R, Levy I, Hasson U. The topography of high-order human object areas. Trends in Cognitive Sciences. 2002;**6**(4):176-184

[90] Tootell RB, Hadjikhani N. Where is 'dorsal V4' in human visual cortex? Retinotopic, topographic and functional evidence. Cerebral Cortex. 2001;**11**(4):298-311

[91] Larsson J, Landy MS, Heeger DJ. Orientation-selective adaptation to first- and second-order patterns in human visual cortex. Journal of Neurophysiology. 2006;**95**(2):862-881. DOI: 10.1152/jn.00668.2005

[92] Sayres R, Grill-Spector K. Relating retinotopic and object-selective responses in human lateral occipital cortex. Journal of Neurophysiology. 2008;**100**(1):249-267. DOI: 10.1152/jn.01383.2007

[93] McKyton A, Zohary E. Beyond retinotopic mapping: The spatial representation of objects in the human lateral occipital complex. Cerebral Cortex. 2007;**17**(5):1164-1172. DOI: 10.1093/cercor/bhl027

[94] Hemond CC, Kanwisher NG, Op de Beeck HP. A preference for contralateral stimuli in human object- and face-selective cortex. PLoS One. 2007;**2**(6):e574. DOI: 10.1371/journal.pone.0000574

[95] Niemeier M, Goltz HC, Kuchinad A, Tweed DB, Vilis T. A contralateral preference in the lateral occipital area: Sensory and attentional mechanisms. Cerebral Cortex. 2005;**15**(3):325-331. DOI: 10.1093/cercor/bhh134

[96] Huk AC, Dougherty RF, Heeger DJ. Retinotopy and functional subdivision of human areas MT and MST. The Journal of Neuroscience. 2002;**22**(16):7195-7205. DOI: 20026661

[97] Amano K, Wandell BA, Dumoulin SO. Visual field maps, population receptive field sizes, and visual field coverage in the human MT+ complex. Journal of Neurophysiology. 2009;**102**(5):2704-2718. DOI: 10.1152/jn.00102.2009

[98] Newsome WT, Mikami A, Wurtz RH. Motion selectivity in macaque visual cortex. III. Psychophysics and physiology of apparent motion. Journal of Neurophysiology. 1986;**55**(6):1340-1351. DOI: 10.1152/jn.1986.55.6.1340

[99] Hedges JH, Gartshteyn Y, Kohn A, Rust NC, Shadlen MN, Newsome WT, et al. Dissociation of neuronal and psychophysical responses to local and global motion. Current Biology. 2011;**21**(23):2023-2028. DOI: 10.1016/j.cub.2011.10.049

[100] Hoffman EA, Haxby JV. Distinct representations of eye gaze and identity in the distributed human neural system for face perception. Nature Neuroscience. 2000;**3**(1):80-84. DOI: 10.1038/71152

[101] Gilaie-Dotan S, Kanai R, Bahrami B, Rees G, Saygin AP. Neuroanatomical correlates of biological motion detection. Neuropsychologia. 2013;**51**(3):457-463. DOI: 10.1016/j.neuropsychologia.2012.11.027

[102] Beauchamp MS, Lee KE, Argall BD, Martin A. Integration of auditory and visual information about objects in superior temporal sulcus. Neuron. 2004;**41**(5):809-823

[103] Zhu LL, Beauchamp MS. Mouth and voice: A relationship between visual and auditory preference in the human superior temporal sulcus. The Journal of Neuroscience. 2017;**37**(10):2697-2708. DOI: 10.1523/JNEUROSCI.2914-16.2017

[104] Smith AT, Greenlee MW, Singh KD, Kraemer FM, Hennig J. The processing of first- and second-order motion in human visual cortex assessed by functional magnetic resonance imaging (fMRI). The Journal of Neuroscience. 1998;**18**(10):3816-3830

[105] Smith AT, Singh KD, Williams AL, Greenlee MW. Estimating receptive field size from fMRI data in human striate and extrastriate visual cortex. Cerebral Cortex. 2001; **11**(12):1182-1190

[106] Tootell RB, Hadjikhani N, Hall EK, Marrett S, Vanduffel W, Vaughan JT, et al. The retinotopy of visual spatial attention. Neuron. 1998;**21**(6):1409-1422

[107] Tootell RB, Mendola JD, Hadjikhani NK, Ledden PJ, Liu AK, Reppas JB, et al. Functional analysis of V3A and related areas in human visual cortex. The Journal of Neuroscience. 1997;**17**(18):7060-7078

[108] Schluppeck D, Glimcher P, Heeger DJ. Topographic organization for delayed saccades in human posterior parietal cortex. Journal of Neurophysiology. 2005;**94**(2):1372-1384. DOI: 10.1152/jn.01290.2004

[109] Pitzalis S, Galletti C, Huang RS, Patria F, Committeri G, Galati G, et al. Wide-field retinotopy defines human cortical visual area v6. The Journal of Neuroscience. 2006;**26**(30):7962-7973. DOI: 10.1523/JNEUROSCI.0178-06.2006

[110] Pitzalis S, Sereno MI, Committeri G, Fattori P, Galati G, Patria F, et al. Human v6: The medial motion area. Cerebral Cortex. 2010;**20**(2):411-424. DOI: 10.1093/cercor/bhp112

[111] Ress D, Chandrasekaran B. Tonotopic organization in the depth of human inferior colliculus. Frontiers in Human Neuroscience. 2013;**7**:586. DOI: 10.3389/fnhum.2013.00586

[112] Chang KH, Thomas JM, Boynton GM, Fine I. Reconstructing tone sequences from functional magnetic resonance imaging blood-oxygen level dependent responses within human primary auditory cortex. Frontiers in Psychology. 2017;**8**:1983. DOI: 10.3389/fpsyg.2017.01983

[113] Wessinger CM, VanMeter J, Tian B, Van Lare J, Pekar J, Rauschecker JP. Hierarchical organization of the human auditory cortex revealed by functional magnetic resonance imaging. Journal of Cognitive Neuroscience. 2001;**13**(1):1-7

[114] Langner G, Sams M, Heil P, Schulze H. Frequency and periodicity are represented in orthogonal maps in the human auditory cortex: Evidence from magnetoencephalography. Journal of Comparative Physiology. A. 1997;**181**(6):665-676

[115] Baumann S, Griffiths TD, Sun L, Petkov CI, Thiele A, Rees A. Orthogonal representation of sound dimensions in the primate midbrain. Nature Neuroscience. 2011;**14**(4):423-425. DOI: 10.1038/nn.2771

[116] Langner G, Schreiner CE. Periodicity coding in the inferior colliculus of the cat. I. Neuronal mechanisms. Journal of Neurophysiology. 1988;**60**(6):1799-1822

[117] Merzenich MM, Brugge JF. Representation of the cochlear partition of the superior temporal plane of the macaque monkey. Brain Research. 1973;**50**(2):275-296

[118] Galaburda AM, Pandya DN. The intrinsic architectonic and connectional organization of the superior temporal region of the rhesus monkey. The Journal of Comparative Neurology. 1983;**221**(2):169-184. DOI: 10.1002/cne.902210206

[119] Fullerton BC, Pandya DN. Architectonic analysis of the auditory-related areas of the superior temporal region in human brain. The Journal of Comparative Neurology. 2007;**504**(5):470-498. DOI: 10.1002/cne.21432

[120] Sweet RA, Dorph-Petersen KA, Lewis DA. Mapping auditory core, lateral belt, and parabelt cortices in the human superior temporal gyrus. The Journal of Comparative Neurology. 2005;**491**(3):270-289. DOI: 10.1002/cne.20702

[121] Dick F, Tierney AT, Lutti A, Josephs O, Sereno MI, Weiskopf N. In vivo functional and myeloarchitectonic mapping of human primary auditory areas. The Journal of Neuroscience. 2012;**32**(46):16095-16105

[122] Kaas JH, Hackett TA. Subdivisions of auditory cortex and levels of processing in primates. Audiology & Neuro-Otology. 1998;**3**(2-3):73-85

[123] Kaas JH, Hackett TA. Subdivisions of auditory cortex and processing streams in primates. Proceedings of National Academy of Sciences U S A. 2000;**97**(22):11793-11799. DOI: 10.1073/pnas.97.22.11793

[124] Hackett TA. Information flow in the auditory cortical network. Hearing Research. 2011;**271**(1-2):133-146. DOI: 10.1016/j.heares.2010.01.011

[125] Hackett TA, Stepniewska I, Kaas JH. Subdivisions of auditory cortex and ipsilateral cortical connections of the parabelt auditory cortex in macaque monkeys. The Journal of Comparative Neurology. 1998;**394**(4):475-495

[126] Morel A, Garraghty PE, Kaas JH. Tonotopic organization, architectonic fields, and connections of auditory cortex in macaque monkeys. The Journal of Comparative Neurology. 1993;**335**(3):437-459. DOI: 10.1002/cne.903350312

[127] Jones EG, Dell'Anna ME, Molinari M, Rausell E, Hashikawa T. Subdivisions of macaque monkey auditory cortex revealed by calcium-binding protein immunoreactivity. The Journal of Comparative Neurology. 1995;**362**(2):153-170. DOI: 10.1002/cne.903620202

[128] Molinari M, Dell'Anna ME, Rausell E, Leggio MG, Hashikawa T, Jones EG. Auditory thalamocortical pathways defined in monkeys by calcium-binding protein immunoreactivity. The Journal of Comparative Neurology. 1995;**362**(2):171-194. DOI: 10.1002/cne.903620203

[129] Kusmierek P, Rauschecker JP. Functional specialization of medial auditory belt cortex in the alert rhesus monkey. Journal of Neurophysiology. 2009;**102**(3):1606-1622. DOI: 10.1152/jn.00167.2009

[130] Rauschecker JP, Tian B, Hauser M. Processing of complex sounds in the macaque nonprimary auditory cortex. Science. 1995;**268**(5207):111-114

[131] Tian B, Rauschecker JP. Processing of frequency-modulated sounds in the lateral auditory belt cortex of the rhesus monkey. Journal of Neurophysiology. 2004;**92**(5):2993-3013. DOI: 10.1152/jn.00472.2003

[132] Kajikawa Y, Frey S, Ross D, Falchier A, Hackett TA, Schroeder CE. Auditory properties in the parabelt regions of the superior temporal gyrus in the awake macaque monkey: An initial survey. The Journal of Neuroscience. 2015;**35**(10):4140-4150. DOI: 10.1523/JNEUROSCI.3556-14.2015

[133] Hickok G, Poeppel D. The cortical organization of speech processing. Nature Reviews. Neuroscience. 2007;**8**(5):393-402. DOI: 10.1038/nrn2113

[134] Brewer AA, Barton B. Human auditory cortex. In: Hickok G, Small SL, editors. Neurobiology of Language. Cambridge: Academic Press, Elsevier; 2016. pp. 49-58. DOI: 10.1016/B978-0-12-407794-2.00005-5

[135] Dau T, Kollmeier B, Kohlrausch A. Modeling auditory processing of amplitude modulation. II. Spectral and temporal integration. The Journal of the Acoustical Society of America. 1997;**102**(5 Pt 1):2906-2919

[136] Ewert SD, Dau T. Characterizing frequency selectivity for envelope fluctuations. The Journal of the Acoustical Society of America. 2000;**108**(3 Pt 1):1181-1196

[137] Hsieh IH, Saberi K. Detection of sinusoidal amplitude modulation in logarithmic frequency sweeps across wide regions of the spectrum. Hearing Research. 2010;**262**(1-2):9-18. DOI: 10.1016/j.heares.2010.02.002

[138] Langner G, Dinse HR, Godde B. A map of periodicity orthogonal to frequency representation in the cat auditory cortex. Frontiers in Integrative Neuroscience. 2009;**3**:27. DOI: 10.3389/neuro.07.027.2009

[139] de la Mothe LA, Blumell S, Kajikawa Y, Hackett TA. Cortical connections of the auditory cortex in marmoset monkeys: Core and medial belt regions. The Journal of Comparative Neurology 2006;**496**(1):27-71. DOI: 10.1002/cne.20923

[140] Petkov CI, Kayser C, Augath M, Logothetis NK. Functional imaging reveals numerous fields in the monkey auditory cortex. PLoS Biology. 2006;**4**(7):e215. DOI: 10.1371/journal.pbio.0040215

[141] Pandya DN, Sanides F. Architectonic parcellation of the temporal operculum in rhesus monkey and its projection pattern. Zeitschrift für Anatomie und Entwicklungsgeschichte. 1973;**139**(2):127-161

[142] Kayser C, Petkov CI, Augath M, Logothetis NK. Functional imaging reveals visual modulation of specific fields in auditory cortex. The Journal of Neuroscience. 2007; **27**(8):1824-1835. DOI: 10.1523/JNEUROSCI.4737-06.2007

[143] Brewer AA, Press WA, Logothetis NK, Wandell BA. Visual areas in macaque cortex measured using functional magnetic resonance imaging. The Journal of Neuroscience. 2002;**22**(23):10416-10426

[144] Hedges S, Kumar S. Genomic clocks and evolutionary timescales. Trends in Genetics. 2003;**19**:200-206

[145] Krubitzer L. The magnificent compromise: Cortical field evolution in mammals. Neuron. 2007;**56**(2):201-208. DOI: 10.1016/j.neuron.2007.10.002

[146] Mancini F, Haggard P, Iannetti GD, Longo MR, Sereno MI. Fine-grained nociceptive maps in primary somatosensory cortex. The Journal of Neuroscience. 2012;**32**(48): 17155-17162. DOI: 10.1523/JNEUROSCI.3059-12.2012

Edited by Thomas Heinbockel

The sensory nervous system is of critical importance in our daily lives and contributes to our personal well-being and safety as well as communication with others. However, it is only when disease or injury impair its function that we fully appreciate the relevance of our sensory modalities. During the past decades, research of our senses has seen an ever-growing interest in this exciting field of study. This book provides the reader with an overview of the current state-of-the-art of research of our senses and focuses on the most important evidence-based developments in this area. This book addresses both the physiology and pathophysiology of our sensory nervous system ranging from molecular, cellular, and systems to cognitive and behavioral topics. Individual chapters focus on recent advances in specific areas of sensory systems in different model organisms and humans. All chapters represent recent contributions to the rapidly developing field of sensory science.

Published in London, UK

IntechOpen

ISBN 978-1-83881-284-3